Activation of Strong C–H and C–O Bonds for Transition Metal-Catalyzed Cross-Coupling

Garrett Freure

Thesis Supervisor: Stephen G. Newman

A thesis submitted in partial fulfillment of the requirements for the degree of

Master of Science in Chemistry

Department of Chemistry and Biomolecular Sciences,

Faculty of Science, University of Ottawa

© Garrett Freure, Ottawa, Canada, 2021

Abstract:

Transition metal-catalyzed cross-coupling is one of the most dominant fields of modern synthetic organic chemistry. Research is forever ongoing, in which there is constant expansion of the scope of nucleophilic- and electrophilic- coupling partners, and consequently the types of products that can be formed. More specifically, strong bond activation in cross-coupling is an emerging field that can enable late-stage functionalization; by activating inert functional groups that were untouched in earlier synthetic steps, they can be taken advantage of for further derivatization. This thesis will focus on the use of aggressive reagents in the activation of strong C–H and C–O bonds for their use in transition metal-catalyzed cross-coupling.

Chapter 1 will involve the use of organometallic superbases in the palladium-catalyzed cross-coupling of sp^3-hybridized carbon-centered nucleophiles. Deprotonation and subsequent electrophilic quench can be considered the most classical form of C–H activation. While modern approaches frequently focus on radical mechanisms or directing groups as modes of C–H activation, stoichiometric metalation has been largely overlooked in the context of cross-coupling. By using aggressive organometallic superbases to deprotonate very weakly acidic C–H bonds, the resultant organometallic species can be taken advantage of as cross-coupling nucleophiles. This chapter will investigate the coupling of organolithiums and organozincs generated *in situ* in the C(sp^3)–H arylation of an array of unactivated substrate classes.

Chapter 2 will briefly investigate the use of aggressive alkyl metallic additives in the C–O activation of silyl enol ethers as Suzuki-Corriu cross-coupling electrophiles. Converting ketones to substituted olefins using cross-coupling is a common approach in medicinal chemistry for the

synthesis of complex bioactive products. While reliable, this chemistry is generally very inefficient due to multi-step synthesis and the instability of activated intermediates. In contrast, applying modern nickel-catalyzed C–O activation to robust silyl enol ethers made *in situ* could alleviate these limitations. Using triethylborane as an additive, a nickel-catalyzed Suzuki-Corriu cross-coupling of silyl enol ethers was discovered. While ultimately unsuccessful, attempts were also made to optimize, explore the scope, and elucidate the mechanism of this reaction.

Acknowledgements:

Firstly, thank you to the Natural Sciences and Engineering Research Council of Canada (NSERC), the Province of Ontario, and the University of Ottawa, whose generous scholarships made this research possible. Furthermore, thank you to all members of the Newman Lab that I've worked with, past and present. I've learned so much from all of you and I've enjoyed working alongside such a great group of young chemists. Above all, I'd especially like to thank Professor Stephen Newman. You're the best supervisor I could have hoped for. By being both incredibly knowledgeable and understanding, you've made my experience in graduate school something that I can look back on fondly. To Eric Skrotzki, you were a joy to work alongside on the superbase project and I'm excited to be able to continue to work near you in Mississauga. Dr. Ryan Sullivan – working with you during my undergraduate studies was a pleasure and you taught me so much. You've greatly contributed to my skills as a researcher and I'll be forever thankful for that experience. Furthermore, thank you to all of my friends and family who tried to keep me sane during by graduate studies; I couldn't have done it without you. Lastly, I must acknowledge Saeed K. Kashani, a member of the Newman Group who passed away far too young. I'm saddened that his life was cut so short, and I wish I could have seen who he would have grown to become.

Table of Contents:

List of Tables:

List of Schemes:

List of Abbreviations:

Ac	acetyl
Ar	aryl
Bn	benzyl
Boc	*tert*-butyloxycarbonyl
Bu	butyl
C	Celsius
cat.	catalytic or catalyst
cod or COD	1,4-cyclooctadiene
CPME	cyclopentyl methyl ether
Cy	cyclohexyl
Cyp	cyclopentyl
d	doublet
DABCO	1,4-diazabicyclo[2.2.2]octane
DavePhos	2-dicyclohexylphosphino-2′-(*N*,*N*-dimethylamino)biphenyl
dba	dibenzylideneacetone
DCM	dichloromethane
DBU	1,8-diazabicyclo[5.4.0]undec-7-ene
DCYPE	1,2-bis(dicyclohexylphosphino)ethane
DIPEA	*N*,*N*-di(*iso*-propyl)ethylamine
DMAP	*N*,*N*-dimethylpyridin-4-amine
DMF	*N*,*N*-dimethylformamide
DMSO	dimethylsulfoxide
DOM	directed ortho metalation
DPPP	1,3-bis(diphenylphosphino)propane
E or E^+	electrophile
EDG	electron-donating group
EI	electron impact

EN	electronegativity
Equiv	equivalent(s)
Et	ethyl
EtOAc	ethyl acetate
EWG	electron-withdrawing group
E2	bimolecular elimination
g	gram(s)
GC	gas chromatography
h	hour(s)
HAT	hydrogen atom transfer
HRMS	high resolution mass spectrometry
HTE	high-throughput experimentation
Hz	hertz
i	*iso*
ICy	1,3-bis(1-adamantyl)imidazol-2-ylidene
IMes	1,3-bis(2,4,6-trimethylphenyl)imidazol-2-ylidene
IPr	1,3-bis(2,4,6-trimethylphenyl)-1,3-dihydro-2H-imidazol-2-ylidene
IPent	1,3-bis(2,6-di-3-pentylphenyl)imidazol-2-ylidene
J	coupling constant
LA	Lewis acid
LDA	lithium di(*iso*propyl)amide
LHE	lithium-halogen exchange
KHMDS	potassium bis(trimethylsilyl)amide
M	generic metal or molar
m	mass, meta, or multiplet
Me	methyl
MeCN	acetonitrile
mg	milligram(s)

min	minute(s)
mL	milliliter(s)
mol	mole(s)
MS	mass spectrometry
m/z	mass over charge
NHC	*N*-heterocyclic carbene
NMR	nuclear magnetic resonance
Nuc	nucleophile
n-Bu	*n*-butyl
N-XantPhos	4,6-bis(diphenylphosphino)phenoxazine
o	ortho
OTf	triflate
OVAT	one variable-at-a-time
O/N	overnight
p	para
PEPPSI	pyridine-enhanced pre-catalyst preparation stabilization and initiation
Pent	pentyl
Pd-XPhos-G2	chloro(2-dicyclohexylphosphino-2',4',6'-triisopropyl-1,1'-biphenyl)[2-(2'-amino-1,1'-biphenyl)]palladium(II)
PFA	perfluoroalkoxy
PG	protecting group
Ph	phenyl
pK_a	acid dissociation constant
pin	pinacolato
ppm	parts per million
Pr	propyl
q	quartet
quin	quintet

R	generic chemical group
RT	room temperature
SIMes	1,3-bis(2,4,6-trimethylphenyl)-4,5-dihydroimidazolidene
SIPr	1,3-bis(2,6-diisopropylphenyl)-4,5-dihydroimidazolidene
S_NAr	nucleophilic aromatic substitution
S_N2	bimolecular nucleophilic substitution
SPhos	2-dicyclohexylphosphino-2',6'-dimethoxybiphenyl
s-Bu	*sec*-butyl
t	triplet
Temp.	temperature
Tf	trifluoromethanesulfonate
TMEDA	*N*,*N*,*N*',*N*'-tetramethylethylenediamine
TMCDA	*trans*-*N*,*N*,*N*',*N*'-tetramethylcyclohexane-1,2-diamine
TMP	2,2,6,6-tetramethylpiperidine
TBS	*tert*-butyldimethylsilyl
*t*Bu or *t*-Bu	*tert*-butyl
TES	triethylsilyl
THF	tetrahydrofuran
TIPS	tri(*iso*-propyl)silyl
TLC	thin layer chromatography
TMS	trimethylsilyl
UV	ultraviolet
X	generic halide or pseudohalide
XPhos	2-dicyclohexylphosphino-2',4',6'-triisopropylbiphenyl
Y or Z	generic heteroatom

Statement of Contributions:

The project discussed in Chapter 1 was done in collaboration with two colleagues in the Newman Lab. Fellow master's student, Eric A. Skrotzki, aided in the deprotonation of primary benzylic C–H bonds using coordinating-amine superbases. He contributed to the optimization, quantification, kinetics, and scope of the deprotonation of toluene derivatives, as well as attempted to apply our novel deprotonation conditions to other substrate classes. Jean-Danick E. Lavertu, an undergraduate researcher whom I mentored, optimized the deprotonation of secondary benzylic C–H bonds using Schlosser's base. He also attempted to optimize the deprotonation of allylic positions using Schlosser's base. Dr. Ryan J. Sullivan, a former PhD student of the Newman Lab, had previously synthesized Pd-XPhos-G2 and Pd(XPhos)(allyl)Cl, both of which were tested in the optimization process for the direct cross-coupling of benzyl lithiums. Unless otherwise indicated, all deprotonation experiments included in this chapter were performed by me. Furthermore, I did all the optimization for the cross-coupling of superbase-generated benzyl lithiums and organozincs, and isolated all scope examples. The research described in this chapter was published in a peer-review journal (1).

Many of the NHC ligands used in Chapter 2 were synthesized by Dr. Yan-Long Zheng, a former postdoctoral fellow in our group. Otherwise, the project discussed in this chapter is entirely my own work.

(1) Freure, G. P. R.; Skrotzki, E. A.; Lavertu, J.-D. E.; Newman, S. G. Palladium-Catalyzed Cross-Coupling of Superbase-Generated C(sp^3) Nucleophiles. *ACS Catal.* **2021**, *11*, 12258–12263.

Chapter 1: Palladium-Catalyzed Cross-Coupling of Superbase-Generated C(sp^3) Nucleophiles

1.1: Introduction

1.1.1: Palladium-Catalyzed Cross-Coupling for C–C Bond Formation

A significant focus in modern synthetic organic chemistry is transition metal-catalyzed cross-coupling.[1, 2] Since the pioneering work in the 1970s, which was later the subject of the 2010 Nobel Prize in Chemistry, palladium-catalyzed cross-coupling has improved many aspects of organic synthesis, enabling the discovery of new bioactive molecules by the rapid access to structural complexity.[3] Furthermore, finely tuned, mild reaction conditions can enable key carbon-carbon bond formation while providing high chemoselectivity, thus decreasing the stringent requirement of protecting groups in complex molecule synthesis. Implementing cross-coupling-based strategies often improves the efficiency of a given synthesis as it can decrease the number of consecutive steps required, thus reducing chemical waste and increasing overall yield.

Many distinct palladium-catalyzed cross-coupling reactions for C–C bond formation have been developed. The commonalities between these related reactions can be highlighted by examining their general catalytic cycle, which is comprised of a series of elementary steps (**Scheme 1**). First, a Pd(0) active catalyst undergoes oxidative addition into a relatively weak carbon-heteroatom bond of the electrophilic coupling partner (R–X), most commonly an aryl- or

---

[1] Biffis, A.; Centomo, P.; Del Zotto, A.; Zecca, M. *Chem. Rev.* **2018**, *118*, 2249–2295.
[2] Campeau, L.-C.; Hazari, N. *Organometallics* **2019**, *38*, 3–35.
[3] Buskes, M. J.; Blanco, M.-J. *Molecules* **2020**, *25*, 3493.

vinyl- (pseudo)halide. By inserting between this bond, the metal center of the catalyst increases both its oxidation state and coordination number by two. If multiple R–X groups are present on a given substrate, the catalyst will generally insert into the weakest bond.

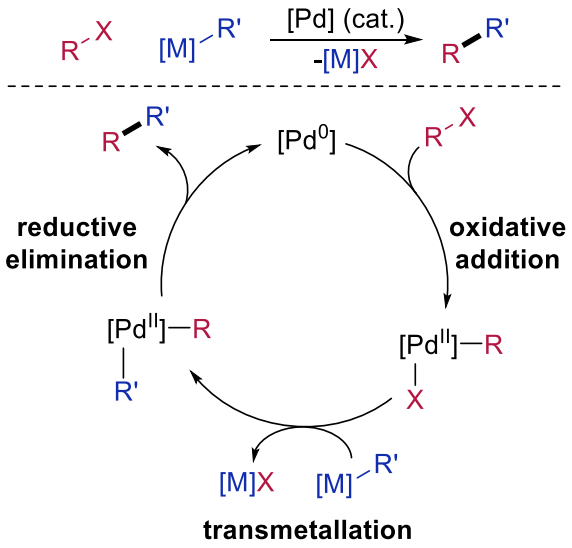

Scheme 1 – General Catalytic Cycle for C–C Bond Formation in Palladium-Catalyzed Cross-Coupling

Following oxidative addition, the nucleophilic coupling partner, most commonly an organometallic species ([M]–R'), undergoes transmetallation with the resultant Pd(II) intermediate. In this step, the polarized organometallic nucleophile exchanges its electron-rich carbon-centered group with the heteroatom-based leaving group of the oxidative addition adduct. A key difference in many types of related cross-coupling reactions involves the identity of the metal bound to the nucleophilic organic fragment. In the pioneering work of the 1970s, these nucleophiles included, but were not limited to, organoborons (Suzuki-Miyaura coupling),[4]

[4] Miyaura, N.; Suzuki, A. *J. Chem. Soc., Chem. Commun.* **1979**, *19*, 866–867.

organotins (Stille coupling),[5] and organomagnesiums (Kumada-Corriu coupling).[6] Since then, there has been a great expansion in the scope of compatible nucleophilic coupling partners. In general, the reactivity of these organometallic nucleophiles is derived from the relative polarity of the R'–M bond. In the context of C–C bond formation, the nucleophiles are carbon atoms, which has an electronegativity (EN) of 2.55. Consequently, the identity of the metal of the organometallic nucleophile influences the degree to which the R'–M bond is polarized. Electropositive metals such as magnesium (EN of 1.31) have a very polarized R'–M bond, making organomagnesiums quite nucleophilic. In contrast, relatively electronegative metals such as tin (EN of 1.96) will have a less polarized bond, making organotins less reactive. The relative nucleophilicity of some common classes of transmetallating agents is shown in **Figure 1**.

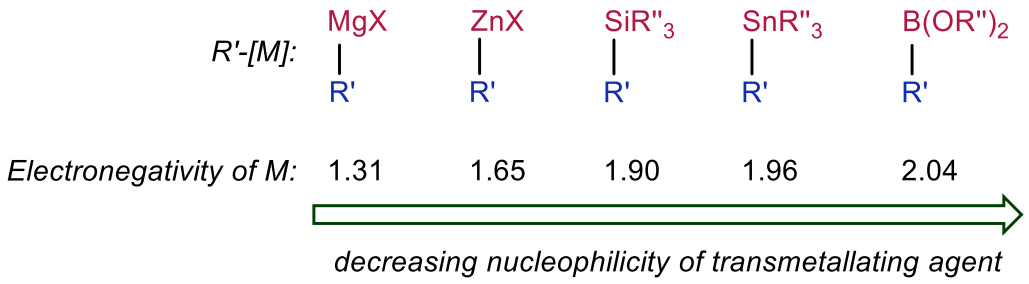

Figure 1 – Relative Nucleophilicity of Common Transmetallating Agent Classes

Relatively weakly-nucleophilic organometallic species often require further activation, as they will not participate in the transmetallation step in the absence of additive. For example, Suzuki-Miyaura coupling (M = boron), almost always requires the presence of an oxygen-centered base (**Scheme 2a**). To aid the transmetallation of trivalent organoborons, a metal alkoxide (R''OM)

[5] Milstein, D.; Stille, J. K. *J. Am. Chem. Soc.* **1979**, *101*, 4992–4998.
[6] Tamao, K.; Sumitani, K.; Kumada, M. *J. Am. Chem. Soc.* **1972**, *94*, 4374–4376.

or similar species can undergo a ligand exchange with the oxidative addition intermediate.[7] This displaces the (pseudo)halide of the Pd(II) oxidative addition adduct. Upon transmetallation, a borate derivative ($B(OR'')_3$) is usually formed, in which the presence of the electron-donating alkoxy/hydroxy groups stabilizes the coordinatively-unsaturated boron center. In the same vein, it is observed that the C–Si bond in Hiyama-Denmark coupling is usually too strong to undergo transmetallation in the absence of additive.[8] By adding a nucleophilic fluoride source to the reaction mixture, a hypervalent silicon species is formed prior to transmetallation that increases the nucleophilicity of the organosilicon (**Scheme 2b**).

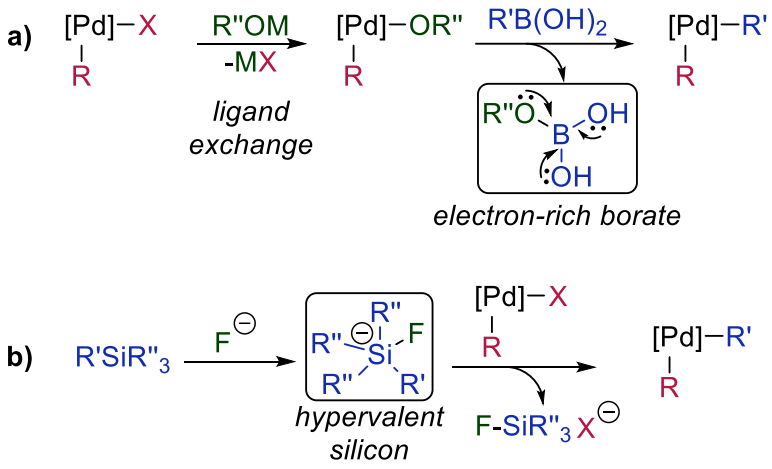

Scheme 2 – Nucleophile Activation in Suzuki-Miyaura and Hiyama-Denmark Coupling

The last step within these catalytic cycles is usually reductive elimination, which is formally the opposite of oxidative addition. Thus, in this step, the oxidation state and coordination number of the final Pd(II) intermediate are decreased by two, forming the key C–C bond and regenerating the active Pd(0) catalyst. Reductive elimination generally requires the groups to be cis, and

[7] Thomas, A. A.; Denmark, S. E. *Science* **2016**, *352*, 329–332.
[8] Hiyama, T. *J. Organomet. Chem.* **2002**, *653,* 1–2.

therefore trans/cis isomerization may be required if the groups are not in the correct configuration.[9] The formation of the cross-coupled product is generally the thermodynamic driving force for the catalytic cycle, since relatively weak R–X and R'–M bonds are replaced with a relatively strong R–R' bond.

As the catalyst continues to turnover by proceeding through this catalytic cycle, more of the cross-coupled product is formed. The efficacy of the catalyst within any desired catalytic cycle often influences the lower bound of the catalyst loadings that are possible; if the catalytic cycle is well behaved, the Pd loading can be very low. However, catalytic cycles are usually imperfect, as the palladium can exist as off-cycle intermediates, often leading to catalyst death, and thus requiring greater catalyst loading. For example, Pd(0) complexes can aggregate to form a palladium black precipitate. While this off-cycle species is known to facilitate heterogeneous catalysis, desired cross-coupling is generally shut down.[10] Furthermore, depending on the kinetics of the rate-determining step, the catalytic cycle may be impractically slow at very low catalyst loadings. Increasing the catalyst loading generally increases the rate of the reaction, thereby providing improved synthetic utility by enabling convenient reaction times.

Palladium-catalyzed cross-coupling is not at all limited to C–C bond formation. Both heteroatom-centered nucleophiles and heteroatom-centered electrophiles have been widely reported in recent years. Beyond organometallic nucleophilic coupling partners, purely organic nucleophiles have also been established in cross-coupling. The most famous of which are the

---

[9] Gillie, A.; Stille, J. K. *J. Am. Chem. Soc.* **1980**, *102*, 4933–4941.
[10] Dziedzic, R. M.; Axtell, J. C.; Rheingold, A. L.; Spokoyny, A. M. *Process Res. Dev*. **2019**, *23*, 1638–1645.

Nobel Prize-winning Mizoroki–Heck reaction with olefins,[11] and Buchwald-Hartwig amination with amines.[12] Furthermore, non-carbon-centered electrophiles have been reported, such as iodosilanes, oxime esters, and chloroamines.[13] However, the overwhelming prevalence of carbon-carbon bonds in organic compounds makes C–C bond formation arguably the most interesting and important application of cross-coupling.

One of the most significant advantages of transition metal-catalyzed cross-coupling is improved scope and functional group tolerance relative to classical methods. For example, nucleophilic aromatic substitution (S_NAr) generally requires aryl halides to be activated to undergo nucleophilic attack. Electron-withdrawing groups (EWG) such as nitros and esters can stabilize the resultant dearomatized anionic intermediate, enabling the product to form (**Scheme 3a**). In contrast, palladium catalysts have frequently been demonstrated to functionalize unactivated and even electron-rich aryl halides for cross-coupling (**Scheme 3b**). Furthermore, because the aryl halide is activated by oxidative addition instead of direct nucleophilic attack, tolerance of electrophilic functional groups is frequently also improved. Therefore, relative to classical methods, cross-coupling can generally enable useful transformations of more complex substrates without inherently requiring activating groups.

[11] Beletskaya, I. P.; Cheprakov, A. V. *Chem. Rev.* **2000**, *100*, 3009–3066.
[12] Ruiz-Castillo, P.; Buchwald, S. L. *Chem. Rev.* **2016**, *116*, 12564–12649.
[13] Korch, K. M.; Watson, D. A. *Chem. Rev*. **2019**, *119*, 8192–8228.

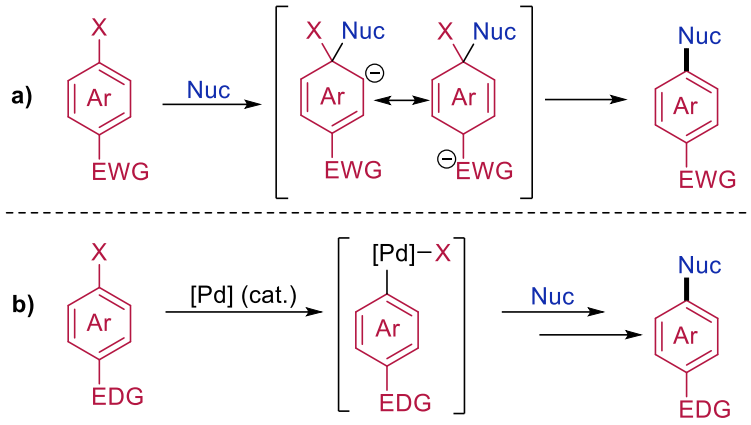

Scheme 3 – Relative Scope of Electrophilic Substrates for S_NAr and Cross-Coupling

While palladium-catalyzed cross-coupling certainly shows some advantages over classical methods, it is not without its limitations. Much of the initial discoveries were largely limited to the formation of $C(sp^2)$–$C(sp^2)$ bonds. As a representative example, one of the seminal reports of Kumada-Corriu coupling involved the cross-coupling of aryl magnesium halide reagents with vinyl bromides in the preparation of stilbenes (**Scheme 4**).[14] In this case, a nickel catalyst was used instead of palladium, which often shows similar catalytic activity.[15] Although this chemistry is useful in the preparation of substituted olefins, it is limited by the difficulty associated with the formation of $C(sp^2)$–$C(sp^3)$ and $C(sp^3)$–$C(sp^3)$ bonds. Therefore, much of the initial reports of transition metal-catalyzed cross-coupling were not suitable to fully overcome the limitations of traditional nucleophilic substitution reactions, such as the classical S_N2 reaction.

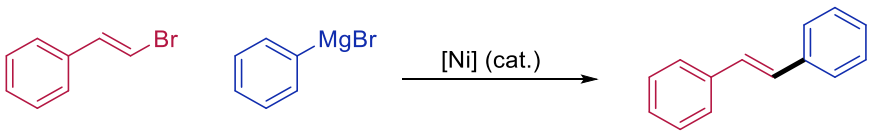

Scheme 4 – Seminal Report of Kumada-Corriu Coupling for $C(sp^2)$–$C(sp^2)$ Bond Formation

[14] Corriu, R. J. P.; Masse, J. P. *J. Chem. Soc., Chem. Commun.* **1972**, *3*, 144.
[15] Tasker, S. Z.; Standley, E. A.; Jamison, T. F. *Nature* **2014**, *509*, 299–309.

Since the inception of cross-coupling, continuous focus has been on the use of C(sp^3)-hybridized coupling partners. A common limitation in cross-coupling is achieving selective functionalization of C(sp^3)–X electrophiles. While oxidative addition into aryl- and vinyl-(pseudo)halides is relatively facile, alkyl halides are much more difficult to activate due to the relative energy of their respective transition states.[16] Consequently, slow oxidative addition makes the use of alkyl halides in cross-coupling a challenge. However, some advancements have been made in this field, such as the palladium-catalyzed Suzuki-Miyaura coupling of benzyl carbonates (**Scheme 5**).[17] In this case, the C(sp^3)–X activation is not as simple as the general oxidative addition previously discussed. Instead, upon decarboxylation of the electrophile, a dearomatized Pd(II) intermediate is formed. While this is an interesting mechanism of C(sp^3)–X oxidative addition, expansion of cross-coupling electrophiles is not the focus of this chapter and therefore will not be discussed in great detail.

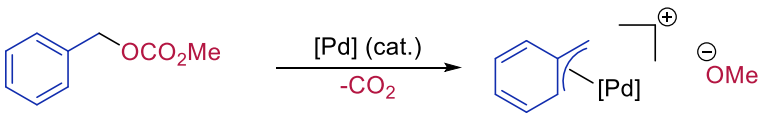

Scheme 5 – Example of Formal Oxidative Addition into a C(sp^3)–X Bond in Cross-Coupling

When it comes to the cross-coupling of C(sp^3)-hybridized nucleophiles, difficulties are typically encountered in the transmetallation step. For example, organoborons are some of the most useful nucleophilic coupling partners because of how well-behaved they are, largely only participating in the desired cross-coupling as opposed to competitive side-reactions.[18] However,

[16] Ariafard, A.; Lin, Z. *Organometallics* **2006**, *25*, 4030–4033.
[17] Ohsumi, M.; Ito, A.; Nishiwaki, N. *RSC Adv.* **2018**, *8*, 35056–35061.
[18] Martin, R.; Buchwald, S. L. *Acc. Chem. Res.* **2008**, *41*, 1461–1473.

alkyl boron species have been shown to be difficult to coerce into undergoing transmetallation, especially when sterics exceed simple primary alkyls.[19] One strategy to overcome this challenge is to use C(sp^3) coupling partners of greater nucleophilicity. For example, Kumada-Corriu cross-coupling has shown to be effective in the coupling of secondary alkyl Grignard reagents (**Scheme 6**).[20]

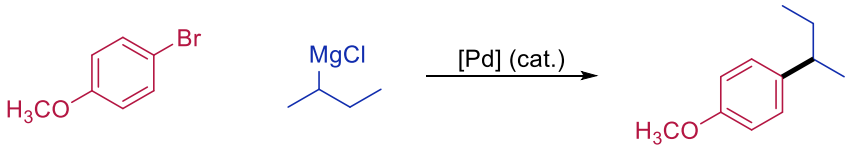

Scheme 6 – Use of Aggressive Nucleophiles for C(sp^3)–C(sp^2) Bond formation in Cross-Coupling

While enabling C(sp^2)–C(sp^3) bond formation, a tradeoff is observed with aggressive nucleophiles as they are more susceptible to side reactions. Due to the nucleophilicity and basicity of Grignard reagents, Kumada-Corriu coupling often has poor tolerance of electrophilic- and acidic- functional groups on the electrophilic coupling partner. However, there have been some recent improvements on this limitation; for example, Buchwald demonstrated that cryogenic reaction temperatures can improve the functional group tolerance of Kumada-Corriu coupling (**Scheme 7**).[21] Although this report exclusively used sp^2-hybridized organomagnesiums, it outlined that if a suitable temperature is identified, transmetallation can outcompete nucleophilic attack onto electrophilic functional groups. Unfortunately, the suitable temperature for this improved chemoselectivity is largely substrate-dependent. Consequently, further

[19] Chemler, S. R.; Trauner, D.; Danishefsky, S. J. *Angew. Chem. Int. Ed.* **2001**, *40*, 4544-4568.
[20] Hayashi, T.; Konishi, M.; Kobori, Y.; Kumada, M.; Higuchi, T.; Hirotsu, K. *J. Am. Chem. Soc.* **1984**, *106*, 158–163.
[21] Martin, R.; Buchwald, S. L. *J. Am. Chem. Soc*. **2007**, *129*, 3844–3845.

optimization relative to the reported conditions is likely required to form cross-coupled products outside of their explicit scope.

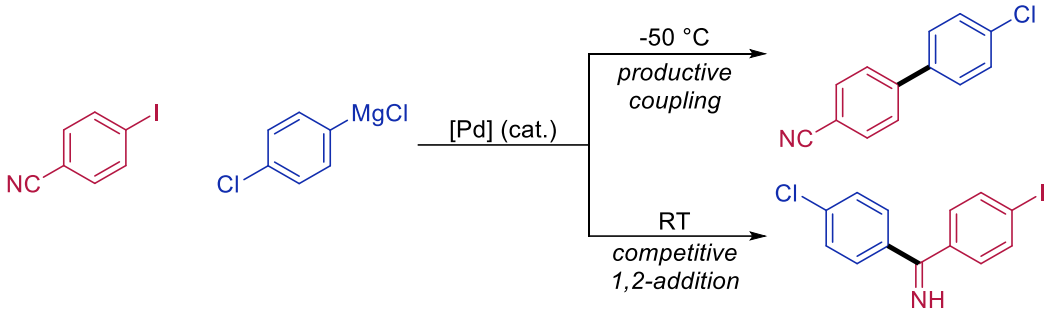

Scheme 7 – Chemoselective Kumada-Corriu Coupling at Cryogenic Temperatures

Alternatively, a balance can be struck between reactivity and chemoselectivity of nucleophilic coupling partners. Organometallic reagents of intermediate nucleophilicity can enable C(sp^3) transmetallation without significant sacrifices to functional group tolerance. For example, the use of alkyl zinc reagents in Negishi coupling can enable C(sp^2)–C(sp^3) bond formation while still having good chemoselectivity in the presence of electrophilic functional groups. This is especially true with modern catalyst design and mild reaction temperatures, which Buchwald demonstrated to enable the tolerance of electrophilic aldehydes in the Negishi coupling of secondary alkyl zincs (**Scheme 8**).[22]

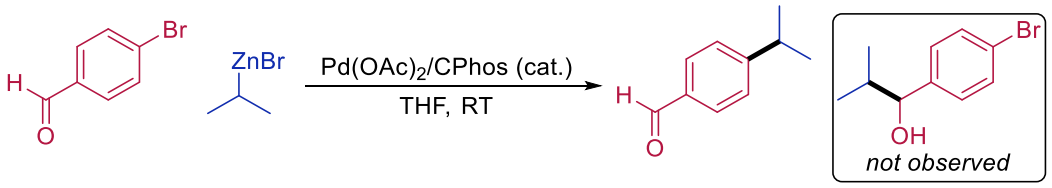

Scheme 8 – Chemoselective Negishi Coupling of C(sp^3) Nucleophiles

[22] Han, C.; Buchwald, S. L. *J. Am. Chem. Soc.* **2009**, *131*, 7532–7533.

Beyond poor transmetallation, another common obstacle in the cross-coupling of C(sp^3) nucleophiles is competitive β-hydride elimination.[23] In competition with reductive elimination, a series of elimination steps can lead to an isomeric mixture of cross-coupled product (**Scheme 9**). After oxidative addition and transmetallation, alkyl palladium intermediates can undergo β-hydride elimination to form an alkene. If the resultant palladium hydride re-inserts into the π-bond of the olefin in the opposite orientation, formal isomerization of the post-transmetallation intermediate is observed. Consequently, undesired isomers of the cross-coupled product can form upon subsequent reductive elimination. This isomerization of bulky alkyl palladiums to a less-hindered species is sometimes referred to as "chain walking".[24]

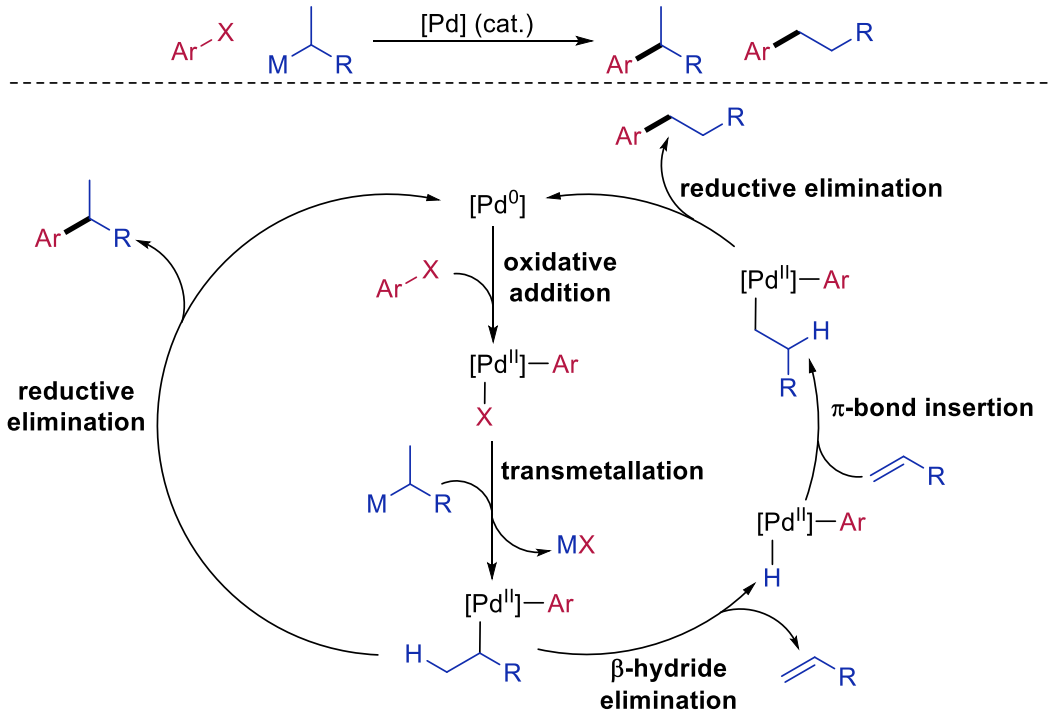

Scheme 9 – Competitive Alkyl Metallic Isomerization in Cross-Coupling of C(sp^3) Nucleophiles

[23] Campeau, L.-C.; Hazari, N. *Organometallics* **2019**, *38*, 3–35.
[24] Sommer, H.; Juliá-Hernández, F.; Martin, R.; Marek, I. *ACS Cent. Sci.* **2018**, *4*, 153–165.

Although innovative ligand design has been demonstrated to help prevent this pathway by favoring reductive elimination over β-hydride elimination,[25] the coupling of C(sp^3)-hybridized nucleophiles remains a common obstacle in modern cross-coupling. Consequently, alternative methods of coupling C(sp^3) nucleophilic coupling partners are continuously being investigated.

1.1.2: C(sp^3)–H Activation of Pronucleophiles in Cross-Coupling

Over the past 20 years, a major focus has been put on the catalytic C–H functionalization of sp^3-hybridized carbon atoms for use in cross-coupling.[26, 27] Although still limited, this chemistry can replace the need for stoichiometric C(sp^3) transmetallating agents; by activating a pro-nucleophilic coupling partner through a different mechanism, the common limitations of C(sp^3) organometallic compounds can often be avoided. A ubiquitous mechanistic step of this chemistry involves C–H functionalization facilitated by the formation of a carbon-palladium bond. This usually proceeds through one of two general mechanisms: deprotonation, oand single-electron r hydrogen atom transfer.

Frequently after oxidative addition, a weakly acidic C(sp^3)–H bond on the pronucleophile can be deprotonated, forming a new C–Pd bond (**Scheme 10**).[28] This deprotonation has been shown to be facilitated by either a basic X-type ligand on the Pd(II) species or an auxiliary stoichiometric base. This mechanism can enable the activation of C–H bonds whose corresponding carbanion would be too unstable for stoichiometric deprotonation (*i.e.* substrates

[25] Lu, X. *Top Catal.* **2005**, *35,* 73–86.
[26] Qiu, G.; Wu, J. *Org. Chem. Front.* **2015**, *2*, 169–178.
[27] Bellina, F.; Rossi, P. *Chem. Rev.* **2010**, *110*, 1082–1146.
[28] Baudoin, O. *Chem. Soc. Rev.* **2011**, *40*, 4902-4911.

that are not sufficiently acidic). Upon subsequent reductive elimination, the cross-coupled product is formed, thus functionalizing the C(sp^3)–H bond. While this chemistry can enable the formation of C(sp^3)–C(sp^2) bonds in addition to having improved atom economy relative to the use of stoichiometric organometallic reagents, it is not without its challenges.

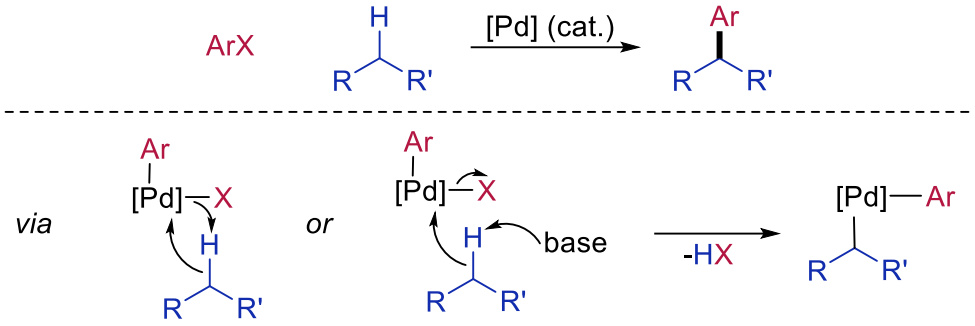

Scheme 10 – General Mechanism of Palladium-Mediated C(sp^3)–H Activation by Deprotonation

Organic compounds are usually rife with a variety of different C–H bonds, and thus their activation can suffer from poor chemo- and regio- selectivity. Due to insufficient distinction, this chemistry can theoretically lead to many different modes of C–H activation. However, pro-nucleophilic coupling partners can be biased to enable selective C–H activation, generally by forcing the catalyst to be in close proximity to a particular C–H bond.

For example, selective intramolecular C(sp^3)–H arylation in cross-coupling was reported by Baudoin (**Scheme 11**).[29] By having the electrophilic- and pro-nucleophilic fragments on the same substrate, a particular C–H bond can be selectively activated due to the close proximity to the Pd(II) after oxidative addition. Unfortunately, intramolecular cross-coupling vastly limits the types of products that can be made to cyclic scaffolds. Furthermore, although intramolecular

[29] Baudoin, O.; Herrbach, A.; Guéritte, F. *Angew. Chem. Int. Ed.* **2003**, *42*, 5736-5740.

C–H activation generally has a lower energy barrier than the intermolecular variant, this chemistry also relies on principles of the Thorpe-Ingold effect. By having steric bulk in the backbone of the alkyl chain, the groups bearing the [Pd]–X and C(sp^3)–H bonds are pushed closer together, increasing the rate of cyclization.[30] Consequently, these extra required modes of activation significantly limit the substrate scope of this chemistry.

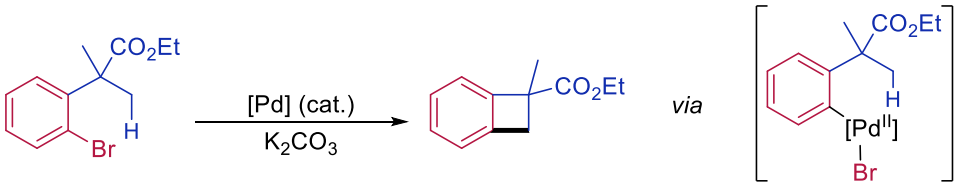

Scheme 11 – Intramolecular Palladium-Mediated C(sp^3)–H Activation in Cross-Coupling

As an example of the intermolecular variant, Daugulis reported the use of a quinoline directing group tethered through an amide linker (**Scheme 12**).[31] In contrast to the general mechanism of C–H activation previously discussed, this chemistry is instead proposed to involve a Pd(II)/Pd(IV) catalytic cycle. Prior to oxidative addition, coordination of the quinoline and the deprotonated amide to Pd(II) brings the catalyst into close proximity to the desired C–H bond of the pro-nucleophile. Oxidative addition into the aryl iodide and C–H activation via deprotonation forms the key C–Pd(IV) bond; however, the order of these two steps is debated. While this representative example extends C(sp^3)–H activation to intermolecular cross-coupling, its synthetic utility is arguably quite limited due to the required directing group. Although the cleverly-designed amide linker can be readily cleaved through hydrolysis, installation and removal

[30] Beesley, R. M.; Ingold, C. K.; Thorpe, J. F. *J. Chem. Soc., Trans.* **1915**, *107*, 1080–1106.
[31] Zaitsev, V. G.; Shabashov, D.; Daugulis, O. *J. Am. Chem. Soc.* **2005**, *127*, 13154–13155.

of the directing group necessitates an additional two synthetic steps to enable the key C(sp^3)–H arylation. Therefore, the inefficiencies associated with multi-step synthesis are significant obstacles for the implementation of this chemistry in complex molecule synthesis.

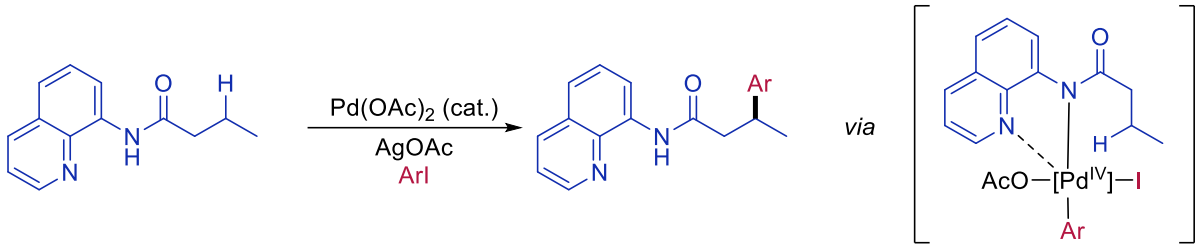

Scheme 12 – Directing Group-Assisted Palladium-Mediated C(sp^3)–H Activation in Cross-Coupling

Lastly, a particularly interesting approach to selectively form a C(sp^3)–Pd bond via deprotonation was reported by Walsh (**Scheme 13**).[32] In contrast to the previous examples, this report outlines the intermolecular C(sp^3)–H arylation of toluene derivatives in the absence of a traditional directing group. The authors propose K(*N*-XantPhos)Pd to be the active catalyst, which forms from the deprotonation of the ligand by KHMDS. By coordination of the toluene derivative to the resultant K^+, the catalyst is brought into close proximity to the acidified benzylic position. Upon deprotonation of the benzylic position and subsequent reductive elimination, a diarylmethane product is formed. Overall, the complex transition state involving the substrate, palladium, ligand, and base, enables the deprotonation of toluene that would otherwise be infeasible (pK_a of toluene and KHMDS are 43 in DMSO and 26 in THF, respectively).

[32] Sha, S.-C.; Tcyrulnikov, S.; Li, M.; Hu, B.; Fu, Y.; Kozlowski, M. C.; Walsh, P. J. *J. Am. Chem. Soc*. **2018**, *140*, 12415–12423.

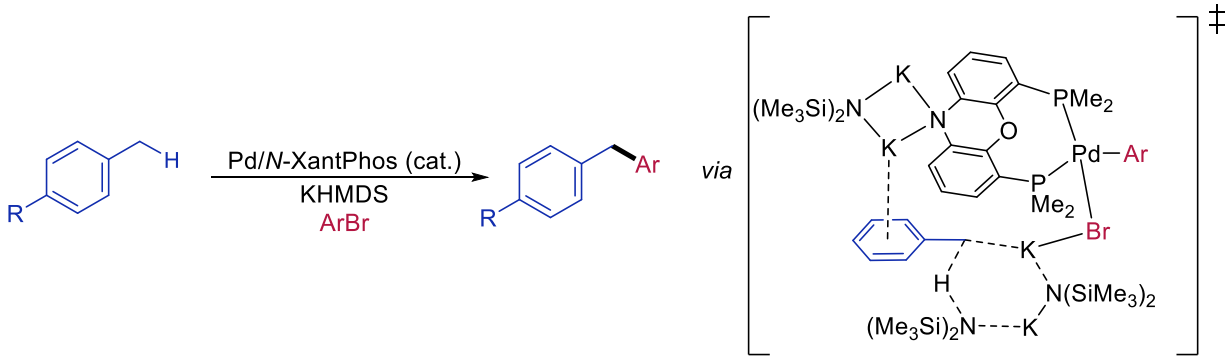

Scheme 13 – Palladium-Mediated C(sp^3)–H Activation in Cross-Coupling using Solvent Quantities

In spite of the apparent advantages of intermolecular C(sp^3)–H activation in the absence of a directing group, a caveat of Walsh's chemistry is that it relies chiefly on solvent quantities of the pro-nucleophilic coupling partner. Due to competitive coordination by aromatic- or ethereal solvents, stoichiometric quantities of toluene derivative cannot be selectively activated. The pro-nucleophilic coupling partner is therefore limited to liquid substrates capable of acting as solvents. Beyond melting point limitations, the use of a reagent in large excess can be very expensive, and may therefore preclude this chemistry from arylating complex toluene derivatives. As such, the scope of nucleophilic coupling partners described by Walsh is largely limited to simple, liquid, inexpensive substrates such as toluene and xylene.

Beyond deprotonations, C(sp^3)–H activation in cross-coupling can also take advantage of radical chemistry.[33] After hydrogen atom transfer (HAT), a transition metal catalyst can trap the resultant carbon-centered radical and incorporate it into its catalytic cycle. While radicals can be generated in a variety of ways, a particularly interesting photoredox approach was reported by

[33] Zhang, C.; Li, Z.-L.; Gu, Q.-S.; Liu, X.-Y. *Nat Commun.* **2021**, *12*, 475–483.

MacMillan (**Scheme 14**).[34] In the presence of a quinuclidine additive, photoexcited Ir(III) can catalyze the HAT of *N*-Boc pyrrolidine to form an sp^3-hybridized carbon-centered radical. After oxidative addition into an aryl bromide, the resultant Ni(II) can trap this radical to achieve arylation. Unfortunately, the principles on which this chemistry relies for selective C(sp^3)–H activation also severely limit the scope. The selective HAT of *N*-Boc pyrrolidine is enabled by the relative stability of the resultant carbon-centered radical. Formally, the *N*-Boc moiety thus acts as an activating group to facilitate the reaction. The scope of this chemistry is therefore limited to biased substrates that can stabilize radical intermediates.

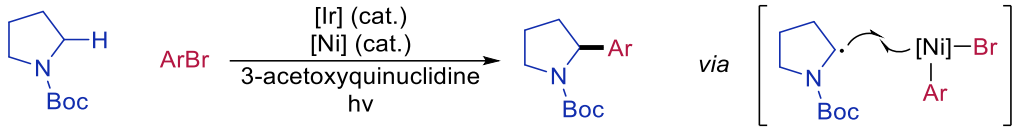

Scheme 14 – Nickel/Photoredox Dual Catalysis for Radical C(sp^3)–H Activation in Cross-Coupling

While current approaches to C(sp^3)–H activation in cross-coupling have their respective benefits, they all have limitations. Intramolecular cyclizations, directing groups, solvent quantities of substrate, and required activating groups, all limit the synthetic utility of established approaches. However, a simpler mechanism of C(sp^3)–H activation has been largely overlooked in the context of cross-coupling – stoichiometric deprotonation.

1.1.3: Classical C(sp^3)–H Activation via Stoichiometric Deprotonation

Stoichiometric metalation and electrophilic quench is one of the most fundamental reactions of organic chemistry. Frequently with a non-nucleophilic base, acidic C(sp^3)–H bonds

[34] Shaw, M. H.; Shurtleff, V. W.; Terrett, J. A.; Cuthbertson, J. D.; MacMillan, D. W. C. *Science* **2016**, *352*, 1304–1308.

can be deprotonated, forming a nucleophilic carbanion/organometallic intermediate. Upon the introduction of an appropriate electrophile, a new C–C bond can be formed, formally functionalizing a C(sp^3)–H bond. This technique is most commonly applied to activated substrates whose resultant anion is significantly stabilized through resonance and/or induction; for example, direct α-functionalization of ketones through a stoichiometric enolate intermediate, as exemplified in the classical aldol reaction (**Scheme 15**).[35] However, using stronger bases, much less activated C(sp^3)–H bonds can be deprotonated and functionalized.

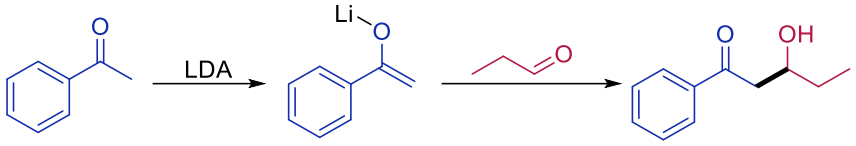

Scheme 15 – Simple Deprotonation and Electrophilic Quench of Ketones

For decades, commercial organolithium compounds such as *n*-BuLi have been used in the preparation of organometallic superbases.[36] Unintuitively, in the context of bases, "super" does not refer to the reactivity of the species. Instead, Caubère's defines a superbase as "…a basic reagent [that] is created by combining the characteristics of several different bases".[37] Thermodynamically, butyl lithium should be able to deprotonate almost any substrate (pK_a ~ 51 in H_2O). However, organolithiums tend to aggregate, which contributes to the high energy of activation that makes many deprotonations kinetically infeasible.[38] Stoichiometric additives have been shown to activate organolithiums to facilitate the deprotonation of very weakly acidic C–H

[35] Park, H. S.; Lee, I. S.; Kwon, D. W.; Kim, Y. H. *Chem. Commun.* **1998**, *24*, 2745–2746.
[36] Clayden, J. Organolithiums: Selectivity for Synthesis, 1st ed.; Tetrahedron Organic Chemistry; Pergamon, 2002; Vol. 23
[37] Caubere, P. *Chem. Rev.* **1993**, *93*, 2317–2334.
[38] Reich, H. J. *Chem. Rev.* **2013**, *113*, 7130–7178.

bonds. There are two main classes of organometallic superbases, which differ by the type of additive used.

One class of superbase involves the use of multidentate amine additives, hereby referred to as "coordinating-amine" superbases. *N*,*N*,*N*',*N*'-tetramethylethylenediamine (TMEDA) and similar additives have been shown to coordinate to lithium, decreasing the aggregation number of the organolithium (**Scheme 16a**).[39] By forming a smaller aggregate of lower steric bulk, difficult deprotonations are made possible due to the lower energy of activation.[40] Furthermore, this amine-coordination weakens and elongates the C–Li bond, increasing the basicity of the carbanion.[41] When C–H bonds are deprotonated by coordinating-amine superbases, they form the corresponding organolithium species, often with the amine still coordinated to the lithium.[42]

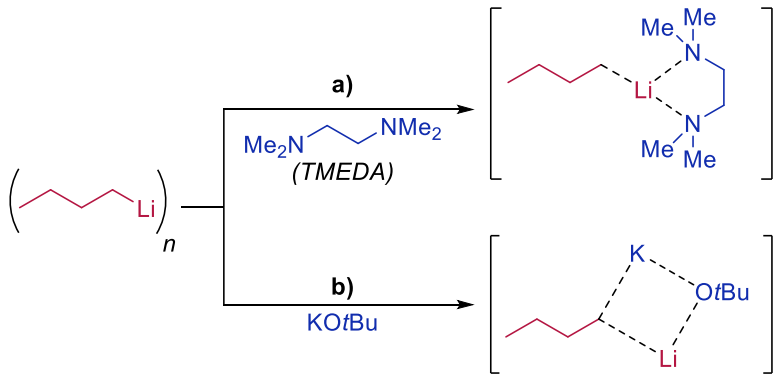

Scheme 16 – Simplified Structures of Active Organometallic Superbase Complexes

[39] Strohmann, C.; Gessner, V. H. *J. Am. Chem. Soc.* **2008**, *130*, 11719–11725.
[40] Nichols, M. A.; Williard, P. G. *J. Am. Chem. Soc.* **1993**, *115*, 1568–1572.
[41] Chadwick, S. T.; Ramirez, A.; Gupta, L.; Collum, D. B. *J. Am. Chem. Soc.* **2007**, *129*, 2259–2268.
[42] Eisch, J. J.; Yu, K.; Rheingold, A. L. *Eur. J. Org. Chem.* **2012**, *2012*, 3165–3171.

The second main class of superbase is Schlosser's base (also known as Lochmann-Schlosser bases or LiCKOR bases), which is comprised of a mixture of alkyl lithium and potassium alkoxide.[43] More specially, Schlosser's base is generally synonymous with BuLi and KO*t*Bu, which have been demonstrated to consist of a butyl anion coordinated to both lithium and potassium cations, which are chelated through a *tert*-butoxide anion (**Scheme 16b**).[44] In addition to the altered aggregation pattern, the increased reactivity of the resultant "ate" complex[45] stems from this species having hybrid Li/K–C bond polarity. The presence of electropositive K^+ puts more electron density on the butyl anion, activating it to facilitate difficult deprotonations. In general, this superbase is significantly more reactive than coordinating-amine superbases. For example, Schlosser's base (and the "ate" complexes that it forms from the deprotonation of substrates) is known to readily deprotonate and decompose solvents such as THF (**Scheme 17**).[46]

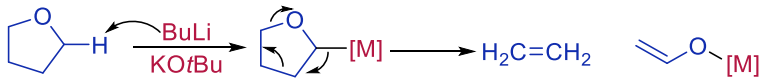

Scheme 17 – Deprotonation and Decomposition of THF with Schlosser's Base

Although coordinating-amine superbases and Schlosser's base are by far the most common, other superbases also exist. Lithium di(*iso*propyl)amide (LDA) and similar bases can also be used in superbase chemistry if the substrate is sufficiently acidic. While unintuitive since LDA is less basic than its BuLi precursor, it is considered a superbase in accordance with Caubère's

[43] Schlosser, M. *Pure & Appl. Chem.* **1988**, *60*, 1627–1634.
[44] Benrath, P.; Kaiser, M.; Limbach, T.; Mondeshki, M.; Klett, J. *Angew. Chem. Int. Ed.* **2016**, *55*, 10886–10889.
[45] Wittig, G. *Angew. Chem.* **1958**, *70,* 65–71.
[46] Giner, J. L.; Margot, C.; Djerassi, C. *J. Org. Chem*. **1989**, *54*, 2117–2125.

definition; LDA combines the strong base properties of BuLi with the non-nucleophilic properties of *i*Pr$_2$NH to form a non-nucleophilic strong base. Consequently, this section will include discussions of LDA in the context of superbases.

There exists decades of literature investigating the use of superbases in stoichiometric C(sp^3)–H metalation reactions. A wide array of functional groups can activate C(sp^3)–H bonds for deprotonation by stabilizing the resultant carbanion. Arguably there are two main mechanisms through which functional groups can be stabilizing: resonance and induction. Substrates bearing unsaturation in the form of π-bonds can stabilize conjugated carbanions through delocalization of the negative charge (**Scheme 18**). For example, among the most commonly-deprotonated by superbases are benzylic positions. Benzyl lithiums have been prepared by the deprotonation of toluene derivatives using *n*-BuLi/TMEDA (**Scheme 18ai**).[47] In most cases, solvent quantities of substrate are required to enable short reaction times, thus limiting the scope to simple, liquid compounds such as toluene and xylene. In contrast, *n*-BuLi/KO*t*Bu, being much more aggressive than *n*-BuLi/TMEDA, can deprotonate non-solvent quantities of substrate to form the corresponding benzyl "ate" complex (**Scheme 18aii**).[48]

[47] Klein, J.; Medlik, A.; Meyer, A. Y. *Tetrahedron* **1976**, *32*, 51–56.
[48] Faigl, F.; Schlosser, M. A. *Tetrahedron Lett.* **1991**, *32*, 3369–3370.

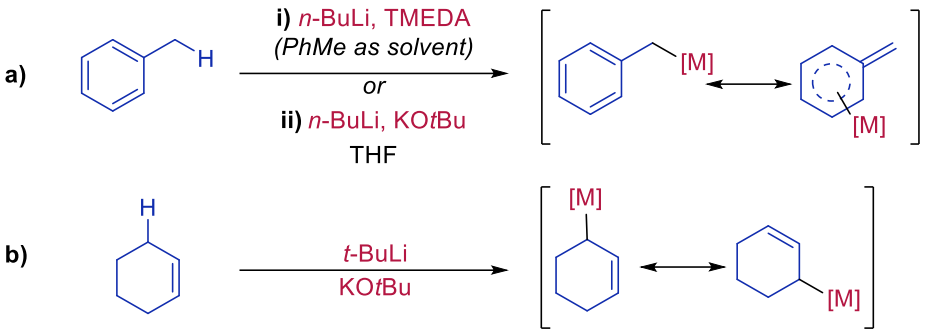

Scheme 18 – Deprotonations of Resonance-Stabilized Substrates by Superbases

In the same vein, C–H bonds α to olefins have also been deprotonated using superbases to form the resultant allylmetal species (**Scheme 18b**).[49] In contrast to benzylic positions, fewer resonance structures and lack of aromaticity makes these species significantly more difficult to metalate. As such, the use of the very aggressive *t*-BuLi variant of Schlosser's base is often required. Moreover, olefins often have multiple sites of acidity, and the resultant allyl metallic species often have multiple sites of nucleophilicity. To improve selectivity, symmetrical olefins such as cyclohexene can be used such that upon electrophilic quench, only one regioisomer of the product can form.

In contrast to resonance, proximity to an electronegative heteroatom can stabilize the negative charge of metalated species through induction (**Scheme 19**). For example, thioanisole can be deprotonated α to sulfur using an *n*-BuLi/DABCO superbase (**Scheme 19a**).[50] In this case, DABCO is used as the stoichiometric amine additive to activate the *n*-BuLi for the deprotonation of thioanisole's methyl group. Phosphorus atoms can also activate substrates for stoichiometric

[49] Schlosser, M. *Mod. Synth. Methods* **1992**, *6*, 227–271.
[50] Epiotis, N. D.; Yates, R. L.; Bernardi, F.; Wolfe, S. *J. Am. Chem. Soc.* **1976**, *98*, 5435–5439.

metalation, such as the deprotonation of diphenylmethylphosphine using *n*-BuLi/TMEDA (**Scheme 19b**).[51] This chemistry has been applied to the derivatization of phosphine ligands, enabling the discovery of new reactivity of transition metal catalysts.[52] As a final example, deprotonation α to oxygen has been established, such as methyl *tert*-butyl ether (MTBE), as reported by Corey (**Scheme 19c**).[53] Due to the difficult nature of this deprotonation, the more aggressive *s*-BuLi variant of Schlosser's base is required. Consequently, this chemistry relies on solvent quantities of substrate to avoid competitive deprotonation of ethereal solvents that are generally used with Schlosser's base. Although nearby heteroatoms can stabilize organolithiums through induction, they can also a destabilizing effect. Alkyl anions α to certain heteroatoms (Y) also have an unfavourable antibonding interaction with the R–Y σ* orbital. Consequently, deprotonation of simple amines α to nitrogen is much more challenging relative to other heteroatoms.[54]

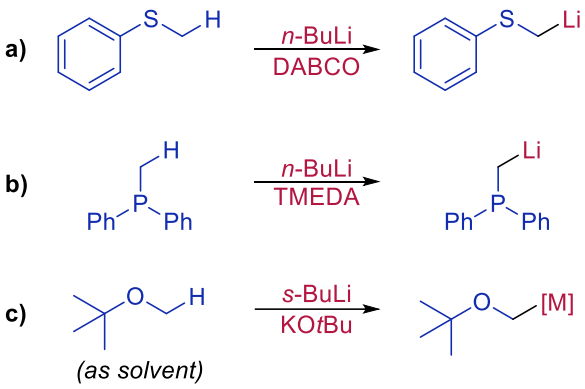

Scheme 19 – Deprotonations of Induction-Stabilized Substrates by Superbases

[51] J. A. Van Doorn, N. Meijboom. *Phosphorus Sulfur Silicon Relat. Elem.* **1989**, *42*, 211–222.
[52] Wei, W.; Yu, B.; Alam, F.; Huang, Y.; Cheng, S.; Jiang, T. *Transit. Met. Chem.* **2019**, *44*, 125–133.
[53] Corey, E. J.; Eckrich, T. M. *Tetrahedron Lett.* **1983**, *24*, 3165–3168.
[54] Ahlbrecht, H.; Dollinger, H. *Tetrahedron Lett.* **1984**, *25*, 1353–1356.

The aforementioned stabilization mechanisms act as a thermodynamic driving force for deprotonations by enabling the metalated intermediate to be relatively low in energy. In the context of a kinetic driving force, directing groups can be used to increase the rate of metalation. As previously mentioned, the high kinetic barrier is generally what prevents BuLi from deprotonating weakly acidic C–H bonds in the absence of stoichiometric additive. Consequently, the presence of directing groups can sometimes enable BuLi to facilitate these metalations in the absence of diamine and potassium alkoxide. Furthermore, directing groups have also been used to improve chemo- and regio- selectivity (**Scheme 20**). In the case of substrates bearing multiple weakly acidic C–H bonds, aggressive bases often don't metalate selectively. However, by using a Lewis basic directing group that can coordinate to the organometallic base, a particular C–H bond can be selectively deprotonated in what's known as lateral metalation.

For example, mesitylene derivatives often have multiple benzylic positions that cannot be differentiated. However, in the presence of a methylenedimethylamino directing group, *n*-BuLi can selectively deprotonate the ortho benzylic position (**Scheme 20a**).[55] Similarly, acyl directing groups can accomplish the same type of lateral metalation (**Scheme 20b**).[56] However, because of the acidity of ketones in the α position, two equivalents of base are required relative to the substrate.

[55] Jones, F. N.; Zinn, M. F.; Hauser, C. R. *J. Org. Chem.* **1963**, *28*, 663–665.
[56] Klein, J.; Medlik-Balan, A. *J. Org. Chem.* **1976**, *41*, 3307–3312.

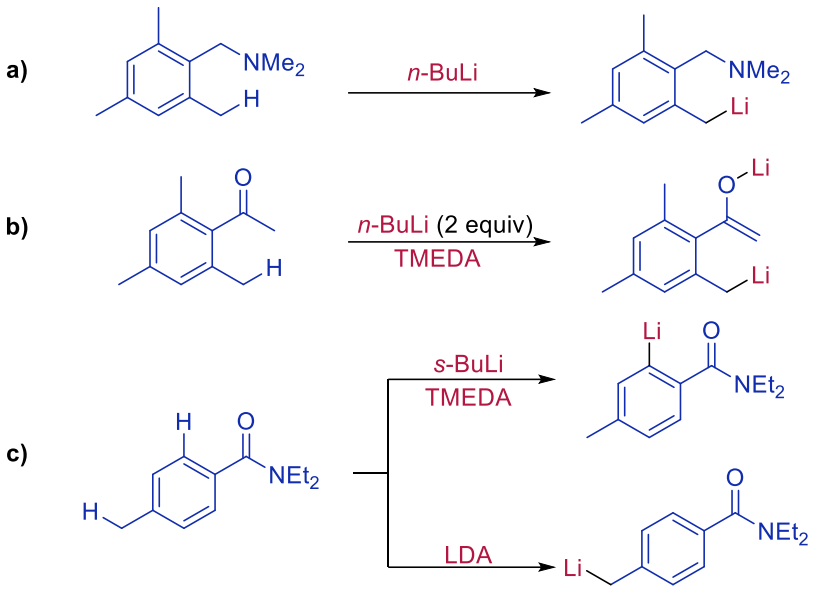

Scheme 20 – Selective Superbase Deprotonations Using Directing Groups

Arguably the most versatile directing groups are those which can influence the selective deprotonation of different C–H bonds depending on the nature of the superbase that is used. This can be enabled using bulky directing groups and bases of varying steric bulk. For example, using an *N*,*N*-diethyl amide directing group in the para position, toluene can be selectively metalated at two unique sites depending on which superbase is used (**Scheme 20c**).[57] With *s*-BuLi/TMEDA, the amide directs to the ortho position. In contrast, LDA, being much bulkier, selectively deprotonates the para benzylic position, far from the bulky directing group.

Overall, superbases have therefore been used in the deprotonation of a wide array of substrate classes bearing C–H bonds with varying degrees of activation. The resultant metalated species tend to be very nucleophilic, and can be quenched with a variety of electrophiles (E^+) to provide a diverse range of possible products (**Scheme 21**). For example, by quenching with D_2O,

[57] Beak, P.; Brown, R. A. *J. Org. Chem*. **1977**, *42*, 1823–1824.

the corresponding deuterated analogue can be formed (**Scheme 21a**).[58] The presence of deuterium on a substrate has been shown to influence the selectivity of subsequent deprotonations due to the kinetic isotope effect.[59] Arguably a more valuable transformations can be accomplished using substitution reactions. For example, Br_2 or I_2 quenches can be used to install versatile halogens, enabling subsequent derivatization (**Scheme 21b**).[60] Similarly, electrophilic quench with the appropriate alkyl halide is also quite common in the preparation of alkylated products (**Scheme 21c**). Also, quenching with electrophilic silicon sources can form the corresponding silylated product (**Scheme 21d**).[61] Metalated species are also commonly used as nucleophiles in 1,2-addition reactions with ketones and other carbonyl compounds (**Scheme 21e**).[62] This can be used in the preparation of tertiary alcohol products, though usually as a mixture of stereoisomers. Lastly, quenching with CO_2, most commonly in the form of dry ice, can be used in the preparation of carboxylic acids (**Scheme 21f**).[63]

[58] McClure, M. S.; Roschanger, F.; Hodson, S. J.; Millar, A.; Osterhout, M. A. *Synthesis.* **2001**, *11*, 1681–1685.
[59] Ahmed, A.; Clayden, J.; Rowley, M. *Tetrahedron Lett*. **1998**, *39*, 6103–6106.
[60] Gilman, H.; Morton, J. W. *Org. Reac.* **1954**, *8*, 258.
[61] Zhang, P.; Gawley, R. E. *J. Org. Chem.* **1993**, *58*, 3223–3224.
[62] Kress, T. J. *J. Org. Chem.* **1979**, *44*, 2081–2082.
[63] Lombardino, J. G. *J. Org. Chem*. **1971**, *36*, 1843–1845.

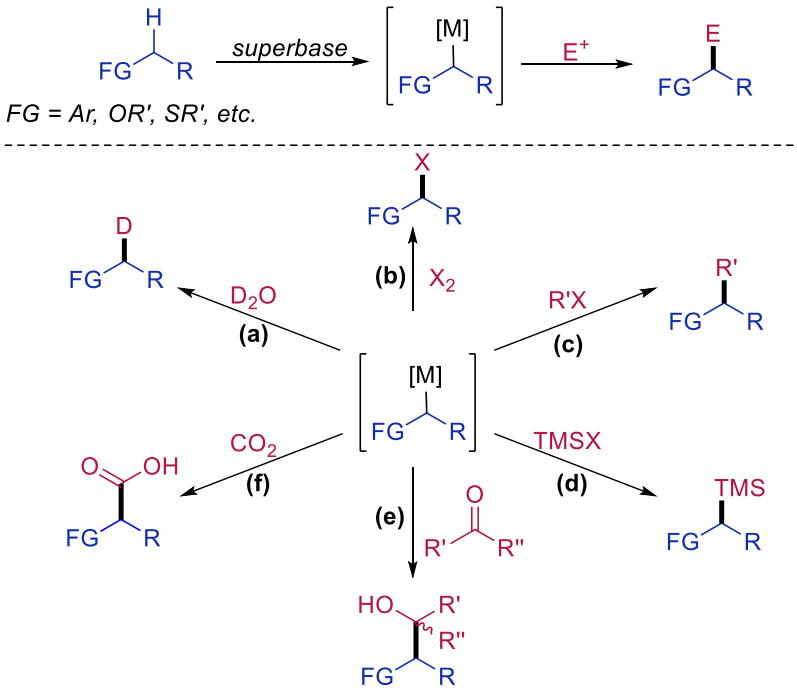

Scheme 21 – Select Precedented Superbase Quenches

While a wide range of quenches have been reported in classical superbase chemistry, the use of these metalated species in cross-coupling reactions has been seldom reported.

1.1.4: Palladium-Catalyzed Cross-Coupling of Organolithiums

The previous section discussed the generation of highly nucleophilic organometallic species, largely developed in the 1960s and 1970s. Over the past decade, there has been growing interest in the use of highly nucleophilic organolithiums (electronegativity of Li is 0.98) in palladium-catalyzed cross-coupling (**Scheme 22**).[64] Although originally discovered in 1979 by

---

[64] a) Vila, C.; Giannerini, M.; Hornillos, V.; Fañanás-Mastral, M.; Feringa, B. L. *Chem. Sci.* **2014**, *5*, 1361–1367.
b) Pinxterhuis, E. B.; Giannerini, M.; Hornillos, V.; Feringa, B. L. *Nat. Commun.* **2016**, *7*, 11698.
c) Hornillos, V.; Giannerini, M.; Vila, C.; Fañanás-Mastral, M.; Feringa, B. L. *Chem. Sci*. **2015**, *6*, 1394–1398.
d) Hornillos, V.; Giannerini, M.; Vila, C.; Fañanás-Mastral, M.; Feringa, B. L. *Org. Lett.* **2013**, *15*, 5114–5117.
e) Vila, C.; Hornillos, V.; Giannerini, M.; Fañanás-Mastral, M.; Feringa, B. L. *Chem. Eur. J.* **2014**, *20*, 13078–13083.
f) Scherpf, T.; Steinert, H.; Großjohann, A.; Dilchert, K.; Tappen, J.; Rodstein, I.; Gessner, V. H. *Angew. Chem Int. Ed.* **2020**, *132*, 20777–20784.

Murahashi,[65] modern catalyst design has recently been demonstrated to bypass some of the limitations outlined in the seminal report. A traditional catalytic cycle is generally accepted, in which a Pd(0) catalyst oxidatively insets into a C(sp^2)–X bond, followed by transmetallation of the organolithium onto the resultant Pd(II) species, then finally reductive elimination to form the key C–C bond and regenerate the active catalyst.

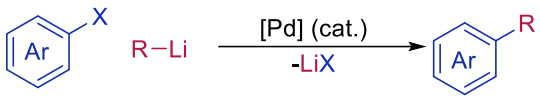

Scheme 22 – General Reaction Scheme of Palladium-Catalyzed Organolithium Coupling

One advantage of modern Murahashi coupling is the ability to couple C(sp^3) nucleophiles, which has been shown to overcome the common issues outlined in **Section 1.1.1**. Due to their significant nucleophilicity, poor transmetallation of organolithiums is seldom an issue. Furthermore, the modern resurgence in this field came from the Feringa group, who demonstrated that modern NHC and Buchwald ligands could drastically minimize competitive β-hydride elimination of alkyl palladium species.[66] Consequently, the use of bulky C(sp^3) nucleophiles that tend to be a challenge in other cross-couplings can readily be used in Murahashi coupling.

Unfortunately, the reactivity of organolithiums comes with the tradeoff of being very prone to side-reactions. In addition to frequently reacting with acidic- and electrophilic-functional groups, organolithiums are prone to lithium-halogen exchange (LHE) with

[65] Murahashi, S.; Yamamura, M.; Yanagisawa, K.; Mita, N.; Kondo, K. *J. Org. Chem.* **1979**, *44*, 2408–2417.
[66] Giannerini, M.; Fañanás-Mastral, M.; Feringa, B. L. *Nature Chem.* **2013**, *5*, 667–672.

organohalides.[67] Consequently, Murahashi coupling generally requires slow addition of the organolithium (**Scheme 23a**) to prevent dehalogenation and homocoupling of the electrophilic coupling partner (**Scheme 23b**). Starving the reaction mixture of nucleophile maintains a relatively high concentration of the oxidative addition adduct, forcing it to be the resting state of the catalytic cycle. As nucleophile is slowly added, the organolithium reacts preferentially with the Pd(II) species instead of directly with the aryl halide. By matching the rate of nucleophile addition to the rate of oxidative addition, productive cross-coupling is enabled. Though arguably logistically inconvenient, slow addition enables the chemoselective cross-coupling of an otherwise problematic nucleophile.

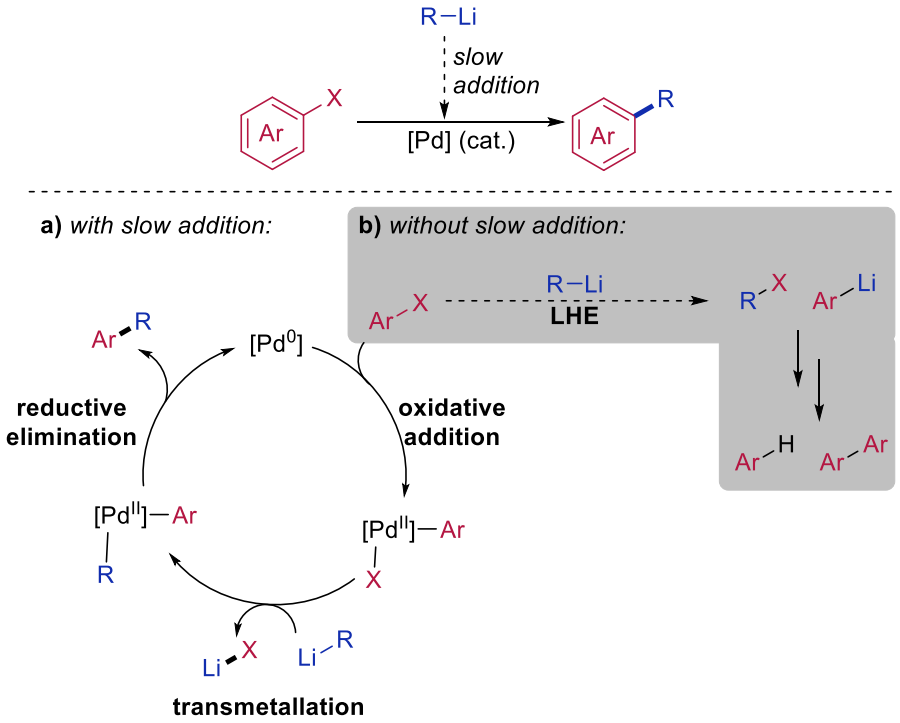

Scheme 23 – Improved Chemoselectivity of Murahashi Coupling via Organolithium Slow Addition

[67] Bailey, W. F.; Patricia, J. J. *J. Organomet. Chem.* **1988**, *352*, 1–46.

Although Murahashi coupling has its benefits, the established scope of sp^3-hybridized organolithiums is unfortunately quite limited. While simple, commercially-available alkyl lithiums (R–Li) such as R = Me, *n*-Bu, *s*-Bu, and CH_2TMS, have been coupled directly (**Scheme 24a**), complexity and diversity are severely lacking. Feringa also reported the coupling of non-commercial organolithium compounds prepared through either directed ortho metalation (DOM) (**Scheme 24b**) or lithium-halogen exchange (**Scheme 24c**), but these advancements have been thus far limited to sp^2-hybridized starting materials, such as furans and aryl halides, respectively.[68] Therefore, the cross-coupling of non-commercial sp^3-hybridized organolithiums remains a largely unexplored area of research in this field.

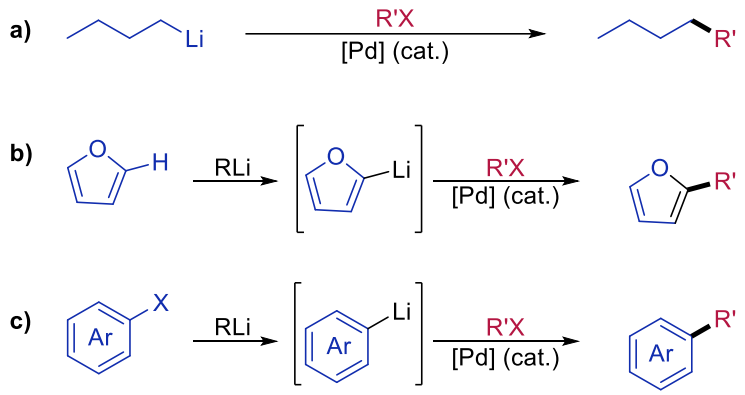

Scheme 24 – Literature Precedent for Direct Organolithium Cross-Coupling

Non-commercial sp^3-hybridized organolithiums can be generated in several ways, however, their use in cross-coupling has mostly yet to be reported. For example, *t*-BuLi has been shown to convert alkyl iodides to the corresponding alkyl lithium via lithium-halogen exchange

[68] Giannerini, M.; Hornillos, V.; Vila, C.; Fañanás-Mastral, M.; Feringa, B. L. *Angew. Chem. Int. Ed.* **2013**, *52*, 13329–13333.

(**Scheme 25a**).[69] The scope of this reaction is limited to sterically unencumbered species in order to avoid elimination and/or substitution of the alkyl halide. Alternatively, using lithium metal, organolithiums can be prepared analogously to Grignard reagents (**Scheme 25b**).[70] Because of the difference in valence between Li and Mg, two equivalents of Li(0) are required to fully convert the substrate. Although this chemistry is fairly robust, in that relatively complex functional groups such as olefins, acetals, silyl groups, and *tert*butyl esters are tolerated, it requires pre-functionalized starting materials. The scope is therefore limited to substrates bearing a C–X bond.

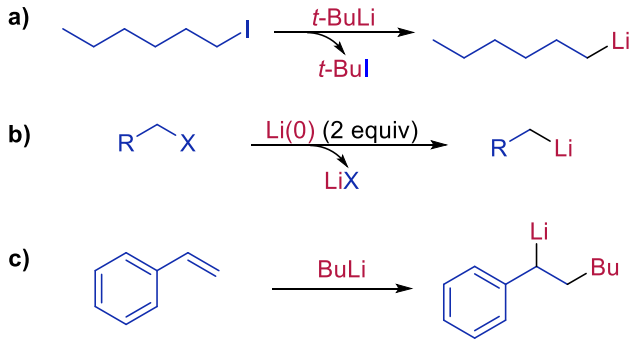

Scheme 25 – Preparation of Non-Commercial C(sp^3)-Hybridized Organolithiums

Lastly, olefins have been shown to react with reagents such as BuLi to form the corresponding carbolithiated product (**Scheme 25c**).[71] This method of organolithium generation is therefore limited to pre-functionalized starting materials bearing an olefin. Furthermore, because both the reagent and product of this reaction are organolithiums, this chemistry is prone to the formation of oligomers, in which the product continues to react with the olefin starting material. Another potential problem is the linear vs. branched selectivity caused by the two

[69] Bailey, W. F.; Patricia, J. J.; Nurmi, T. T.; Wang, W. *Tetrahedron Letters* **1986**, *27*, 1861–1864.
[70] Anker, R. M.; Cook, A. H. *J. Chem. Soc.* **1941**, 323–331.
[71] Alazet, S.; West, M. S.; Patel, P.; Rousseaux, S. A. L. *Angew. Chem. Int. Ed.* **2019**, *58*, 10300–10304.

competitive orientations of olefin insertion. Biased substrates such as styrene can influence the selectivity due to the relative stability of the organolithium being conjugated to the arene. Overall, these methods to prepare non-commercial sp^3-hybridized organolithiums are largely limited by the requirement of pre-functionalized starting materials, and therefore have limited scope.

Of course, as discussed in **Section 1.1.3**, superbases have been used in the generation of a variety of organolithiums. A notable advantage to this chemistry is the ability to prepare non-commercial C(sp^3) organolithiums without necessitating pre-functionalized starting materials such as organohalides and olefins. However, the generation of C(sp^3) nucleophilic coupling partners using superbases is remarkably under-investigated. Though some related mechanisms have been reported, they each possess substantial limitations that hamper their synthetic utility.

For example, using a chiral *s*-BuLi/(-)-sparteine superbase, Campos *et. al.* reported the enantioselective deprotonation and cross-coupling of *N*-Boc pyrrolidines (**Scheme 26a**).[72] To avoid epimerization of the deprotonated species, the authors coupled the corresponding organozinc after treatment with $ZnCl_2$. Although this chemistry generates enantio-enriched products, sparteine has become incredibly expensive and borderline unavailable since the 1960s.[73] Furthermore, the starting materials in this chemistry are significantly activated by the presence of the carbamate directing group. Therefore, to incorporate this reaction into a synthesis, reduced yield and atom economy would result from the installation and removal of the directing group.

---

[72] Campos, K. R.; Klapars, A.; Waldman, J. H.; Dormer, P. G.; Chen, C. *J. Am. Chem. Soc.* **2006**, *128*, 3538–3539.
[73] O'Brien, P. *Chem. Commun.* **2008**, *6*, 655–667.

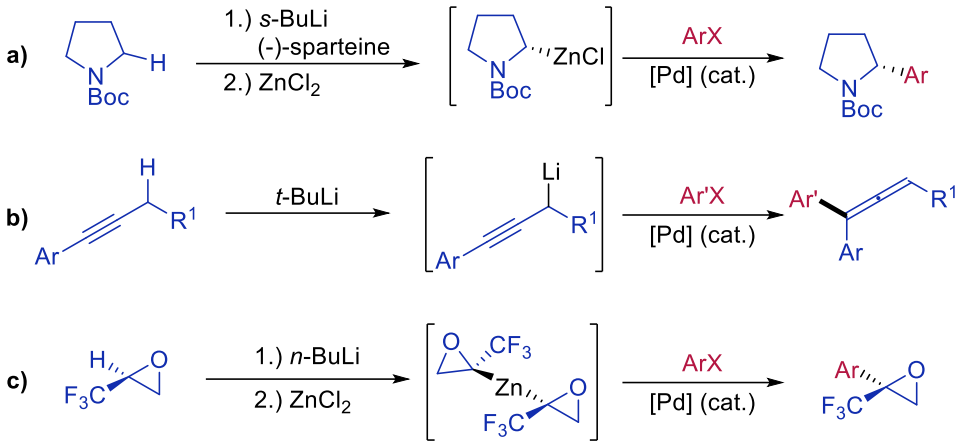

Scheme 26 – Precedent for Stoichiometric Deprotonation and Cross-Coupling of C(sp^3)–H Bonds

Also, Feringa reported the deprotonation and cross-coupling adjacent to alkynes (**Scheme 26b**).[74] Although a C(sp^3)–H bond is deprotonated and coupled, a C(sp^2)–C(sp^2) bond is formed, as they selectively observe the corresponding allene product. Therefore, this chemistry isn't exactly fitting with the previous discussion of C(sp^3)–H deprotonation and cross-coupling. Lastly, Buchwald reported the enantio-retentive metalation and cross-coupling of an enantio-pure trifluoromethyl-containing epoxide (**Scheme 26c**).[75] Analogous to the Campos report, this chemistry requires cross-coupling of the corresponding organozinc. The scope of this reaction is significantly limited, as only one substrate could be used as the pronucleophile. Furthermore, the ability to deprotonate the trifluoromethyl-containing epoxide with *n*-BuLi alone highlights the degree to which the substrate is activated. Overall, precedent for the deprotonation and cross-coupling of unactivated C(sp^3)–H bonds is very limited.

[74] Mateos-Gil, J.; Mondal, A.; Castiñeira Reis, M.; Feringa, B. L. *Angew. Chem. Int. Ed.* **2020**, *59*, 7823–7829.
[75] Zhang, H.; Buchwald, S. L. *J. Am. Chem. Soc,* **2017**, *139*, 11590-11594.

1.2: Project Goals

We hypothesized that there was untapped potential in the overlapping areas of organolithium coupling and superbase chemistry. By deprotonating very weakly acidic C(sp^3)–H bonds using organometallic superbases, non-commercial C(sp^3) organolithiums could be prepared *in situ* and used as cross-coupling nucleophiles (**Scheme 27**). Slowly adding the resultant organolithium to a mixture of palladium catalyst and aryl halide could enable the C(sp^3)–H bond functionalization of a variety of substrate classes. If this approach could be applied to the intermolecular cross-coupling of unactivated pronucleophiles, much of the limitations of established C(sp^3)–H activation strategies could be overcome.

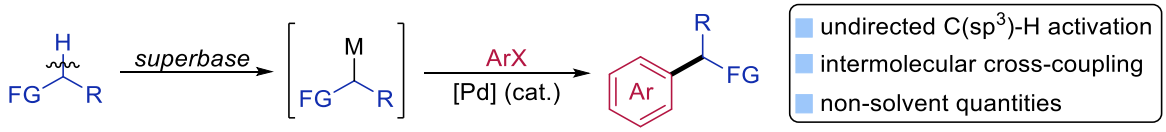

Scheme 27 – Goals for the Deprotonation and Cross-Coupling of C(sp^3)–H Bonds

The initial focus of this project was on the arylation of unactivated benzylic positions. This is formally the same transformation as reported by Walsh, which is severely limited by the required solvent quantities of toluene derivative.[76] Therefore, to improve upon this report, we emphasized the importance of the deprotonation and cross-coupling of toluene derivatives in non-solvent quantities. Furthermore, the cross-coupling of benzyl lithiums has never been reported to our knowledge; we were therefore interested in optimizing their use as cross-coupling nucleophiles and studying their functional group tolerance.

---

[76] Sha, S.-C.; Tcyrulnikov, S.; Li, M.; Hu, B.; Fu, Y.; Kozlowski, M. C.; Walsh, P. J. *J. Am. Chem. Soc.* **2018**, *140*, 12415–12423.

1.3: Results and Discussion

1.3.1: Preparation of Primary Benzyl Lithiums using Superbases

We first investigated the use of a coordinating-amine superbase in the deprotonation of toluene for its subsequent use in cross-coupling. As previously mentioned in **Section 1.1.3**, precedent using this class of superbase requires solvent quantities of toluene and is generally performed at cryogenic temperatures.[77] Although Schlosser's base can enable non-solvent quantities of substrate, we suspected the resultant "ate" complex would be too reactive to couple directly. Due to the relatively tame nature of organolithiums, we opted to optimize the deprotonation of stoichiometric quantities of toluene using *n*-BuLi/TMEDA.

We therefore required a solvent that could facilitate the deprotonation without directly reacting with the superbase. We expected dilution with a solvent would drastically reduce the rate of the deprotonation. To avoid impractically-long reaction times, we increased the temperature of the deprotonation to room temperature and quenched it after 1 hour. We deemed it important to have full conversion of *n*-BuLi to BnLi to avoid the formation of butylated arene side-products when applied to the subsequent cross-coupling (**Scheme 28**).

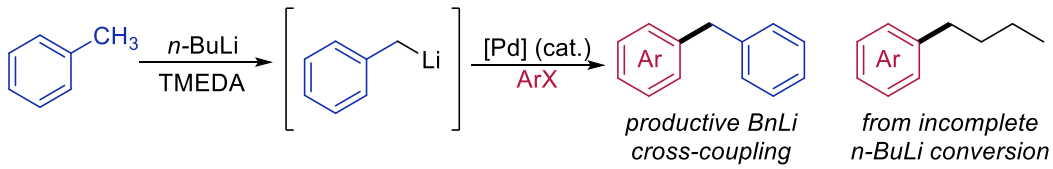

Scheme 28 – Incomplete BuLi Conversion in the Deprotonation and Coupling of Toluene

---

[77] a) Klein, J.; Medlik, A.; Meyer, A. Y. *Tetrahedron* **1976**, *32*, 51–56.
b) Fuchibe, K.; Jyono, H.; Fujiwara, M.; Kudo, T.; Yokota, M.; Ichikawa, J. *Chem. Eur. J.* **2011**, *17*, 12175– 12185.
c) Siu, P. W.; Serin, S. C.; Krummenacher, I.; Hey, T. W.; Gates, D. P. *Angew. Chem. Int. Ed.* **2013**, *52*, 6967–6970.

To monitor the progress of the deprotonation, we used a precedented 1,2-addition quench as previously discussed in **Section 1.1.3**. The 1,2-addition reactions of *n*-BuLi and BnLi with benzophenone form the corresponding lithium alkoxide products. Upon protonation with a Bronsted acid during workup, the resultant alcohols could be readily detected and differentiated by GC-MS. Although the 1,2-addition between benzyl lithium and benzophenone is generally not quantitative, with yields usually reported around 85%,[78] we prioritized confirming full *n*-BuLi conversion over knowing the exact yield of benzyl lithium formation. A slight excess of toluene (1.25 equiv) was used relative to *n*-BuLi/TMEDA to ensure there was enough substrate to be deprotonated. In contrast, using exactly 1:1 stoichiometry of toluene:superbase could result in small amounts of remaining *n*-BuLi due to experimental error. Using these conditions, a variety of solvents were screened, the results of which are summarized in **Table 1**.

[78] Eberhardt, G. G.; Butte, W. A. A *J. Org. Chem.* **1964**, *29*, 2928–2932.

Table 1 – Solvent Screen for Toluene Deprotonation by n-BuLi/TMEDA[a]

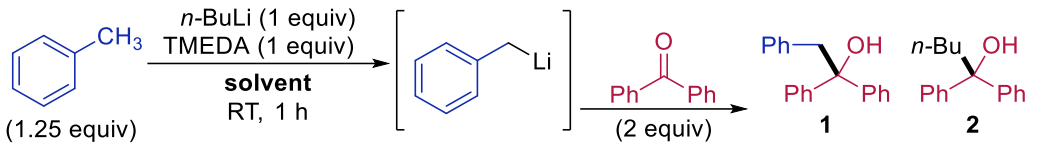

Entry	Solvent	Yield of **1** (%)	Yield of **2** (%)
1	Benzene	Trace	Trace
2	$PhCF_3$	0	Trace
3	Glyme	0	0
4	Diglyme	0	0
5	*n*-Bu_2O	Trace	Trace
6	CPME	Trace	Trace
7	MTBE	Trace	Trace
8	(*i*-Pr)$_2O$	Trace	4

[a]Reactions were run on a 0.1 mmol scale of superbase. Yields are reported by GC-MS using a 5-point calibration curve relative to 1,3,5-trimethoxybenzene as an internal standard. Trace yield indicates product was detected by GC-MS, but calculated yield was < 1%.

Unfortunately, the yields of both benzyl- and butyl- 1,2-addition adducts with benzophenone were very poor with all of the solvents screened (**Table 1**). Under the assumption that all *n*-BuLi added into the reaction should result in formation of alcohols **1** or **2**, this poor mass balance suggests consumption of *n*-BuLi via unproductive side-reactions. When using benzene (entry 1), only trace amounts of products **1** and **2** were observed by GC-MS. Instead, a significant side-product with an m/z value of 260 was identified, suggesting benzene was deprotonated and acted as the nucleophile in the 1,2-addition (**Scheme 29a**). Although benzene is less acidic than toluene (pK_a of 43 and 41 in H_2O, respectively), its presence in large excess likely made its deprotonation both kinetically- and thermodynamically- favourable. A similar result of suspected solvent reactivity was observed with benzotrifluoride (entry 2), having observed an m/z value of 328 (**Scheme 29b**).

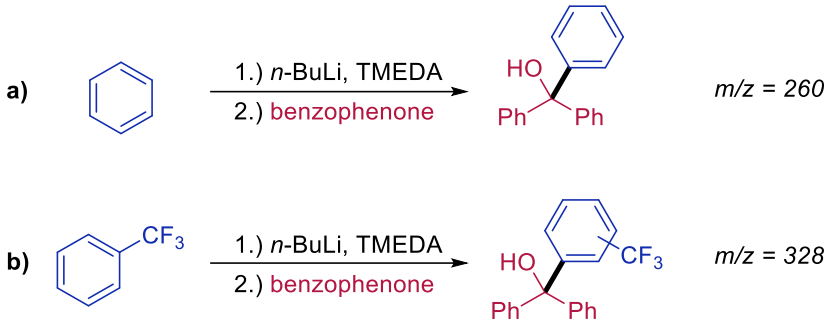

Scheme 29 – Observed Solvent Reactivity in the Deprotonation of Toluene by n-BuLi/TMEDA

Ethereal solvents including glyme, diglyme, dibutyl ether, cyclopentyl methyl ether (CPME), methyl *tert*-butyl ether (MTBE), and di(*iso*-propyl) ether (**Table 1**, entries 3-8) led to zero-to-trace yields of alcohol **1** and no suspected solvent reactivity was identified. This may be due to these ethereal solvents having undergone deprotonation and decomposition similar to THF (see **Scheme 17** in **Section 1.1.3**). Furthermore, trace formation of alcohol **2** was frequently observed, suggesting the reactions were not run long enough to provide full conversion of *n*-BuLi.

We suspected that biasing the reaction conditions to greatly increase the rate of deprotonation while minimizing solvent reactivity would be beneficial. We thus decided to do the deprotonation in only the solvent present in the *n*-BuLi solution (1.6 M in hexanes) without any further dilution. Indeed, these so-called "solvent-free" conditions drastically improved the mass balance of the reaction. In comparison to the solvent screen which resulted in a < 5% mass balance in all cases (**Table 1**), mass balance using no addition solvent was increased to 54% (**Table 2**, entry 1). By performing the deprotonation in an aliphatic hydrocarbon solvent that is inert to superbases,[79] observed solvent reactivity was avoided. Furthermore, the conversion from

[79] Clayden, J. Organolithiums: Selectivity for Synthesis, 1st ed.; Tetrahedron Organic Chemistry; Pergamon, 2002; Vol. 23

n-BuLi to BnLi was greatly improved, presumably from the elevated concentration having increased the rate of the reaction. With 50% yield of alcohol **1** and 4% of alcohol **2**, there was near full conversion of *n*-BuLi under these reaction conditions. Although complete conversion could likely be observed if the deprotonation was run longer, short reaction times were identified as a target goal of this project. Upon heating the "solvent-free" deprotonation to 60 °C (the approximate boiling point of the *n*-BuLi in hexanes), full conversion of *n*-BuLi was observed within 15 minutes, providing a 45% yield of alcohol **1** (**Table 2**, entry 2). These conditions were therefore suitable for the fast conversion of *n*-BuLi to BnLi using non-solvent quantities of toluene.

Table 2 – Optimization of "Solvent-free" Deprotonation of Toluene by n-BuLi/TMEDA[a]

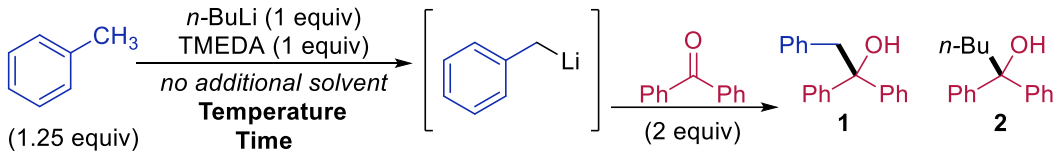

Entry	Temperature (°C)	Time (min)	Yield of **1** (%)	Yield of **2** (%)
1	RT	60	50	4
2	60	15	45	0

[a]Reactions were run on a 0.1 mmol scale of superbase. Yields are reported by GC-MS using a 5-point calibration curve relative to 1,3,5-trimethoxybenzene as an internal standard.

Unfortunately, these short deprotonation times had the apparent trade-off of moderate yield, with the most likely culprit being *n*-BuLi decomposition. At elevated temperatures, alkyl lithiums are known to undergo β-hydride elimination to form lithium hydride and an olefin (**Scheme 30a**).[80] Therefore, these harsh deprotonation conditions likely not only increased the rate of deprotonation, but also the rate of *n*-BuLi decomposition. In contrast, benzyl lithium

[80] T. Thomson, T. S. Stevens, *J. Chem. Soc.* **1933**, 555–557.

cannot decompose under this mechanism due to the lack of a β-hydride (**Scheme 30b**). Moreover, resonance stabilization of the BnLi was suspected to further stabilize the deprotonated species, further minimizing its decomposition.

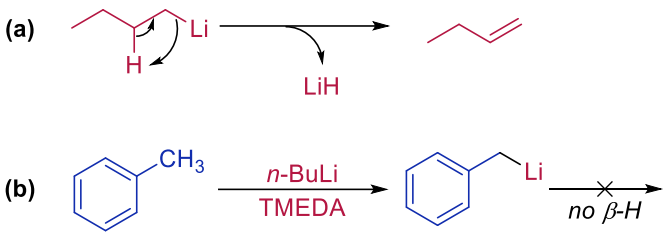

Scheme 30 – Relative Decomposition Pathways of n-BuLi and BnLi

Although having diminished the yield of the deprotonation, the partial decomposition of *n*-BuLi presumably also contributed to its conversion. By having some of the *n*-BuLi selectively decompose, the formation of alcohol **2** was entirely prevented under the harsh deprotonation conditions. To avoid competitive cross-coupling of remaining *n*-BuLi, we prioritized full *n*-BuLi conversion over yield of the deprotonation. With the optimized conditions providing full conversion of *n*-BuLi in the deprotonation of non-solvent quantities of toluene in short reaction times, we moved on to the direct cross-coupling of the resultant benzyl lithium.

1.3.2: Cross-Coupling of Superbase-Generated Primary Benzyl Lithiums

The literature precedent for palladium-catalyzed Murahashi coupling was consulted when designing the experiments for the cross-coupling of benzyl lithiums.[81] A summary of the variables

---

[81] [a] Giannerini, M.; Fañanás-Mastral, M.; Feringa, B. L. *Nature Chem.* **2013**, *5*, 667–672.
[b] Vila, C.; Giannerini, M.; Hornillos, V.; Fañanás-Mastral, M.; Feringa, B. L. *Chem. Sci.* **2014**, *5*, 1361–1367.
[c] Pinxterhuis, E. B.; Giannerini, M.; Hornillos, V.; Feringa, B. L. *Nat. Commun.* **2016**, *7*, 11698.
[d] Hornillos, V.; Giannerini, M.; Vila, C.; Fañanás-Mastral, M.; Feringa, B. L. *Chem. Sci*. **2015**, *6*, 1394–1398.
[e] Hornillos, V.; Giannerini, M.; Vila, C.; Fañanás-Mastral, M.; Feringa, B. L. *Org. Lett.* **2013**, *15*, 5114–5117.
[f] Vila, C.; Hornillos, V.; Giannerini, M.; Fañanás-Mastral, M.; Feringa, B. L. *Chem. Eur. J.* **2014**, *20*, 13078–13083.
[g] Giannerini, M.; Hornillos, V.; Vila, C.; Fañanás-Mastral, M.; Feringa, B. L. *Angew. Chem. Int. Ed.* **2013**, *52*, 13329–13333.

screened, including catalyst system, solvent, temperature, aryl halide, stoichiometry, and duration of nucleophile addition is indicated in **Scheme 31**. Feringa, who has published extensively on the subject of direct organolithium coupling, frequently uses a small selection of catalyst systems. Among the most common is Pd_2dba_3/XPhos, which has been shown to be suitable for the coupling of a variety of nucleophiles and electrophiles, including alkyl-, aryl-, and alkenyl- lithiums with aryl- chlorides and bromides. With its low cost and stability in air, Pd_2dba_3/XPhos was chosen to be the initial catalyst system used for the direct cross-coupling of benzyl lithiums.

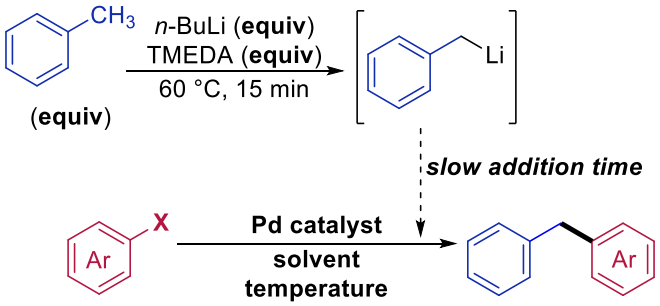

Scheme 31 – Optimization Variables for the Direct Cross-Coupling of Benzyl Lithium

Also, Feringa usually employs toluene as the solvent in organolithium coupling. However, we suspected even remotely acidic solvents would result in reactivity with the benzyl lithium. Instead, we opted to perform the cross-coupling in cyclohexane, which we observed to be inert to such deprotonations at elevated temperatures (see **Section 1.3.1**). However, the Pd_2dba_3/XPhos catalyst system was found to poorly soluble in cyclohexane at room temperature. We suspected that if not fully dissolved, poor metal-ligand interaction could perturb the efficacy of the cross-coupling. We therefore decided to initially perform the cross-coupling at 60 °C to help

solubilize the catalyst system, as well as it being logistically convenient, since that temperature was used for the deprotonation as well.

Aryl bromides were our initial choice of electrophilic coupling partner as they are known to undergo oxidative addition more easily than aryl chlorides. We suspected this would enable less stringent nucleophile addition times. More specifically, 2-bromonaphthalene was used because any homocoupling, dehalogenation, or butylation of the aryl halide could be detected by GC-MS (**Scheme 32**). By being able to observe these side-products, a more systematic optimization could be conducted by considering their respective mechanisms of formation.

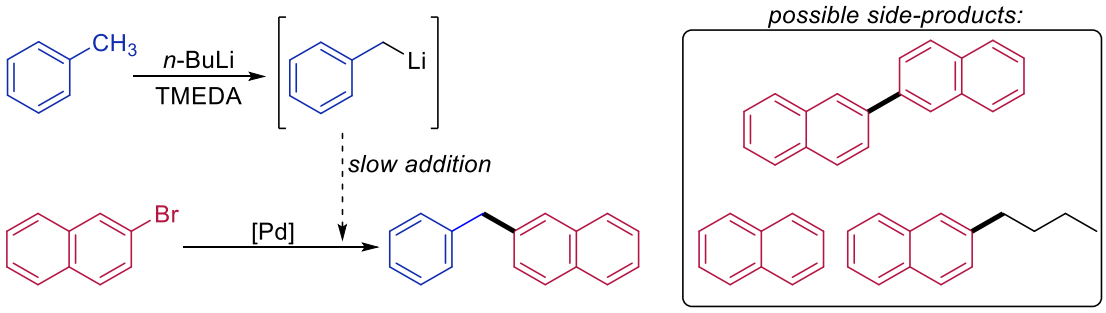

Scheme 32 – Possible Products for the Deprotonation and Cross-Coupling of Toluene

Lastly, there were logistical considerations regarding the slow addition of the benzyl lithium nucleophile. Because the deprotonation was done very concentrated, it involved impractically small volumes to handle on the optimization scale of 0.1 mmol. Consequently, it was diluted with cyclohexane prior to its addition to the coupling mixture. For the slow addition, a syringe pump was used to reliably provide consistent rates of addition. Furthermore, use of a syringe pump enabled long addition times that would be impractical if done manually. A photograph of the general reaction setup for the direct cross-coupling of benzyl lithium is

illustrated in **Figure 2**. With the initial variables identified, the direct benzyl lithium cross-coupling was attempted.

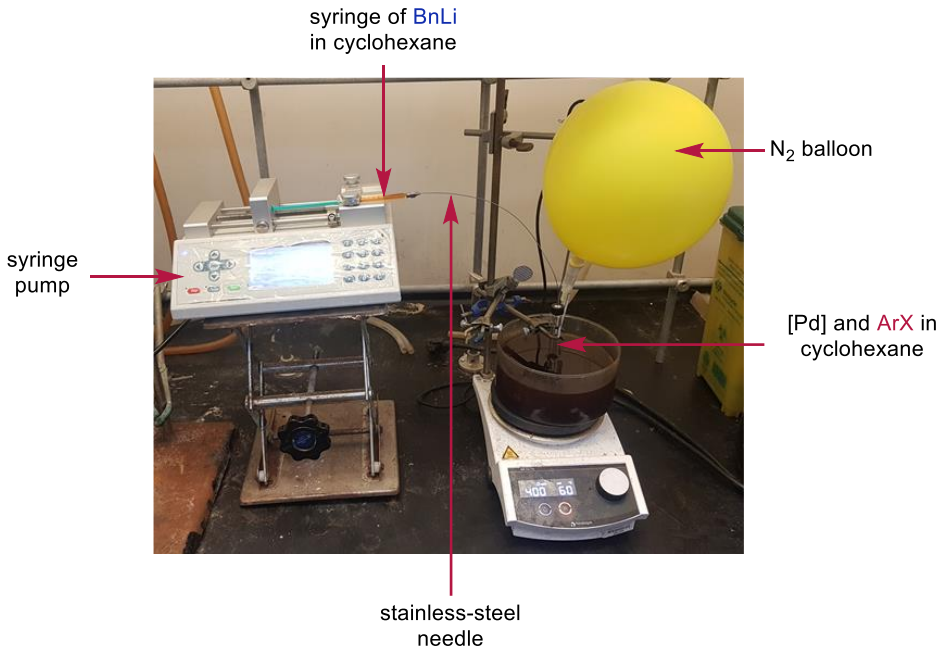

Figure 2 – Reactor Setup for the Cross-Coupling of Benzyl Lithium via Nucleophile Slow Addition

Since the yield of our optimized deprotonation conditions was found to be 45% (**Section 1.3.1**), the first variable screened was the equivalents of the deprotonation mixture relative to the aryl halide limiting reagent. As shown in **Table 3**, 1 or 1.5 equivalents of superbase (entries 1-2) led to 25% and 29% yield of diarylmethane **3**, respectively, with recovery of aryl bromide being observed by GC-MS (m/z of 207). In contrast to other cross-couplings in which starting material recovery may stem from catalyst death or insufficient reaction time, organolithiums can directly react with organohalides via LHE, sometimes in rates comparable to proton transfers.[82] Therefore, recovery of aryl halide suggested an insufficient quantity of the deprotonation mixture was used.

[82] Bailey, W. F.; Patricia, J. J.; Nurmi, T. T.; Wang, W. *Tetrahedron Lett.* **1986**, *27*, 1861–1864.

Table 3 – Effect of Stoichiometry in the Direct Cross-Coupling of Benzyl Lithium

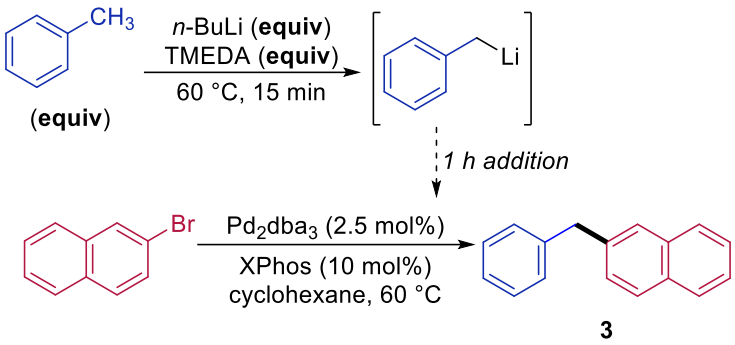

Entry	PhMe:*n*-BuLi:TMEDA:ArX (equiv)	Yield of **3** (%)[a]
1	1.25:1:1:1	25
2	1.875:1.5:1.5:1	29
3	2.5:2:2:1	36
4	3.125:2.5:2.5:1	34

[a]Reactions were run on a 0.1 mmol scale of aryl halide. Yields are reported by ^{1}H NMR using 1,3,5-trimethoxybenzene as an internal standard.

When the amount of superbase was increased to 2 equivalents (**Table 3**, entry 3), a 36% yield of the cross-coupled product was observed with no recovery of aryl halide observed by GC-MS. Upon increasing the amount of superbase to 2.5 equivalents (**Table 3**, entry 4), a negligible decrease in yield to 34% was observed. In all of these experiments, significant naphthalene was observed by GC-MS (m/z of 128), contributing to the poor yields. We suspected LHE was responsible for this dehalogenation side-product. Therefore, with full conversion of aryl halide achieved using 2 equivalents of the deprotonation mixture, focus was shifted to favour productive cross-coupling over competitive LHE.

We hypothesized that aryl chlorides would be less prone to decomposition by LHE due to the stronger Ar-X bond.[83] Indeed, relative to the best previous result of 34% yield using 2-bromonapthalane (**Table 4**, entry 1), switching to 2-chloronaphthalene provided an improved yield of 43% (entry 2). In addition to being beneficial in this reaction, aryl chlorides are generally desirable for use in cross-coupling because of their relatively low cost and greater commercial availability relative to aryl- bromides and iodides.[84]

Table 4 – Effect of Naphthyl Halide in the Direct Cross-Coupling of Benzyl Lithium

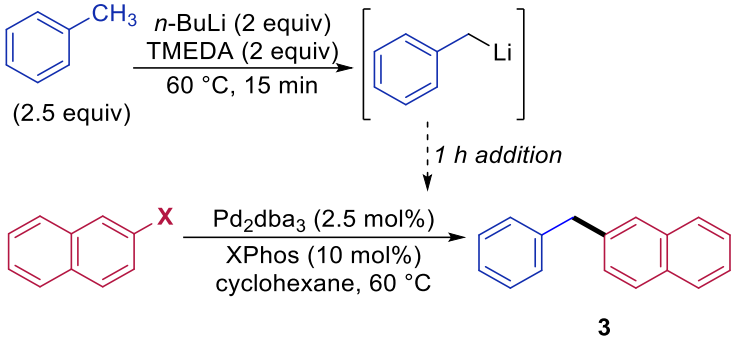

Entry	X	Yield of **3** (%)[a]
1	Br	34
2	Cl	43

[a]Reactions were run on a 0.1 mmol scale of aryl halide. Yields are reported by ^{1}H NMR using 1,3,5-trimethoxybenzene as an internal standard.

Unfortunately, when attempting to replicate this result, a significant reproducibility issue was observed with only trace amounts of the expected product being observed (**Table 5**, entry 1). Furthermore, significant aryl chloride recovery was also identified by GC-MS (m/z of 162), suggesting possible nucleophile decomposition. During the slow addition of this failed experiment, the benzyl lithium solution entering the needle was its characteristic vibrant orange

[83] Lam, K. C.; Marder, T. B.; Lin, Z. *Organometallics* **2007**, *26*, 758–760.
[84] Littke, A. F.; Fu, G. C. *Angew. Chem. Int. Ed.* **2002**, *41*, 4176–4211.

colour, but colourless coming out. We thus suspected that repeated exposure of BnLi to the same 12” stainless-steel needle (**Figure 3a**) had corroded the metal. Upon replacing the needle with a fresh one, the characteristic orange colour of the benzyl lithium was once again observed coming out of the needle and the expected yield was obtained (**Table 5,** entry 2). To prevent future corrosion, PFA tubing was investigated as an alternative material for the slow addition (see Supporting Information **Section 3.1.2**). With the appropriate luers, this highly robust polymer, commonly used in HPLC and flow chemistry, could be readily attached to a disposable plastic syringe at one end, and a disposable 1.5” stainless-steel needle on the other (**Figure 3b**).

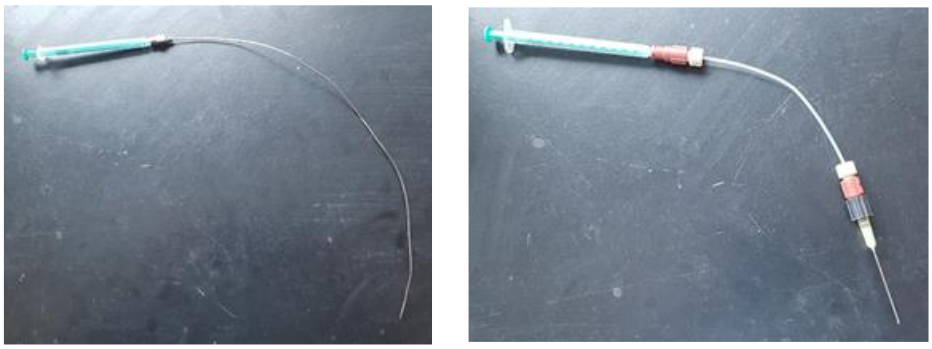

(a) (b)

Figure 3 – Different Slow Addition Materials for the Direct Cross-Coupling of Benzyl Lithium

Interestingly, switching to PFA tubing resulted in an unexpected improvement in yield to 51% (**Table 5,** entry 3). The likely explanation for this was the relative concentration of the nucleophile during the slow addition. To account for the dead volume of the deprotonation flask and slow addition material, an excess of nucleophile stock solution was prepared for these coupling reactions. To avoid unnecessary waste of reagents, the nucleophile was diluted more when the PFA tubing was used, which has a greater volume than the stainless-steel needle. The concentration of benzyl lithium was therefore lower when PFA tubing was used compared to the

needle (0.2 M and 0.3 M, respectively). Greater nucleophile dilution may have improved the efficacy of the slow addition by maintaining a low concentration of BnLi in the cross-coupling mixture, making productive coupling more competitive than LHE. However, further diluting the nucleophile to 0.13 M prior to slow addition led to a negligible change in yield (entry 4), suggesting 0.2 M was optimal. Therefore, PFA tubing and a nucleophile concentration of 0.2 M was used for subsequent variable screening.

Table 5 – Effect of Slow Addition Material and Nucleophile Concentration in the Direct Cross-Coupling of Benzyl Lithium[a]

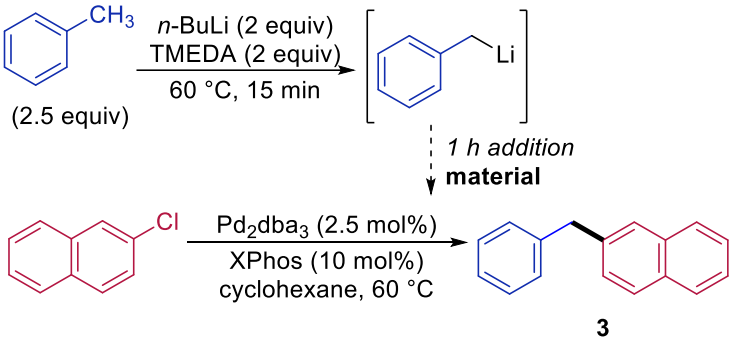

Entry	Slow Addition Material	[Nuc] (M)[b]	Yield of **3** (%)
1	stainless steel needle (old)	0.30	Trace
2	stainless steel needle (new)	0.30	43
3	PFA tubing	0.20	51
4	PFA tubing	0.13	53

[a]Reactions were run on a 0.1 mmol scale of aryl halide. Yields are reported by ^{1}H NMR using 1,3,5-trimethoxybenzene as an internal standard. Trace yield indicates m/z was detected by GC-MS, but calculated yield was < 1 %. [b][Nuc] is reported relative to *n*-BuLi/TMEDA limiting reagents.

Unfortunately, when attempting to repeat this result, a separate reproducibility issue was observed in which the yield plummeted to 20% (**Table 6**, entry 1). In contrast to BnLi decomposition with a stainless steel needle, no aryl chloride was observed by GC-MS, suggesting there was a different problem. For the first time, *N*,*N*-dimethyl-2-naphthylamine **4** was observed by GC-MS (m/z of 171), likely forming from the decomposition and cross-coupling of TMEDA.

Butyl lithium is known to deprotonate TMEDA in an elimination reaction to form butane, *N*,*N*-dimethylvinylamine, and lithium dimethylamide (**Scheme 33a**).[85] These types of lithium amides have precedent to undergo palladium-catalyzed Buchwald-Hartwig amination with aryl halides in the synthesis of aniline derivatives (**Scheme 33b**).[86]

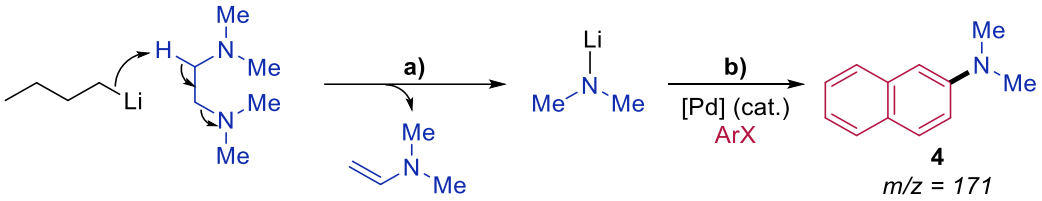

Scheme 33 – Aniline Side-Product from the Decomposition and Cross-Coupling of TMEDA

Although precedented, it was unclear what had sparked TMEDA decomposition, as many deprotonation/cross-coupling reactions were performed without ever observing the amine side-product. We instead investigated the use of an alternative superbase; *trans*-*N*,*N*,*N*',*N*'-tetramethyl-1,2-diaminocyclohexane (TMCDA) is known to be a more robust additive used in the preparation of coordinating-amine superbases.[87] The organolithium-induced decomposition of TMCDA has been shown to be much less prevalent than TMEDA due to the thermodynamically favoured chair conformation not having any antiperiplanar β-hydrogens, thus minimizing an E2-type elimination (**Scheme 34**).

[85] Eberhardt, G. G.; Butte, W. A. *J. Org. Chem.* **1964**, *29*, 2928–2932.
[86] Shen, Q.; Hartwig, J. F. *J. Am. Chem. Soc.* **2006**, *128*, 10028–10029.
[87] Strohmann, C.; Gessner, V. H. *J. Am. Chem. Soc.* **2008**, *130*, 11719–11725.

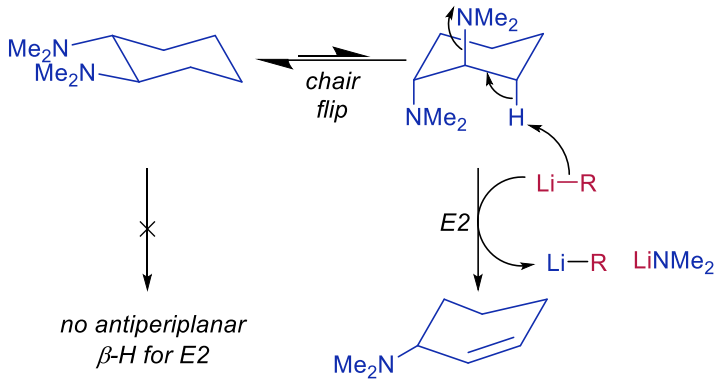

Scheme 34 – Mechanistic Justification for the Robustness of TMCDA to Organolithiums

Relative to the irreproducible results with TMEDA (**Table 6**, entries 1-2), use of TMCDA provided approximately 50% yield for two identical experiments (entries 3-4). To our advantage, no re-optimization of the deprotonation conditions was required, as no butylated aryl halide was observed. Although amine **4** was still observed, it was in negligibly low yields of 2-4%. With these two reproducibility issues overcome, the optimization process could be continued using PFA tubing and TMCDA instead of stainless-steel needles and TMEDA.

While we found aryl chlorides to be beneficial in the cross-coupling of benzyl lithium, presumably by minimizing LHE, their relatively strong Ar–X bond also makes them sluggish to undergo oxidative addition relative to aryl bromides.[88] We hypothesized that by increasing the time over which the nucleophile was added could account for the relatively slow oxidative addition,[89] thus further decreasing LHE. Indeed, a longer slow addition of 1.5 hours provided an improved yield of 57% (**Table 6**, entry 5), again with minimal formation of amine **4**. Further increasing the addition time to 2 hours had a negligible change in yield of the coupling (entry 6),

[88] Barrios-Landeros, F.; Hartwig, J. F. *J. Am. Chem. Soc.* **2005**, , 6944−6945.
[89] Sullivan, R. J.; Freure, G. P. R.; Newman, S. G. *ACS Catal.* **2019**, *9*, 5623–5630.

and dehalogenation was still observed. We therefore suspected there was an inherent competition in reaction rates between transmetallation and LHE, regardless of the concentration of the oxidative addiction adduct. With no added benefit provided by a 2 hour nucleophile slow addition, further optimization was performed using a 1.5 hour addition.

Table 6 – Effect of Diamine and Addition Rate in the Deprotonation and Cross-Coupling of Toluene[a]

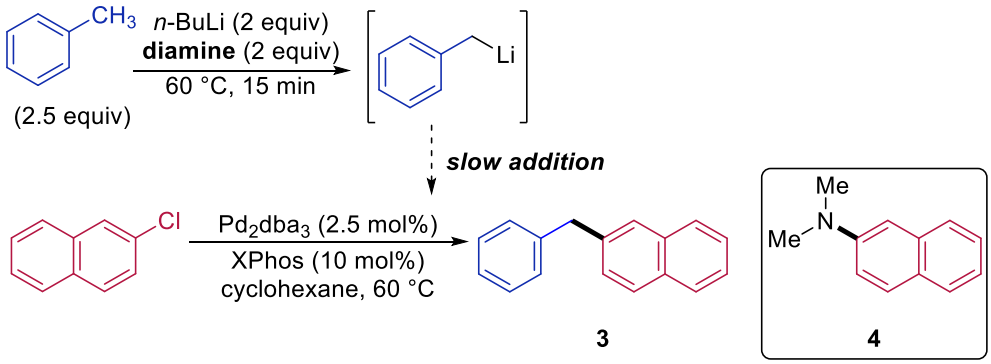

Entry	Diamine	Slow Addition Time (h)	Yield of **3** (%)	Yield of **4** (%)
1	TMEDA	1	51[b]	0
2	TMEDA	1	20[b]	41
3	TMCDA	1	51[c]	4
4	TMCDA	1	48[c]	2
5	TMCDA	1.5	57	2
6	TMCDA	2	59	2

[a]Reactions were run on a 0.1 mmol scale of aryl halide. Yields are reported by ^{1}H NMR using 1,3,5-trimethoxybenzene as an internal standard. [b]Results from two identical experiments show irreproducibility. [c]Results from two identical experiments show reproducibility.

We hypothesized there was a temperature at which productive transmetallation could outcompete LHE. Reducing the coupling temperature to 40 °C significantly decreased the yield of the reaction relative to 60 °C (**Table 7**, entries 1-2). With a yield of 29%, significant naphthalene was observed by GC-MS, suggesting LHE had dominated the reaction. Upon increasing the temperature to 80 °C (entry 3), the observed yield improved to 82%, suggesting productive

coupling was favored at this temperature. To heat the cross-coupling to 95 °C, heptane was used in the place of cyclohexane because of their relative boiling points (98 °C and 81 °C, respectively), providing a diminished of 40% (entry 4). However, this did not appear to be an issue of the relative rates of transmetallation and LHE, as significant aryl chloride recovery was observed by GC-MS. Furthermore, during the slow addition, an orange precipitate was observed in the syringe, most likely being the BnLi/TMCDA complex,[90] likely due to poor solubility in heptane. This precipitation likely resulted in inconsistent flow rates, clogging of the slow addition, and most importantly, decomposition of benzyl lithium leading to recovery of aryl halide. Therefore, we settled on 80 °C in cyclohexane as the optimal temperature and solvent for use in further optimization studies.

Table 7 – Effect of Temperature in the Direct Cross-Coupling of Benzyl Lithium

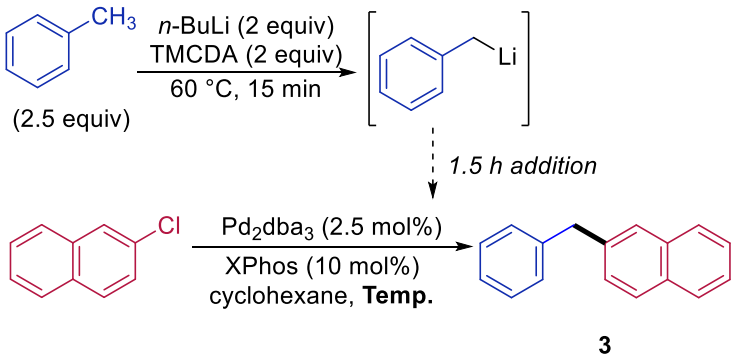

3

Entry	Temperature (°C)	Yield of **3** (%)[a]
1	40	29
2	60	57
3	80	82
4	95[b]	40

[a]Reactions were run on a 0.1 mmol scale of aryl halide. Yields are reported by ^{1}H NMR using 1,3,5-trimethoxybenzene as an internal standard. [b]Heptane used instead of cyclohexane.

[90] Eisch, J. J.; Yu, K.; Rheingold, A. L. *Eur. J. Org. Chem.* **2012**, *2012*, 3165–3171.

Next, focus was shifted to the catalyst system; although Pd_2dba_3/XPhos worked well under these coupling conditions, there was no certainty as to whether or not it was indeed the optimal catalyst system. Therefore a variety of catalyst systems were screened, again using Feringa's precedent in organolithium coupling. With Pd_2dba_3 as the pre-catalyst, a small range of additional Buchwald ligands were tested, which are known to favor both oxidative addition and reductive elimination.[91] Relative to 82% with XPhos (**Table 8**, entry 1), SPhos, DavePhos, and JohnPhos were found to perform significantly worse, with yields ranging from 38-54% (entries 2-4). Significant naphthalene was observed by GC-MS, suggesting LHE was more competitive to transmetallation with these ligands. Pd-PEPPSI-IPent and $Pd[P(tBu)_3]_2$ involved changing both the pre-catalyst and the ligand, since these complexes exist with the ligand bound to the metal. Again, both of these catalysts provided reduced yields of 68% and 33%, respectively (entries 5-6). Therefore, XPhos was the best ligand of those screened.

The efficacy of Pd_2dba_3 forming an active catalyst in the presence of phosphine ligands is known to be very dependent on the specific reaction conditions used.[92] Theoretically, if a pre-catalyst is used that already has the XPhos coordinated to the metal, catalyst activation should be easier. However, relative to Pd_2dba_3/XPhos, Pd-XPhos-G2 and Pd(XPhos)(allyl)Cl led to comparable and worse yield, respectively (**Table 8**, entries 7-8). One potential limitation of these pre-catalysts lies with the fact that they exist in the Pd(II) oxidation state, and their activation to Pd(0) requires reaction with BnLi. This may have contributed to greater LHE if the catalyst

[91] Old, D. W.; Wolfe, J. P.; Buchwald, S. L. *J. Am. Chem. Soc.* **1998**, *120*, 9722-9723.
[92] Janusson, E.; Zijlstra, H. S.; Nguyen, P. P. T.; MacGillivray, L.; Martelino, J.; McIndoe, J. S. *Chem. Commun.* **2017**, *53*, 854–856.

activation was not sufficiently fast. With an inexpensive, air-stable catalyst system of Pd_2dba_3/XPhos having provided an 82% yield for the coupling of toluene with 2-chloronapthalene, the optimization process was concluded.

Table 8 – Effect of Catalyst System in the Direct Cross-Coupling of Benzyl Lithium[a]

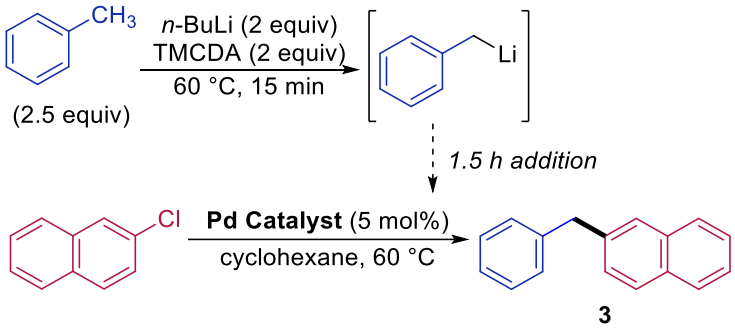

Entry	Pd Catalyst[b]	Yield of **3** (%)
1	Pd_2dba_3/XPhos	82
2	Pd_2dba_3/SPhos	44
3	Pd_2dba_3/DavePhos	54
4	Pd_2dba_3/JohnPhos	38
5	Pd-PEPPSI-IPent	68
6	$Pd[P(tBu)_3]_2$	33
7	Pd-XPhos-G2	77
8	Pd(XPhos)(allyl)Cl	64

[a]Reactions were run on a 0.1 mmol scale of aryl halide. Yields are reported by ^{1}H NMR using 1,3,5-trimethoxybenzene as an internal standard. [b]Pd monomers were used in 5 mol% and Pd dimers were used in 2.5 mol%. Monodentate phosphine ligands were used in 10 mol%.

With our optimized conditions in hand, we investigated the scope of aryl chlorides and toluene derivatives for this deprotonation and cross-coupling sequence (**Table 9**). After isolation, 2-benzylnaphthalene **3** provided an isolated yield of 76% (entry 1), largely consistent with the observed crude NMR yield. We were very interested in investigating the use of solid toluene

derivatives, since they are incompatible with Walsh's chemistry requiring solvent quantities.[93] With our method, however, non-solvent quantities of the toluene derivative enabled solid substrates, such as 3,5-*di*terbutyltoluene, to be deprotonated and coupled to form **5** without a diminished yield (entry 2). Steric hindrance on the aryl chloride was also tolerated, with 2-chlorobiphenyl having provided a 78% yield of **6** when coupled with toluene (entry 3). Furthermore, the aryl chloride did not inherently require activation by the presence of extended conjugation (naphthyl or biphenyl), as undecorated chlorobenzene provided **7** in 69% (entry 4) when coupled with 1,1,4,4,6-pentamethyl-1,2,3,4-tetrahydronaphthalene, another solid toluene derivative.

Due to the inherent reactivity of benzyl lithiums, functional group tolerance on the aryl chloride was found to be limited, consistent with other organolithium coupling reported by Feringa.[94] However, a benzotrifluoride moiety, being fairly inert while also electron-withdrawing, was tolerated to give **8** in 84% yield (entry 5), an improvement relative to electron-neutral aryl chlorides. Lastly, presumably due to the relatively slow rate of oxidative addition, electron-rich aryl chlorides such as 4-chloroanisole (entry 6) and *N*-methyl-4-chloroindole (entry 7) benefited from a longer addition time of 3 hours, but still led to diminished yields of 58% of **9** and 63% of **10**, respectively. These reduced yields can likely be attributed to the electron-rich Pd(II) oxidative addition adduct undergoing transmetallation slower, making the benzyl lithium more prone to react directly with the aryl chloride via LHE. In hindsight, it may have been beneficial to use an

[93] Sha, S.-C.; Tcyrulnikov, S.; Li, M.; Hu, B.; Fu, Y.; Kozlowski, M. C.; Walsh, P. J. *J. Am. Chem. Soc*. **2018**, *140*, 12415–12423.
[94] Hornillos, V.; Giannerini, M.; Vila, C.; Fañanás-Mastral, M.; Feringa, B. L. *Org. Lett.* **2013**, *15*, 5114–5117.

electron-rich aryl halide for the optimization; by optimizing with a challenging substrate, overall higher yields may have been obtained. However, the potential lack of ability to easily observe recovery or dehalogenation of aryl halide would have made the optimization process significantly more difficult, as it would be less clear what was responsible for poor yields.

Table 9 – Substrate Scope for the Deprotonation and Cross-Coupling of Toluene Derivatives[a]

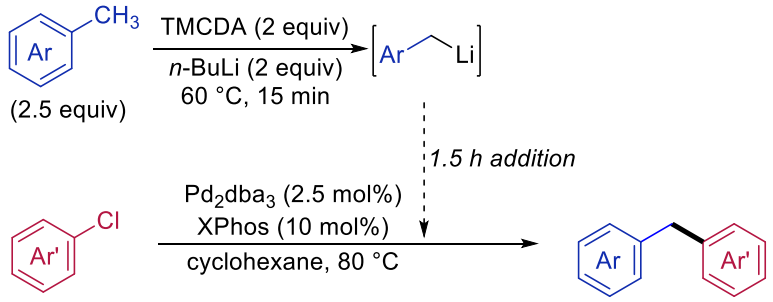

Entry	Product	Yield (%)	Entry	Product	Yield (%)
1	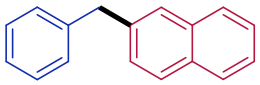 **3**	76%	5	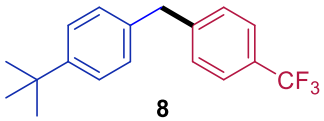 **8**	84%
2	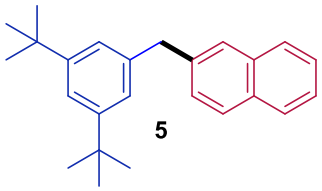 **5**	76%	6	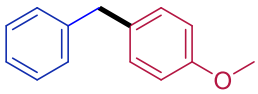 **9**	58%[b]
3	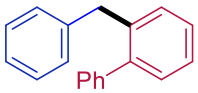 **6**	78%	7	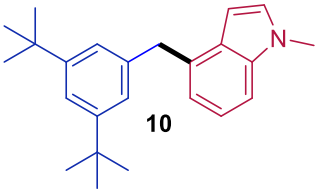 **10**	63%[b]
4	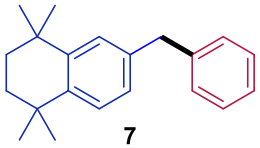 **7**	69%			

[a]Reactions were run on a 0.2 mmol scale of aryl halide. Yields are reported after isolation by column chromatography. [b]Nucleophile added to electron-rich aryl chlorides over 3 h.

Many decorated aryl chlorides were found to be incompatible in the direct cross-coupling of benzyl lithiums. Our group previously took advantage of nucleophile slow addition to expand the functional group tolerance of Kumada-Corriu coupling with aryl chlorides.[95] By slowly adding the Grignard reagent to the coupling mixture, it preferentially reacts with the oxidative addition adduct, enabling the aryl chloride to bear electrophilic functional groups such as amides, nitriles, ketones, and esters. We hoped this technique would also work for benzyl lithium coupling; however, many electrophilic functional groups were found to be too reactive for such an aggressive nucleophile. As shown in **Scheme 35**, ketone **11**, α,β-unsaturated ketone **12**, nitrile **13**, tertiary amide **14**, and heterocyclic methyl ester **15** were all found to be incompatible. All of these substrates provided zero-to-trace yields of their respective cross-coupled products. In some cases, the 1,2-addition adducts of the aryl chlorides were observed by GC-MS, indicating the benzyl lithium reacted faster with the electrophilic functional groups than in cross-coupling or lithium-halogen exchange.

Aryl chlorides bearing mildly acidic functional groups such as terminal alkyne **16** and tolyl-containing **17** were also not tolerated. In these cases, the benzyl lithium may have been quenched by the deprotonation of these species. This could potentially lead to dimerization of the aryl halide, though this was not specifically observed. Also, 4-chlorothioanisole **18** was observed to react at both the Ar–Cl and Ar–SCH_3 bonds leading to a mixture of cross-coupled products. The

[95] Hua, X.; Masson-Makdissi, J.; Sullivan, R. J.; Newman, S. G. *Org. Lett.* **2016**, *18*, 5312–5315.

palladium-catalyzed cross-coupling of thioanisole has been previously reported, so this mode of C–S activation is not unprecedented.[96]

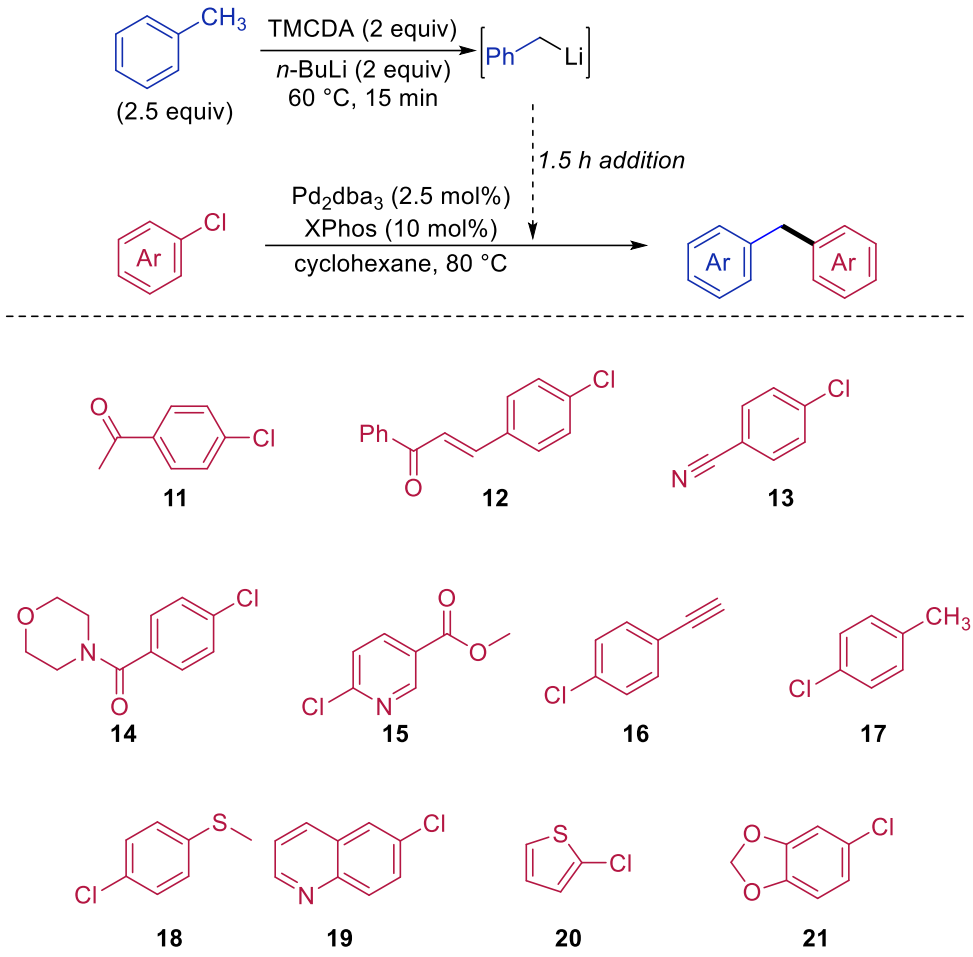

Scheme 35 – Failed Electrophiles for the Direct Cross-Coupling of Benzyl Lithium

Lastly, several heterocyclic substrates were not tolerated, such as quinoline **19**, thiophene **20**, and benzodioxole **21**. Heterocycles have been shown to undergo deprotonation by organolithiums, commonly through directed ortho metalation.[97] Therefore, competitive aryl

[96] Zhu, F.; Wang, Z.-X. *Org. Lett.* **2015**, *17*, 1601–1604.
[97] Quéguiner, G.; Marsais, F.; Snieckus, V.; Epsztajn, *J. Adv. Heterocyclic Chem*. **1991**, *52*, 187–304.

chloride deprotonation by BnLi may have outcompeted productive cross-coupling. Interestingly, Feringa has reported the organolithium cross-coupling of heterocyclic aryl chlorides including thiophenes and furans.[98] A possible explanation for why similar substrates failed in our chemistry is that upon deprotonation of C–H bonds with coordinating-amine superbase, the resultant organolithium can exist with the amine still coordinated to the lithium cation (**Scheme 36**).[99] This may activate the BnLi in a similar mechanism to how diamines activate *n*-BuLi. Consequently, it is reasonable for the coupling of non-commercial organolithiums generated in this manner to have worse functional group tolerance than those that are commercially available.

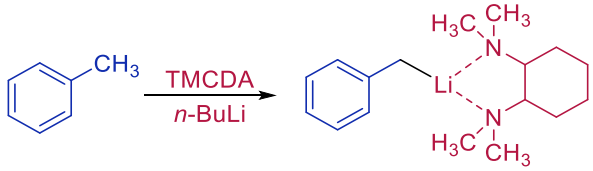

Scheme 36 – Plausible Explanation for the Reactivity of Superbase-Generated Benzyl Lithium

In conclusion, we have outlined a reasonable set of deprotonation- and cross-coupling conditions to enable the C(sp^3)–H arylation of toluene derivatives using non-solvent quantities of substrate. While functional group tolerance was found to be limited due to the aggressive nature of superbases and benzyl lithiums, this chemistry improves upon the biggest limitation of Walsh's chemistry[100] by enabling the functionalization of solid toluene derivatives. Furthermore, our deprotonation and cross-coupling methodology of unactivated starting materials contributes to the field of Murahashi coupling by including non-commercial C(sp^3) organolithiums.

---

[98] Hornillos, V.; Giannerini, M.; Vila, C.; Fañanás-Mastral, M.; Feringa, B. L. *Org. Lett*. **2013**, *15*), 5114–5117.
[99] Eisch, J. J.; Yu, K.; Rheingold, A. L. *Eur. J. Org. Chem.* **2012**, *2012*, 3165–3171.
[100] Sha, S.-C.; Tcyrulnikov, S.; Li, M.; Hu, B.; Fu, Y.; Kozlowski, M. C.; Walsh, P. J. *J. Am. Chem. Soc.* **2018**, *140*, 12415–12423.

1.3.3: Cross-Coupling of Superbase-Generated Primary Benzyl Zincs

We were interested in improving upon the stringent limitations of direct benzyl lithium coupling to enable the formation of more complex products using our benzylic C(sp^3)–H deprotonation and coupling methodology. Poor scope, imperfect yield, relatively high catalyst loading, and the required slow addition significantly limit the synthetic utility of this chemistry. We therefore investigated zinc chloride as an additive, which is known to transmetallate with reactive organometallic nucleophiles to form the more well behaved organozinc.[101, 102] Although generally prepared from zinc metal and benzyl halides, benzyl zincs have been used in palladium-catalyzed cross-coupling of functional group-dense aryl halides without requiring nucleophile slow addition.[103] **Table 10** shows the steps that were taken to form benzyl zincs *in situ* for their use in cross-coupling without nucleophile slow addition.

After the deprotonation of toluene using our optimized conditions (**Section 1.3.1**), zinc chloride was added as a stock solution in THF. This caused an immediate loss of the characteristic orange colour of the benzyl lithium, suggesting the transmetallation took place. Upon treating the resultant benzyl zinc with 2-chloronaphthalene under the optimized conditions described in **Section 1.3.2**, a 90% yield was of **3** observed (**Table 10**, entry 1). Although this Negishi coupling proceeded very smoothly with no change to the coupling conditions, THF was investigated as the coupling solvent because of its improved ability to solubilize the catalyst system relative to cyclohexane. As it has a lower boiling (66 °C), performing the coupling in THF at 60 °C provided **3**

---

[101] Asako, S.; Nakajima, H.; Takai, K. *Nat. Catal.* **2019**, *2*, 297–303.
[102] Zhang, H.; Buchwald, S. L. *J. Am. Chem. Soc.* **2017**, *139*, 11590–11594.
[103] Pompeo, M.; Froese, R. D. J.; Hadei, N.; Organ, M. G. *Angew. Chem. Int. Ed.* **2012**, *51*, 11354–11357.

in 88% yield (entry 2), a negligible change compared to cyclohexane at 80 °C. Lastly, catalyst loading could be reduced from 2.5 mol% to 1 mol% without a significant change in yield (entry 3), thus further validating the use of organozincs. Therefore, by being less prone to metal-halogen exchange, proceeding through a benzyl zinc intermediate alleviated the need for nucleophile slow addition while providing improved yields at a lower catalyst loading.

Table 10 – Effect of $ZnCl_2$ as an Additive in the Deprotonation and Cross-Coupling of Toluene[a]

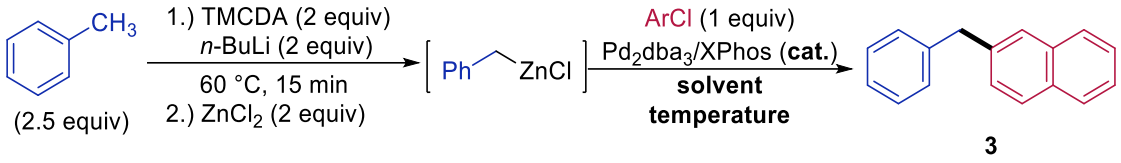

Entry	Solvent	Temperature (°C)	Catalyst Loading (mol%)[b]	Yield of **3** (%)
1	Cyclohexane	80	2.5	90
2	THF	60	2.5	88
3	THF	60	1	89

[a]Reactions were run on a 0.1 mmol scale of aryl halide. Yields are reported by ^{1}H NMR using 1,3,5-trimethoxybenzene as an internal standard. [b]Catalyst loading is reported relative to Pd_2dba_3, with a respective four equivalents of XPhos.

It's interesting that the cross-coupling conditions which were optimized for benzyl lithium transferred so smoothly to benzyl zinc. It is very common for palladium-catalyzed Negishi coupling to require salt additives to improve reactivity of the organozinc.[104] Super-stoichiometric lithium chloride is most commonly used, which is proposed to enable the *in situ* formation of higher-order zincates that are the active transmetallating species (**Scheme 37**). However, under our deprotonation and transmetallation conditions, lithium chloride is generated as a by-product

[104] Eckert, P.; Sharif, S.; Organ, M. G. *Angew. Chem. Int. Ed.* **2020**, *60*, 12224–12241.

from the organolithium transmetallating with zinc chloride. Consequently, this method of organozinc generation is likely beneficial to the subsequent Negishi coupling.

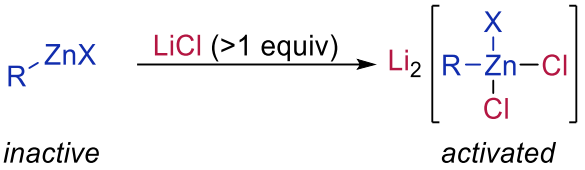

Scheme 37 – Role of Salt Additives in Organozinc Activation

TMCDA may also play a role in the cross-coupling of the organozinc. TMEDA has been shown to be beneficial in the Negishi coupling of benzyl zincs (generated from Zn dust/powder and benzyl halide) in aqueous media.[105] However, its exact role in aprotic organic solvents has not yet been elucidated to our knowledge. In our case, perhaps the coordination of TMCDA to the organozinc activates the nucleophile analogously to the activation of *n*-BuLi (**Scheme 38**). With this facile incorporation of $ZnCl_2$ providing immediate benefits to the cross-coupling condition, we quickly moved on to explore the difference in scope of this deprotonation and cross-coupling methodology.

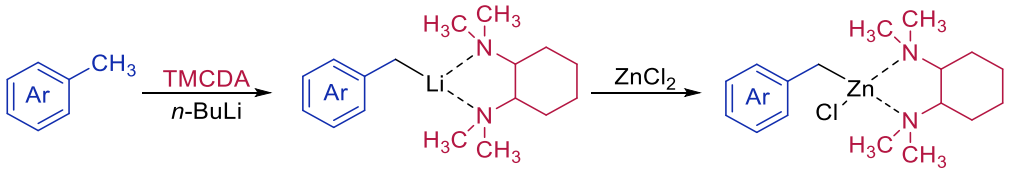

Scheme 38 – Plausible Mechanism of Activation of Benzyl Zincs with TMCDA

Proceeding through an organozinc intermediate was found to significantly improve the scope of the electrophilic coupling partner for the deprotonation and cross-coupling of toluene

[105] Duplais, C.; Krasovskiy, A.; Wattenberg, A.; Lipshutz, B. H. *Chem. Commun.* **2010**, *46*, 562–564.

derivatives (**Table 11**). For example, challenges associated with heterocycles and electrophilic esters were overcome in the preparation of nicotinate **22** in 91% yield (entry 1), highlighting the tamed nucleophilicity and basicity of organozincs. Also, while electron-rich aryl chlorides were challenging in the benzyl lithium coupling, 2-chloro-1,3,5-trimethoxybenzene, coupled smoothly with toluene-d_8 to give **23** in 77% yield (entry 2), provided the catalyst loading was increased to 2.5 mol%. Although the deprotonation of toluene-d_8 required a longer deprotonation time of 1 hour to provide full *n*-BuLi conversion because of the kinetic isotope effect, non-solvent quantities of substrate enabled the relatively inexpensive synthesis of a deuterated product using this methodology. Furthermore, expansion of the scope to include aryl- bromides and iodides are exemplified by the syntheses of difluoroarene **24**, phenylacetonitrile **25**, and azaindole **26** in 69-85% yield (entries 3-5).

While likely also compatible in the benzyl lithium coupling, mesitylene, which bears multiple potential sites of acidity, selectively underwent mono functionalization under these conditions to provide pyridine **27** in 90% yield (**Table 11**, entry 6). Also, moderately acidic aniline **28** was prepared in 93% yield (entry 7), requiring twice as much nucleophile to provide full aryl halide conversion. Presumably stoichiometric deprotonation of the N–H bond quenched significant amounts of the benzyl zinc (pK_a in DMSO ~ 31 for aniline compared to 43 for toluene), with the excess participating in the cross-coupling. Lastly, antihistamine loratadine (brand name Claratin) was coupled to give **29** in 99% yield (entry 8), demonstrating this methodology is suitable for the derivatization of drug scaffolds.

Table 11 – Substrate Scope for the Cross-Coupling of Benzyl Zincs Generated by Deprotonation[a]

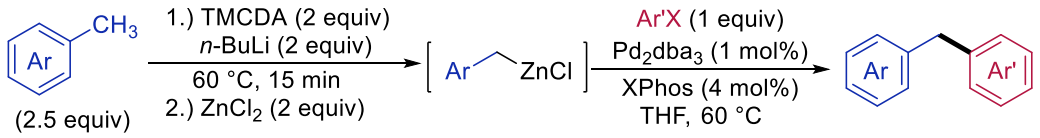

Entry	X	Product	Yield (%)	Entry	X	Product	Yield (%)
1	Cl	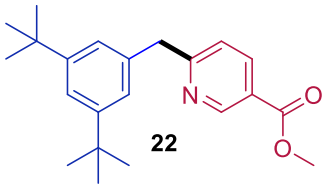 **22**	91%	5	I	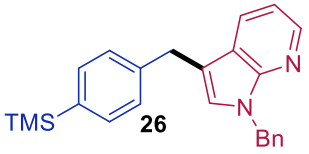 **26**	69%[c]
2	Cl	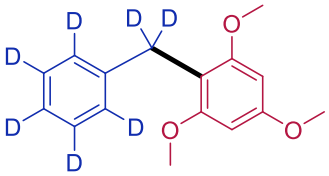 **23**	77%[b,c]	6	Cl	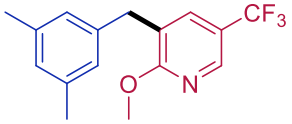 **27**	90%
3	Br	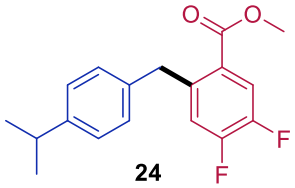 **24**	84%	7	Br	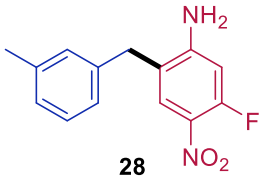 **28**	93%[d]
4	Br	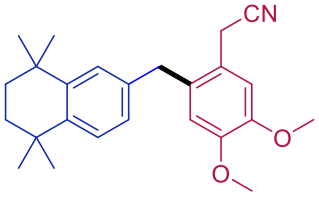 **25**	85%	8	Cl	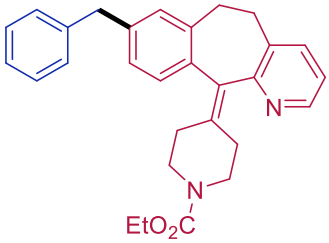 **29**	99%[c]

[a]Reactions were run on a 0.2 mmol scale of aryl halide. Yields are reported after isolation by column chromatography. [b]Deprotonation of toluene-d_8 over 1 h. [c]2.5 mol% Pd_2dba_3 and 10 mol% XPhos. [d]$ArCH_3$ (5 equiv), TMCDA (4 equiv), and *n*-BuLi (4 equiv).

Unsurprisingly, not all functional groups were tolerated on the aryl halide for the benzyl zinc coupling (**Scheme 39)**. Heterocycles bearing multiple heteroatoms often led to significant aryl halide recovery observed by GC-MS, including thiadiazole **30**, imidazopyridine **31**, and

pyrimidine **32**. This may be due to catalyst death stemming from oxidative addition into the arene of the heterocycles.[106] Furthermore, acidic 4-chlorophenol **33** and 4-chlorobenzoic **34** failed to give any product, even when double the equivalents of nucleophile were used. Also, benzaldehyde **35** and styrene **36** were not tolerated, possibly due to competitive 1,2-addition[107] and Mizoroki-Heck[108] reactions, respectively. Lastly, trifluoromethoxy-containing **37** led to a mixture of both Ar–Cl and Ar–OCF_3 activation products observed by GC-MS.

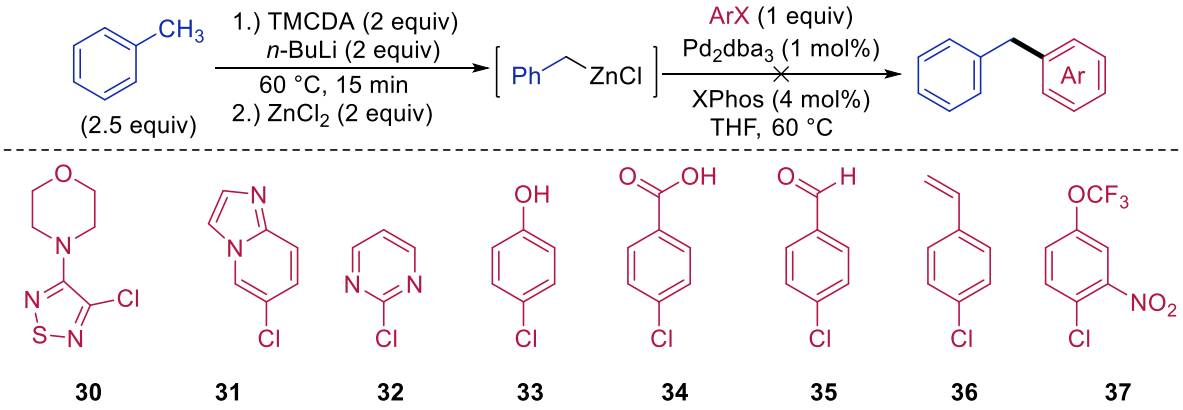

Scheme 39 – Failed Electrophiles for the Coupling of Benzyl Zincs Generated by Deprotonation

There were also some scope limitations of the nucleophilic coupling partner. For example, upon applying the optimal conditions to 4-methylanisole **38**, we expected the deprotonation to be slow because of its electron-rich nature, destabilizing the resultant anionic species. However, ortho arylation was observed, suggesting the methoxy group facilitated directed ortho metalation that outcompeted the desired benzylic deprotonation (**Scheme 40a**). This highlights a significant limitation to this deprotonation and cross-coupling methodology. Not only are most electron-

[106] Ahneman, D. T.; Estrada, J. G.; Lin, S.; Dreher, S. D.; Doyle, A. G. *Science* **2018**, *360*, 186–190.
[107] Cho, H.-H.; Kim, S.-H. *Bull. Korean Chem. Soc.* **2015**, *36*, 1274–1277.
[108] Fristrup, P.; Le Quement, S.; Tanner, D.; Norrby, P.-O. *Organometallics* **2004**, *23*, 6160–6165.

withdrawing groups likely not tolerant of the deprotonation conditions because of their frequent electrophilic nature, but electron-donating groups are likely to facilitate DOM via heteroatoms coordinating to the superbase. Competitive DOM is a known problem in the deprotonation of 4-methylanisole,[109] suggesting this may be an inherent limitation of superbases that cannot be prevented by further optimization.

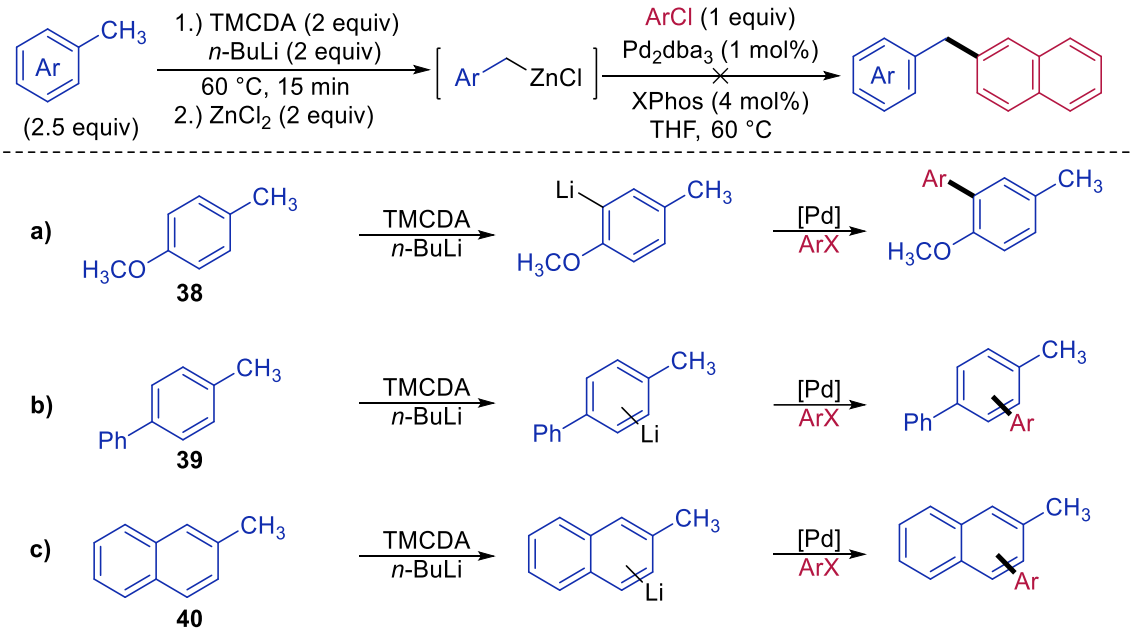

Scheme 40 – Failed Nucleophiles and Observed Side-Products for the Cross-Coupling of Benzyl Zincs Generated by Deprotonation

Interestingly, toluene derivatives bearing extended conjugation were also not tolerated. For example, 4-methylbiphenyl **39** led to numerous isomers detected by GC-MS (m/z of 294), suggesting competitive Ar–H functionalization (**Scheme 40b**). A similar result was observed with 2-methylnaphthalene **40**, which led to several products with m/z of 294 (**Scheme 40c**). This

[109] Bates, R. B.; Siahaan, T. J.; Suvannachut, K. *J. Org. Chem.* **1990**, *55*, 1328–1334.

substrate has been shown to be deprotonated by *n*-BuLi in the absence of additive, [110] indicating it's an activated substrate. Since we were solely interested in the functionalization of inert C(sp^3)–H bonds using superbases, we did not investigate the use of *n*-BuLi alone for the deprotonation and cross-coupling of 2-methylnaphthalene.

In summary, proceeding through a benzyl zinc intermediate drastically improved the cross-coupling of superbase-generated nucleophiles relative to benzyl lithiums. Stringent limitations of our benzyl lithium coupling such as high catalyst loading, nucleophile slow addition, relatively low yields, and poor functional group tolerance, could largely be overcome by instead using the more robust Negishi coupling. While functional group tolerance on the nucleophilic coupling partner is limited due to the harsh nature of the deprotonation conditions, the broad scope of functional group-dense aryl halides enabled the synthesis of a variety of complex products. The preparation of drug derivatives and deuterated products demonstrates the potential uses of this transformation in the fine chemical industry.

1.3.4: Cross-Coupling of Superbase-Generated Secondary Benzyl Zincs

With the deprotonation and cross-coupling of toluene derivatives achieved, the intuitive next step is the arylation of secondary benzylic C(sp3)–H bonds. Although coordinating-amine superbases are precedented to provide poor selectivity between benzylic- and aryl-deprotonation of ethylbenzene, we thought it was worthwhile to investigate our novel deprotonation conditions. By monitoring the kinetics of the deprotonation of ethylbenzene after quenching with benzophenone, full conversion of n-BuLi was observed within 90 minutes

[110] Kawabata, T.; Nagato, M.; Takasu, K.; Fuji, K. *J. Am. Chem. Soc.* **1997**, *119*, 3169–3170.

(performed by Eric A. Skrotzki). The optimized benzyl lithium and benzyl zinc coupling conditions discussed in **Sections 1.3.2** and **1.3.3**, respectively, were then applied to the ethylbenzene-derived nucleophiles. Unfortunately, this led to very poor yields of 19% and 27% of the desired cross-coupled product, respectively (**Table 12**, entries **1**-**2**). Although there was full conversion of aryl halide, substantial formation of the ortho, meta, and para arylated isomers was observed, explaining the poor yields. Notably, the mass balance when accounting for these isomers was better with the organozinc, further suggesting these milder nucleophiles reduce competitive metal-halogen exchange. We therefore concluded that our novel deprotonation conditions for toluene were not transferable to ethylbenzene due to competitive aryl lithiation.

Table 12 – Deprotonation and Coupling of Ethylbenzene Using n-BuLi/TMCDA[a]

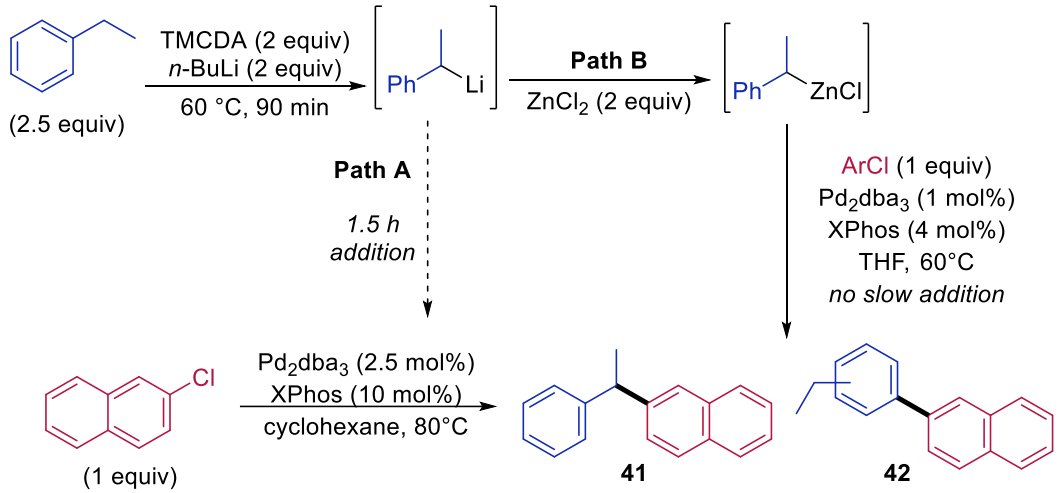

Entry	Path	Yield of **41** (%)	Yield of **42** (%)[b]
1	A	19	47
2	B	27	61

[a]Reactions were run on a 0.1 mmol scale of aryl halide. Yields are reported by ^{1}H NMR using 1,3,5-trimethoxybenzene as an internal standard. [b]Yield of **42** is reported as a mixture of ortho, meta, and para isomers.

We hypothesized a biased ethylbenzene derivative bearing steric bulk on the arene would favour benzylic arylation without having to change the deprotonation or coupling conditions.

Indeed, 4-*tert*-butyl-1-ethylbenzene provided far better benzylic selectivity when the corresponding organozinc was coupled (**Table 13**, entry 1). However, even with less-competitive aryl reactivity, yield was still poor with only 19% of the benzylic isomer **43** and significant aryl chloride recovery observed by GC-MS. Although LiCl as an additive is known to be beneficial in Negishi coupling,[111] it provided a negligible change in this case (entry 2). This is intuitive, given that stoichiometric LiCl should already be present from the deprotonation and $ZnCl_2$ quench. However, the presence of KO*t*Bu improved the yield to 36% (entry 3), but still led to significant aryl halide recovery. It was unclear why the presence of the para *tert*-butyl group influenced the degree of aryl halide conversion.

Table 13 – Effect of Salt Additives and a Biased Substrate for Secondary Benzylic Coupling[a]

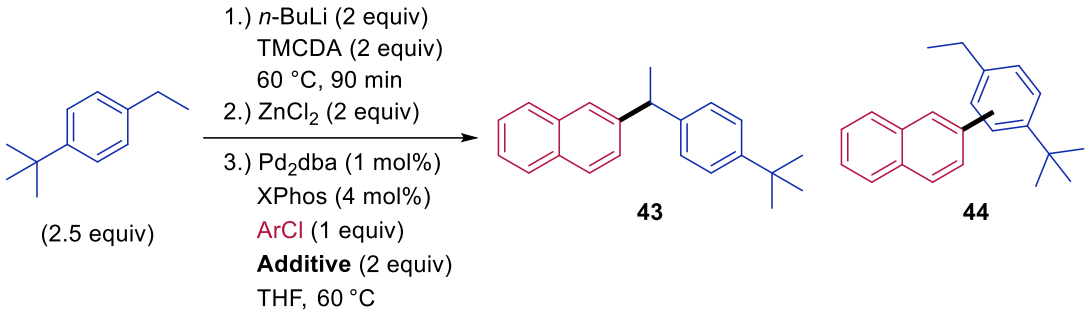

Entry	Additive	Yield of **43** (%)	Yield of **44** (%)[b]
1	None	19	3
2	LiCl	16	Trace
3	KO*t*Bu	36	Trace

[a]Reactions were run on a 0.1 mmol scale of aryl halide. Yields are reported by ^{1}H NMR using 1,3,5-trimethoxybenzene as an internal standard. Yield of **44** is reported a mixture of ortho and meta isomers with respect to aryl and *tert*-butyl groups. Trace yield indicates product was observed by GC-MS, but calculated yield was < 1%.

[111] Eckert, P.; Sharif, S.; Organ, M. G. *Angew. Chem. Int. Ed.* **2020**, *60*, 12224–12241.

As previously mentioned in **Section 1.3.1**, the use of Schlosser's base was initially avoided because of the known reactivity of the corresponding "ate" complexes likely making them impractical to couple directly. However, not only is Schlosser's base precedented to deprotonate ethylbenzene derivatives with high benzylic selectivity in non-solvent quantities,[112] our salt additive investigation suggested the KO*t*Bu that would also be present from Schlosser's base was beneficial in the coupling of the corresponding benzyl zinc. In contrast to the known reactivity with ethereal solvents, a slurry of *n*-BuLi/KO*t*Bu in aliphatic solvents has been demonstrated to selectively deprotonate ethylbenzene derivatives without observed solvent reactivity.[113] Upon applying a slightly modified version of these known deprotonation conditions to our benzyl zinc cross-coupling, ethylbenzene was coupled with 2-chloronaphthalene in 96% yield (**Table 14**, entry 1). A similar result was observed with octylbenzene, providing an 84% yield (entry 2). Unfortunately, tetralin, a more complex bicyclic derivative, led to a 0% yield (entry 3). With significant aryl chloride recovery observed by GC-MS, we suspected the metalated tetralin species had decomposed under the elevated reaction temperatures. Therefore, we instead investigated cryogenic Schlosser's base conditions in ethereal solvents.

[112] Guggisberg, Y.; Faigl, F.; Schlosser, M. *J. Organomet. Chem.* **1991**, *415*, 1–6.
[113] Faigl, F.; Schlosser, M. *Tetrahedron Lett.* **1991**, *32*, 3369–3370.

Table 14 – Cross-Coupling of Secondary Benzyl Zincs Generated using a Schlosser's Base Slurry

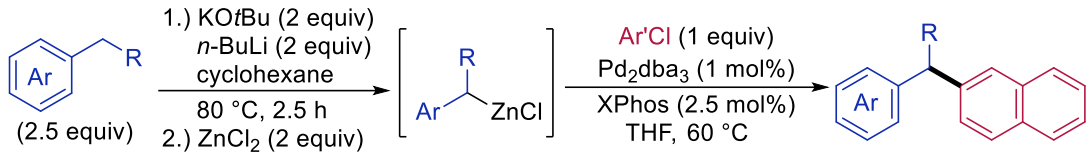

Entry	$ArCH_2R$ Substate	Yield (%)[a]
1	Ethylbenzene	96
2	Octylbenzene	84
3	Tetralin	0

[a]Reactions were run on a 0.1 mmol scale of aryl halide. Yields are reported by ^1H NMR using 1,3,5-trimethoxybenzene as an internal standard. 0% yield indicates the expected m/z value was not observed by GC-MS.

Using conditions modified by Guggisberg *et. al.,*[114] Jean-Danick E. Lavertu optimized the deprotonation of ethylbenzene for its subsequent use in our optimized benzyl zinc coupling (**Scheme 41**). By monitoring the formation of the butyl arene and arylated THF side-products, he optimized the temperature and time of the deprotonation to maximize the formation of the desired 1,1-diarylethane product **41**. He found that 10 minutes and -40 °C provided full conversion of *n*-BuLi, as no butyl arene was observed by GC-MS. Furthermore, by removing the deprotonation mixture from the cold bath for 1 minute before the addition of $ZnCl_2$, he observed selective decomposition of the deprotonated THF. With otherwise unchanged coupling conditions, **41** was formed in quantitative yield. Using his optimized deprotonation and transmetallation conditions, we explored the scope of the cross-coupling.

[114] Guggisberg, Y.; Faigl, F.; Schlosser, M. *J. Organomet. Chem.* **1991**, *415*, 1–6.

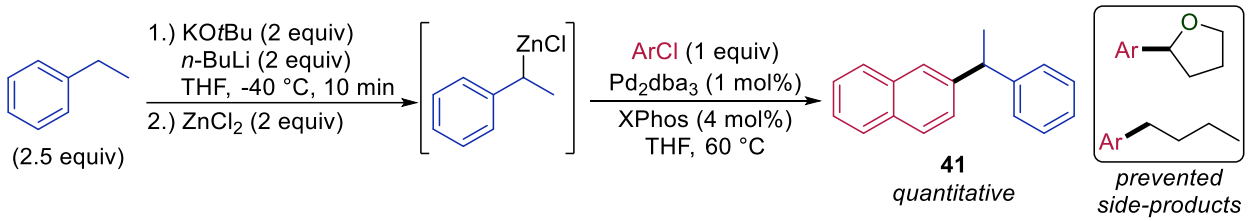

Scheme 41 – Optimized Deprotonation and Cross-Coupling of Ethylbenzene using Schlosser's base in THF

When coupled with a variety of complex electrophilic coupling partners, excellent selectivity of benzylic arylation was observed for all $ArCH_2R$ pronucleophiles tested (**Table 15**). Furthermore, likely due to the identical coupling conditions, functional group tolerance on the aryl- chlorides and bromides was found to be very similar to the primary benzyl zinc coupling; electrophilic, electron-rich, electron-poor, heterocyclic, and bioactive aryl halides were all tolerated. Simple secondary benzylic compounds such as ethylbenzene and 4-*tert*-butyl-1-ethylbenzene were coupled in 72-76% yield (entries 1-2). Interestingly, by presumably deprotonating the aryl halide *in situ*, anti-psychotic Chlorpromazine was used directly as the HCl salt to give **45**, provided double the equivalents of nucleophile was used. Substrates bearing multiple sites of potential acidity such as 1,4-diethylbenzene (entry 3) and 1,3,5-triethylbenzene (entry 4) selectively formed the mono-arylation products **47** and **48** in 80-89% yield. In contrast to the slurry conditions, tetralin was successfully coupled with bioactive fenofibrate to give **49** in 91% yield (entry 5). Similarly, bicyclic indane could also be coupled to give 64% yield of **50** (entry 6). Octylbenzene (entry 7), bearing the long aliphatic chain, was coupled selectively in 69% yield without any observed chain walking isomerization. Analogous to the primary benzylic scope, the Ar–Si bond of 4-trimethylsilyl-1-ethylbenzene was tolerated in the synthesis of **52** in 73% yield (entry 8).

Table 15 –Scope for the Cross-Coupling of Superbase-Generated Secondary Benzyl Zincs[a]

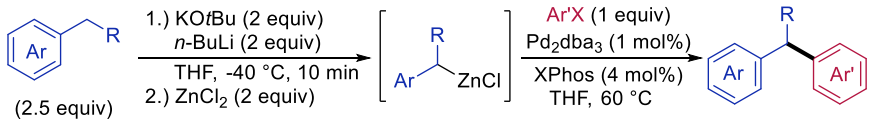

Entry	X	Product	Yield (%)	Entry	X	Product	Yield (%)
1	Cl	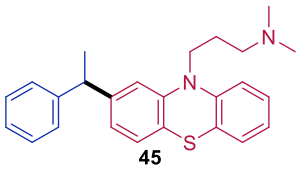 **45**	72% [b]	6	Br	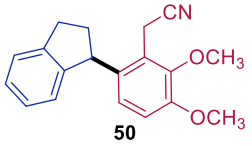 **50**	64%
2	Br	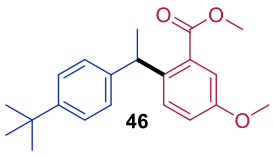 **46**	76%	7	Cl	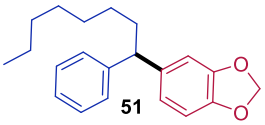 **51**	69%
3	Br	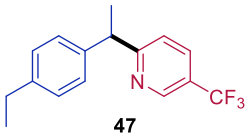 **47**	80%	8	Cl	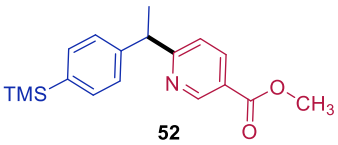 **52**	73%
4	Cl	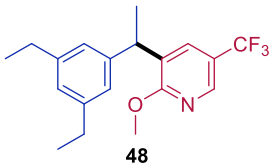 **48**	89%	9	Br	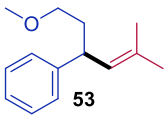 **53**	76%
5	Cl	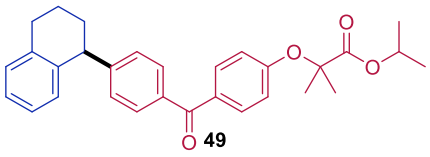 **49**	91%	10	Cl	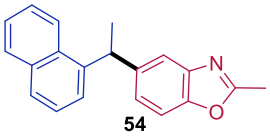 **54**	89%
				11	Cl	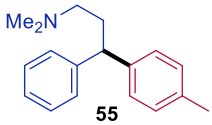 **55**	76%

[a]Reactions were run on a 0.2 mmol scale of aryl halide. Yields are reported after isolation by column chromatography. [b]ArX used as the HCl salt with $ArCH_2R$ (5 equiv), KO*t*Bu (4 equiv), and *n*-BuLi (4 equiv).

In contrast to the harsh *n*-BuLi/TMCDA deprotonation conditions used in the primary benzyl zinc scope, the more dilute, cryogenic nature of these Schlosser's base conditions enabled greater functionality on the nucleophilic coupling partner. For example, 3-methoxypropylbenzene was coupled with a vinyl bromide to give **53** in 76% yield (**Table 15**, entry 9), demonstrating

tolerance of a distal methoxy group on the nucleophile while showing this chemistry is not inherently limited to aryl halides as electrophilic coupling partners. Furthermore, while 2-methylnaphthalene failed with *n*-BuLi/TMCDA, 2-ethylnaphthalene reacted smoothly to give **54** in 89% yield (entry 10) with no aryl C–H deprotonation side-products observed. Lastly, a distal dimethylamino group was tolerated and was used for the synthesis of anti-histamine tolpropamine **55** in 76% yield (entry 11), a significantly more efficient route than established methods.[115]

The improvement in nucleophile scope highlights some advantages of Schlosser's base relative to *n*-BuLi/TMCDA. Not only is *n*-BuLi/TMCDA incompatible with secondary benzylic C–H bond deprotonation due to competitive aryl metalation, the harsh deprotonation conditions required for fast *n*-BuLi conversion largely limited the scope of nucleophilic coupling partners to undecorated toluene derivatives. Although *n*-BuLi/TMCDA enabled the direct cross-coupling of the deprotonated species, the benzyl lithium coupling was found to have severe limitations relative to the benzyl zinc coupling. While the direct coupling of the Schlosser's base-generated "ate" complex was not explicitly tested, the unmatched synthetic utility of Negishi coupling suggests the use of Schlosser's base is more versatile than *n*-BuLi/TMCDA. Furthermore, although we did not investigate the use of Schlosser's base in the arylation of primary benzylic positions, its use in the deprotonation of toluene derivatives in non-solvent quantities is precedented,[116] and the subsequent $ZnCl_2$ quench and cross-coupling would likely proceed smoothly.

---

[115] Prediger, P.; da Silva, A. R.; Correia, C. R. D. *Tetrahedron* **2014**, *70*, 3333–3341.
[116] Yamaguchi, T.; Yamamoto, Y.; Fujiwara, Y.; Tanimoto, Y. *Org. Lett.* **2005**, *7*, 2739–2742.

However, Schlosser's base is not perfect, as it also has some functional group limitations of the nucleophilic coupling partner (**Scheme 42**). While 3-methoxypropylbenzene was tolerated, 2-methoxyethylbenzene **56** was not. Also, 4-phenyl-1-butene **57** and 4-fluoro-1-ethylbenzene **58** both led to no product formation. In all cases, significant aryl halide recovery was observed by GC-MS, possibly suggesting decomposition of the metalated substrates.

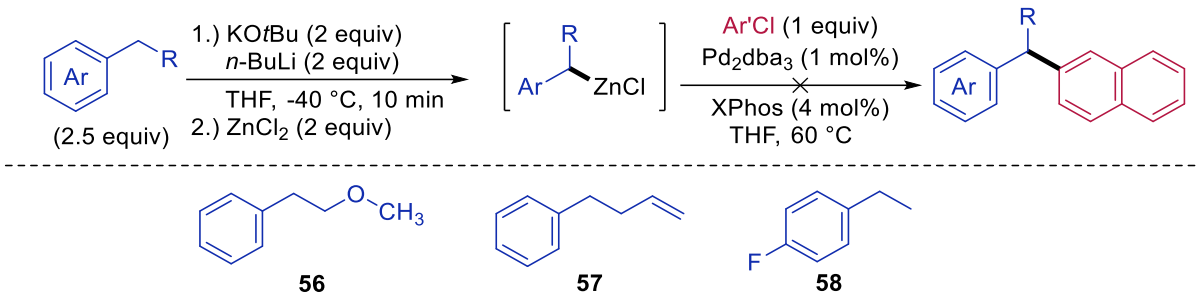

Scheme 42 – Failed Nucleophiles for the Cross-Coupling of Secondary Benzyl Zincs Generated by Deprotonation

This methodology of stoichiometric deprotonation, transmetallation with $ZnCl_2$, and cross-coupling can hereby be extended to include secondary benzylic positions. The use of Schlosser's base enables the deprotonation of unactivated, undirected ethylbenzene derivatives in non-solvent quantities for the generation of secondary C(sp^3)-hybridized benzyl zincs. The subsequent Negishi coupling was again found to be quite selective, enabling the preparation of a diverse range of complex 1,1-diaryl alkane products, including the synthesis- and derivatization-of bioactive compounds. However, much of the classical superbase literature remains unexplored in the context of cross-coupling. Therefore, we then set our sights on expanding this superbase-coupling methodology to other substrate classes previously described in **Section 1.1.3**.

1.3.5: Deprotonation and Cross-Coupling α to Heteroatoms

Due to the vast abundance of oxygen in organic compounds, C(sp^3)–H arylation α to oxygen is a sought-after transformation. In fact, nickel/photoredox dual catalysis has recently been demonstrated to arylate THF and similar substrates using a radical mechanism.[117] Using the deprotonation conditions reported by Corey,[118] methyl *tert*-butyl ether (MTBE) was subsequently quenched with $ZnCl_2$ and treated to the optimized Negishi conditions described in **Section 1.3.3**. When coupled with 2-chloronaphthalene, **59** was isolated in 84% yield (**Table 16**, entry 1). The most significant limitation to this chemistry is the need for solvent quantities of substrate, which could otherwise lead to competitive solvent deprotonation. However, benzyl *tert*-butyl ether, being both α to oxygen and benzylic, was suspected to be sufficiently activated such that it could be used in non-solvent quantities in the presence of THF. Indeed, using the same deprotonation and cross-coupling conditions previously used for secondary benzylic positions (**Section 1.3.4**), BnO*t*Bu was successfully coupled with methyl 6-chloronicotinate to give **60** in 76% (**Table 16**, entry 2). While not explicitly investigated, this methodology of deprotonation and cross-coupling is likely applicable to other ethers of varying activation.

---

[117] Zhang, L.; Si, X.; Yang, Y.; Zimmer, M.; Witzel, S.; Sekine, K.; Rudolph, M.; Hashmi, A. S. K. *Angew. Chem. Int. Ed.* **2019**, *58*, 1823–1827.
[118] Corey, E. J.; Eckrich, T. M. *Tetrahedron Lett.* **1983**, *24*, 3165–3168.

Table 16 – Deprotonation and Cross-Coupling α to Heteroatom[a]

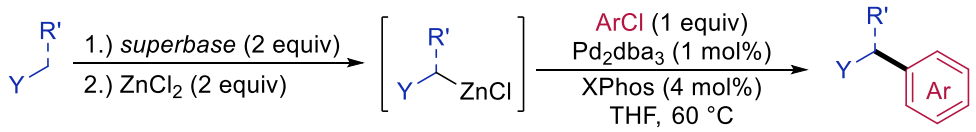

Entry	Substrate	Superbase Conditions	Product	Yield (%)
1	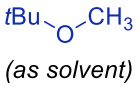 *(as solvent)*	KO*t*Bu, *s*-BuLi -78 °C, 2 h	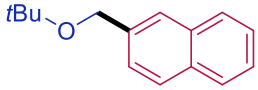 **59**	84%
2	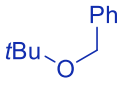 (2.5 equiv)	KO*t*Bu, *n*-BuLi THF, -40 °C, 15 min	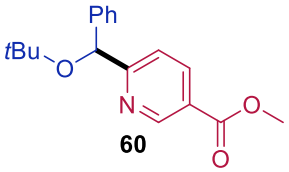 **60**	76%
3	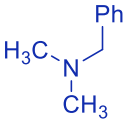 (2.5 equiv)	KO*t*Bu, *n*-BuLi THF, 0 °C, 15 min	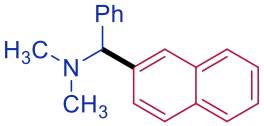 **61**	83%

[a]Reactions were run on 0.2 mmol scale of aryl halide. Yields reported after isolation by column chromatography.

Unlike α to oxygen, organometallic species α to nitrogen are destabilized by the proximity to the heteroatom.[119] Consequently, simple amines cannot be deprotonated in the same way as simple ethers. Instead, an azo derivative of benzyl *tert*butyl ether was investigated, such that the deprotonated species would be stabilized by conjugation with the phenyl group. Using literature deprotonation conditions,[120] *N*,*N*-dimethylbenzylamine was treated to our optimized benzyl zinc coupling conditions, providing an 83% yield of **61** when coupled with 2-chloronaphthalene **(Table 16**, entry 3). The C(sp^3)–H arylation of benzylamines is analogous to *N*-Boc pyrrolidine reported by Campos *et. al.* that was previously discussed in **Section 1.1.4**.[121] With sufficient activation,

[119] Hillis, L. R.; Ronald, *R. C. J. Org. Chem.* **1981**, *46,* 3349–3352.
[120] Maeda, Y.; Sato, Y. *J. Chem. Soc., Perkin Trans. 1*, **1997**, *10*, 1491-1493.
[121] Campos, K. R.; Klapars, A.; Waldman, J. H.; Dormer, P. G.; Chen, C. *J. Am. Chem. Soc.* **2006**, *128*, 3538–3539.

deprotonation and cross-coupling α to nitrogen can be achieved. By diversifying the class and position of the activating group relative to the site of acidity, the synthetic utility of this methodology is improved by formally expanding the scope of compatible pronucleophiles (**Scheme 43**).

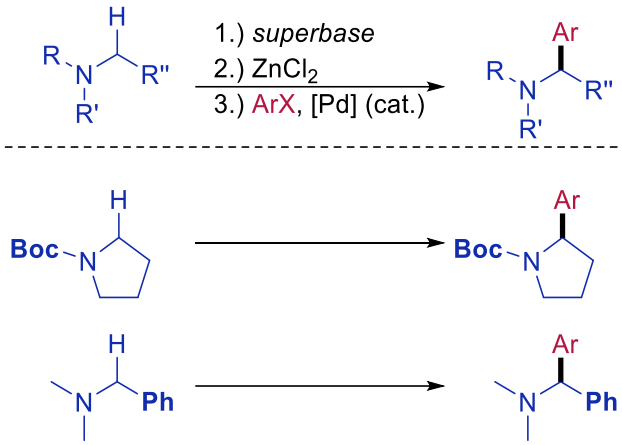

Scheme 43 – Unique Activating Groups for the Deprotonation and Cross-Coupling α to Nitrogen

The immediate successes of MTBE, BnO*t*Bu, and $BnNMe_2$ having provided facile $C(sp^3)$–H arylation using Schlosser's base were very promising. We therefore suspected that there were likely many other classes of substrate in the classical superbase literature that could be applied to this methodology. Unfortunately, some of the other substrate classes that were investigated were not functionalized so easily.

1.3.6: Unsuccessful Substrates Classes for C(sp^3)–H Deprotonation and Coupling

C(sp^3)–H bonds α to olefins were identified as an interesting class of substrate for this deprotonation and coupling methodology. There is lots of interest in the field of functionalizing allylic positions, particularly with radical chemistry.[122] In addition, one of Walsh's many contributions to the field of C(sp^3)–H deprotonation and cross-coupling is the functionalization of allyl benzenes (**Scheme 44**).[123] While interesting, this report highlights the benefit of activated olefin substrates, in which the presence of the aryl group acidifies the allylic C–H bond for deprotonation. We were therefore interested in the deprotonation and cross-coupling of truly unactivated allylic positions through a deprotonation and cross-coupling mechanism.

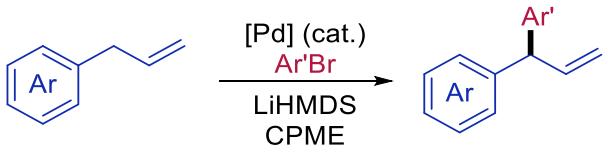

Scheme 44 – Deprotonation and Cross-Coupling of Allyl Benzenes

Jean-Danick E. Lavertu rigorously attempted to optimize the deprotonation of simple olefins. Unfortunately, he was unable to reproduce literature conditions that were transferable to cross-coupling. In addition, his attempts to use novel conditions also led to a range of side-products that are summarized in **Scheme 45**. A common problem he encountered was achieving selectivity between substrate deprotonation and solvent deprotonation. THF was consistently arylated, having a drastic influence on the yield of the reaction. Even when the deprotonation

[122] Wang, R.; Luan, Y.; Ye, M. *Chin. J. Chem.* **2019**, *37*, 720–743.
[123] Hussain, N.; Frensch, G.; Zhang, J.; Walsh, P. J. *Angew. Chem. Int. Ed.* **2014**, *53*, 3693–3697.

was incomplete (*i.e.* observed formation of the butylated aryl halide), solvent reactivity was still observed. This suggested there was an inherent competition between the two deprotonations, as opposed to the metalated olefin reacting with solvent if the deprotonation was run for too long.

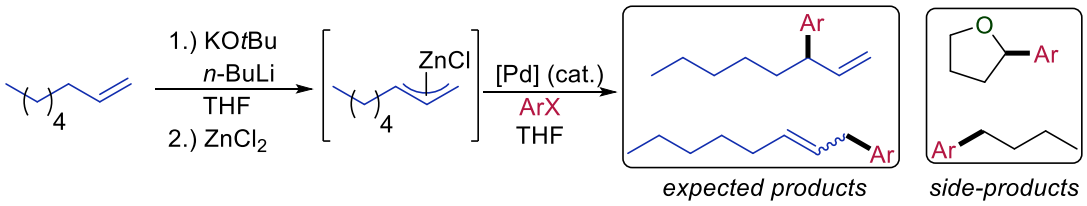

Scheme 45 – Products and Side-Products for Olefin Deprotonation and Cross-Coupling

Jean-Danick also observed a mixture of isomers when attempting to deprotonate and cross-couple 1-octene and other similar olefins. Once deprotonated, the allyl metallic species is presumably nucleophilic at two sites. However, with symmetrical olefins, the two sites are equivalent, and therefore should not have such selectivity issues (**Scheme 46**). Therefore, we investigated the functionalization of cyclohexene using a Schlosser's base slurry in an attempt to prevent solvent deprotonation and to bias the reaction towards a single isomer of the cross-coupled product.

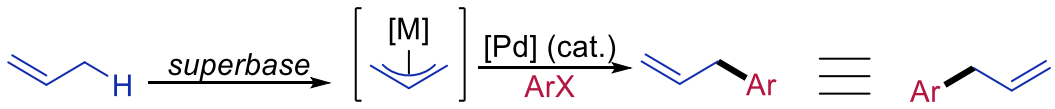

Scheme 46 – Improved Selectivity in the Deprotonation and Cross-Coupling of Symmetrical Olefins

Although the deprotonation of cyclohexene using a Schlosser's base slurry has been reported, applications are limited to simple S_N2 and 1,2-addition quenches.[124] Using the literature deprotonation conditions, our organozinc protocol outlined in **Section 1.3.3-1.3.5** led to no product being observed (**Table 17**, entry 1). Furthermore, significant recovery of aryl halide was observed by GC-MS, suggesting possible nucleophile decomposition. We hypothesized this decomposition was occurring via deprotonation of the THF in the $ZnCl_2$ stock solution. However, cooling the deprotonation mixture to -78 °C prior to the addition of the $ZnCl_2$ solution provided the same result (entry 2).

Table 17 – Cyclohexene Deprotonation and Coupling

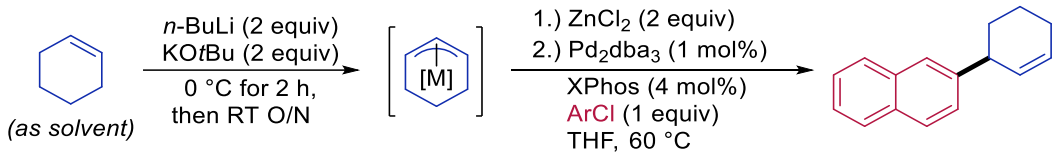

Entry	Deviation from Standard Conditions	Yield (%)[a]
1	None	0
2	$ZnCl_2$ added at -78 °C	0
3	$ZnCl_2$ added in 2-MeTHF	0
4	$ZnCl_2$·TMEDA instead of in THF	0

[a]Reactions were run on a 0.1 mmol scale of aryl halide. 0% yield indicate the product was not observed by GC-MS or ^{1}H NMR.

The $ZnCl_2$ quench was also done using a stock solution in 2-MeTHF, which has been shown to be less prone to metalation by superbases.[125] Unfortunately, this also led to no conversion of aryl halide (entry 3). To add the zinc chloride in the absence of ethereal solvent, a TMEDA complex

[124] Wu, Z.; Fatuzzo, N.; Dong, G. *J. Am. Chem. Soc.* **2020**, *142* (6), 2715–2720.
[125] Lee, H.; Kim, H.; Kim, D. *Chem. Eur. J.* **2019**, *25*, 11641–11645.

of $ZnCl_2$ was used, which has been shown to be more soluble in hydrocarbon solvents.[126] However, this also led to 0% yield of the cross-coupled product (entry 4). With this set of experiments leading to no trace of the desired allylic C(sp^3)–H arylation product, in addition to Jean-Danick Lavertu's work, attempts to deprotonate and couple allylic positions were halted here.

As previously mentioned in **Section 1.1.3**, thioansiole is precedented to undergo selective lithiation by an *n*-BuLi/DABCO superbase.[127] Using the established conditions, thioanisole was deprotonated and quenched with benzophenone (**Table 18**, entry 1). This provided an 88% yield of the desired product with no observed formation of the 1,2-addition adduct between *n*-BuLi and benzophenone. Unfortunately, this deprotonation did not seamlessly transfer to cross-coupling. After deprotonation and quench with $ZnCl_2$, cross-coupling of the corresponding organozinc of thioanisole led to no conversion of aryl halide (entry 2), again suggesting possible nucleophile decomposition. If a carbon-metal bond is adjacent to a sufficiently good leaving group, the species can undergo elimination to form the corresponding carbene,[128] effectively decomposing the organometallic. In the case of thioanisole, this would form methylene and lithium thiophenolate (**Scheme 47a**). In an attempt to prevent this possible decomposition, the coupling was performed using milder conditions, in which the organozinc was added to the coupling mixture at 0 °C, then slowly warmed to room temperature overnight. Unfortunately this also led to no product being observed (entry 3).

---

[126] Asako, S.; Nakajima, H.; Takai, K. *Nat. Catal.* **2019**, *2*, 297–303.
[127] Epiotis, N. D.; Yates, R. L.; Bernardi, F.; Wolfe, S. *J. Am. Chem. Soc.* **1976**, *98*, 5435–5439.
[128] Ishii, S.; Zhao, S.; Mehta, G.; Knors, C. J.; Helquist, P. *J. Org. Chem.* **2001**, *66*, 3449–3458.

Table 18 – Deprotonation and Cross-Coupling of Thioanisole

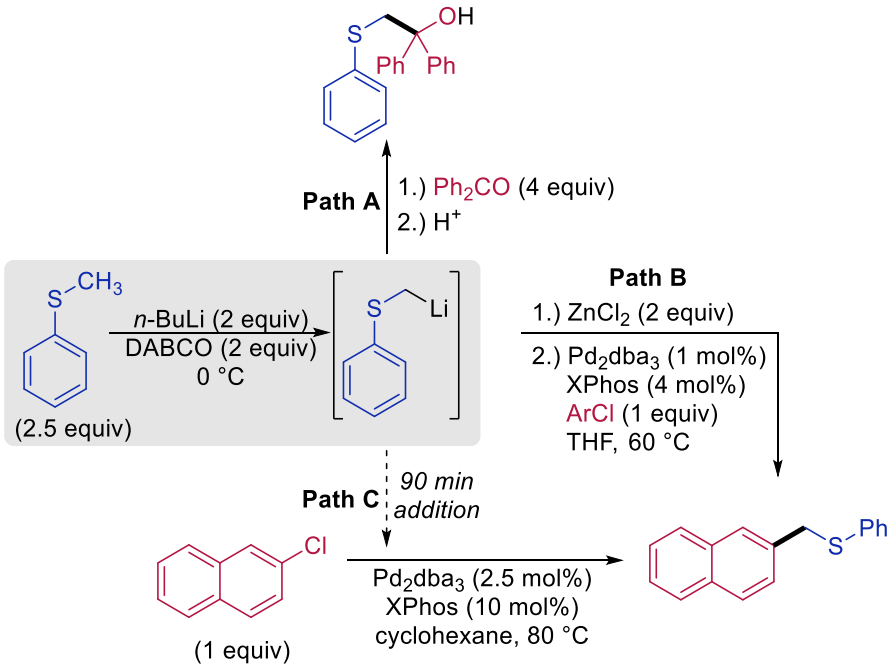

Entry	Path	Deviation from Standard Conditions	Yield (%)[a]
1	A	None	88
2	B	None	0
3	B	Couple at 0 °C to RT	0
4	C	None	0
5	C	Couple at RT; ArBr used instead of ArCl	0

[a]Reactions were run on a 0.1 mmol of electrophile. Yield is reported by ^{1}H NMR relative to 1,3,5-trimethoxybenzene as an internal standard. 0% yield indicates no product was observed by GC-MS or ^{1}H NMR.

When coupling of the corresponding organolithium of $PhSCH_3$ was attempted, no product was observed once again (**Table 18**, entry 4). Instead, a compound consistent with 2-naphthyl phenyl sulfide was observed by GC-MS (m/z of 236), suggesting the decomposed nucleophile participated in the cross-coupling (**Scheme 47b**). This side-product is not particularly interesting, as it could be prepared more easily by the precedented deprotonation and coupling of

thiophenol.[129] Milder organolithium coupling conditions were then tested, in which 2-bromonaphthalene was used and the coupling was performed at room temperature. Unfortunately, this also led to no product formation with substantial amounts of recovered aryl halide detected by GC-MS (**Table 18**, entry 5). With the suspected instability of metalated thioanisole, attempts to deprotonate and couple this substrate were stopped here.

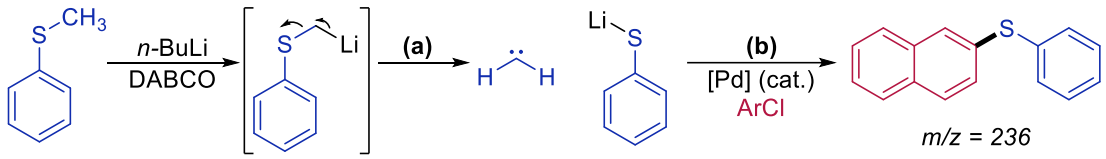

Scheme 47 – Plausible Mechanism for the Deprotonation, Decomposition, and Cross-Coupling of Thioanisole

The failed substrate classes of α to olefin and α to sulfur suggest possible limitations to this deprotonation and cross-coupling methodology. Just because a precedented deprotonation is facile, does not mean the subsequent cross-coupling is possible. The instability of the deprotonated species in the form of an "ate" complex, an organolithium, or the corresponding organozinc, may prevent the coupling from being successful. In much of the classical literature, deprotonation and electrophilic quench were done cryogenically to prevent side reactivity.[130] This may suggest cryogenic temperatures could be a suitable approach for the cross-coupling of unstable organometallic nucleophiles generated by the C(sp^3)–H deprotonation by superbases.

[129] Itoh, T.; Mase, T. *Org. Lett.* **2004**, *6*, 4587–4590.
[130] Clayden, J. Organolithiums: Selectivity for Synthesis, 1st ed.; Tetrahedron Organic Chemistry; Pergamon, 2002; Vol. 23

1.3.7: Cross-Coupling of Superbase-Generated Benzyl Lithiums with Aryl Fluorides

During the optimization of the direct benzyl lithium cross-coupling discussed in **Section 1.3.2**, poor yields likely stemming from LHE presented a significant challenge. We hypothesized that the use of aryl fluorides as electrophilic coupling partners could help with this, as the strong Ar–F bond should make LHE less competitive. However, the strength of this bond has a history of making activation of aryl fluorides nearly impossible with palladium, but possible with nickel. Using a precedented nickel catalyst for Ar–F activation,[131] the direct cross-coupling of benzyl lithium with aryl fluorides was investigated (**Table 19**).

Table 19 – Optimization of Benzyl Lithium Coupling with Aryl Fluorides[a]

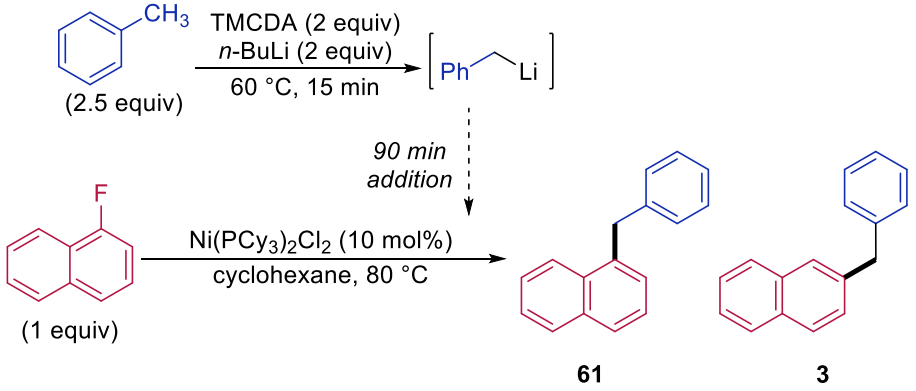

Entry	Deviation from Standard Conditions	Yield of **61** (%)	Yield of **3** (%)
1	None	38	7
2	No catalyst	24	26
3	4h addition	8	Trace

[a]Reactions were run on 0.1 mmol of aryl halide. Yields reported ^{1}H NMR relative to 1,3,5-trimethoxy benzene as an internal standard. Trace yield indicates product was detected by GC-MS, but calculated yield was < 1 %.

[131] Zhu, F.; Wang, Z.-X. *J. Org. Chem.* **2014**, *79*, 4285–4292.

After the deprotonation of toluene using our optimized *n*-BuLi/TMCDA conditions, benzyl lithium was added over 1.5 hours to a mixture of 1-fluoronaphthelene and $Ni(PCy_3)_2Cl_2$ catalyst in cyclohexane at 80 °C. This led to a yield of 38% of **61** (**Table 19**, entry 1). Interestingly, although 1-fluoronaphthalene was used as the electrophilic coupling partner, 7% of the 2- isomer **3** was observed, suggesting a competitive pathway had taken place. By deprotonating ortho to the C–F bond using BnLi, an elimination reaction to displace fluoride could form 1-naphthyne. Upon subsequent attack by another equivalent of BnLi, the formal cross-coupled product could form as a mixture of isomers (**Scheme 48**). Assuming the two electrophilic sites of the naphthyne are approximately equally reactive, this would lead to a 1:1 mixture of isomers if this proposed mechanism was followed exclusively.

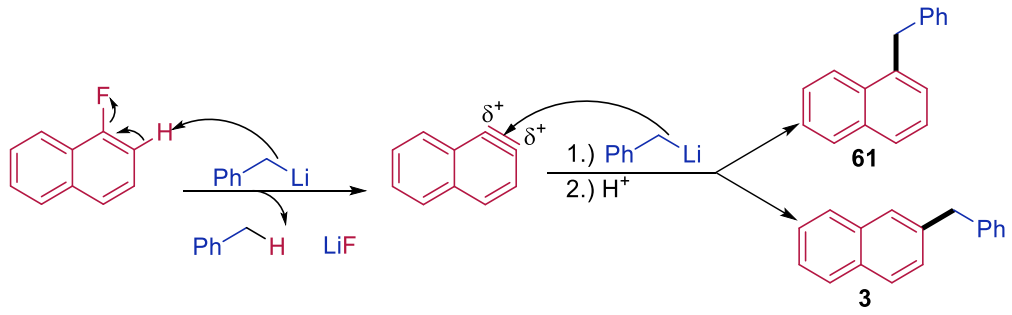

Scheme 48 – Proposed Naphthyne Mechanism in Benzyl Lithium Coupling with Aryl Fluorides

In the absence of catalyst, an approximate 1:1 mixture of isomers was observed with 24% yield of **61** (**Table 19**, entry 2), helping to validate the proposed mechanism. Since we suspected naphthyne to form by the BnLi reacting directly with aryl fluoride, a longer slow addition was suspected be beneficial, similar to what was observed with the coupling of aryl chlorides. However, although increasing the duration of the BnLi addition to 4 hours drastically improved the selectivity of the desired isomer, the yield decreased to 8% (entry 3). Significant aryl fluoride

was observed by GC-MS (m/z of 146), suggesting nucleophile decomposition. If small leaks were present in the slow addition apparatus, extended reaction times could enable atmospheric moisture to permeate into the reaction and quench the benzyl lithium.

Although aryl fluorides were found to be beneficial in helping to prevent competitive LHE, they provided poor regioselectivity due to a competitive benzyne mechanism. We therefore saw little benefit of the strong Ar–F bond in the direct cross-coupling of benzyl lithiums. Consequently, this approach was not investigated further.

1.3.8: Conclusions and Future Outlooks

By merging modern transition metal-catalyzed cross-coupling with classical superbase chemistry, we have demonstrated the selective C(sp^3)–H arylation of unactivated benzylic positions. Using novel deprotonation conditions to enable non-solvent quantities of substrate, primary benzyl lithiums could be prepared *in situ* for the first-of-their-kind use in palladium-catalyzed cross-coupling. While benzyl lithium coupling is believed to have inherent functional group limitations on the electrophilic coupling partner, proceeding through an *in situ* benzyl zinc enabled the synthesis of complex products without the stringent need for nucleophile slow addition. The preparation of drug derivatives and deuterated products demonstrates the potential uses of this transformation in the fine chemical industry.

Furthermore, we demonstrated this deprotonation, transmetallation with zinc chloride, and cross-coupling methodology is suitable for an array of substrate classes, including secondary benzylic, α to oxygen, and α to nitrogen. The intermolecular cross-coupling of unactivated, undirected C(sp^3)–H bonds using non-solvent quantities of substrates improves upon some of the biggest limitations of modern C–H activation. This approach remains to be applied to much of the classical superbase literature, which could enable the cross-coupling of even more diverse nucleophiles. However, we suspect some metalated substrate classes are prone to decomposition, including α to olefin and α to sulfur. Cryogenic coupling conditions may provide reactivity without possible nucleophile decomposition.

Lastly, if kinetic resolution were to be applied to the deprotonation and cross-coupling of secondary benzylic positions or other prochiral pronucleophiles, the chemistry developed in this chapter may be suitable for the formation of enantio-enriched products (**Scheme 49**). Using a

chiral ligand on the palladium catalyst (PdL*), one enantiomer of the racemic nucleophile generated by deprotonation may be able to react preferentially in the transmetallation step. In fact, an enantio-convergent variant of the work previously discussed by Campos[132] was subsequently reported by Fu[133] using this chiral ligand approach. Incorporating asymmetric catalysis into our deprotonation and coupling methodology would further validate its synthetic utility in complex molecule synthesis.

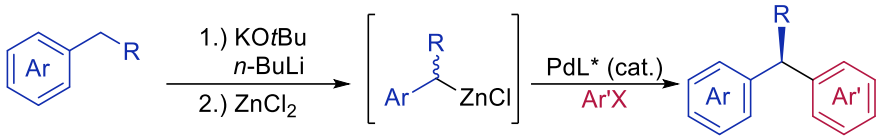

Scheme 49 – Potential Kinetic Resolution of Secondary Benzyl Zincs

With Chapter 1 largely focusing on novel nucleophile generation for transition metal-catalyzed cross-coupling, Chapter 2 will focus on expanding the scope of possible cross-coupling electrophiles.

[132] Campos, K. R.; Klapars, A.; Waldman, J. H.; Dormer, P. G.; Chen, C. *J. Am. Chem. Soc.* **2006**, *128*, 3538–3539.
[133] Cordier, C. J.; Lundgren, R. J.; Fu, G. C. *J. Am. Chem. Soc.* **2013**, *135*, 10946–10949.

Chapter 2: Nickel-Catalyzed Suzuki-Miyaura Coupling of Silyl Enol Ethers

2.1: Introduction

2.1.1: Converting Ketones to Substituted-Olefins with Cross-Coupling

Many examples of converting ketones to substituted olefins with cross-coupling have been reported, usually through multi-step synthesis (**Scheme 50**). Starting from a ketone, an activated vinyl (pseudo)halide species can be prepared, most commonly a vinyl triflate. The weak C–X bond can enable the vinylic species to act as an electrophilic coupling partner. When coupled with an appropriate nucleophile, this chemistry can form highly-substituted olefin products. This methodology is frequently used in medicinal chemistry because of its reliable and robust nature, thus highlighting the importance of highly-substituted olefins in biologically-relevant compounds.

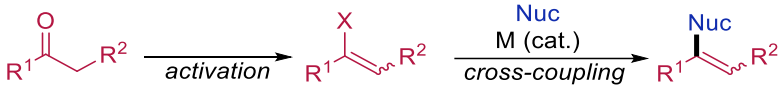

Scheme 50 – Generic Ketone-to-Substituted-Olefin Sequence in Cross-Coupling

For example, Inoue *et. al.* converted a complex ketone into a substituted olefin for the total synthesis of 1-hydroxytaxinine (**Scheme 51**).[134] Preparation of the olefin required a three-step synthesis; first was to convert ketone **63** to hydrazone **64** using stoichiometric hydrazine. Next, treatment with molecular iodine formed the corresponding vinyl iodide **65**. Lastly, the use of a palladium catalyst with methyl acrylate enabled a Mizoroki-Heck reaction to form the

[134] Imamura, Y.; Yoshioka, S.; Nagatomo, M.; Inoue, M. *Angew. Chem. Int. Ed.* **2019**, *58*, 12159–12163.

substituted olefin **66**, which in this case, was also a diene. This substituted olefin moiety was retained in the final structure of the bioactive 1-hydroxytaxinine **67**.

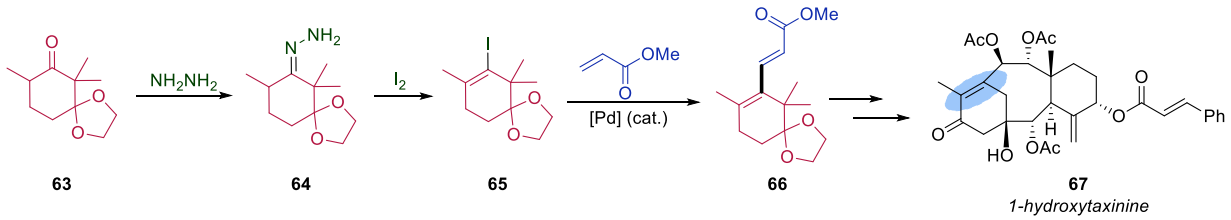

Scheme 51 – Ketone-to-Substituted-Olefin in the Synthesis of 1-hydroxytaxinine

In contrast to the previous example, activated vinyl triflate intermediates can be prepared in a one-step synthesis from ketones. For example, O'Donnell and coworkers treated ketone **68** with bis(trifluoromethanesulfonyl)aniline and LiHMDS to form vinyl triflate **69** directly (**Scheme 52**).[135] The resultant vinyl triflate was then used in the palladium-catalyzed Suzuki-Miyaura coupling to form substituted olefin **70**, with this moiety retained in the final product Pibrestasvir (VI) **71**.

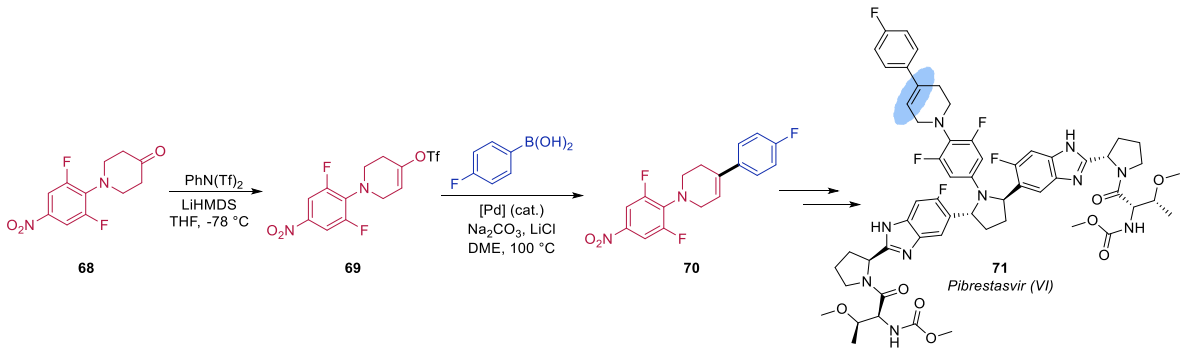

Scheme 52 – Ketone-to-Substituted-Olefin in the Synthesis of Pibrestasvir (VI)

[135] Flick, A. C.; Leverett, C. A.; Ding, H. X.; McInturff, E.; Fink, S. J.; Helal, C. J.; O'Donnell, C. J. *J. Med. Chem.* **2019**, *62*, 7340–7382.

Another example of multi-step synthesis for converting ketones to substituted olefins in cross-coupling was reported by the Snyder group (**Scheme 53**).[136] In this case, the authors again converted ketone **72** to hydrazone **73** using a stoichiometric hydrazine derivative. This intermediate was then alkylated at the α relative to the hydrazone via simple deprotonation and electrophilic quench to form hydrazone **74**. Next, triflation using *N*-(5-chloro-2-pyridyl)bis(trifluoromethanesulfonimide), also known as Comins' reagent, formed vinyl triflate **75**. Finally, a palladium-catalyzed Mizoroki-Heck-like cyclization was carried out which simultaneously acetylated the olefin to form **76**. This chemistry was used in the total synthesis of Conidgenone C and D, which differ by the stereochemistry at the indicated chiral center of **77**. In contrast to the previous examples discussed, this synthesis does not retain the olefin in the final bioactive compound, as it is subsequently derivatized in a later step of the synthesis.

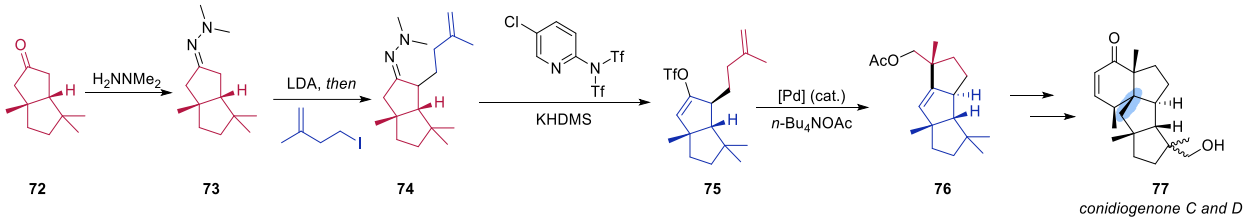

Scheme 53 – Ketone-to-Substituted-Olefin in the Synthesis of Conidgenone C and D

Somovilla *et. al.* also used Comins' reagent for the key triflation step (**Scheme 54**).[137] Treatment of α-amino ketone **78** with this reagent formed vinyl triflate **79**. Subsequent palladium-catalyzed Sonogashira coupling with trimethylsilylacetylene formed substituted olefin **80**. In this

[136] Hu, P.; Chi, H. M.; DeBacker, K. C.; Gong, X.; Keim, J. H.; Hsu, I. T.; Snyder, S. *Nature* **2019**, *569*, 703–707.
[137] Quiñones-Reyes, G.; Agulló, C.; Mercader, J. V.; Abad-Somovilla, A.; Abad-Fuentes, A. *Angew. Chem. Int. Ed.* **2019**, *58*, 9134–9139.

case, the intermediate is a conjugated enyne, with the olefin being retained at the end of the total synthesis of a variety of cyanotoxins, including **81.**

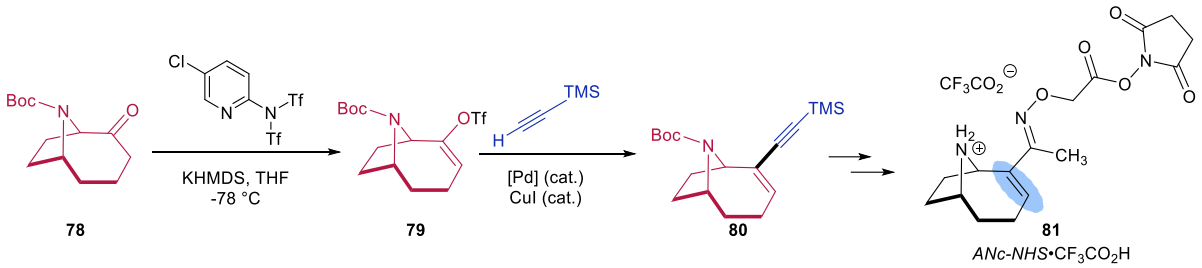

Scheme 54 – Ketone-to-Substituted-Olefin in the Synthesis of Cyanotoxins

Less activated vinyl derivatives can also be used for ketone activation in cross-coupling. The So group reported the use of dimethylcarbamyl chloride to convert ketone **82** into a mixture of *E* and *Z* vinyl carbamates **83** (**Scheme 55**).[138] After separation, each of these isomers then underwent palladium-catalyzed Kumada-Corriu coupling with an aryl Grignard reagent to form *(E)* and *(Z)* Tamoxifen **84**. Therefore, this chemistry of converting ketones to substituted-olefins using cross-coupling can be the key step in the synthesis of biologically-relevant compounds.

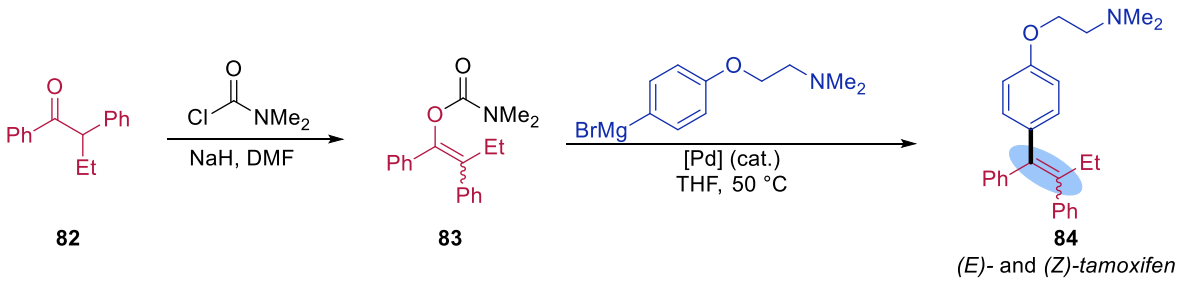

Scheme 55 – Ketone-to-Substituted-Olefin in the Synthesis of (E) and (Z) Tamoxifen

[138] Chen, Z.; So, C. M. *Org. Lett.* **2020**, *22*, 3879–3883.

All of the aforementioned examples take advantage of a palladium catalyst to oxidatively insert into the relatively weak C–X bond of vinyl (pseudo)halides. However, nickel has also been used, which can enable the oxidative addition into less activated intermediates. For example, the Shi group reported the nickel-catalyzed Suzuki-Miyaura coupling of vinyl acetates (**Scheme 56**).[139] With a representative scope example showing this chemistry's versatility in the synthesis of biologically-relevant compounds, treatment of estrone **85** with *iso*propenyl acetate formed the corresponding steroidal vinyl acetate **86**. Subsequent treatment with a nickel catalyst and an organoboron reagent formed a cross-coupled steroid derivative **87**. Unfortunately, this cross-coupling provided a modest yield of 43%, suggesting less activated vinyl ether species are difficult to implement in cross-coupling, even in the presence of a nickel catalyst.

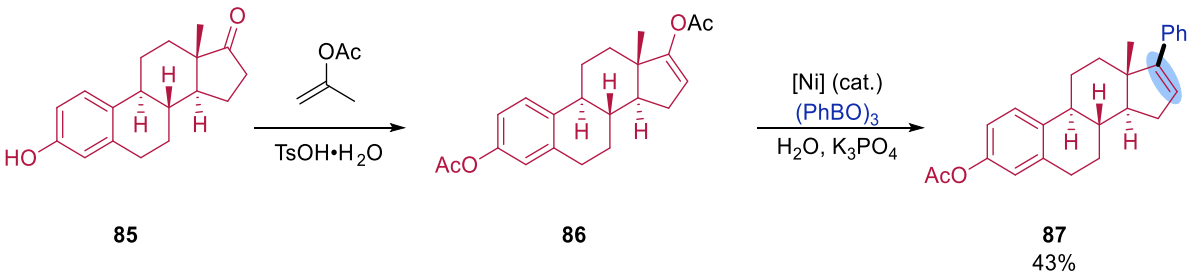

85 **86** **87**
43%

Scheme 56 – Ketone-to-Substituted-Olefin in the Derivatization of Estrone

While these examples highlight the utility of this chemistry in the synthesis of bioactive compounds, in general, this approach is very inefficient. Converting ketones to substituted-olefins using multi-step synthesis requires isolation of the activated C–X intermediate. Whether it's a vinyl- iodide, triflate, carbamate, or acetate, adding an extra step to a synthesis usually decreases overall yield. In some cases, the synthesis of these vinyl (pseudo)halides requires multi-step

[139] Sun, C.-L.; Wang, Y.; Zhou, X.; Wu, Z.-H.; Li, B.-J.; Guan, B.-T.; Shi, Z.-J. *Chem. Eur. J.* **2010**, *16*, 5844–5847.

syntheses just for the preparation of the intermediate that will subsequently undergo cross-coupling, further highlighting the synthetic inefficiency. Also, the preparation of these activated intermediates frequently suffers from poor atom economy because of the required reagents. For example, in addition to being relatively expensive, bis(trifluoromethanesulfonyl)aniline and Comins' reagent have high molecular weight and are required stoichiometrically. Because the vinyl triflate is used solely as an activated intermediate, the C–OTf functional group does get incorporated into the cross-coupled product, thus hindering the atom economy of these syntheses.

Since the preparation of these vinyl (pseudo)halides provides a weak C–X bond for cross-coupling, these intermediates are usually not very well behaved. Sensitive functional groups such as vinyl triflates are very prone to decompose under a variety of reaction conditions. This is exemplified by the fact that in all of the aforementioned examples, the activated vinyl species were prepared in the step immediately before cross-coupling. This therefore limits this method of ketone functionalization to linear syntheses.

In contrast, divergent synthesis could be enabled by the use of a more stable protected vinyl species (**Scheme 57**). By balancing reactivity and stability, a protected enol could potentially be selectively activated for cross-coupling, while still being robust enough to tolerate a variety of reaction conditions for other functional group manipulations. Divergent syntheses generally provide improved efficiency relative to linear syntheses; by being able to form significantly different products from the same precursor, a variety of structurally-complex scaffolds can be obtained more easily.

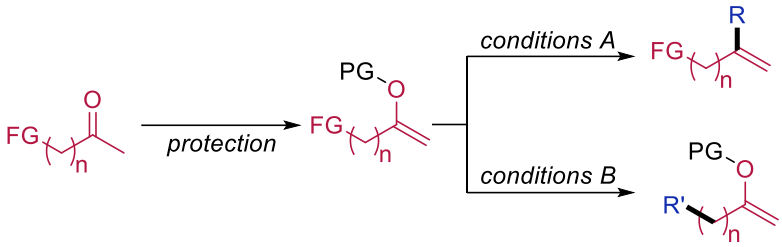

Scheme 57 – Potential Divergent Synthesis in the Cross-Coupling of Protected Enols

An alternative method for converting ketones to olefins without requiring an activated intermediate has also been established. Rather than oxidative addition into a vinylic species, the Zhou group demonstrated ketone activation involving a nickel catalyst undergoing oxidative cyclization into the C=O bond to form a metallacycle (**Scheme 58**).[140] Consequently, the issues of poor atom economy and reduced yield due to multi-step synthesis that were previously discussed can be largely avoided. However, this chemistry is mostly limited to aryl ketones, as most dialkyl ketones led to a mixture of regio- and stereo- isomers.

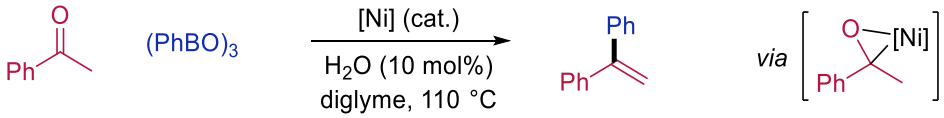

Scheme 58 – Metallacycle Mechanism of Ketone Activation in Cross-Coupling

Overall, while these reports of converting ketones to substituted-olefins have their benefits and medicinal chemistry applications, they are largely limited by inefficient multi-step synthesis and/or poor selectivity.

[140] Lei, C.; Yip, Y. J.; Zhou, J. S. *J. Am. Chem. Soc.* **2017**, *139*, 6086–6089.

2.1.2: Activation of Strong C–O Bonds as Electrophiles

The nickel-catalyzed activation of strong C–O bonds is a field of significant interest in modern synthetic organic chemistry.[141] The prevalence of oxygen in organic compounds makes C–O bonds obvious candidates for their use as electrophiles in metal-catalyzed cross-coupling. Furthermore, strong bond activation can enable late-stage functionalization, as functional groups that were untouched in earlier synthetic steps can be taken advantage of for further derivatization. For example, the nickel-catalyzed cross-coupling of anisoles has been reported with a variety of nucleophilic coupling partners, such as Suzuki-Miyaura coupling with organoborons,[142] Buchwald-Hartwig amination with secondary amines,[143] and alkylations with organoaluminums[144] (**Scheme 59a**). This chemistry generally takes advantage of traditional oxidative addition into the strong C–O bond.

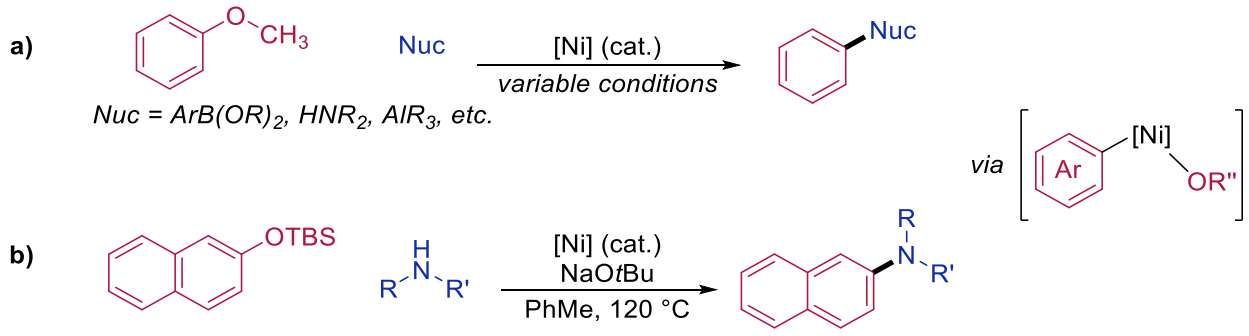

Scheme 59 – Activation of Strong C–O Bonds in Nickel-Catalyzed Cross-Coupling

---

[141] Rosen, B. M.; Quasdorf, K. W.; Wilson, D. A.; Zhang, N.; Resmerita, A.-M.; Garg, N. K. ; Percec, V. *Chem. Rev.* **2011**, *111*, 1346–1416.
[142] Tobisu, M.; Shimasaki, T.; Chatani, N. *Angew. Chem. Int. Ed.* **2008**, *47*, 4866–4869.
[143] Tobisu, M.; Shimasaki, T.; Chatani, N. *Chem. Lett.* **2009**, *38*, 710–711.
[144] X. Liu, C. Hsiao, I. Kalvet, M. Leiendecker, L. Guo, F. Schoenebeck, M. Rueping, *Angew. Chem. Int. Ed.* **2016**, *55*, 6093–6098.

In a similar vein, the Montgomery group reported the use of TBS-protected phenol derivatives as cross-coupling electrophiles for Buchwald-Hartwig amination (**Scheme 59b**).[145] However, this report is mostly limited to activated electrophilic coupling partners with extended conjugation of the aryl ring to promote oxidative addition, such as naphthyl- and biphenyl- type silyl ethers. Interestingly, the Montgomery group also demonstrated their conditions for silyl ether cross-coupling are complementary to the alkylative anisole activation conditions described by Rueping. Because of their unique respective reaction conditions, C–O functionalization can occur selectively at either the Ar–OTBS or Ar–OMe of a doubly-functionalized substrate (**Scheme 60**). This divergent synthesis emphasizes one of the benefits of the activation of robust cross-coupling electrophiles. Because the respective strong C–O bonds are tolerant to a variety of reaction conditions, significantly different cross-coupled products can be generated from the same precursor, thus enabling more efficient syntheses.

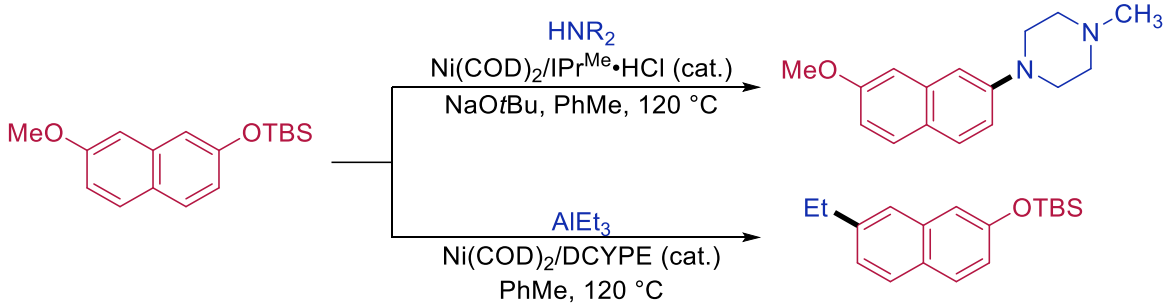

Scheme 60 – Divergent Synthesis of Silyl Ethers and Alkyl Ethers as Cross-Coupling Electrophiles

As previously mentioned in **Section 2.1.1**, the C–O activation of robust protected enol derivatives could have potential applications in divergent synthesis. More specifically, silyl enol ethers have been used as robust protecting groups for carbonyls as well as their nucleophilicity

[145] Wiensch, E. M.; Todd, D. P.; Montgomery, J. *ACS Catal.* **2017**, *7*, 5568–5571.

at the α position. This dual nature of silyl enol ethers has been taken advantage of in the total synthesis of a variety of natural products.[146] Therefore, activation of the strong C–O bond of silyl enol ethers in cross-coupling could have significant utility in improving synthetic efficiency.

To our knowledge, established methods for the use of silyl enol ethers as cross-coupling electrophiles are limited exclusively to Kumada-Corriu coupling. For example, in 1980, Kumada reported the cross-coupling of a variety of dialkyl silyl enol ethers with alkyl- and aryl- Grignard reagents in the preparation of highly-substituted olefins (**Scheme 61a**).[147] Years later, Shi reported a similar transformation, though their scope was quite limited to only a couple of substrate examples (**Scheme 61b**).[148] While these are interesting transformations, they both suffer from the use of aggressive nucleophilic coupling partners. Grignard reagents are inherently quite nucleophilic and basic, thus limiting the scope of compatible functional groups on the silyl ether.

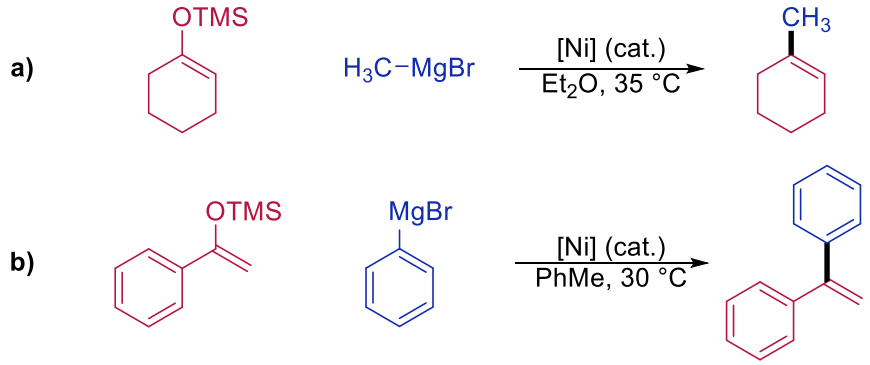

Scheme 61 – Nickel-Catalyzed Kumada-Corriu Coupling of Silyl Enol Ethers

---

[146] a) Alonso, D.; Caballero, E.; Medarde, M.; Tomé, F. *Tetrahedron Lett.* **2005**, *46*, 4839–4841.
b) Lee, G. S.; Namkoong, G.; Park, J.; Chen, D. Y. -K. *Chem. Eur. J.* **2017**, *23*, 16189–16193.
c) Nicolaou, K.C.; Jautelat, R.; Vassilikogiannakis, G.; Baran, P. S.; Simonsen, K. B. *Chem. Eur. J.* **1999**, *5*, 3651–3665.
[147] Hayashi, T.; Katsuro, Y.; Kumada, M. *Tetrahedron Lett.* **1980**, *21*, 3915–3918.
[148] Zhao, F.; Yu, D.-G.; Zhu, R.-Y.; Xi, Z.; Shi, Z.-J. *Chem. Lett.* **2011**, *40*, 1001–1003.

There are also examples of other silicon protecting groups enabling strong C–O bond activation outside of the realm of cross-coupling. For example, the Fussell group reported the use of $Si(OMe)_4$ as an in situ protecting group for carboxylic acids to enable subsequent amidation by the use of an amine nucleophile (**Scheme 62a**).[149] This under-studied reagent protects the carboxylic acid that would otherwise participate in unproductive side-reactions. For instance, upon deprotonation, the resultant carboxylate is prone to decarboxylation to form a nucleophilic carbanion intermediate. Furthermore, by protection as the silyl ester, the electrophilicity of the C–O bond is increased relative to the carboxylic acid because of the relative stability of $(MeOSi)_3O^-$ and hydroxide as leaving groups. Charette reported the use of a different silicon reagent in an analogous transformation (**Scheme 62b**).[150] A similar mechanism was proposed involving another activated silylated carboxylate intermediate. Furthermore, this chemistry was implemented in the formation of key linkages between amino acid residues without a loss of enantiomeric excess, thus showing its applications in the synthesis of biologically-relevant compounds.

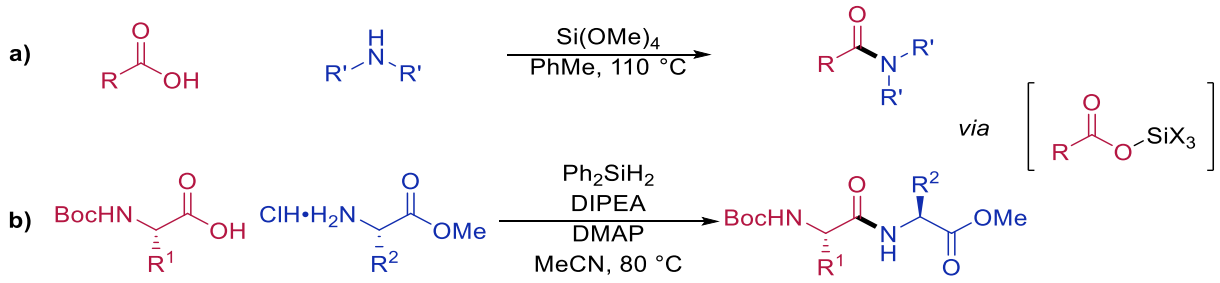

Scheme 62 – Use of Silicon Protecting Groups in Carboxylic Acid C–O Activation

[149] Braddock, D. C.; Lickiss, P. D.; Rowley, B. C.; Pugh, D.; Purnomo, T.; Santhakumar, G.; Fussell, S. J. *Org. Lett.* **2018**, *20*, 950–953.
[150] Sayes, M.; Charette, A. B. *Green Chem.* **2017**, *19*, 5060–5064.

Although not transition metal-catalyzed cross-coupling, these reports outline the use of silicon reagents as *in situ* protecting groups in strong C–O bond activation. Furthermore, the Weix group reported the use of chlorotriethylsilane and related silicon reagents in a nickel-catalyzed reductive cross-coupling for the preparation of substituted silyl enol ethers (**Scheme 63**).[151] This therefore indicates ketone silylation conditions and nickel-catalyzed cross-coupling conditions can be complementary and not inherently incompatible.

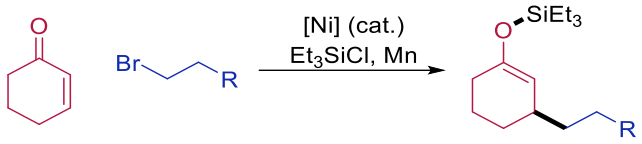

Scheme 63 – Tolerance of Silylating Agents in Nickel-Catalyzed Cross-Coupling

[151] Huihui, K. M. M.; Shrestha, R.; Weix, D. J. *Org. Lett.* **2017**, *19*, 340–343.

2.1.3: Project Goals

We hypothesized that a few of the reports discussed thus far could be combined and expanded upon. Although converting ketones to substituted-olefins is an invaluable tool in the synthesis of bioactive compounds, this chemistry is greatly limited by the poor atom economy of the required activating agents, poor overall yields stemming from multi-step syntheses, and the implementation of divergent syntheses being largely prohibited because of the instability of the activated vinyl (pseudo)halide intermediates. Relative to vinyl triflates, the C–O cross-coupling of more robust silyl enol ethers is very scarce, and to our knowledge, has only been reported in Kumada-Corriu coupling. The poor chemoselectivity of aggressive Grignard reagents severely limits the scope of products that can be made with this method. If these types of electrophiles could be used in Suzuki-Miyaura coupling, the functional group tolerance could likely be greatly improved. The discussed literature precedent for strong C–O bond activation in nickel-catalyzed cross-coupling could provide useful information for the functionalization of largely inert silyl enol ethers.

Furthermore, the reports by Fussell, Charette, and Weix suggest the possibility of forming activated silyl-protected substrates in situ, potentially enabling the conversion of ketones to substituted olefins in one step (**Scheme 64**). Alternatively, a one-pot/two-step approach could be suitable for first converting ketones to silyl enol ethers, and subsequently cross-coupling them without isolating the intermediate. Although the formal Suzuki-Miyaura coupling of ketone-to-substituted-olefin has already been reported by Zhou, the mechanism is inherently flawed, frequently providing poor regio- and stereo- selectivity. In contrast, the selective formation of

vinyl (pseudo)halides from ketones is well established, and has been implemented in cross-coupling for the formation of olefins with high selectivity.[152]

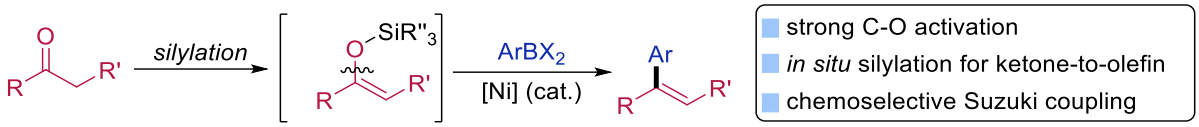

Scheme 64 – Project Goals for the Nickel-Catalyzed Suzuki-Miyaura coupling of Silyl Enol Ethers

We therefore sought to discover a nickel-catalyzed Suzuki-Miyaura coupling of silyl enol ethers. Once optimized, a potential *in situ* or 1-pot/2-step approach to silylation and cross-coupling could then be investigated. This chemistry could therefore enable the efficient synthesis of substituted-olefins from ketones with high chemo-, regio-, and stereo- selectivity.

[152] Poirier, J.-M. *Org. Prep. Proced. Int.* **1988**, *20*, 317–369.

2.2: Results and Discussion

2.2.1: Discovery and Optimization of the Suzuki-Miyaura Coupling of Silyl Enol Ethers

Reaction conditions were screened to discover a nickel-catalyzed Suzuki-Miyaura coupling of silyl enol ethers. For each of a diverse range of electrophilic coupling partners, a series of 7 experiments were performed, varying ligand, base, and additive. For fixed variables, Ni(COD)2 was chosen to be the pre-catalyst as it is known to readily interact with strong σ donor ligands.[153] Toluene was chosen as the solvent because of its frequent use in cross-coupling as well as having a relatively high boiling point, enabling an elevated reaction temperature of 110 °C which was suspected to be beneficial in the desired strong bond activation. Lastly, phenyl boronic acid was used as the nucleophilic Suzuki-Miyaura coupling partner, as it is commercially available, inexpensive, and air-stable. The choice of ligands was inspired from the literature discussed in **Section 2.1.2**. We hypothesized that ligands frequently used in nickel-catalyzed cross-coupling of strong C–O bonds could be beneficial in the activation of inert silyl enol ethers. A relatively diverse range of phosphine and NHC ligands were screened, including PCy_3, DPPP, DCYPE, and IPr·HCl. The structure of these ligands as well as the fixed variables are illustrated in **Scheme 65**.

[153] Tran, V. T.; Li, Z.; Apolinar, O.; Derosa, J.; Joannou, M. V.; Wisniewski, S. R.; Eastgate, M. D.; Engle, K. M. *Angew. Chem. Int. Ed.* **2020**, *59*, 7409–7413.

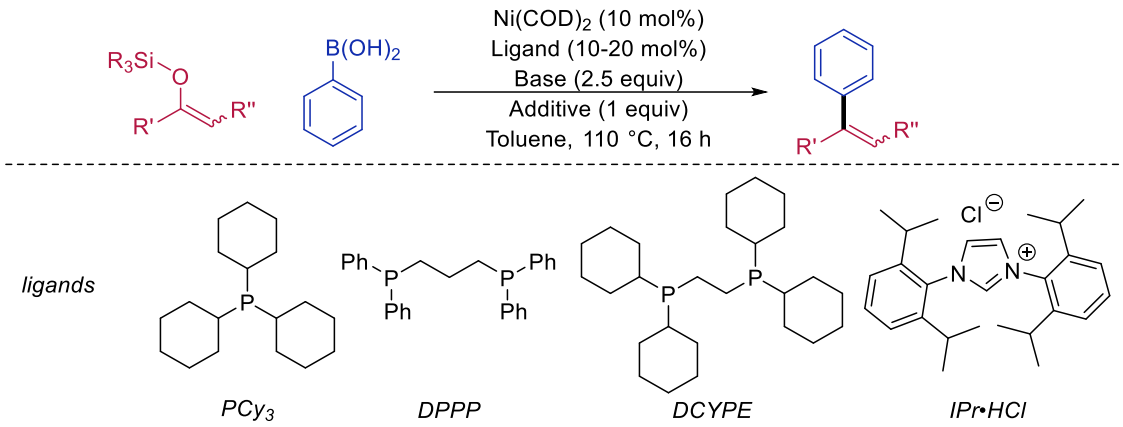

Scheme 65 – Initial Choice of Ligands and Fixed Variables for the Suzuki-Miyaura coupling of Silyl Enol Ethers

Suzuki-Miyaura coupling generally requires the use of an oxygen-centered base to aid the transmetallation step.[154] K_3PO_4 and NaO*t*Bu were selected, as they are frequently used in the nickel-catalyzed C–O activation of protected phenol derivatives,[155] and have also been shown to activate NHC salts by deprotonation.[156,157] Cesium fluoride and triethylborane were also chosen as additives in select experiments. Although some fluoride additives are known to cleave silyl protecting groups, CsF has been shown to activate organoborons in the Suzuki-Miyaura coupling involving strong bond activation.[158] In addition, BEt_3 has been shown to facilitate the nickel-catalyzed C–O activation of aryl- and enol- ethers.[159]

Silyl enol ether substrates were chosen to maximize the diversity of activation and stability. It was hypothesized that if they're too stable, the substrates may not react in the cross-coupling; conversely, if too reactive, they may decompose under the reaction conditions. The

[154] Smith, G. B.; Dezeny, G. C.; Hughes, D. L.; King, A. O.; Verhoeven, T. R. *J. Org. Chem.* **1994**, *59*, 8151–8156.
[155] Tobisu, M.; Chatani, N. *Top Curr Chem (Z)* **2016**, *374*, 41.
[156] Arduengo, A. J.; Harlow, R. L.; Kline, M. *J. Am. Chem. Soc.* **1991**, *113*, 361–363.
[157] Bhunia, A.; Yetra, S. R.; Gonnade, R. G.; Biju, A. T. *Org. Biomol. Chem.* **2016**, *14*, 5612–5616.
[158] Zhang, T.; Nohira, I.; Chatani, N. *Org. Chem. Front.* **2021**, *8*, 3783–3787.
[159] Guo, L.; Liu, X.; Baumann, C.; Rueping, M. *Angew. Chem. Int. Ed.* **2016**, *55*, 15415–15419.

structures of the selected ketones are illustrated in **Scheme 66**. Arguably the most activated ketone used was ethyl acetoacetate **88**. The nearby ester in the β position could potentially coordinate to the catalyst, aiding in the oxidative addition step. 1-indanone **89** was used as an aryl ketone example. The conjugation with the arene was thought to aid oxidative addition by stabilizing the resultant organometallic species. Lastly, 4-*tert*-butyl-cyclohexanone **90** was chosen as an unactivated dialkyl ketone, which lacks both of the aforementioned mechanisms of activation.

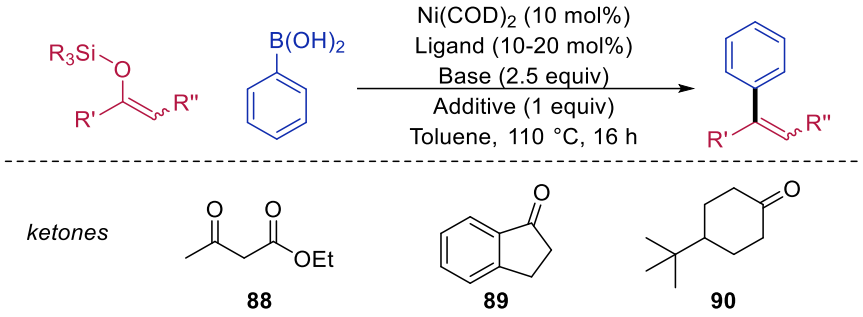

Scheme 66 – Initial Choice of Ketones for the Suzuki-Miyaura Coupling of Silyl Enol Ethers

A variety of silyl protecting groups were also selected to diversify reactivity and stability. In general, bulky R groups on the –SiR3 moiety stabilize silylated species in both acidic and basic media. The general stability is as follows: trimethylsilyl (TMS) < triethylsilyl (TES) < *tert*butyldimethylsilyl (TBS) < tri*iso*propylsilyl (TIPS), as shown **Scheme 67**. The smallest and least stable silyl group chosen was TMS, which was used for the aforementioned mentioned reports of Kumada-Corriu coupling of silyl enol ethers (**Section 2.1.2**).[160, 161] The low steric bulk of this group

[160] Hayashi, T.; Katsuro, Y.; Kumada, M. *Tetrahedron Lett.* **1980**, *21*, 3915–3918.
[161] Zhao, F.; Yu, D.-G.; Zhu, R.-Y.; Xi, Z.; Shi, Z.-J. *Chem. Lett.* **2011**, *40*, 1001–1003.

may enable the catalyst to insert into the C–O bond more easily than bulkier silyl groups. In contrast, TIPS is among the bulkiest of silyl protecting groups, which although makes TIPS-protected species less prone to decomposition, may result in a more challenging oxidative addition step. Lastly, TBS was used as a silyl group of intermediate bulk, which may provide a balance between the stability and reactivity of the silyl enol ether. Furthermore, as previously mentioned, TBS-protected phenol derivatives were used in the nickel-catalyzed Buchwald-Hartwig amination reported by Montgomery.[162]

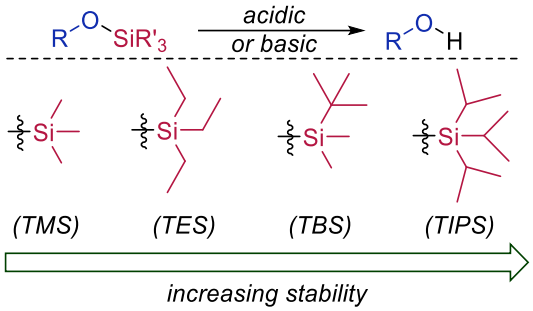

Scheme 67 – Relative Stability of Different Silyl Protecting Groups

Treating the aforementioned ketones with trialkyl silyl halides in the presence of an amine base enabled the facile preparation of silyl enol ethers. Three substrates were isolated, each from a distinct combination of ketone and silyl group, and were subjected to the set of designed experiments. The results of this screening of reaction conditions are summarized in **Table 20**. Most reaction conditions did not lead to any product. Recovery of silyl enol ether starting material was frequently observed by GC-MS, indicating lack of reactivity.

[162] Wiensch, E. M.; Todd, D. P.; Montgomery, J. *ACS Catal.* **2017**, *7*, 5568–5571.

Table 20 – Screened Reaction Conditions for the Nickel-Catalyzed Suzuki-Miyaura Coupling of Silyl Enol Ethers[a]

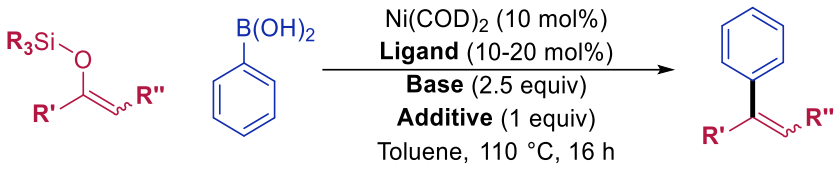

Entry	Silyl Enol Ether	Ligand[b]	Base	Additive	Yield (%)
1		IPr·HCl	K_3PO_4	--	0
2		IPr·HCl	NaO*t*Bu	--	0
3	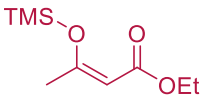	IPr·HCl	NaO*t*Bu	CsF	0
4		IPr·HCl	NaO*t*Bu	BEt_3	0
5	**91**	PCy_3	NaO*t*Bu	--	0
6		DPPP	NaO*t*Bu	--	0
7		DCYPE	NaO*t*Bu	--	0
8		IPr·HCl	K_3PO_4	--	0
9		IPr·HCl	NaO*t*Bu	--	0
10	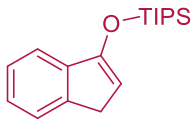	IPr·HCl	NaO*t*Bu	CsF	0
11		IPr·HCl	NaO*t*Bu	BEt_3	11
12	**92**	PCy_3	NaO*t*Bu	--	0
13		DPPP	NaO*t*Bu	--	0
14		DCYPE	NaO*t*Bu	--	0
15		IPr·HCl	K_3PO_4	--	0
16		IPr·HCl	NaO*t*Bu	--	0
17	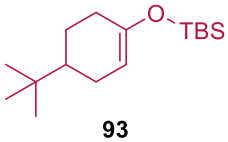	IPr·HCl	NaO*t*Bu	CsF	0
18		IPr·HCl	NaO*t*Bu	BEt_3	0
19	**93**	PCy_3	NaO*t*Bu	--	0
20		DPPP	NaO*t*Bu	--	0
21		DCYPE	NaO*t*Bu	--	0

[a]Reactions were run on 0.1 mmol of silyl enol ether. Yields are reported by ^1H NMR relative to 1,3,5-trimethoxybenzene as an internal standard. Yields of 0% indicate the m/z value of the desired product was not observed by GC-MS. [b]Monodentate ligands were used in 10 mol% and bidentate ligands were used in 20 mol%.

However, a single set of conditions provided the desired cross-coupled product for one of the silyl enol ether substrates; in the presence of triethylborane as an additive, TIPS-protected 1-indanone **92** gave the tri-substituted olefin product **94** in 11% yield (**Table 20**, entry 11). Furthermore, significant recovery of silyl enol ether was observed by GC-MS (m/z of 288). Interestingly, as shown in **Scheme 68**, trace amounts of a side-product consistent with the ethyl-substituted olefin **95** were also observed by GC-MS (m/z of 144). Theoretically, this side-product could form from the competitive transmetallation of BEt_3. However, the lack of product with the otherwise same conditions in the absence of BEt_3 (**Table 20**, entry 9) suggests the triethyl borane is somehow involved in the mechanism of electrophile activation.

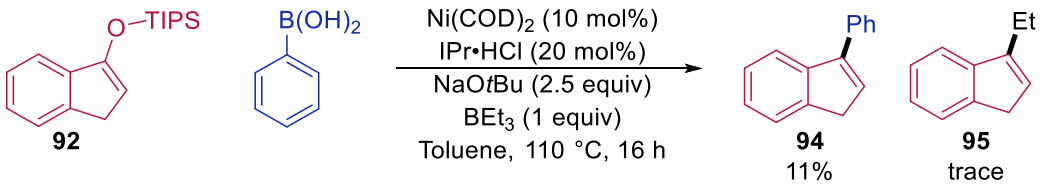

Scheme 68 – Initial Hit for the Nickel-Catalyzed Suzuki-Miyaura Coupling of Silyl Enol Ethers

We hypothesized that BEt_3 serves as a Lewis acid with the boron coordinated by the oxygen of the silyl enol ether, pulling electron density away from the C–O bond to weaken it enough for oxidative addition (**Scheme 69**). Competitive transmetallation by $PhB(OH)_2$ and BEt_3 could lead to the formation of both olefins **94** and **95**. This would be consistent with what was reported by Rueping, in which BEt_3 is proposed to act as both the nucleophilic coupling partner and a Lewis acid additive to activate the anisole electrophile.[163]

[163] Guo, L.; Liu, X.; Baumann, C.; Rueping, M. *Angew. Chem. Int. Ed.* **2016**, *55*, 15415–15419.

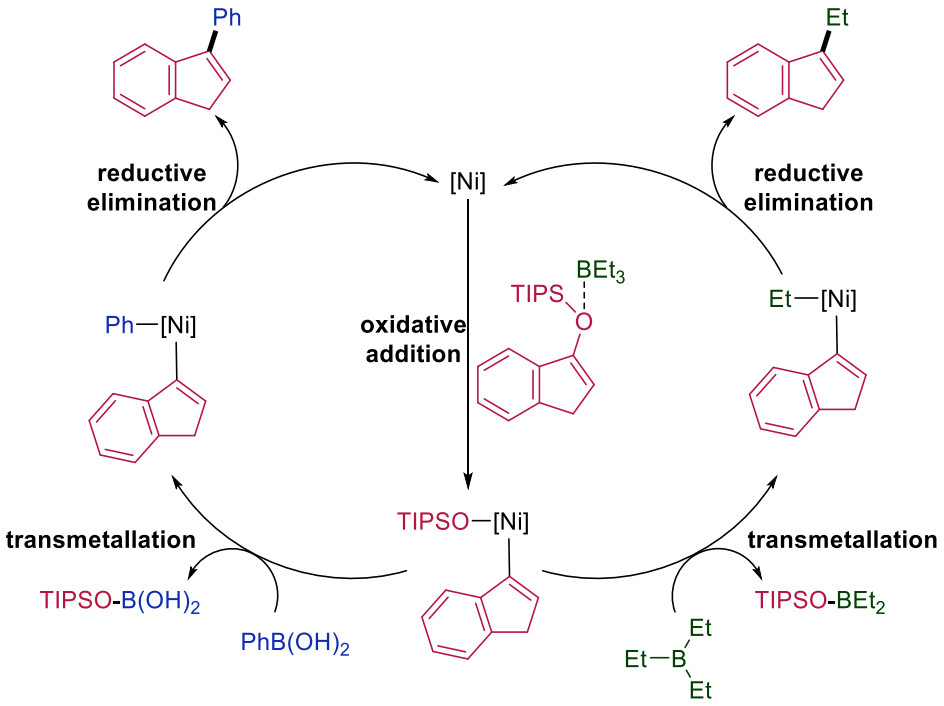

Scheme 69 – Proposed Competitive Catalytic Cycles for the Nickel-Catalyzed Suzuki-Miyaura Coupling of Silyl Enol Ethers

To optimize this reaction, a variety of other additives were screened, under the assumption that BEt_3 activated the C–O bond for cross-coupling via a Lewis acid-base interaction (**Table 21**). Relative to BEt_3 with 11% yield (entry 1), other boron reagents including boric acid, borane (complexed with THF), and tris(pentafluorophenyl)borane, all led to 0% yield (entries 2-4). Metal salts including silver triflate, lithium chloride, scandium triflate, and zinc chloride, also led to no product formation (entries 5-8). Overall, the lack of product seemed to stem from poor starting material conversion, as substantial recovery of the silyl enol ether was observed by GC-MS (m/z of 288). Due to the observed reactivity with BEt_3, this additive was used as a fixed variable for subsequent optimization.

Table 21 – Effect of Lewis Acid Additives in the Suzuki-Miyaura Coupling of Silyl Enol Ethers

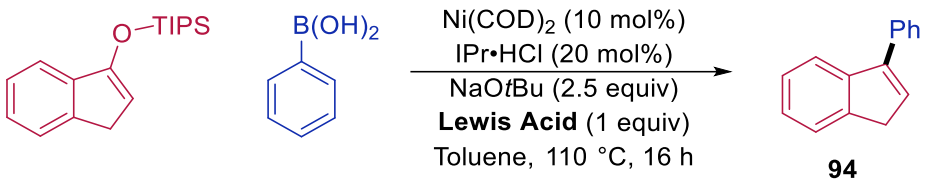

Entry	Lewis Acid	Yield of **94** (%)[a]	Entry	Lewis Acid	Yield of **94** (%)[a]
1	BEt_3	11	5	AgOTf	0
2	$B(OH)_3$	0	6	LiCl	0
3	BH_3·THF	0	7	$Sc(OTf)_3$	0
4	$B(C_6F_5)_3$	0	8	$ZnCl_2$	0

[a]Reactions were run on 0.1 mmol of silyl enol ether. Yields are reported by ^{1}H NMR relative to 1,3,5-trimethoxybenzene as an internal standard. Yields of 0% indicate the m/z value of the desired product was not observed by GC-MS.

As previously mentioned, we suspected the identity of the silyl group could provide a useful balance of stability and reactivity of the silyl enol ether. Consequently, two additional silyl enol ether analogues of 1-indanone were screened (TES and TBS) at different coupling temperatures (**Table 22**). At 60 °C, no product was observed regardless of the silyl group (entries 1-3). Significant recovery of silyl enol ether was observed by GC-MS, suggesting lack of reactivity at this temperature. An intermediate temperature of 110 °C seemed to balance reactivity and stability, providing product in variable yields (entries 4-6). While there didn't appear to be decomposition to the ketone, significant recovery of silyl enol ether was detected by GC-MS. At this temperature, TES, the least bulky of the silyl groups tested, provided the worst yield of 6% (entry 4). In contrast, TBS, a silyl group of intermediate bulk, provided the highest yield of 17% (entry 5). Lastly, TIPS, the bulkiest silyl group, provided an intermediate yield of 11% (entry 6). Heating the reaction to 160 °C appeared to be too aggressive regardless of the silyl group, as product formed in zero-to-trace yields (entries 7-9), and significant amounts of ketone were

observed by GC-MS. Therefore, at 110 °C, a TBS protecting group on 1-indanone provided the highest yield. This combination of silyl group and temperature was thus used for subsequent optimization of the Suzuki-Miyaura coupling of 1-indanone.

Table 22 – Effect of Silyl Group in the Suzuki-Miyaura Coupling of Silyl Enol Ethers

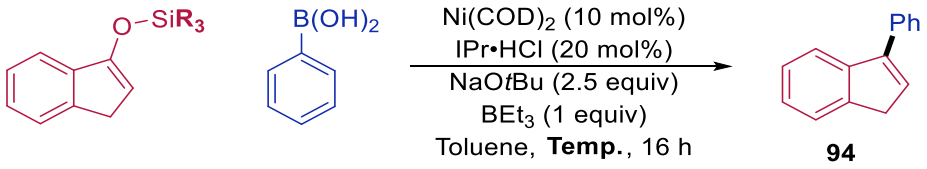

Entry	Temperature (°C)	Silyl Group	Yield of **94** (%)
1	60	TES	0
2	60	TBS	0
3	60	TIPS	0
4	110	TES	6
5	110	TBS	17
6	110	TIPS	11
7	160	TES	Trace
8	160	TBS	0
9	160	TIPS	0

[a]Reactions were run on 0.1 mmol of silyl enol ether. Yields are reported by ^{1}H NMR relative to 1,3,5-trimethoxybenzene as an internal standard. Yields of 0% indicate the m/z value of the desired product was not observed by GC-MS. Trace yields indicate the product was observed by GC-MS, but calculated yield was < 1 %.

The identity of the nucleophilic coupling partner was then investigated. Since we were interested solely in the Suzuki-Miyaura coupling of silyl enol ethers, several different organoboron nucleophiles were screened (**Table 23**) and compared to $PhB(OH)_2$ (entry 1). Chatani found organoboronic esters to be more active in his reports of anisole C–O bond activation.[164] However,

[164] Tobisu, M.; Shimasaki, T.; Chatani, N. *Angew. Chem. Int. Ed.* **2008**, *47*, 4866–4869.

boronic acid pinacol ester **97** led to no product formation (entry 2). Furthermore, aryl potassium trifluoroborate **98**, which has been shown to have improved stability in Suzuki-Miyaura couplings relative to other organoboron reagents,[165] was found to be unsuitable here, providing 0% yield (entry 3). Lastly, bis(pinacolato)diboron **99**, which was tested as a borylation reagent, provided no conversion of silyl enol ether (entry 4). With none of the additional nucleophiles leading to product formation, we suspected some sort of complexity in the reaction mechanism in which multiple reagents may have acted in tandem for the activation of silyl enol ethers.

Table 23 – Effect of Organoboron Nucleophile in the Suzuki-Miyaura coupling of Silyl Enol Ethers

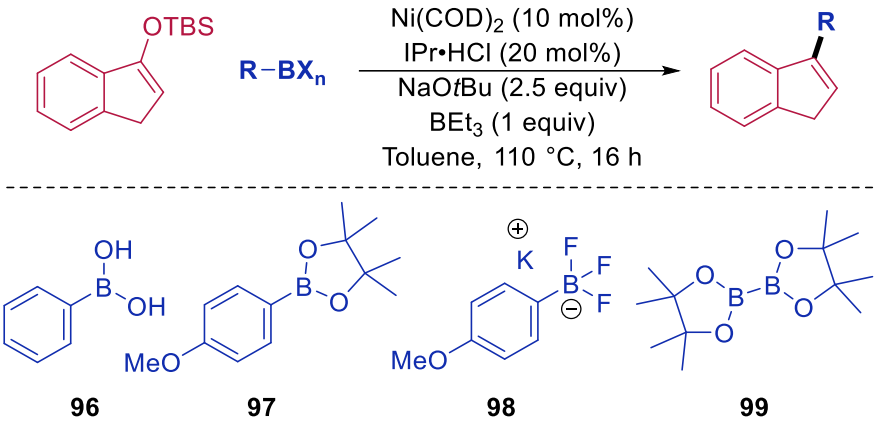

96 **97** **98** **99**

Entry	RBX_n	Yield (%)[a]
1	**96**	17
2	**97**	0
3	**98**	0
4	**99**	0

[a]Reactions were run on 0.1 mmol of silyl enol ether. Yields are reported by ^{1}H NMR relative to 1,3,5-trimethoxybenzene as an internal standard. Yields of 0% indicate the m/z value of the desired product was not observed by GC-MS or ^{1}H NMR.

[165] Molander, G. A.; Ellis, N. *Acc. Chem. Res.* **2007**, *40*, 275–286.

Given the observed influence of BEt_3 and $PhB(OH)_2$, we hypothesized the identity of the base may also play an important role in the Suzuki-Miyaura coupling of silyl enol ethers. A variety of both organic- and inorganic- bases were therefore screened (**Table 24**). As a precaution to ensure IPr·HCl was activated, weak amine bases that are potentially not strong enough to deprotonate this ligand were dosed with an additional 20 mol% of NaO*t*Bu.

Table 24 – Effect of Base in the Suzuki-Miyaura Coupling of Silyl Enol Ethers

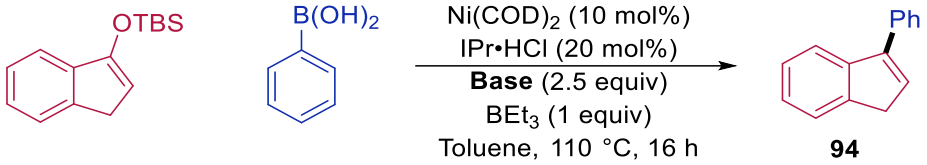

Entry	Base	Yield of **94** (%)[a]	Entry	Base	Yield of **94** (%)[a]
1	Et_3N[b]	0	8	HCO_2Na	0
2	TMP[b]	0	9	$NaHCO_3$	0
3	DBU[b]	0	10	KF	0
4	DIPEA[b]	0	11	PhOK	<1
5	Pyridine[b]	0	12	LiO*t*Bu	0
6	Morpholine[b]	0	13	KO*t*Bu	12
7	Li_2CO_3	0	14	NaO*t*Bu	17

[a]Reactions were run on 0.1 mmol of silyl enol ether. Yields are reported by ^1H NMR relative to 1,3,5-trimethoxybenzene as an internal standard. Yields of 0% indicate the m/z value of the desired product was not observed by GC-MS. [b] Amine bases were dosed with an additional 20 mol% of NaO*t*Bu for activation of the NHC ligand.

Unfortunately, none of the amine bases that were screened led to the formation of product (**Table 24**, entries 1-6). Even in the presence of catalytic NaO*t*Bu to enable ligand activation, triethylamine, tetramethylpiperidine (TMP), DBU, Hunig's base, pyridine, and morpholine, were found to be unsuitable for this reaction. In general, amine bases are less reactive than NaO*t*Bu, and are seldom used in Suzuki-Miyaura coupling. However, the inorganic

bases that were screened also led to little-to-no product formation in most cases. Li_2CO_3, HCO_2Na, $NaHCO_3$, and KF led to no product formation, (entries 7-10) possibly due to lack of activation of IPr·HCl. Although PhOK led to trace product formation (entry 11), significant ketone and PhOTBS (m/z of 208) were observed by GC-MS, suggesting the silicon atom of the starting material was attacked by the nucleophilic base (**Scheme 70**). Surprisingly, other *tert*-butoxides such as KO*t*Bu and LiO*t*Bu led to diminished and 0% yield, respectively (entries 12-13) relative to NaO*t*Bu (entry 14). Interestingly, although of identical pK_a, the counter-cation of these respective *tert*-butoxide bases had a significant effect on outcome of this reaction. Since it was the best base of those tested, the continued use of NaO*t*Bu was investigated for subsequent optimization of the reaction conditions.

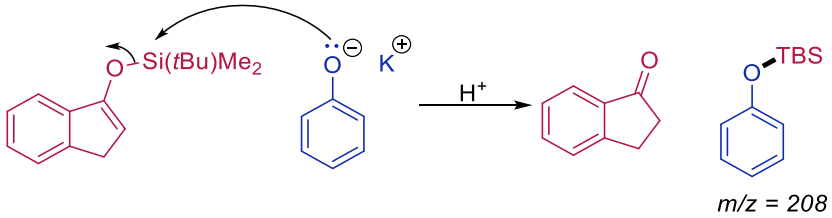

Scheme 70 – Plausible Mechanism of Silyl Enol Ether Decomposition with PhOK

The steric and electronic properties of NHC ligands can be tuned to promote challenging cross-coupling reactions.[166] Consequently, a diverse range of twelve NHC salts were screened. In addition to being complex, some of the ligands used are not commercially-available and do not have generic names, so their structures are indicated in **Figure 4**.

[166] Herrmann, W. A. *Angew. Chem. Int. Ed.* **2002**, *41*, 1290–1309.

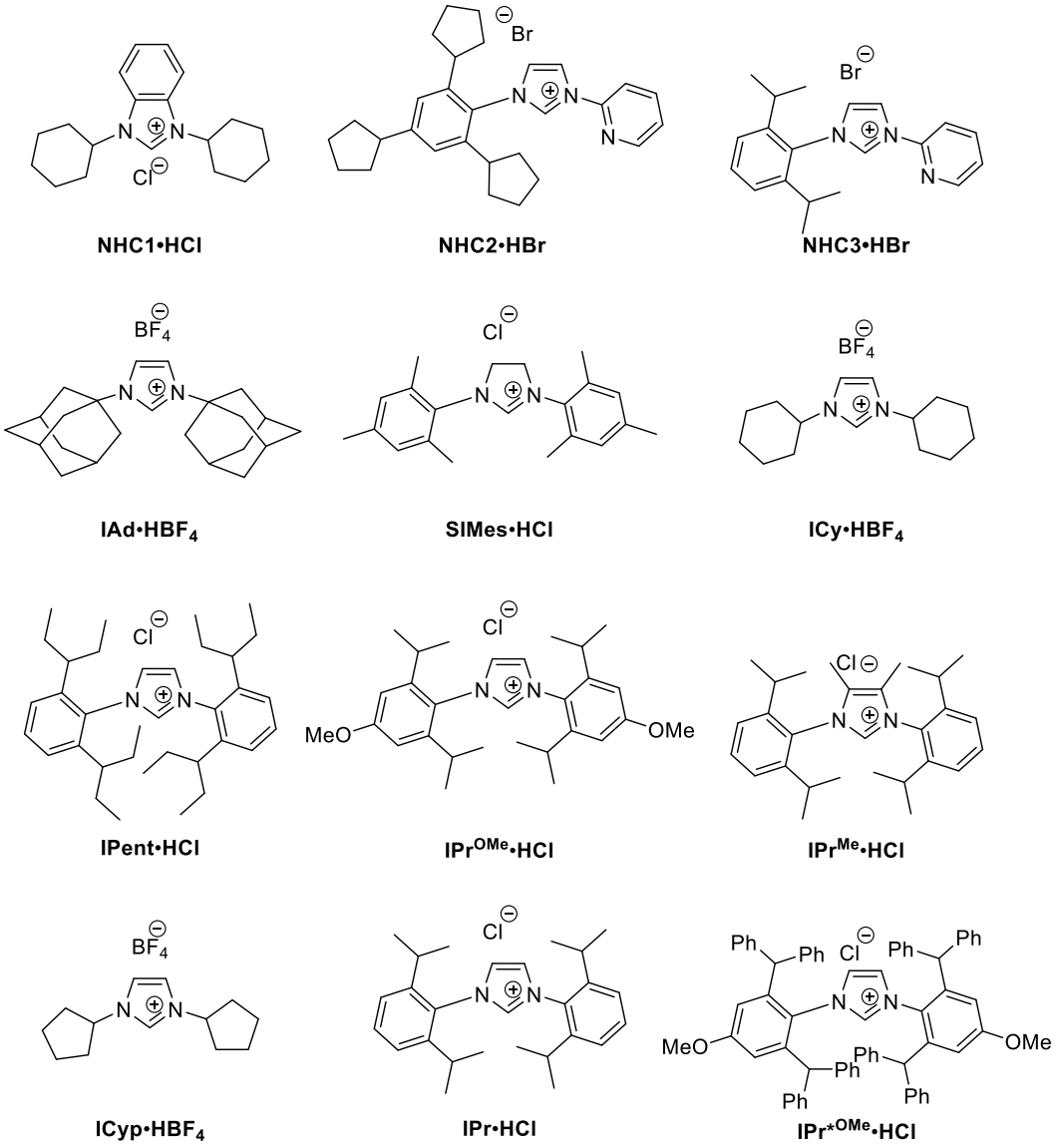

Figure 4 – Structures of Select NHC·HX Ligands

The ligands screened provided a diverse range in yields of the reaction (**Table 25**). However, some recovery of silyl enol ether was observed by GC-MS, regardless of the ligand. NHC1·HCl, NHC2·HBr, NHC3·HBr, IAd·HBF_4, SIMes·HCl, and ICy·HBF_4 all led to 0-3% yield (entries 1-6). Furthermore, IPent·HCl, IPr^{OMe}·HCl, IPr^{Me}·HCl, and ICy·HBF_4 were slightly higher-yielding, ranging from 6-8% (entries 7-10). Notably IPr·HCl, which was used for the reaction discovery and optimization up to this point, was among the highest-yielding experiments with 17% (entry 11).

Lastly, among the most electron-rich and sterically-hindered ligands was IPr*^{OMe}·HCl, which provided the best yield of 27% (entry 12). Furthermore, this ligand has been proposed to form particularly stable Pd(0)–NHC complexes at elevated temperatures,[167] which may have been beneficial under the relatively harsh reaction conditions. As it was the best ligand screened, IPr*^{OMe}·HCl was used for subsequent optimization experiments.

Table 25 – Effect of NHC Ligand in the Suzuki-Miyaura coupling of Silyl Enol Ethers

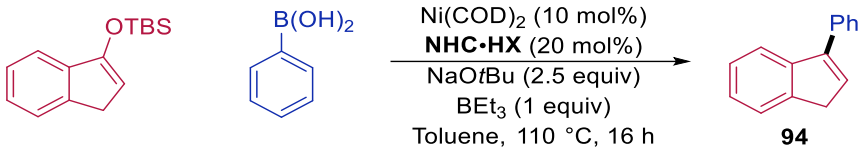

Entry	NHC·HX	Yield of **94** (%)[a]	Entry	NHC·HX	Yield of **94** (%)[a]
1	NHC1·HCl	3	7	IPent·HCl	6
2	NHC2·HBF_4	0	8	IPr^{OMe}·HCl	7
3	NHC3·HBr	0	9	IPr^{Me}·HCl	8
4	IAd·HBF_4	0	10	ICyp·BF_4	8
5	SIMes·HCl	1	11	IPr·HCl	17
6	ICy·HBF_4	2	12	IPr*^{OMe}·HCl	27

[a]Reactions were run on 0.1 mmol of silyl enol ether. Yields are reported by ^{1}H NMR relative to 1,3,5-trimethoxybenzene as an internal standard. Yields of 0% indicate the m/z value of the desired product was not observed by GC-MS.

Due to the seemingly inherent reactivity of BEt_3 enabling this reaction via a largely unknown mechanism, trimethyl aluminum and diethyl zinc were also investigated as stoichiometric additives (**Table 26**). Relative to 27% yield of **94** with BEt_3 (entry 1), $ZnEt_2$ and $AlMe_3$ led to diminished yields of 12% (entry 2) and 8% (entry 3), respectively. Interestingly, trace

[167] Meiries, S.; Speck, K.; Cordes, D. B.; Slawin, A. M. Z.; Nolan, S. P. *Organometallics* **2013**, *32*, 330–339.

quantities of the ethyl- and methyl- substituted olefin side-products **95** and **100** were also detected by GC-MS for these respective additives. Therefore, it appears that mechanisms of C–O bond activation and alkyl-substituted olefin side-product formation are closely related. Both $ZnEt_2$ and $AlMe_3$ are precedented nucleophiles in nickel-catalyzed cross-coupling of strong C–O bonds.[168, 169] This, in combination with the fact that none of the Lewis acids screened led to observed product formation, may suggest an alternative mechanism of C–O activation than what was previously proposed.

Table 26 – Effect of Alkyl Metallic Additives in the Suzuki-Miyaura coupling of Silyl Enol Ethers[a]

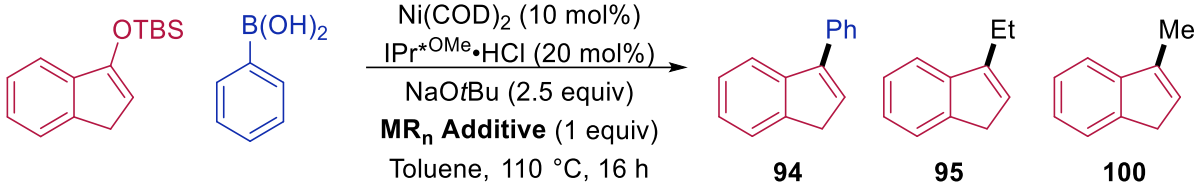

Entry	MR_n Additive	Yield of **94** (%)	Yield of **95** (%)	Yield of **100** (%)
1	BEt_3	27	Trace	0
2	$ZnEt_2$	12	Trace	0
3	$AlMe_3$	8	0	Trace

[a]Reactions were run on 0.1 mmol of silyl enol ether. Yields are reported by ^1H NMR relative to 1,3,5-trimethoxybenzene as an internal standard. Trace yields indicate m/z was detected by GC-MS, but calculated yield was < 1 %.

If BEt_3 could transmetallate onto Ni(0), possibly aided by a Lewis acid-base interaction with NaO*t*Bu,[170] an anionic nickel(0) species could form (**Scheme 71**). Because of their electron-rich nature, anionic catalyst intermediates have been shown to enable oxidative addition into

[168] Morioka, T.; Nishizawa, A.; Nakamura, K.; Tobisu, M.; Chatani, N. *Chem. Lett.* **2015**, *44*, 1729–1731.
[169] Wisniewska, H. M.; Swift, E. C.; Jarvo, E. R. *J. Am. Chem. Soc.* **2013**, *135*, 9083–9090.
[170] Yao, W.; Wang, J.; Zhong, A.; Wang, S.; Shao, Y. *Org. Chem. Front.* **2020**, *7*, 3515–3520.

other types of strong bonds, such as alkyl fluorides.[171] After oxidative addition into the C–O bond of the silyl enol ether, subsequent transmetallation with $PhB(OH)_2$ would form an anionic nickel species bearing three carbon-centered groups. Upon reductive elimination, the desired phenyl-substituted product **94**, the ethyl-substituted side-product **95**, and ethyl benzene, could all theoretically form. However, ethylbenzene would be difficult to detect due to its volatility. If correct, this proposed mechanism could explain the unique affect alkylmetal additives have on this C–O activation in addition to the formation of the observed alkyl-substituted side-products.

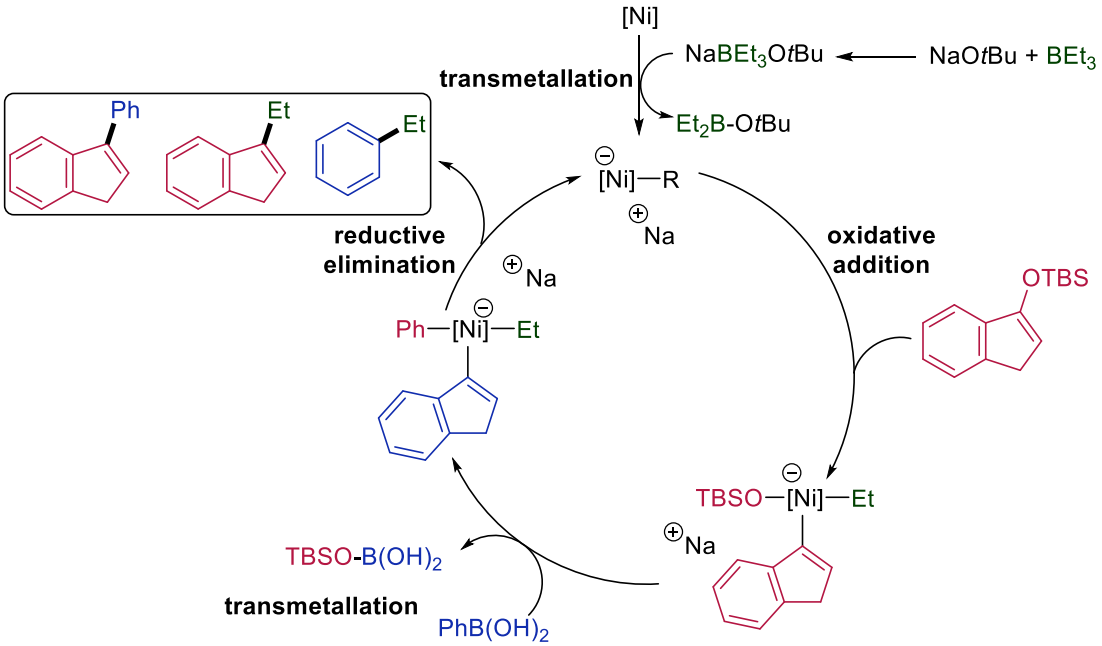

Scheme 71 – Revised Proposed Catalytic Cycle for Silyl Enol Ether Activation with BEt_3

Over the course of the optimization process, the one-variable-at-a-time screening had provided minimal improvements to the Suzuki-Miyaura coupling of silyl enol ethers, only increasing the yield from 11% to 27%. For the most part, the screening of conditions did not

[171] Iwasaki, T.; Fukuoka, A.; Yokoyama, W.; Min, X.; Hisaki, I.; Yang, T.; Ehara, M.; Kuniyasu, H.; Kambe, N. *Chem. Sci.* **2018**, *9*, 2195–2211.

provide significant deviations relative to the initial reaction discovery. Though changes such as silyl protecting group and ligand led to slightly improved yield, other variables such as temperature, nucleophilic coupling partner, additive, and base, did not provide any improved reactivity. Also, since the initial hit failed with the other two silyl enol ether substrates that were tested in the initial reaction discovery phase, we had growing concerns that we had stumbled upon a unique set of conditions that provided only poor yields to a very narrow range of substrates. We therefore applied the slightly improved reaction conditions to a variety of silyl enol ether substrates to determine if the reaction was worth investigating any further.

Unfortunately, all of the additional TBS silyl enol ethers that were screened did not form any product (**Table 27**). Consequently, it was difficult to explain what seemed to be unique reactivity with 1-indanone (entry 1). It isn't too surprising that an unactivated substrate such as TBS-protected dialkyl ketone **102** failed to yield product (entry 2). Presumably the presence of the conjugated aryl group in 1-indanone aids in the activation of the substrate, possibly via resonance of the oxidative addition intermediate. However, TBS-protected electron-deficient aryl ketone **103** also failed (entry 3). Even with aryl conjugation and an electron-withdrawing group, this substrate did not lead to any product formation under the reaction conditions. Furthermore, TBS-protected β-keto ester **104** also led to no product, even with the potential ability to coordinate to the catalyst (entry 4). What is truly detrimental to this chemistry is that TBS-protected α-tetralone **105** failed to provide product (entry 5). The only difference between 1-indanone and α-tetralone is the size of the aryl-fused alkyl ring; the presence of an additional methylene in the backbone apparently stopped the chemistry from working.

Table 27 – Scope of the Suzuki-Miyaura Coupling of Silyl Enol Ethers

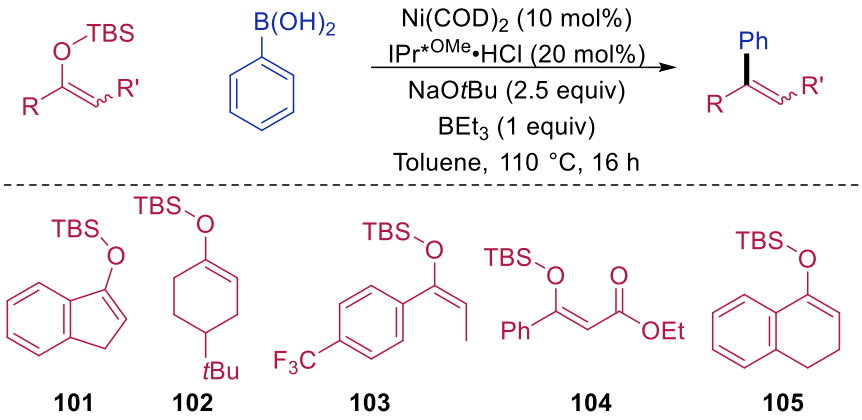

Entry	Silyl Enol Ether	Yield (%)[a]
1	**101**	27
2	**102**	0
3	**103**	0
4	**104**	0
5	**105**	0

[a]Reactions were run on 0.1 mmol of silyl enol ether. Yields are reported by ^{1}H NMR relative to 1,3,5-trimethoxybenzene as an internal standard. Yields of 0% indicate the m/z value of the desired product was not observed by GC-MS.

Due to the disappointing scope of this reaction, work on this project was halted and it was ultimately deemed unsuccessful.

2.2.2: Conclusions and Future Outlooks

A set of reaction conditions were discovered for the nickel-catalyzed Suzuki-Miyaura coupling of silyl enol ethers. While attempts were made to optimize this reaction, only small deviations in conditions were found to moderately increase the yield. Consequently, the initial goal of a 1-pot/2-step or *in situ* silylation and cross-coupling sequence was not investigated. Furthermore, all silyl enol ethers that were tested beyond 1-indanone-derived substrates failed for largely unknown reasons. Therefore, because of the abhorrent scope of electrophilic coupling partner, this chemistry is not synthetically useful, even if the yield were to be improved.

One-variable-at-a-time optimization is inherently flawed by the inability to efficiently screen the effect that multiple variables have on each other. Suspected key variables in this chemistry such as nucleophilic coupling partner, additive, and base, may have a complex interaction that could not be confidently elucidated during the optimization. If screened simultaneously, perhaps improved reactivity and mechanistic understanding could be uncovered. Consequently, a high-throughput approach to reaction optimization may be suitable for future work on this project. However, further optimization of indanone-derived silyl enol ethers would not be advisable, since it has shown unusually reactivity compared to similar substrates.

Chapter 3: Supporting Information

3.1: Palladium-Catalyzed Cross-Coupling of Superbase-Generated C(sp^3) Nucleophiles

3.1.1: Experimental Details and General Procedures

Unless otherwise indicated, reagents were obtained from Sigma Aldrich, Acros, Alfa Aesar, Matrix Scientific, Oakwood, or Combi-Blocks, and used as received. Pd_2dba_3 was obtained from Johnson Matthey, and XPhos (98%) from Combi-Blocks. KO*t*Bu (reagent grade, ≥ 98%), $ZnCl_2$ (anhydrous, ≥ 98%), *n*-BuLi (1.6 M in hexanes), and *s*-BuLi (1.4 M in cyclohexane) were obtained from Sigma Aldrich. Butyl lithium was used fresh and not titrated. Stock solutions of $ZnCl_2$, KO*t*Bu, and benzophenone in tetrahydrofuran were prepared inside of a glovebox and stored under N_2. ACS grade cyclohexane was purchased from Fisher Chemical, purged with UHP N_2, dried with molecular sieves, and stored under N_2. Tetrahydrofuran and toluene were degassed with N_2 and passed through a PureSolv solvent purification system before use. Unless otherwise indicated, all reactions were carried out in oven-dried glassware under an N_2 atmosphere.

(±)-*trans*-*N*,*N*,*N*',*N*'-tetramethylcyclohexane-1,2-diamine (TMCDA),[172] 4-(trimethylsilyl)toluene,[173] 4-chloro-1-methyl-1H-indole,[174] 3-methoxypropylbenzene,[175] 4-(trimethylsilyl)ethylbenzene,[176] *N*,*N*-dimethyl-3-phenylpropylamine,[177] and benzyl *tert*-butyl ether,[178] were all prepared by literature procedures and their characterization data were all in agreement with that reported by the authors.

Silicycle F60 40-63 µm silica gel was used for column chromatography. Analytical thin layer chromatography (TLC) was conducted using aluminum-backed EMD Millipore Silica Gel 60. Visualization of developed plates was performed under UV light (254 nm) and/or using $KMnO_4$ stain. Yields for optimization were determined by ^{1}H NMR or GC analysis of the crude reaction mixture using 1,3,5-trimethoxybenzene as an internal standard.

NMR spectra were collected on a Bruker Avance 400 MHz spectrometer. Data for ^{1}H NMR are reported as follows: chemical shift (δ ppm), multiplicity (s = singlet, d = doublet, t = triplet, q = quartet, m = multiplet), coupling constant (Hz), integration. ^{1}H and ^{13}C chemical shifts were referenced to residual solvent signals. IR spectra of compounds were obtained using an Agilent Technologies Cary 630 FTIR (diamond crystal). Accurate mass data (EI) was obtained from an Agilent 5977A GC/MSD using MassWorks 4.0 from CERNO bioscience.

---

[172] Remenar, J. F.; Lucht, B. L.; Collum, D. B. *J. Am. Chem. Soc.* **1997**, *119*, 5567–5572.
[173] Doszczak, L.; Kraft, P.; Weber, H.-P.; Bertermann, R.; Triller, A.; Hatt, H.; Tacke, R. *Angew. Chem. Int. Ed.* **2007**, *46*, 3367–3371.
[174] Jayaraman, A.; Misal Castro, L. C.; Fontaine, F.-G. *Org. Process Res. Dev.* **2018**, *22*, 1489–1499.
[175] Ayub, R.; Papadakis, R.; Jorner, K.; Zietz, B.; Ottosson, H. *Chem. Eur. J.* **2017**, *23*, 13684–13695.
[176] Ball, L. T.; Lloyd-Jones, G. C.; Russell, C. A. *J. Am. Chem. Soc.* **2014**, *136*, 254–264.
[177] Mbofana, C. T.; Chong, E.; Lawniczak, J.; Sanford, M. S. *Org. Lett.* **2016**, *18*, 4258–4261.
[178] Yasukawa, N.; Kanie, T.; Kuwata, M.; Monguchi, Y.; Sajiki, H.; Sawama, Y. *Chem. Eur. J.* **2017**, *23*, 10974–10977.

3.1.1.1: General Procedure A: Coupling of Aryl Chlorides with Primary Benzyl Lithiums Generated by Deprotonation

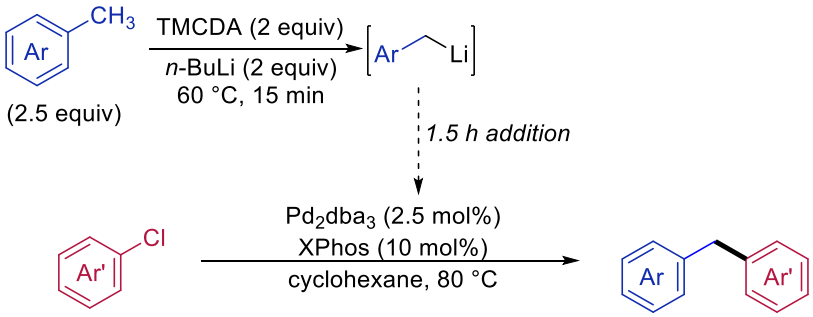

Pd_2dba_3 (4.6 mg, 2.5 mol%, 5 µmol), XPhos (9.5 mg, 10 mol%, 20 µmol) and aryl chloride (if solid; 1 equiv, 0.2 mmol) were placed in an 8 mL screw-top tube and flushed with N_2. Cyclohexane (2 mL) and aryl chloride (if liquid; 1 equiv, 0.2 mmol) were added and the solution and stirred at 80 °C for 15 min. Separately, the toluene derivative (2.5 equiv, 0.5 mmol) and TMCDA (74 µL, 2 equiv, 0.4 mmol) were added to a 4 mL screw-top vial under N_2. *n*-BuLi 1.6 M in hexanes (250 µL, 2 equiv, 0.4 mmol) was added dropwise over approximately 1 min at room temperature before heating to 60 °C for 15 min. During this time, the solution turned dark orange, with the colour varying slightly depending on the substrate. The deprotonated toluene derivative was then diluted with cyclohexane to a total volume of 2 mL, taken up into a 3 mL plastic HSW syringe bearing a PFA tube instead of a traditional stainless-steel needle (see **Section 3.1.2** on Troubleshooting), placed on a NewEra NE-300 syringe pump, and added to the solution of catalyst and aryl chloride at a rate of 1333.3 µL/h for 1.5 h (2 mL total). The reaction was stirred an additional 15 min after the addition was complete, then quenched with methanol (2 mL), dry-loaded onto silica gel, and purified by flash column chromatography.

3.1.1.2: General Procedure B: Coupling of Aryl Halides with Primary Benzyl Zincs Generated by Deprotonation

Pd_2dba_3 (1.8 mg, 1 mol%, 2 µmol), XPhos (3.8 mg, 4 mol%, 8 µmol) and aryl halide (if solid; 1 equiv, 0.2 mmol) were placed in an 8 mL screw-top tube and flushed with N_2. Tetrahydrofuran (2 mL) and aryl halide (if liquid; 1 equiv, 0.2 mmol) were added to the solution which was then stirred for approximately 15 min at room temperature. Separately, the toluene derivative (2.5 equiv, 0.5 mmol) and TMCDA (74 µL, 2 equiv, 0.4 mmol) were added to a 4 mL screw-top vial under N_2. *n*-BuLi 1.6 M in hexanes (250 µL, 2 equiv, 0.4 mmol) was added dropwise over approximately 1 minute at room temperature before heating to 60 °C for 15 min. During this time, the solution turned dark orange, with the colour varying slightly depending on the substrate. A solution of $ZnCl_2$ 0.5 M in tetrahydrofuran (800 µL, 2 equiv, 0.4 mmol) was then added to the benzyl lithium solution at room temperature over approximately 3 seconds to form a colourless solution, followed by dilution with tetrahydrofuran to a total volume of 2 mL. The resultant benzyl zinc solution was then added to the mixture of catalyst and aryl halide and stirred at 60 °C. Once the reaction was complete (i.e. full consumption of aryl halide observed by GC-MS; usually less than 3 hours), the mixture was then quenched with methanol (2 mL), dry loaded onto silica gel, and purified by flash column chromatography.

3.1.1.3: General Procedure C: Coupling of Aryl Halides with Secondary Benzyl Zincs Generated by Deprotonation

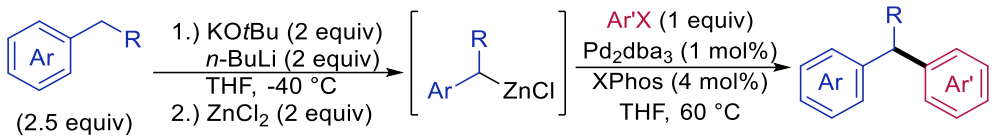

Pd_2dba_3 (1.8 mg, 1 mol%, 2 µmol), XPhos (3.8 mg, 4 mol%, 8 µmol) and aryl halide (if solid; 1 equiv, 0.2 mmol) were placed in an 8 mL screw-top tube and flushed with N_2. Tetrahydrofuran (2 mL) and aryl halide (if liquid; 1 equiv, 0.2 mmol) were added to the vial and stirred at room temperature for approximately 15 min. Separately, the ethylbenzene derivative (2.5 equiv, 0.5 mmol) and 1.0 M KO*t*Bu in tetrahydrofuran (400 µL, 2 equiv, 0.4 mmol) were added to a 4 mL screw-top vial at room temperature. The mixture was then diluted with tetrahydrofuran to a total volume of 1.2 mL before being cooled to -40 °C. *n*-BuLi 1.6 M in hexanes (250 µL, 2 equiv, 0.4 mmol) was added dropwise over approximately 1 min at -40 °C. The mixture was stirred for 10 min at -40 °C, during which time the solution turned dark red, with the colour varying slightly depending on the substrate. The solution was then removed from the cold bath for 60 seconds before the addition of $ZnCl_2$ 0.5 M in tetrahydrofuran (800 µL, 2 equiv, 0.4 mmol) over approximately 3 seconds to form a colourless solution. The resultant benzyl zinc solution was then added to the mixture of catalyst and aryl halide, then warmed to 60 °C. Once the reaction was complete (i.e. full consumption of aryl halide observed by GC-MS; usually less than 3 hours), the mixture was then quenched with methanol (2 mL), dry loaded onto silica gel, and purified by flash column chromatography.

3.1.2: Reactor Setup and Trouble Shooting

The deprotonation of toluene derivatives using *n*-BuLi/TMCDA or Schlosser's base led to characteristic vibrant orange and red colours, respectively. Upon being quenched with zinc chloride, these colours fade to form a colourless solution. Consequently, if this colour fades at any other point in the reaction, the nucleophile was somehow quenched, usually by oxygen or water. This is often the cause for incomplete aryl halide conversion in the cross-coupling. If a noticeable loss of colour is observed, we recommend setting up a new deprotonation, ensuring reagents and glassware are clean and dry, and the reaction is maintained under an inert atmosphere.

Figure 5 shows the general reaction setup for the direct palladium-catalyzed cross-coupling of benzyl lithium with aryl chlorides described in General Procedure A. Because a 1.5 h nucleophile slow addition was determined to be optimal, it is best to use a syringe pump (we used a NewEra NE-300). This allows for reliable and consistent flow rates which can be programmed and left unattended for the duration of the slow addition.

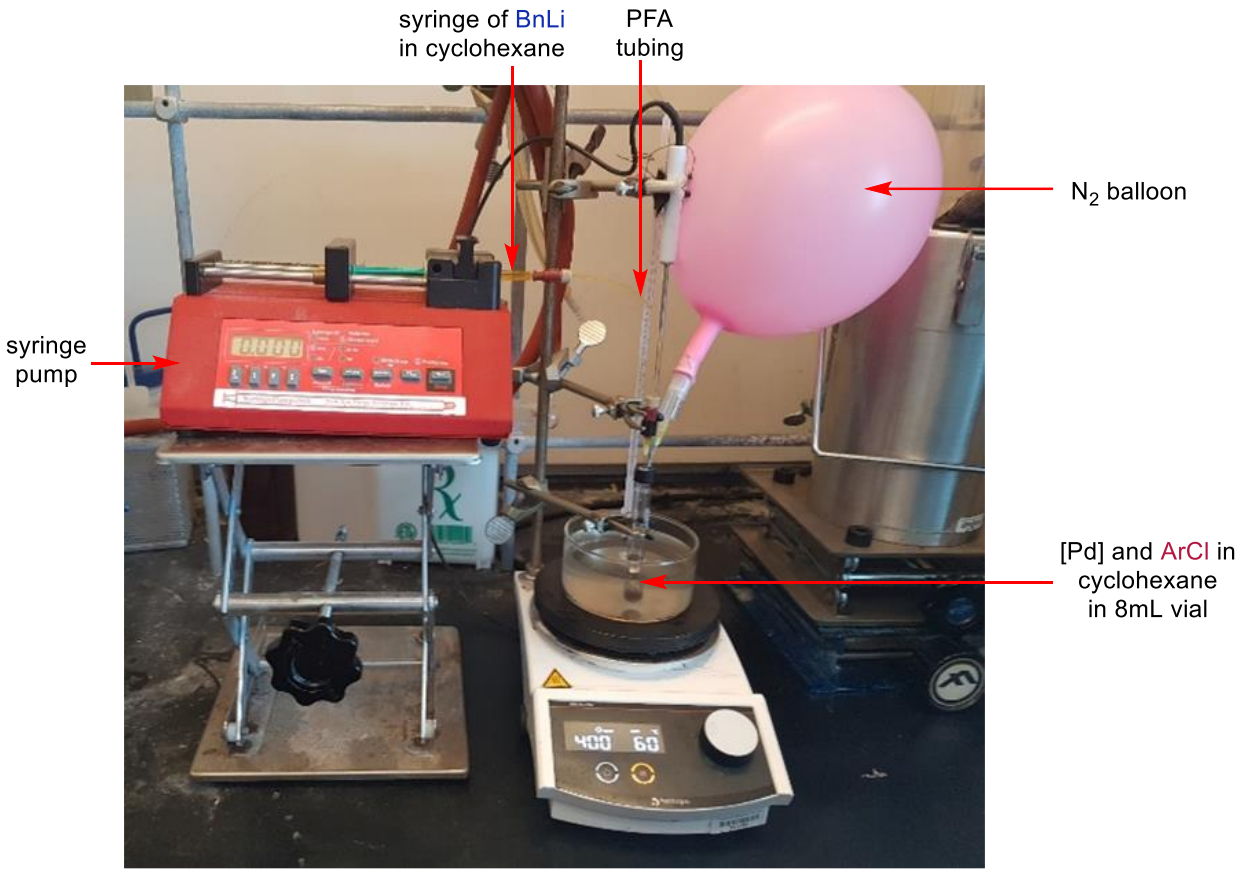

Figure 5 – Reactor Setup for Benzyl Lithium Slow-Addition

Furthermore, as previously discussed, the use of a typical 12” 20-gauge stainless steel needle led to reproducibility problems due to corrosion of the steel over multiple uses. This is evident by the solution entering the needle being orange but being fainter or entirely colourless coming out. If this issue is observed, we recommend using PFA tubing (Figure S1) in place of stainless-steel needles. With the appropriate luers, standard disposable plastic syringes and 1.5” stainless-steel needles can be attached on either end of the PFA tubing. We used materials from Idex Health & Science with the followings part numbers.

- PFA Tubing Natural 1/16" OD x .040" ID (Part # 1507L)
- Flangeless Fitting Short, PEEK, 1/4-28 Flat-Bottom for 1/16" OD Natural (Part # XP-235X)
- Nut SF Short 1/16in PEEK Nat (Part # LT-115)
- Adapter, Luer (Female) to 1/4"-28 Flat Bottom (Female), ETFE (Part # P-678)

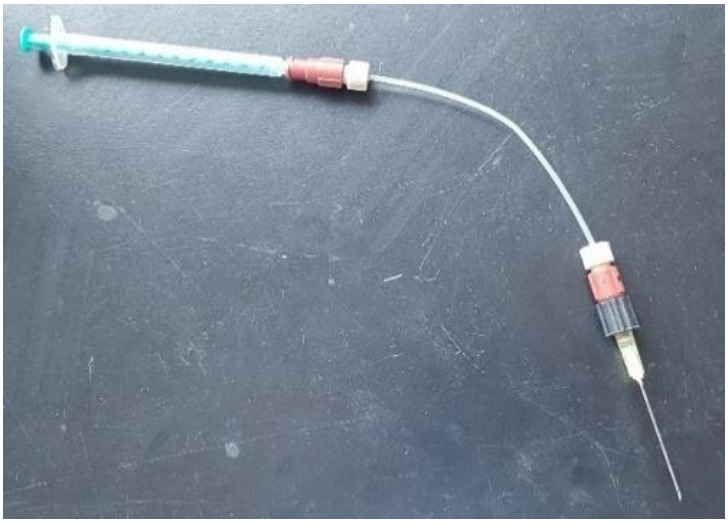

Figure 6 – PFA Tubing for Benzyl Lithium Slow Addition

It is also important to have the benzyl lithium solution dropping *directly* into the coupling solution, not dripping down the side of the reaction vessel. Otherwise, the benzyl lithium is prone to precipitate on the side of the flask, preventing it from entering the solution and participating in the reaction. This is another potential cause of incomplete aryl halide conversion.

For our optimization and scope of the deprotonation and coupling sequence of primary benzylic positions, we ensured to use fresh *n*-BuLi such that the concentration is close to 1.6 M. If a white precipitate is observed in the *n*-BuLi bottle, we recommend opening a fresh bottle or ensure the desired stoichiometry is used. If titration indicates the *n*-BuLi is substantially below 1.6 M concentration, an extended reaction time (on the order of 1 hour) is suggested.

3.1.3: Characterization Data for Products

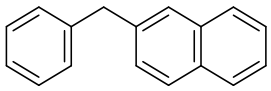

2-benzylnaphthalene (3) was prepared from toluene and 2-chloronaphthalene by general procedure A. Purified on silica eluting with 1% Et_2O in hexanes. Yield 33.1 mg (76%) white solid. Characterization data were in agreement with the literature.[179] **^{1}H NMR** (400 MHz, $CDCl_3$) δ 7.81-7.75 (m, 3H), 7.64 (s, 1H), 7.48-7.41 (m, 2H), 7.34-7.28 (m, 3H), 7.25-7.19 (m, 3H), 4.15 (s, 2H). **^{13}C{^{1}H} NMR** (100 MHz, CDCl3) δ 141.0, 138.6, 133.6, 132.1, 129.0, 128.5, 128.1, 127.64, 127.62, 127.5, 127.1, 126.1, 125.6, 125.3, 42.1.

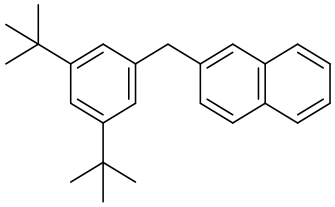

2-(3,5-di(*tert*-butyl)benzyl)naphthalene (5) was prepared from 3,5-di(*tert*-butyl)toluene and 2-chloronapthalene by general procedure A. Purified on silica eluting with 1% Et_2O in hexanes. Yield 50.5 mg (76%) white solid, melting point 113 °C. **^{1}H NMR** (400 MHz, $CDCl_3$) δ 7.84-7.75 (m, 3H), 7.66 (s, 1H), 7.50-7.43 (m, 2H), 7.37 (dd, J = 1.5, 8.5 Hz, 1H), 7.30 (t, J = 2.0 Hz, 1H), 7.11 (d, J = 2.0 Hz, 2H), 4.16 (s, 2H), 1.31 (s, 18 H). **^{13}C{^{1}H} NMR** (100 MHz, $CDCl_3$) δ 150.8, 139.9, 139.0, 133.7, 132.1, 127.9, 127.8, 127.64, 127.63, 127.0, 125.9, 125.2, 123.3, 120.2, 42.6, 34.8, 31.5. **IR** ν(neat) 1508, 1593, 2865, 2895, 2960 cm^{-1}. **Accurate Mass** (EI) m/z calculated for $C_{25}H_{30}$ 330.2348, found 330.2342, spectral accuracy 98.6%.

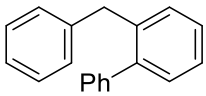

2-benzyl-1,1'-biphenyl (6) was prepared from toluene and 2-chlorobiphenyl by general procedure A. Purified on silica eluting with 1% Et_2O in hexanes. Yield 38.0 mg (78%) white solid. Characterization data were in agreement with the literature.[180] **^{1}H NMR** (400 MHz, $CDCl_3$) δ 7.38-7.14 (m, 14H), 6.98 (d, J = 7.5 Hz, 2H), 3.96 (s, 2H). **^{13}C{^{1}H} NMR** (100 MHz, $CDCl_3$) δ 142.3, 141.6, 141.5, 138.2, 130.3, 130.1, 129.3, 128.8, 128.2, 128.0, 127.5, 126.9, 126.1, 125.8, 39.0.

---

[179] Zhao, C.; Zha, G.-F.; Fang, W.-Y.; Rakesh, K. P.; Qin, H.-L. *Eur. J. Org. Chem.* **2019**, *2019*, 1801–1807.

[180] Sengupta, D.; Pandey, M. K.; Mondal, D.; Radhakrishna, L.; Balakrishna, M. S. *Eur. J. Inorg. Chem.* **2018**, *2018*, 3374–3383.

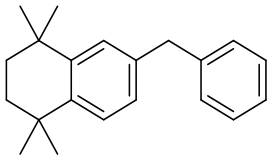

6-benzyl-1,1,4,4-tetramethyl-1,2,3,4-tetrahydronaphthalene (7) was prepared from 1,1,4,4,6-pentamethyl-1,2,3,4-tetrahydronaphthalene and chlorobenzene by general procedure A. Purified on silica eluting with 1% Et_2O in hexanes. Yield 38.7 mg (69%) colourless oil. **^{1}H NMR** (400 MHz, $CDCl_3$) δ 7.31-7.27 (m, 2H), 7.21-7.19 (m, 5H), 6.91 (dd, J = 2.0, 8.0 Hz, 1H), 3.93 (s, 2H), 1.67 (s, 4H), 1.25 (s, 12H). **^{13}C{^{1}H} NMR** (100 MHz, $CDCl_3$) δ 144.8, 142.5, 141.3, 137.8, 129.0, 128.4, 126.9, 126.6, 126.1, 125.9, 41.7, 35.2, 35.1, 34.2, 34.0, 31.89, 31.87. **IR** ν(neat) 1454, 1597, 1655, 2861, 2919, 2958 cm^{-1}. **Accurate Mass** (EI) m/z calculated for $C_{21}H_{26}$ 278.2035, found 278.2029, spectral accuracy 98.5%.

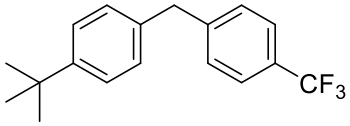

1-(*tert*-butyl)-4-[(4-trifluoromethyl)benzyl]benzene (8) was prepared from 4-*tert*-butyltoluene and 4-chlorobenzotrifluoride by general procedure A. Purified on silica eluting with 1% Et_2O in hexanes. Yield 48.9 mg (84%) colourless oil. Characterization data were in agreement with the literature.[181] **^{1}H NMR** (400 MHz, $CDCl_3$) δ 7.54 (d, J = 8.0 Hz, 2H), 7.32 (t, J = 8.0 Hz, 4H), 7.11 (d, J = 8.0 Hz, 2H), 4.00 (s, 2H), 1.31 (s, 9H). **^{13}C{^{1}H} NMR** (100 MHz, $CDCl_3$) δ 149.3, 145.4 (q, $^4J_{C,F}$ = 1.5 Hz), 136.9, 129.2, 128.5, 128.4 (q, $^2J_{C,F}$ = 32.0 Hz), 125.6, 125.4 (q, $^3J_{C,F}$ = 4.0 Hz), 124.3 (q, $^1J_{C,F}$ = 272.0 Hz), 41.2, 34.4, 31.4. **^{19}F NMR** (376 MHz, $CDCl_3$) δ -62.3.

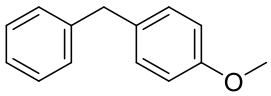

4-benzylanisole (9) was prepared from toluene and 4-chloroanisole by a modified version of general procedure A using a 3-hour slow addition. Purified on silica eluting with 1% Et_2O in hexanes. Yield 22.8 mg (58%) colourless oil. Characterization data were in agreement with the literature.[182] **^{1}H NMR** (400 MHz, $CDCl_3$) δ 7.30-7.26 (m, 2H), 7.21-7.15 (m, 3H), 7.12-7.08 (m, 2H), 6.83 (d, J = 8.5 Hz, 2H), 3.93 (s, 2H), 3.78 (s, 3H). **^{13}C{^{1}H} NMR** (100 MHz, $CDCl_3$) δ 158.0, 141.6, 133.3, 129.9, 128.8, 128.4, 126.0, 113.9, 55.3, 41.0.

[181] Benischke, A.; Desaintjean, A.; Juli, T.; Cahiez, G.; Knochel, P. *Synthesis* **2017**, *49*, 5396–5412.
[182] Chang, S.-T.; Li, Q.; Chiang, R.-T.; Gau, H.-M. *Tetrahedron* **2012**, *68*, 3956–3962.

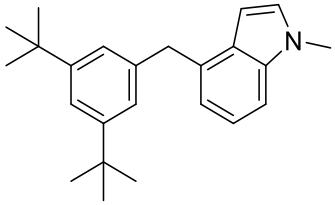

***N*-methyl-4-(3,5-di(*tert*-butyl)benzyl)indole (10)** was prepared from 3,5-di(*tert*-butyl)toluene and N-methyl-4-chloroindole by a modified version of general procedure A using a 3-hour slow addition. Purified on silica eluting with 5% EtOAc in hexanes with 1% Et_3N. Yield 42.3 mg (63%) red oil. **^{1}H NMR** (400 MHz, $CDCl_3$) δ 7.31 (t, J = 1.5 Hz, 1H), 7.25-7.17 (m, 4H), 7.07 (d, J = 3.0 Hz, 1H), 6.91 (d, J = 6.5 Hz, 1H), 6.61 (d, J = 3.0 Hz, 1H), 4.30 (s, 2H), 3.81 (s, 3H), 1.34 (s, 18H). **^{13}C{^{1}H} NMR** (100 MHz, $CDCl_3$) δ 150.5, 146.0, 139.8, 136.7, 133.9, 128.3, 128.1, 123.5, 121.7, 119.8, 119.3, 107.2, 99.6, 39.9, 34.8, 33.0, 31.6. **IR** ν(neat) 1577, 1597, 1739, 2870, 2954 cm^{-1}. **Accurate Mass** (EI) m/z calculated for $C_{24}H_{31}N$ 333.2457, found 333.2451, spectral accuracy 97.6%.

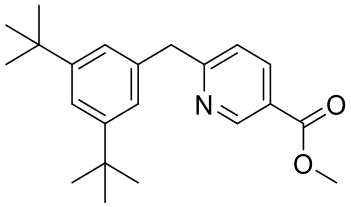

6-(3,5-di(tert-butyl)benzyl)nicotinate (22) was prepared from 3,5-di(*tert*-butyl)toluene and methyl 6-chloronicotinate by general procedure B. Purified on silica eluting with a gradient of 0-20% EtOAc in hexanes. Yield 61.8 mg (91%) off-white solid, melting point 105 °C. **^{1}H NMR** (400 MHz, $CDCl_3$) δ 9.16 (d, J = 2.0 Hz, 1H), 8.17 (dd, J = 2.0, 8.0 Hz, 1H), 7.31 (t, J = 1.5 Hz, 1H), 7.19 (d, J = 8.0 Hz, 1H), 7.11 (d, J = 1.5 Hz, 2H), 4.22, (s, 2H), 3.93 (s, 3H), 1.30 (s, 18H).**^{13}C{^{1}H} NMR** (100 MHz, $CDCl_3$) δ 166.1, 166.0, 151.1, 150.5, 137.5, 135.0, 123.7, 123.4, 122.7, 120.7, 52.2, 45.4, 34.8, 31.5. **IR** ν(neat) 1439, 1593, 1707, 2870, 2952 cm^{-1}. **Accurate Mass** (EI) m/z calculated for $C_{22}H_{29}NO_2$ 339.2198, found 339.2193, spectral accuracy 96.7%.

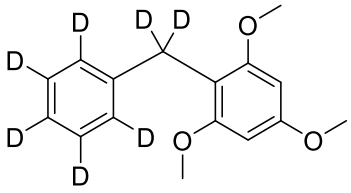

2-(heptadeuterobenzyl)-1,3,5-trimethoxybenzene (23) was prepared from toluene-d_8 and 2-chloro-1,3,5-trimethoxybenzene using a modified version of general procedure B using a 1-hour deprotonation and 2.5 mol% Pd_2dba_3 and 10 mol% XPhos. Purified on silica eluting with a gradient of 0-5% EtOAc in hexanes. Yield 41.0 mg (77%) white solid. Characterization data were in

agreement with the literature for the non-deuterated derivative.[183] **^{1}H NMR** (400 MHz, $CDCl_3$) δ 6.16 (s, 2H), 3.82 (s, 3H), 3.80 (s, 6H). **^{13}C{^{1}H} NMR** (75 MHz, $CDCl_3$) δ 159.7, 158.9, 142.0, 128.4-127.9 (m), 127.8-127.2 (m), 125.0-124.5 (m), 110.3, 90.6, 55.7, 55.3, 29.8-29.6 (m).

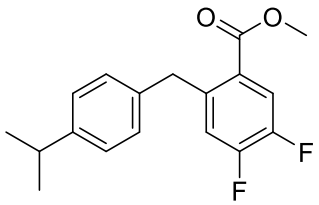

Methyl 2-(4-isopropylbenzyl)-4,5-difluorobenzoate (24) was prepared from *p*-cymene and methyl 2-bromo-4,5-difluorobenzoate by general procedure B. Purified on silica eluting with a gradient of 1-5% Et_2O in hexanes. Yield 51.3 mg (84%) colourless oil. **^{1}H NMR** (400 MHz, $CDCl_3$) δ 7.77 (dd, J = 11.5, 8.0 Hz, 1H), 7.18-7.13 (m, 2H), 7.08-7.03 (m, 2H), 6.96 (dd, J = 11.0, 8.0 Hz, 1H), 4.32 (s, 2H), 3.85 (s, 3H), 2.88 (quin, J = 7.0 Hz, 1H), 1.24 (d, J = 7.0 Hz, 6H). **^{13}C{^{1}H} NMR** (100 MHz, $CDCl_3$) δ 166.6 (d, $^{4}J_{C,F}$ = 2.0 Hz), 152.4 (dd, $^{1}J_{C,F}$ = 254.8 Hz, $^{2}J_{C,F}$ = 12.4 Hz), 148.2 ($^{1}J_{C,F}$ = 248.0 Hz, $^{2}J_{C,F}$ = 13.0 Hz), 147.0, 141.1 (dd, $^{3}J_{C,F}$ = 6.0 Hz, $^{4}J_{C,F}$ = 4.0 Hz), 137.0, 128.8, 126.6, 125.9 (dd, $^{3}J_{C,F}$ = 5.0 Hz, $^{4}J_{C,F}$ = 3.5 Hz), 120.1 (d, $^{2}J_{C,F}$ = 17.5 Hz), 120.0 (dd, $^{2}J_{C,F}$ = 19.0 Hz, $^{3}J_{C,F}$ = 1.5 Hz), 52.2, 38.4, 33.7, 24.0. **^{19}F NMR** (376 MHz, $CDCl_3$) δ -131.48 (d, J = 22.0 Hz), 140.52 (d, J = 22.0 Hz). **IR** ν(neat) 1176, 1178, 1508, 1599, 1726, 2876, 2928, 2960 cm^{-1}. **Accurate Mass** (EI) m/z calculated for $C_{18}H_{18}F_2O_2$ 304.1275, found 304.1269, spectral accuracy 97.7%.

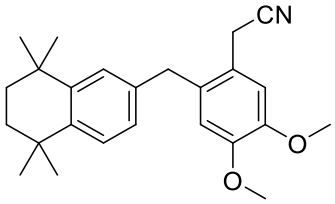

2-(4,5-dimethoxy-2-((5,5,8,8-tetramethyl-5,6,7,8-tetrahydronaphthalen-2-yl)methyl)phenyl)acetonitrile (25) was prepared from 1,1,4,4,6-pentamethyl-1,2,3,4-tetrahydronaphthalene and 2-bromo-4,5-dimethoxyphenylacetonitrile by general procedure B. Purified on silica eluting with a gradient of 0-30% EtOAc in hexanes. Yield 64.1 mg (85%) off-white solid, melting point 84 °C. **^{1}H NMR** (400 MHz, $CDCl_3$) δ 7.21 (d, J = 8.5 Hz, 1H), 7.04 (s, 1H), 6.92 (s, 1H), 6.78 (d, J = 7.5 Hz, 1H), 6.72 (s, 1H), 3.92-3.91 (m, 5H), 3.85 (s, 3H), 3.55 (s, 2H), 1.67 (s, 4H), 1.25 (d, J = 9.5 Hz, 12H). **^{13}C{^{1}H} NMR** (100 MHz, $CDCl_3$) δ 148.7, 147.9, 145.2, 143.1, 135.9, 130.8, 126.9, 126.3, 125.4, 120.5, 118.1, 114.3, 112.2, 65.3, 56.1, 56.0, 38.4, 35.09, 35.06, 34.2, 34.0, 31.9, 21.1. **IR** ν(neat) 1517, 1608, 2255, 2861, 2923, 2958 cm^{-1}. **Accurate Mass** (EI) m/z calculated for $C_{25}H_{31}NO_2$ 377.2355, found 377.2349, spectral accuracy 98.4%.

[183] Nagashima, H.; Kubo, Y.; Kawamura, M.; Nishikata, T.; Motoyama, Y. *Tetrahedron* **2011**, *67*, 7667–7672.

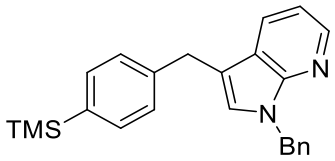

1-benzyl-3-(4-(trimethylsily)benzyl)-1H-pyrrolo[2,3-b]pyridine (26) was prepared from 4-(trimethylsilyl)toluene and 1-benzyl-3-iodo-1H-pyrrolo[2,3-b]pyridine using general procedure B. Purified on silica eluting with a gradient of 0-10% EtOAc in hexanes. Yield 51.3 mg (69%) yellow oil. **^{1}H NMR** (400 MHz, CDCl3) δ 8.36 (dd, J = 4.0, 1.5 Hz, 1H), 7.81 (dd, J = 8.0, 1.5 Hz, 1H), 7.48-7.46 (m, 2H) 7.33-7.27 (m, 5H), 7.25-7.20 (m, 2H), 7.04 (dd, J = 8.0, 4.5 Hz, 1H), 7.00 (s, 1H), 5.49 (s, 2H), 4.09 (s, 2H), 0.28 (s, 9H). **^{13}C{^{1}H} NMR** (100 MHz, $CDCl_3$) δ 148.2, 143.1, 141.4, 138.1, 137.8, 133.5, 128.7, 128.0, 127.5, 127.4, 127.4, 125.9, 120.2, 115.4, 113.2, 47.6, 31.7, -1.0. **IR** ν(neat) 1450, 1599, 1702, 1716, 2852, 2921 cm^{-1}. **Accurate Mass** (EI) m/z calculated for $C_{24}H_{26}N_2Si$ 370.1865, found 370.1860, spectral accuracy 98.2%.

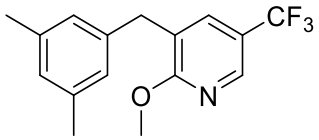

3-(3,5-dimethylbenzyl)-2-methoxy-5-(trifluoromethyl)pyridine (27) was prepared from mesitylene and 3-chloro-2-methoxy-5-(trifluoromethyl)pyridine using a modified version of general procedure B in which butyl lithium was added over 10 minutes. Purified on silica eluting with a gradient of 0-10% EtOAc in hexanes. Yield 53.1 mg (90%) colourless oil. **^{1}H NMR** (400 MHz, $CDCl_3$) δ 8.33 (s, 1H), 7.45 (d, J = 2.0 Hz, 1H), 6.90 (s, 1H), 6.82 (s, 2H), 4.04 (s, 3H), 3.88 (s, 2H), 2.31 (s, 6H). **^{13}C{^{1}H} NMR** (100 MHz, $CDCl_3$) δ 164.1, 142.4 (q, $^{3}J_{C,F}$ = 4.5 Hz), 138.3, 138.2, 134.7 (q, $^{3}J_{C,F}$ = 3.0 Hz), 128.3, 126.8, 124.5, 124.1 (q, $^{1}J_{C,F}$ = 271.5 Hz), 119.9 (q, $^{2}J_{C,F}$ = 32.5 Hz), 54.1, 35.2, 21.3. **^{19}F NMR** (376 MHz, $CDCl_3$) δ -61.3. **IR** ν(neat) 1116, 1482, 1624, 2867, 2926, 3018 cm^{-1}. **Accurate Mass** (EI) m/z calculated for $C_{16}H_{16}F_3NO$ 295.1184, found 295.1178, spectral accuracy 98.7%.

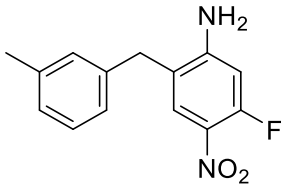

2-(3-methylbenzyl)-5-fluoro-4-nitroaniline (28) was prepared from *m*-xylene and 2-bromo-5-fluoro-4-nitroaniline by a modified version of general procedure B in which butyl lithium was added over 10 minutes and double the equivalents of *m*-xylene, *n*-BuLi, and TMCDA. Purified on silica eluting with 0-40% EtOAc in hexanes. Yield 48.6 mg (93%) yellow solid, melting point 122 °C. **^{1}H NMR** (400 MHz, $CDCl_3$) δ 7.92 (d, J = 8.5 Hz, 1H), 7.24-7.19 (m, 1H), 7.08 (d, J = 8.0 Hz, 1H), 6.99-6.95 (m, 2H), 6.38 (d, J = 13.0 Hz, 1H), 4.32 (s, 2H), 3.85 (s, 2H), 2.32 (s, 3H). **^{13}C{^{1}H} NMR** (100 MHz, $CDCl_3$) δ 157.0 (d, $^{1}J_{C,F}$ = 262.0 Hz), 152.0 (d, $^{3}J_{C,F}$ = 11.5 Hz), 138.9, 137.0, 129.17,

129.16, 129.0 (d, $^{3}J_{C,F}$ = 7.5 Hz), 128.0, 127.6 (d, $^{2}J_{C,F}$ = 19.0 Hz) 125.3, 120.0 (d, $^{4}J_{C,F}$ = 2.5 Hz), 102.5 (d, $^{2}J_{C,F}$ = 24.5 Hz), 37.2, 21.4. **^{19}F NMR** (376 MHz, $CDCl_3$) δ -177.1. **IR** ν(neat) 1299, 1489, 1629, 2855, 2924, 3357, 3482 cm^{-1}. **Accurate Mass** (EI) m/z calculated for $C_{14}H_{13}FN_2O_2$ 260.0961, found 260.0956, spectral accuracy 99.0%.

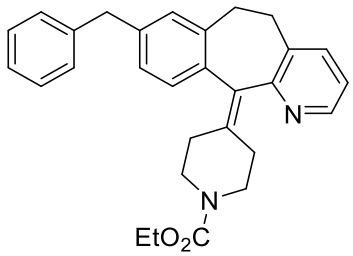

4-(8-benzyl-5,6-dihydro-11H-benzo[5,6]cyclohepta[1,2-b]pyridin-11-ylidene-1-piperidinecarboxylic acid ethyl ester (29) was prepared from toluene and loratadine using a modified version of general procedure B using 2.5 mol% Pd_2dba_3 and 10 mol% XPhos. Purified on silica eluting with a gradient of 0-60% EtOAc in hexanes with 1% Et_3N. Yield 86.8 mg (99%) yellow solid, melting point 51 °C. **^{1}H NMR** (400 MHz, $CDCl_3$) δ 8.38 (d, J = 4.0 Hz, 1H), 7.43-7.37 (m, 1H), 7.31-7.34 (m, 2H), 7.22-7.16 (m, 3H), 7.14-7.10 (m, 1H), 7.08-7.03 (m, 1H), 7.01 – 6.97 (m, 2H), 4.14 (q, J = 7.0 Hz, 2H), 3.92 (s, 2H), 3.82 (s, 2H), 3.42-3.29 (m, 2H), 3.19-3.09 (m, 2H), 2.85-2.74 (m, 2H), 2.52-2.29 (m, 4H), 1.25 (t, J = 7.0 Hz, 3H). **^{13}C{^{1}H} NMR** (100 MHz, $CDCl_3$) δ 157.9, 155.5, 146.5, 140.1, 140.3, 137.6, 137.3, 136.9, 135.2, 133.7, 129.6, 129.4, 129.0, 128.5, 126.5, 126.1, 122.1, 61.3, 45.0, 44.9, 41.6, 31.9, 31.7, 30.7, 30.6, 14.7. **IR** ν(neat) 1431, 1690, 2879, 2924 cm^{-1}. **Accurate Mass** (EI) m/z calculated for $C_{29}H_{30}N_2O_2$ 438.2307, found 438.2302, spectral accuracy 98.7%.

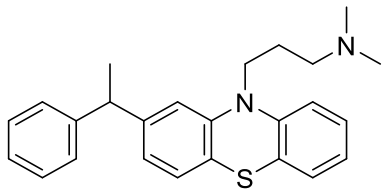

2-(1-phenylethyl)-10-(3-dimethylaminopropyl)phenothiazine (45) was prepared from ethylbenzene and chlorpromazine hydrochloride by a modified version of general procedure C using double the equivalents of ethylbenzene, *n*-BuLi, and KO*t*Bu. Purified on silica eluting with 0-5% MeOH in CH_2Cl_2 with 1% Et_3N. Yield 55.8 mg (72%) yellow oil. **^{1}H NMR** (400 MHz, $CDCl_3$) δ 7.31-7.26 (m, 2H), 7.23-7.09 (m, 5H), 7.07-7.03 (m, 1H), 6.92-6.79 (m, 3H), 6.70-6.67 (m, 1H), 4.09 (q, J = 7.0 Hz, 1H), 3.86 (t, J = 7.0 Hz, 2H), 2.43 (t, J = 6.0 Hz, 2H), 2.22 (s, 6H), 1.92 (quin, J = 7.0 Hz, 2H), 1.61 (d, J = 7.5 Hz, 3H). **^{13}C{^{1}H} NMR** (100 MHz, $CDCl_3$) δ 146.0, 145.9, 145.3, 145.0, 128.4, 127.5, 127.4, 127.24, 127.20, 126.15, 125.4, 122.7, 122.4, 121.7, 115.6, 115.4, 57.0, 45.3, 45.2, 44.6, 29.7, 24.6, 21.8. **IR** ν(neat) 1416, 1457, 1585, 2757, 2930, 2965, 3029, 3062 cm^{-1}. **Accurate Mass** (EI) m/z calculated for $C_{25}H_{28}N_2S$ 388.1973, found 388.1968, spectral accuracy 98.2%.

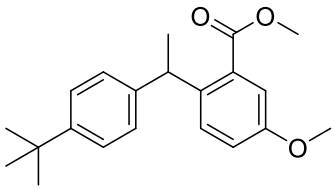

Methyl 2-(1-(4-tertbutylphenyl)ethyl)-5-methoxybenzoate (46) was prepared from 1-*tert*-butyl-4-ethylbenzene and methyl 2-bromo-5-methoxybenzoate by general procedure C. Purified on silica eluting with 0-5% EtOAc in hexanes. Yield 49.5 mg (76%) colourless oil. **^{1}H NMR** (400 MHz, $CDCl_3$) δ 7.29-7.23 (m, 3H), 7.20-7.10 (m, 3H), 6.98-6.93 (m, 1H), 4.96 (q, J = 7.0 Hz, 1H), 3.82 (s, 3H), 3.79 (s, 3H). 1.58 (d, J = 7.0 Hz, 3H), 1.27 (s, 9H). **^{13}C{^{1}H} NMR** (100 MHz, $CDCl_3$) δ 168.5, 157.2, 148.5, 143.2, 139.8, 131.0, 129.6, 127.3, 125.0, 118.0, 114.4, 55.4, 52.0, 38.8, 34.3, 31.4, 22.1. **IR** ν(neat) 1215, 1433, 1496, 1720, 2872, 2960 cm^{-1}. **Accurate Mass** (EI) m/z calculated for $C_{21}H_{26}O_3$ 326.1882, found 326.1876, spectral accuracy 97.5%.

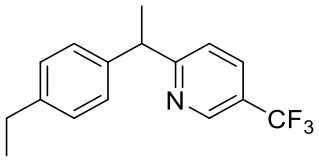

2-(1-(4-ethylphenyl)ethyl)-5-trifluoromethylpyridine (47) was prepared from 1,4-diethylbenzene and 2-bromo-5-trifluoromethylpyridine using general procedure C. Purified on silica eluting with 5% Et_2O in hexanes with 1 % Et_3N. Yield 44.8 mg (80%) colourless oil. **^{1}H NMR** (400 MHz, $CDCl_3$) δ 8.82 (s, 1H), 7.78 (dd, J = 8.0, 2.5 Hz, 1H), 7.27-7.19 (m, 3H), 7.18-7.13 (m, 2H), 4.34 (q, J = 7.0 Hz, 1H), 2.63 (q, J = 7.5 Hz, 2H), 1.72 (d, J = 7.0 Hz, 3H), 1.23 (t, J = 7.5 Hz, 3H). **^{13}C{^{1}H} NMR** (100 MHz, $CDCl_3$) δ 169.3 (q, $^{4}J_{C,F}$ = 1.5 Hz), 146.1 (q, $^{3}J_{C,F}$ = 4.0 Hz), 142.7, 141.3, 133.5 (q, $^{3}J_{C,F}$ = 3.5 Hz), 128.1, 127.6, 124.0 (q, $^{2}J_{C,F}$ = 33.0 Hz), 123.7 (q, $^{1}J_{C,F}$ = 272.5 Hz), 121.9, 47.1, 28.4, 20.6, 15.5. **^{19}F NMR** (376 MHz, $CDCl_3$) δ -62.3. **IR** ν(neat) 1129, 1325, 1392, 1605, 2880, 2934, 2969 cm^{-1}. **Accurate Mass** (EI) m/z calculated for $C_{16}H_{16}F_3N$ 279.1235, found 279.1229, spectral accuracy 98.2%.

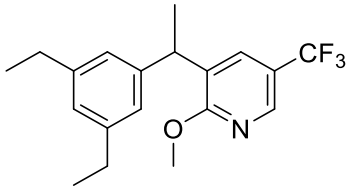

3-(1-(3,5-diethylphenyl)ethyl)-2-methoxy-5-(trifluoromethyl)pyridine (48) was prepared from 1,3,5-triethylbenzene and 3-chloro-2-methoxy-5-(trifluoromethyl)pyridine using general procedure C. Purified on silica eluting with a gradient of 0-5% EtOAc in hexanes. Yield 60.0 mg (89%) yellow oil. **^{1}H NMR** (400 MHz, $CDCl_3$) δ 8.32-8.29 (m, 1H), 7.58 (d, J = 2.5 Hz, 1H), 6.92 (s, 1H), 6.88 (s, 2H), 4.40 (q, J = 7.0 Hz, 1H), 4.00 (s, 3H), 2.62 (q, J = 7.5 Hz, 4H), 1.60 (d, J = 7.5 Hz, 3H), 1.23 (t, J = 7.5 Hz, 6H). **^{13}C{^{1}H} NMR** (100 MHz, $CDCl_3$) δ 163.6, 144.4, 143.8, 142.0 (q, $^{3}J_{C,F}$ = 4.5 Hz), 132.5 (q, $^{3}J_{C,F}$ = 3.0 Hz), 129.9, 125.7, 124.6, 122.8 (q, $^{1}J_{C,F}$ = 271.5 Hz), 120.0 (q, $^{2}J_{C,F}$ = 32.5

Hz), 54.0, 37.8, 28.9, 20.3, 15.6. **^{19}F NMR** (376 MHz, $CDCl_3$) δ -61.3. **IR** ν(neat) 1435, 1594, 1720, 2930, 2969. **Accurate Mass** (EI) m/z calculated for $C_{19}H_{22}F_3NO$ 337.1653, found 337.1648, spectral accuracy 97.8%.

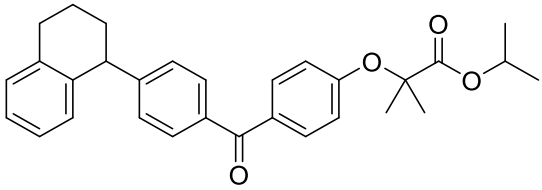

2-[4-(4-(1,2,3,4-tetrahydro-1-naphthyl)benzoyl)phenoxy]-2-methylpropanoic acid isopropyl ester (49) was prepared from tetralin and fenofibrate by general procedure C. Purified on silica eluting with a gradient of 0-10% EtOAc in hexanes. Yield 85.8 mg (91%) colourless oil. **^{1}H NMR** (400 MHz, $CDCl_3$) δ 7.77 (d, J = 8.5 Hz, 2H), 7.69 (d, J = 8.5 Hz, 2H), 7.22-7.02 (m, 5H), 6.89-6.82 (m, 3H), 5.09 (sept, J = 6.0 Hz, 1H), 4.21 (t, J = 6.5 Hz, 1H), 3.00-2.80 (m, 2H), 2.26-2.16 (m, 1H), 1.96-1.84 (m, 2H), 1.83-1.72 (m, 1H), 1.67 (s, 6H), 1.20 (d, J = 6.0 Hz, 6H). **^{13}C{^{1}H} NMR** (100 MHz, $CDCl_3$) δ 196.2, 173.2, 159.4, 152.1, 138.5, 137.6, 135.9, 132.0, 130.9, 130.1, 130.0, 129.2, 128.7, 126.2, 125.8, 117.2, 79.4, 69.3, 45.7, 33.1, 29.7, 25.4, 21.5, 20.9. **IR** ν(neat) 1385, 1501, 1597, 1651, 1726, 2861, 2932, 2982 cm^{-1}. **Accurate Mass** (EI) m/z calculated for $C_{30}H_{32}O_4$ 456.2301, found 456.2295, spectral accuracy 97.4%.

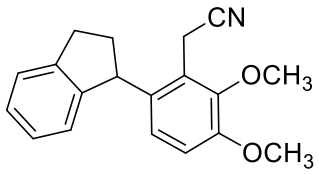

2-(2,3-dihydro-1H-inden-1-yl)-4,5-dimethoxyphenylacetonitrile (50) was prepared from indane and 1-(4-chloro-3-(trifluoromethyl)phenyl)ethenone by general procedure C. Purified on silica eluting with a gradient of 0-20% EtOAc in hexanes. Yield 37.6 mg (64%) yellow solid, melting point 38 °C. **^{1}H NMR** (400 MHz, $CDCl_3$) δ 7.32 (d, J = 7.5 Hz, 1H), 7.24-7.14 (dt, J = 24.5, 7.0 Hz, 2H), 6.94 (d, J = 7.5 Hz, 1H), 6.90 (s, 1H), 6.52 (s, 1H), 4.44 (t, J = 8.5 Hz, 1H), 3.91 (s, 3H), 3.75 (s, 2H), 3.70 (s, 3H), 3.12-2.93 (m, 2H), 2.69-260 (m, 1H), 2.02-1.89 (m, 1H). **^{13}C{^{1}H} NMR** (100 MHz, $CDCl_3$) δ 149.1, 147.7, 145.5, 144.2, 135.5, 126.9, 126.6, 124.7, 124.6, 120.0, 118.3, 112.2, 111.8, 56.0, 55.9, 47.5, 35.6, 31.6, 21.2. **IR** ν(neat) 1129, 1325, 1392, 1605, 2880, 2934, 2969 cm^{-1}. **Accurate Mass** (EI) m/z calculated for $C_{19}H_{19}NO_2$ 293.1416, found 293.1410, spectral accuracy 97.6%.

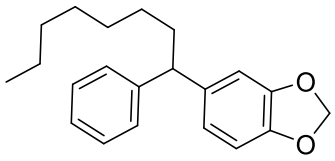

5-(1-phenyloctyl)-1,3-benzodioxole (51) was prepared from 1-phenyloctane and 5-chloro-1,3-benzodioxole using general procedure C. Purified on silica eluting with a gradient of 0-5% EtOAc in hexanes. Yield 43.0 mg (69%). Colourless oil. **^{1}H NMR** (400 MHz, $CDCl_3$) δ 7.28-7.15 (m, 5H), 6.71 (s, 3H), 5.90 (s, 2H), 3.80 (t, J = 7.5 Hz, 1H), 2.02-1.93 (m, 2H), 1.29-1.22 (m, 10H), 0.86 (t, J = 6.5 Hz, 3H). **^{13}C{^{1}H} NMR** (100 MHz, $CDCl_3$) δ 147.6, 145.7, 145.5, 139.4, 128.4, 127.7, 126.0, 120.7, 108.2, 108.0, 100.8, 51.0, 35.8, 31.8, 29.6, 29.2, 28.0, 22.6, 14.1. **IR** ν(neat) 1422, 1452, 1634, 2854, 2919 cm^{-1}. **Accurate Mass** (EI) m/z calculated for $C_{21}H_{26}O_2$ 310.1993, found 310.1927, spectral accuracy 96.9%.

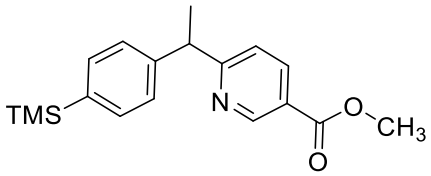

6-(1-(4-trimethylsilylphenyl)ethyl)nicotinate (52) was prepared from (4-ethylphenyl)trimethylsilane and methyl 6-chloronicotinate using general procedure C. Purified on silica eluting with a gradient of 0-15% EtOAc in hexanes. Yield 46.0 mg (73%) off-white solid, melting point 51 °C. **^{1}H NMR** (400 MHz, $CDCl_3$) δ 9.17 (d, J = 2.0 Hz, 1H), 8.16 (dd, J = 8.5, 2.5 Hz, 1H), 7.49-7.43 (m, 2H), 7.31-7.27 (m, 2H), 7.24-7.27 (m, 1H), 4.34 (q, J = 7.5 Hz, 1H), 3.92 (s, 3H), 1.72 (d, J = 7.0 Hz, 3H), 0.24 (s, 9H). **^{13}C{^{1}H} NMR** (100 MHz, $CDCl_3$) δ 169.4, 165.9, 150.5, 144.7, 138.4, 137.4, 133.6, 127.1, 123.7, 121.8, 52.2, 47.5, 20.4, -1.2. **IR** ν(neat) 1433, 1476, 1593, 1719, 2239, 2954. **Accurate Mass** (EI) m/z calculated for $C_{18}H_{23}NO_2Si$ 313.1498, found 313.1493, spectral accuracy 95.9%.

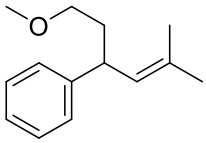

3-methyl-1-phenyl-1-(2-methoxy-ethyl)-but-2-ene (53) was prepared from 3-methoxypropylbenzene and 2-methyl-1-propenylbromide using general procedure C. Purified on silica eluting with a gradient of 0-5% Et_2O in hexanes. Yield 31.2 mg (76%). Colourless oil. **^{1}H NMR** (400 MHz, $CDCl_3$) δ 7.32-7.26 (m, 2H), 7.24-7.14 (m, 3H), 5.26 (d, J = 10.0 Hz, 1H), 3.73-3.64 (m, 1H), 3.30 (s, 3H), 3.30 (t, J = 6.0 Hz, 2H), 2.01-1.91 (m, 1H), 1.89-1.81 (m, 1H), 1.71 (s, 3H), 1.68 (s, 3H). **^{13}C{^{1}H} NMR** (100 MHz, $CDCl_3$) δ 145.7, 131.9, 128.4, 128.2, 127.3, 125.8, 70.6, 58.5, 40.6, 36.7, 25.9, 18.0. **IR** ν(neat) 1448, 1601, 2874, 2926, 2971 cm^{-1}. **Accurate Mass** (EI) m/z calculated for $C_{14}H_{20}O$ 204.1514; found 204.1509, spectral accuracy 96.2%.

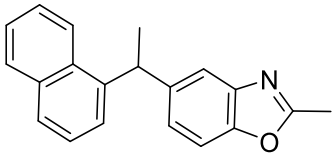

5-(1-(naphthalen-2-yl)ethyl)-2-methylbenzoxzole (54) was prepared from 2-ethylnaphthalene and 5-chloro-2-methylbenzoxazole using general procedure C. Purified on silica eluting with a gradient of 0-20% EtOAc in hexanes. Yield 51.2 mg (89%). Yellow oil. **^{1}H NMR** (400 MHz, $CDCl_3$) δ 8.06-8.02 (m, 1H), 7.86-7.73 (m, 2H), 7.57-7.30 (m, 6H), 7.17-7.12 (m, 1H), 5.05 (q, J = 7.0 Hz, 1H), 2.59 (s, 3H), 1.82 (d, J = 7.0 Hz, 3H). **^{13}C{^{1}H} NMR** (100 MHz, $CDCl_3$) δ 164.1, 149.4, 143.2, 141.8, 141.4, 134.1, 131.7, 128.8, 127.1, 125.9, 125.4, 125.3, 124.31, 124.27, 124.0, 118.2, 109.9, 40.6, 23.0, 14.5. **IR** ν(neat) 1474, 1508, 1576, 2926, 2964, 3047. **Accurate Mass** (EI) m/z calculated for $C_{20}H_{17}NO$ 287.1310, found 287.1315, spectral accuracy 95.9%.

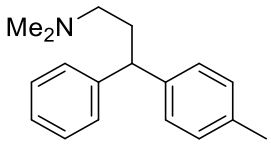

Tolpropamine (55) was prepared from *N*,*N*-dimethyl-3-phenylpropylamine and 4-chlorotoluene using general procedure C. Purified on silica gel eluting with a gradient of 0-10% MeOH in DCM. Yield 42.1 mg (83%) yellow oil. Characterization data were in agreement with the literature.[184] **^{1}H NMR** (400 MHz, $CDCl_3$) δ 7.30-7.23 (m, 4H), 7.18-7.06 (m, 5H), 3.95 (t, J = 6.5 Hz, 1H), 2.30 (s, 3H), 2.27-2.19 (m, 10H). **^{13}C{^{1}H} NMR** δ 145.1, 141.8, 135.7, 129.2, 128.5, 127.8, 127.7, 126.1, 58.1, 48.7, 45.4, 33.5, 21.0.

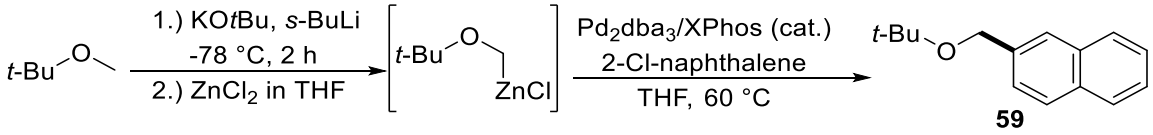

2-(*tert*-butoxymethyl)naphthalene (59) was prepared from methyl *tert*-butyl ether and 2-chloronaphthalene. Pd_2dba_3 (2.3 mg, 2.5 mol%, 2.5 µmol), XPhos (4.7 mg, 10 mol%, 10 µmol) and 2-chloronaphthalene (16.3 mg, 1 equiv, 0.1 mmol) were placed in an 8 mL screw-top tube and flushed with N_2. Tetrahydrofuran (2 mL) was added to the vial. Separately, KO*t*Bu (22.4 mg, 2 eq, 0.2 mmol) was weighed inside of a glovebox under a N_2 atmosphere. Methyl tert-butyl ether (1.33 mL) was added, and the mixture was cooled to -78 °C. *s*-BuLi 1.4 M in cyclohexane (143 µL, 2 equiv, 0.2 mmol) was added dropwise over approximately 1 minute. The mixture was stirred for 2 hours at -78 °C, during which time the solution turned pale yellow. A solution of $ZnCl_2$ 0.5 M in 2-MeTHF (400 µL, 2 equiv, 0.2 mmol) was then added dropwise over approximately 1 minute to the mixture at -78 °C to form a colourless solution. The resultant organozinc solution was then

[184] Gu, F.; Huang, W.; Liu, X.; Chen, W.; Cheng, X. *Adv. Synth. Catal.* **2018**, *360*, 925–931.

added to the mixture of catalyst and aryl halide and stirred at 60 °C. Once the reaction was complete (i.e. full consumption of aryl halide observed by GC-MS; less than 3 hours), the mixture was then quenched with methanol (2 mL), dry loaded onto silica gel, and purified by flash column chromatography eluting with 1% Et_2O in hexanes. Yield 18.0 mg (84%) off-white solid. Characterization data were in agreement with the literature.[185] **^{1}H NMR** (400 MHz, $CDCl_3$) δ 7.86-7.78 (m, 4H), 7.51-7.42 (m, 3H), 4.62 (s, 2H), 1.35 (s, 9H). **^{13}C{^{1}H} NMR** (100 MHz, $CDCl_3$) δ 137.4, 133.4, 132.8, 127.9, 127.8, 127.6, 125.84, 125.79, 127.75, 125.5, 73.6, 64.3, 27.8.

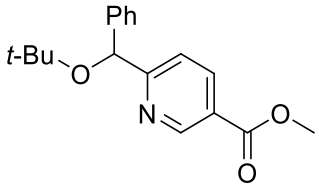

Methyl 6-(*tert*-butoxy(phenyl)methyl)nicotinate (60) was prepared from benzyl *tert*-butyl ether and 2-chloronaphthalene using general procedure C. Purified on silica eluting with a gradient of 0-15% EtOAc. Yield 45.6 mg (76%) yellow solid, melting point 72 °C. **^{1}H NMR** (400 MHz, $CDCl_3$) δ 9.09 (d, J = 1.5 Hz, 1H), 8.24 (dd, J = 8.0, 2.0 Hz, 1H), 7.70 (d, J = 8.5 Hz, 1H), 7.47-7.41 (m, 2H), 7.28 (t, J = 7.5 Hz, 2H), 7.23-7.16 (m, 1H), 5.78 (s, 1H), 3.92 (s, 3H), 1.23 (s, 9H). **^{13}C{^{1}H} NMR** (100 MHz, $CDCl_3$) δ 169.1, 165.8, 149.9, 143.0, 137.7, 128.3, 127.2, 126.5, 124.3, 120.6, 76.9, 75.5, 52.2, 28.5. **IR** ν(neat) 1435, 1471, 1594, 1719, 2854, 2926, 2971. **Accurate Mass** (EI) m/z calculated for $C_{18}H_{21}NO_3$ 299.1521, found 299.1516, spectral accuracy 97.9%.

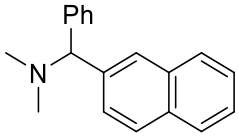

N,N-dimethyl-1-(naphthalen-2-yl)-1-phenylmethanamine (61) was prepared from N,N-dimethylbenzylamine and 2-chloronaphthalene using a modified version of general procedure C in which the deprotonation was done at 0 °C for 30 minutes. Purified on silica eluting with 89:10:1 hexanes:EtO_2:Et_3N. Yield 43.5 mg (83%) off-white solid. Characterization data were in agreement with the literature.[186] **^{1}H NMR** (400 MHz, $CDCl_3$) δ 7.87 (s, 1H), 7.83-7.74 (m, 3H), 7.61 (dd, J = 8.5, 1.5 Hz, 1H), 7.53-7.48 (m, 2H), 7.47-7.39 (m, 2H), 7.31-7.28 (m, 1H), 7.28-7.25 (m, 1H), 7.21-7.15 (m, 1H), 4.25 (s, 1H), 2.26 (s, 6H). **^{13}C{^{1}H} NMR** (100 MHz, $CDCl_3$) δ 143.2, 141.0, 133.5, 132.7, 128.5, 128.2, 127.8, 127.6, 126.9, 126.2, 125.9, 125.8, 125.5, 78.1, 44.8.

[185] Tait, K.; Alrifai, O.; Boutin, R.; Haner, J.; Tam, W. *J. Org. Chem.* **2016**, *12*, 2189–2196.
[186] Ong, D. Y.; Fan, D.; Dixon, D. J.; Chiba, S. *Angew. Chem. Int. Ed.* **2020**, *59*, 11903–11907.

3.1.4: NMR Spectra

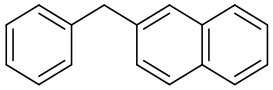

3 (^{1}H NMR, $CDCl_3$, 400 MHz)

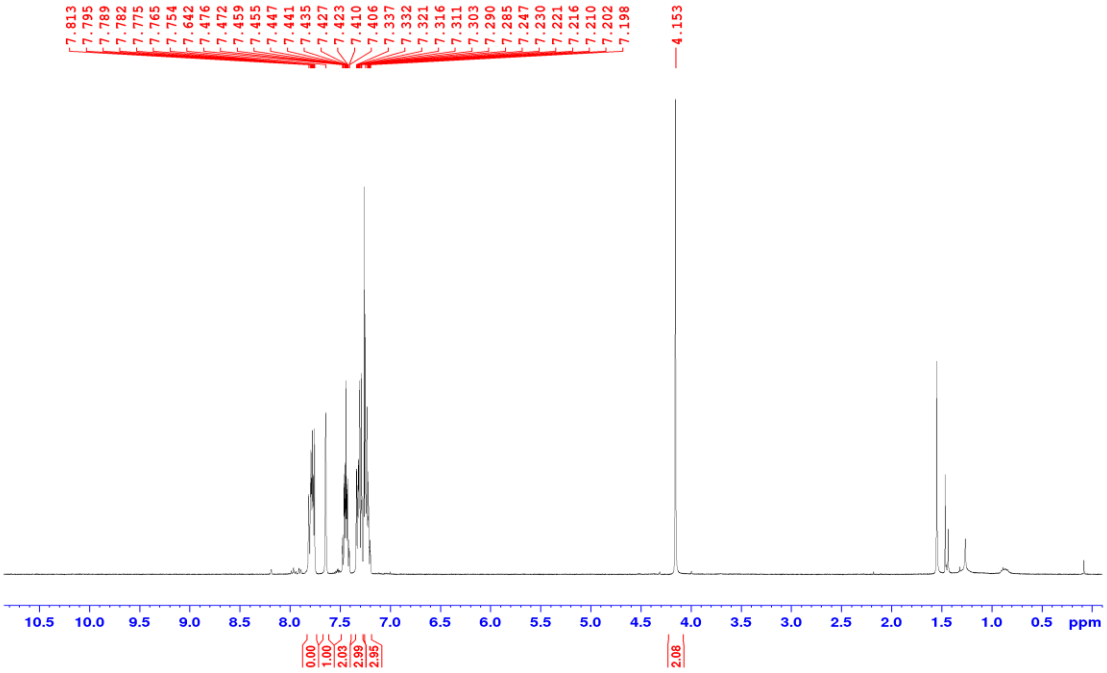

2 (^{13}C NMR, $CDCl_3$, 100 MHz)

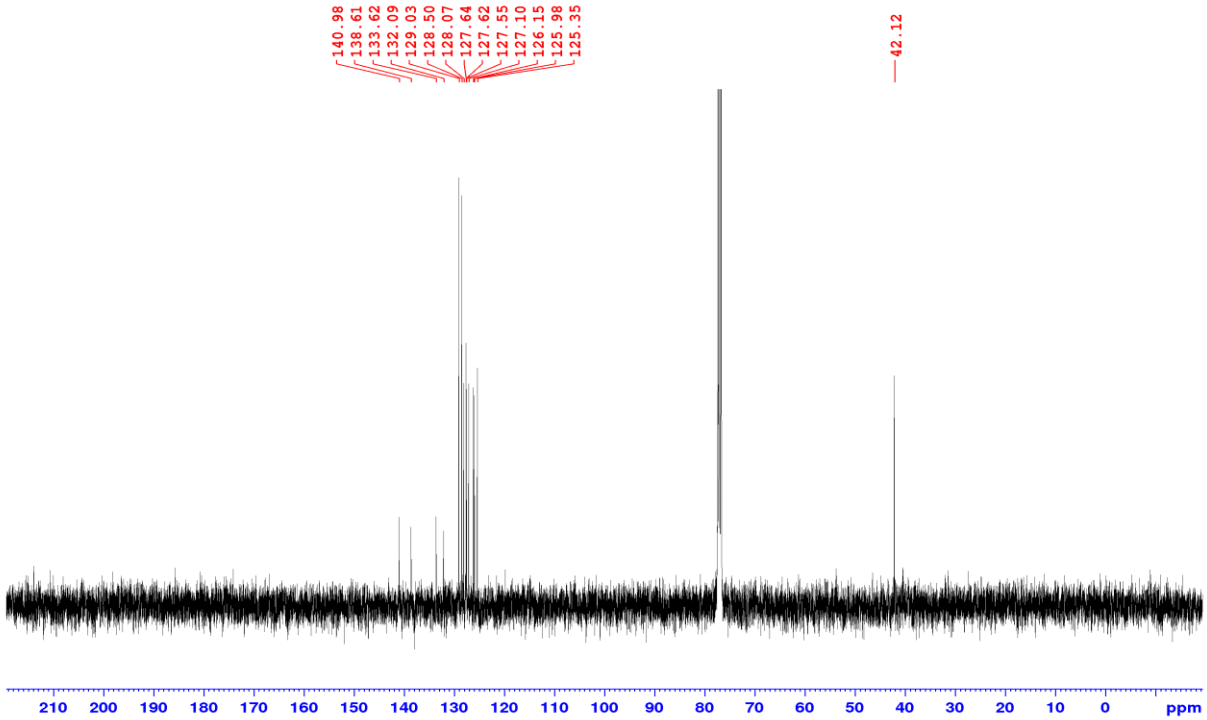

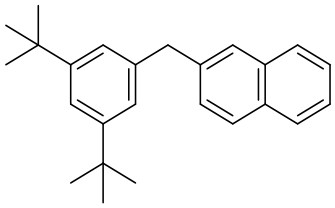

5 (^{1}H NMR, $CDCl_3$, 400 MHz)

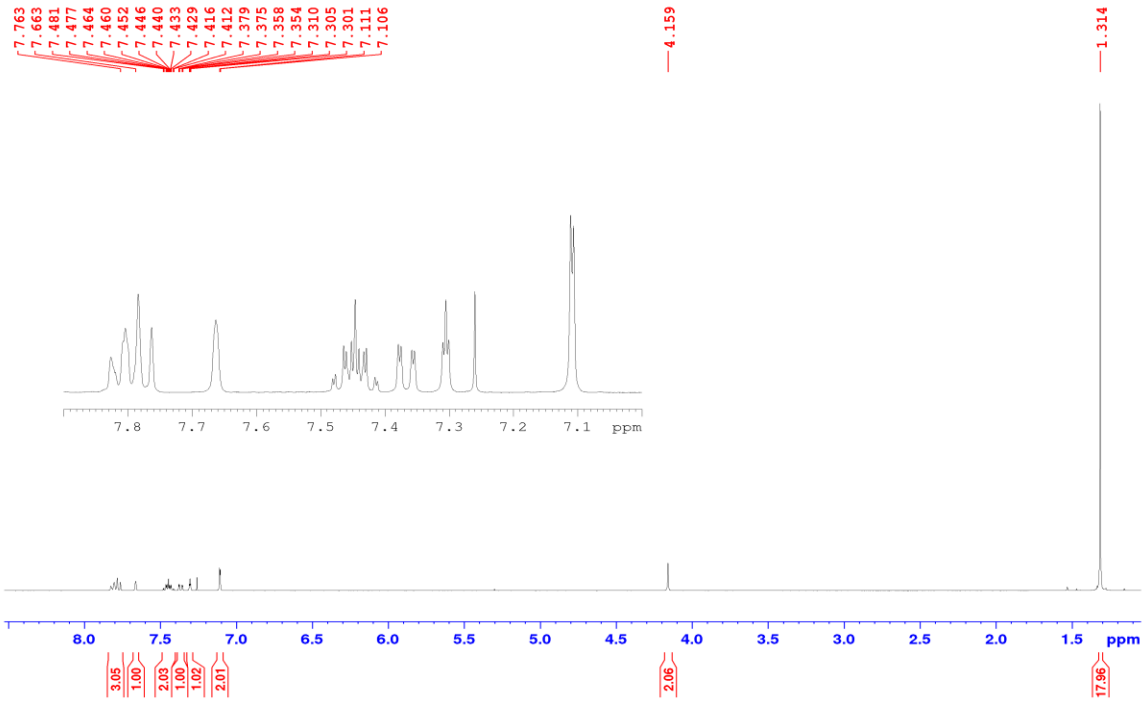

5 (^{13}C NMR, $CDCl_3$, 100 MHz)

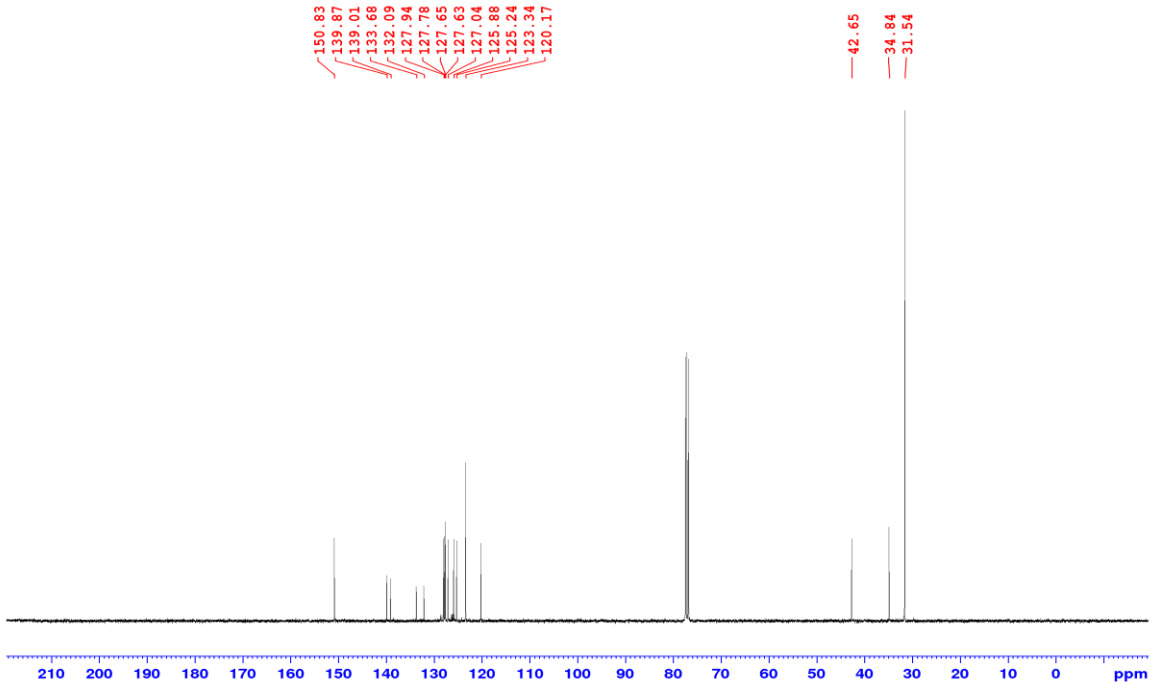

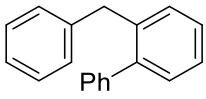

6 (^{1}H NMR, $CDCl_3$, 400 MHz)

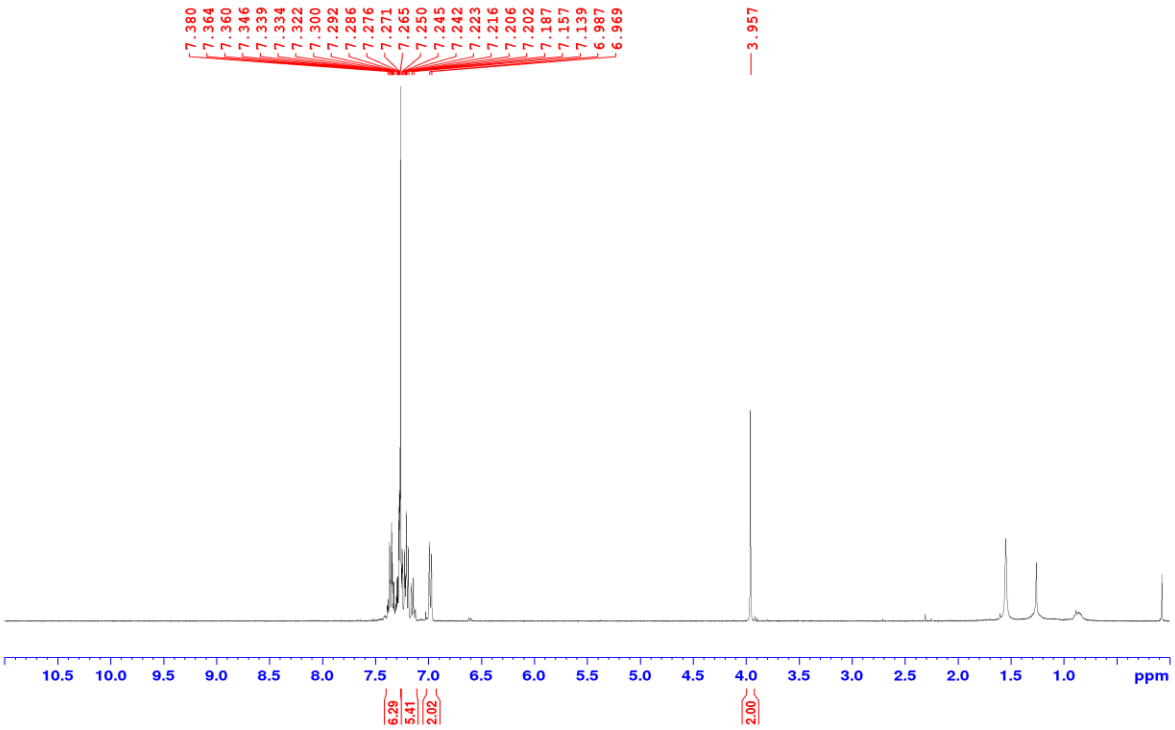

6 (^{13}C NMR, $CDCl_3$, 100 MHz)

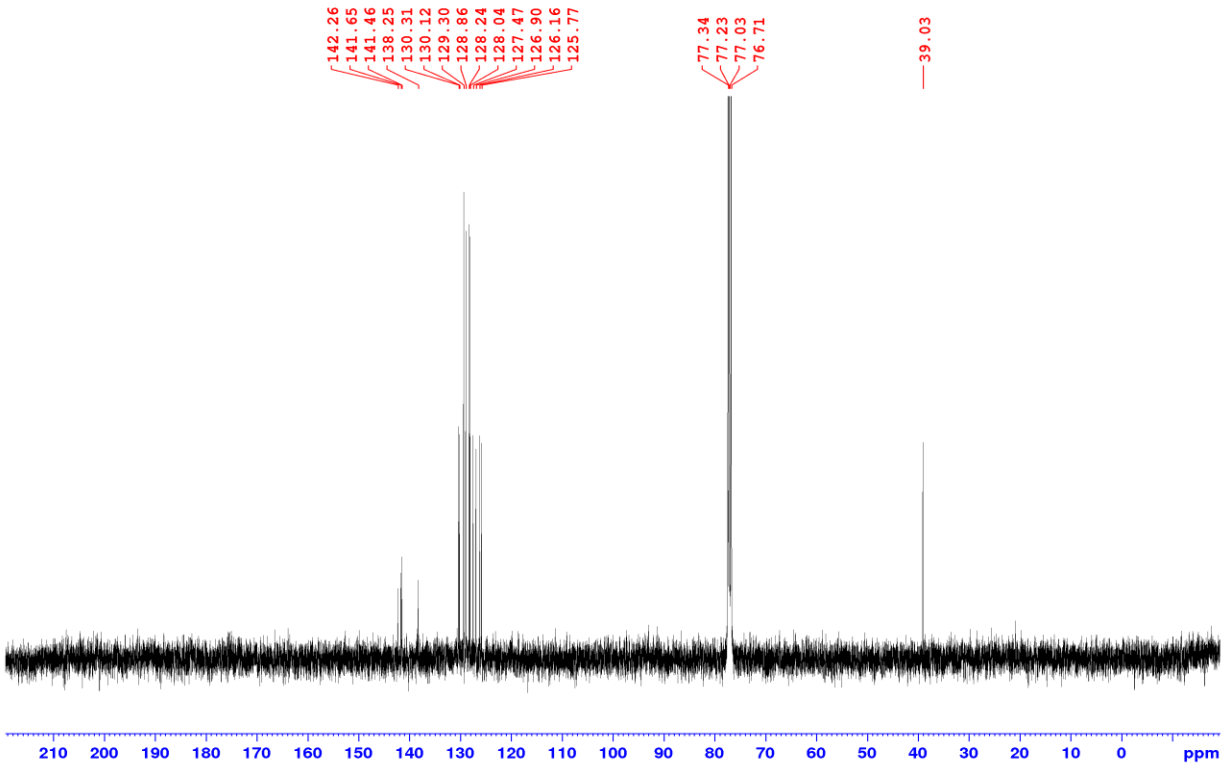

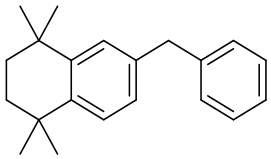

7 (^{1}H NMR, $CDCl_3$, 400 MHz)

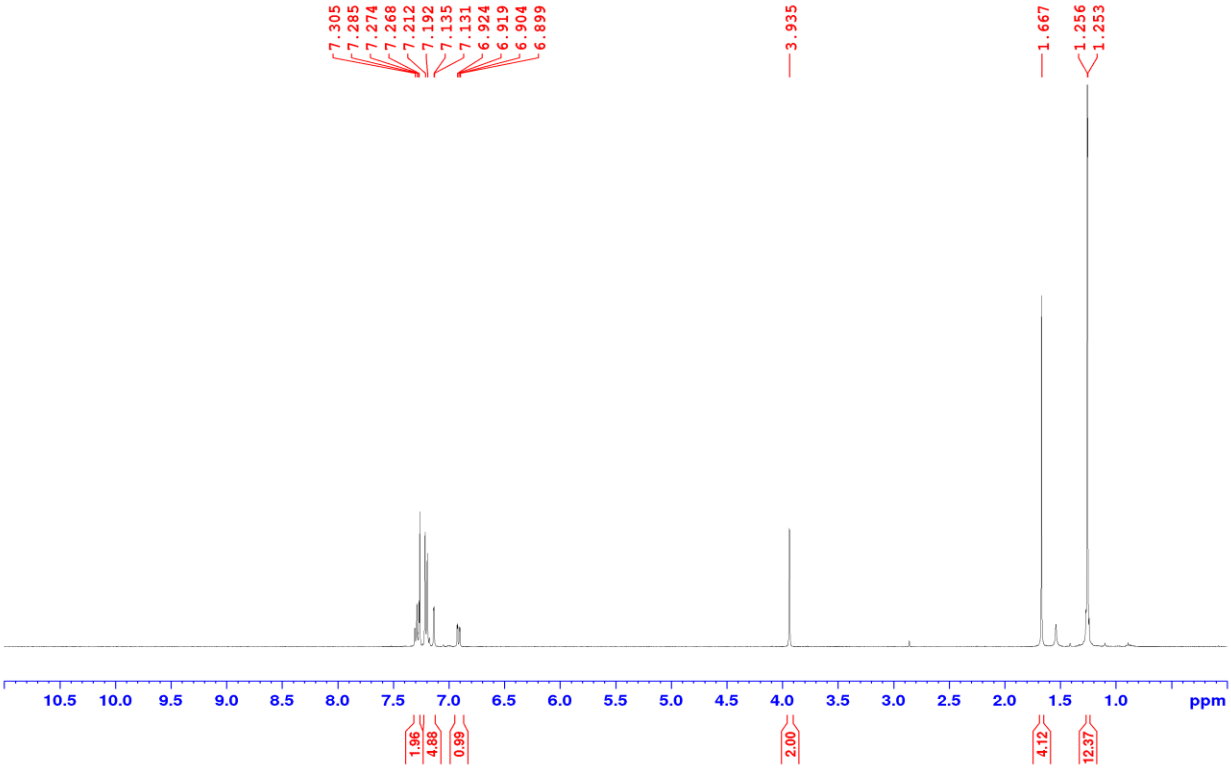

7 (^{13}C NMR, $CDCl_3$, 100 MHz)

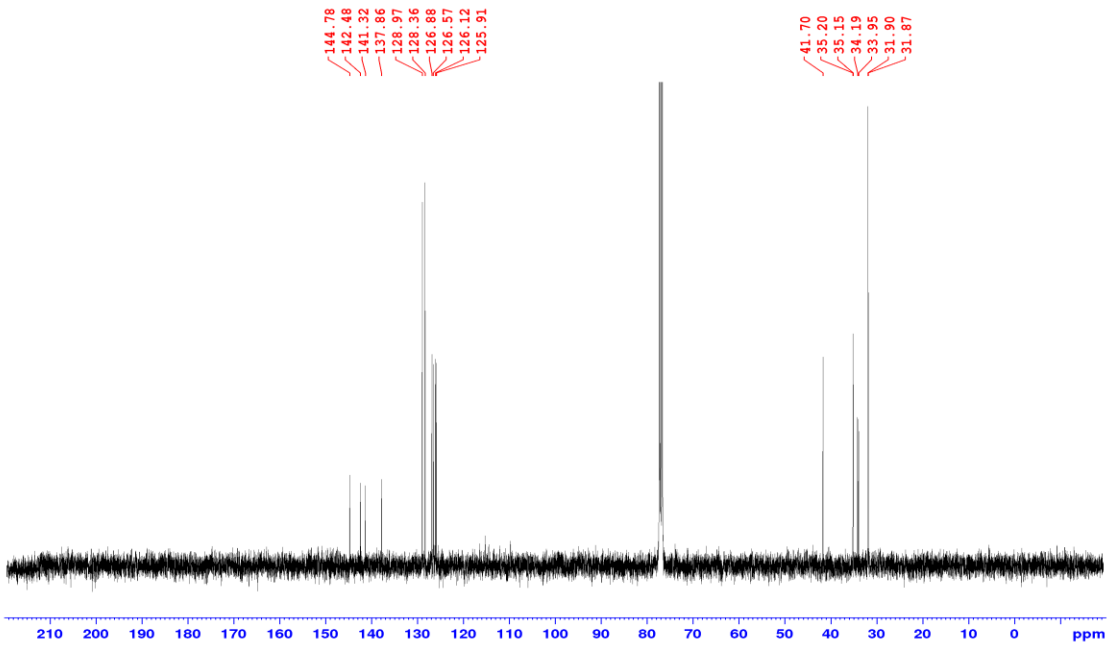

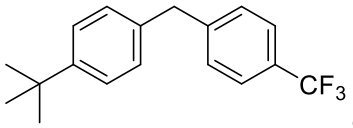

8 (^{1}H NMR, $CDCl_3$, 400 MHz)

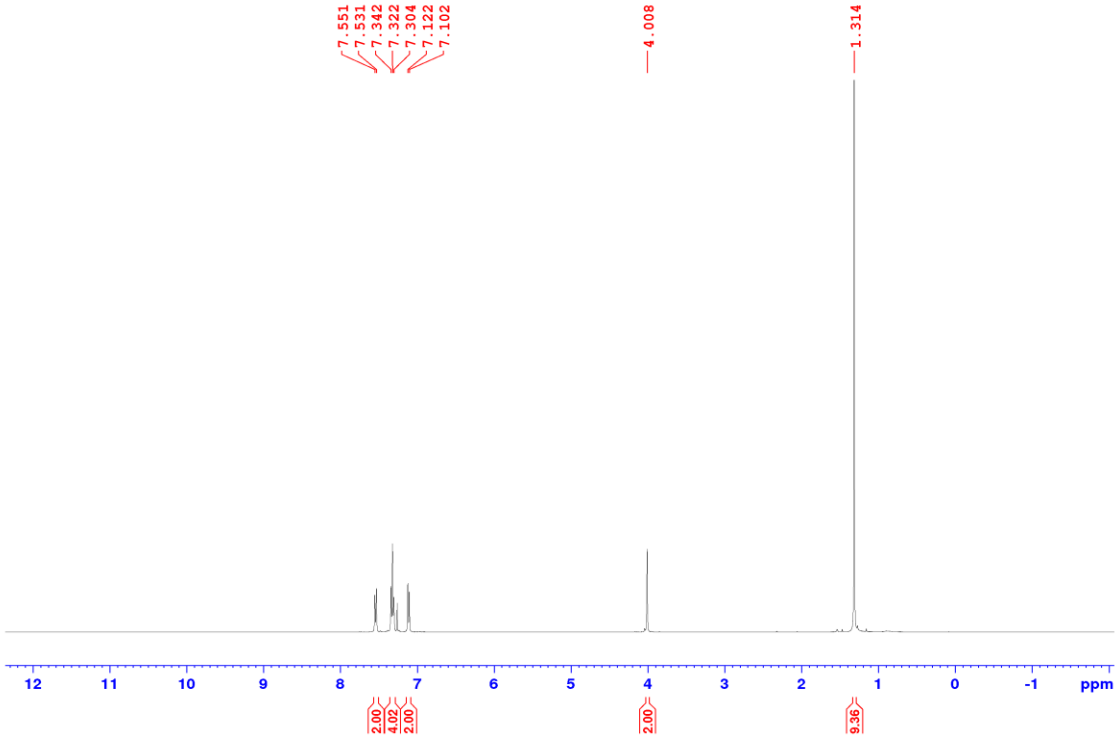

8 (^{13}C NMR, $CDCl_3$, 100 MHz)

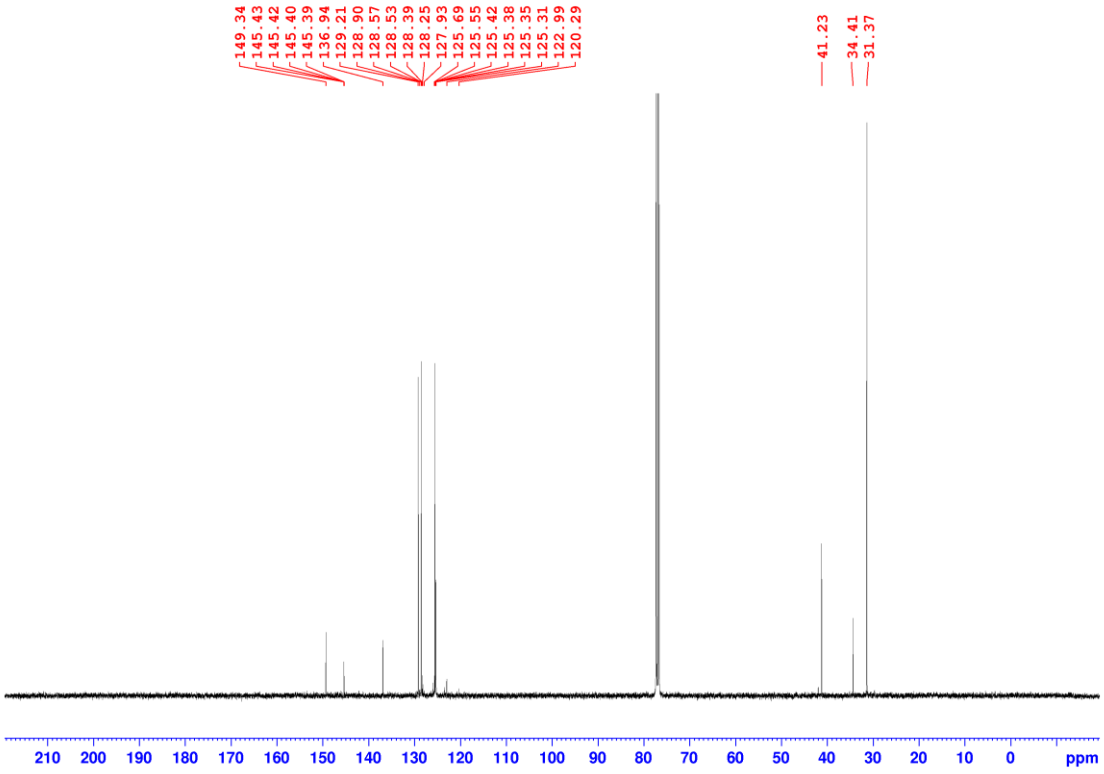

8 (^{19}F NMR, $CDCl_3$, 75 MHz)

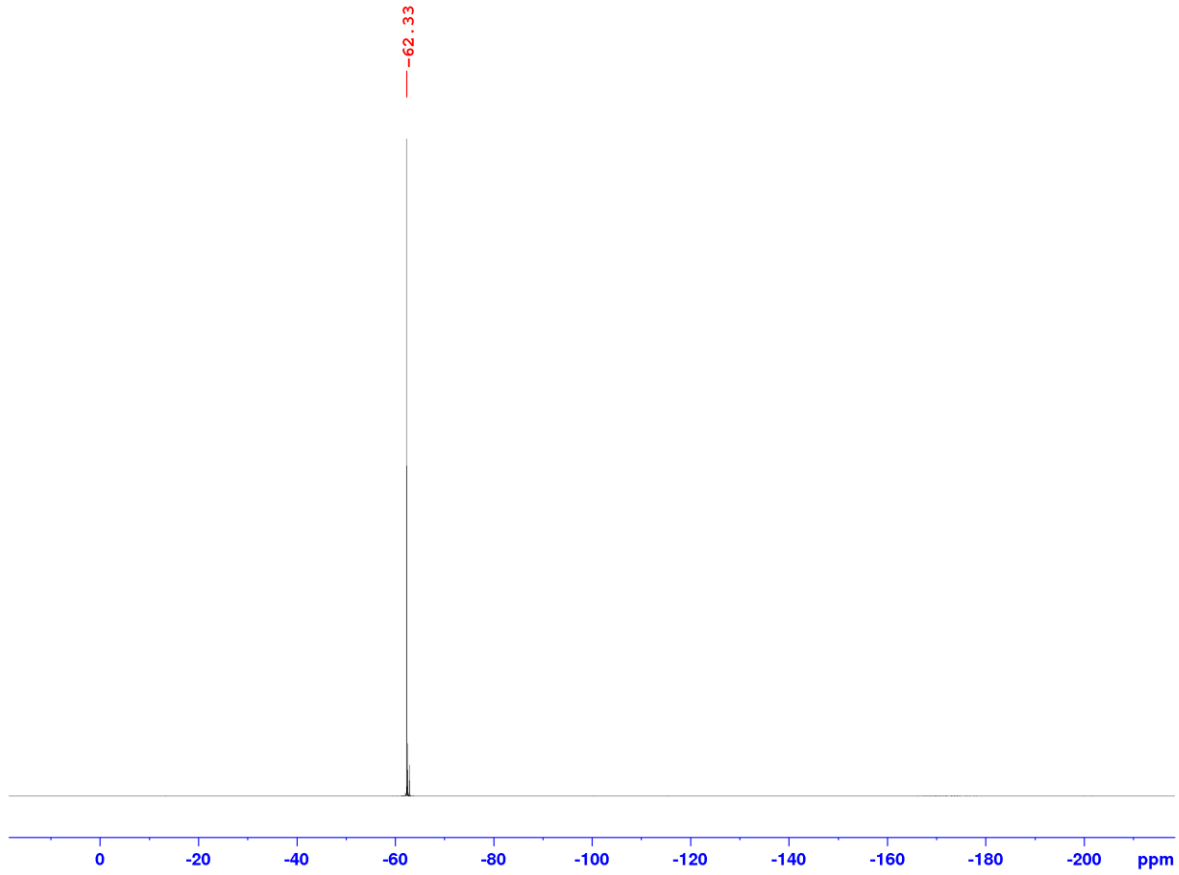

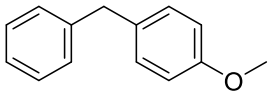

9 (^{1}H NMR, $CDCl_3$, 400 MHz)

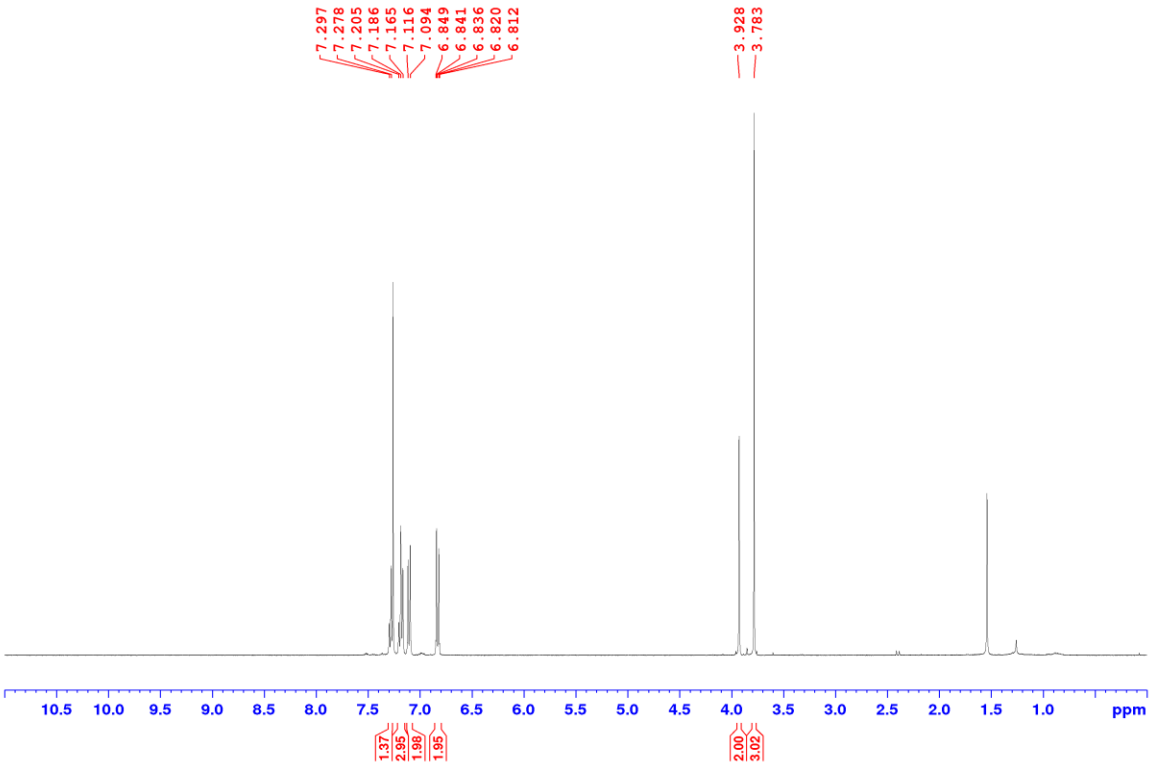

9 (^{13}C NMR, $CDCl_3$, 100 MHz)

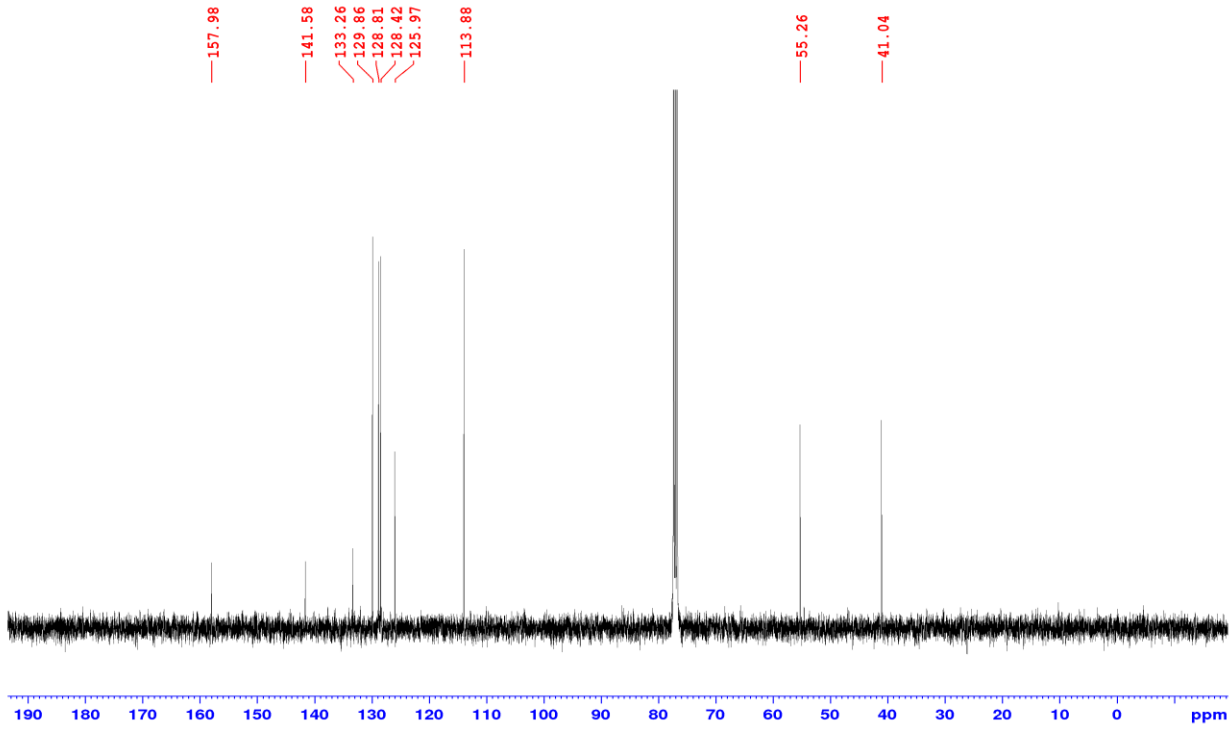

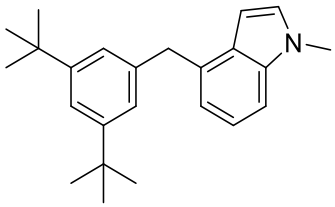

10 (^{1}H NMR, $CDCl_3$, 400 MHz)

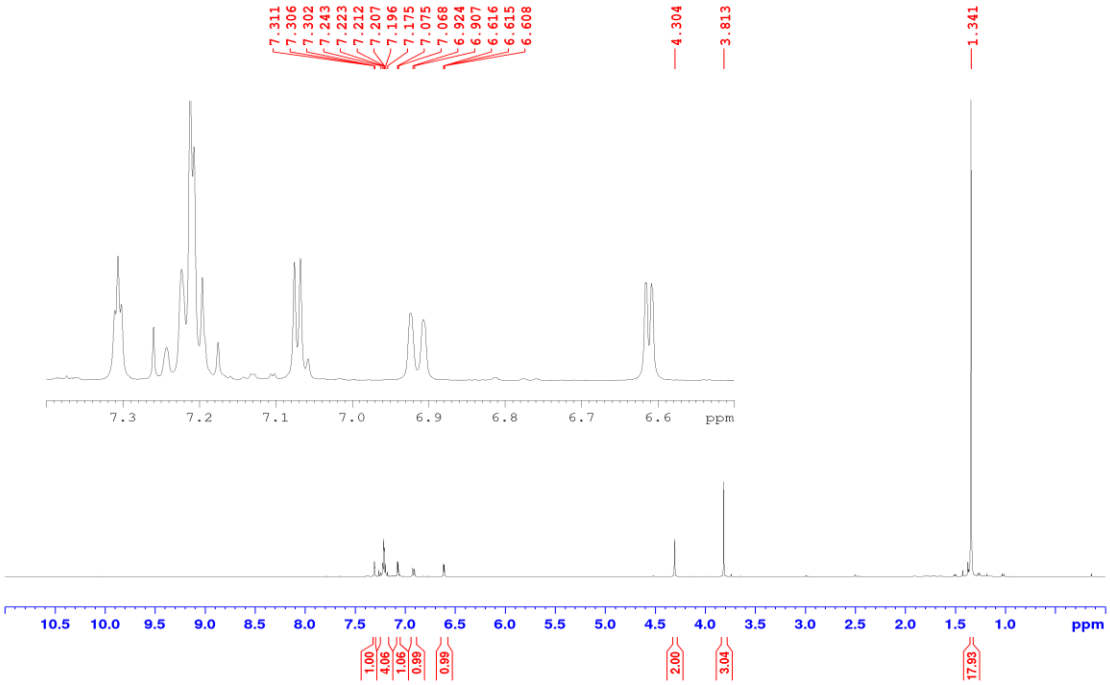

10 (^{13}C NMR, $CDCl_3$, 100 MHz)

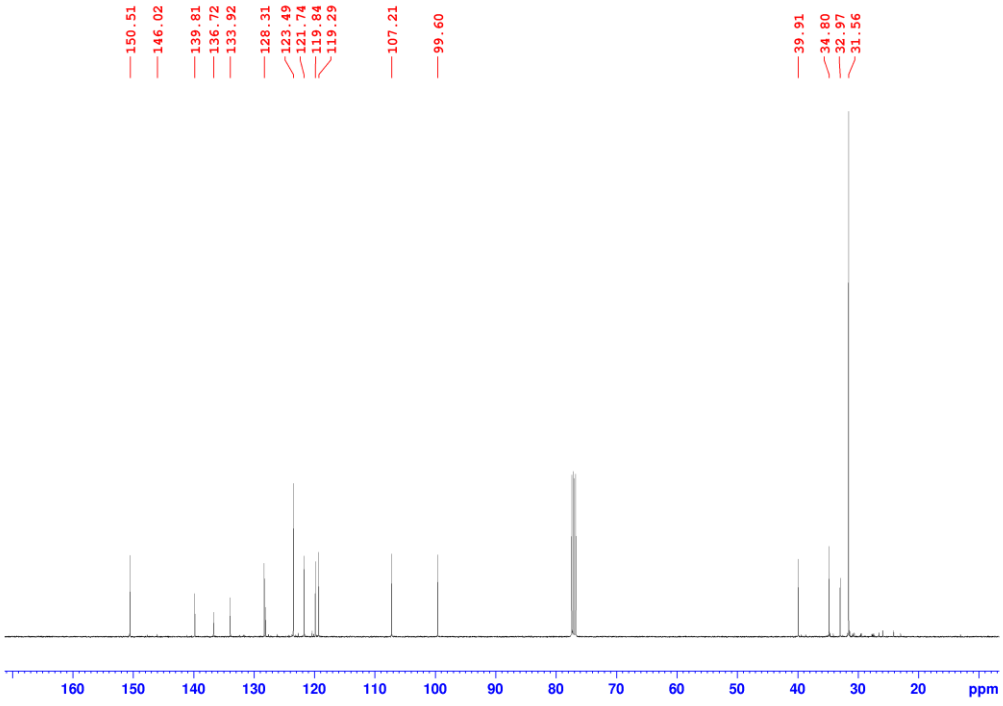

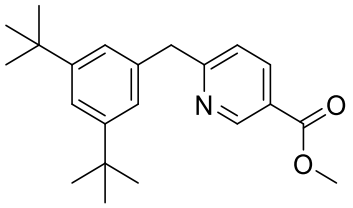

22 (^{1}H NMR, $CDCl_3$, 400 MHz)

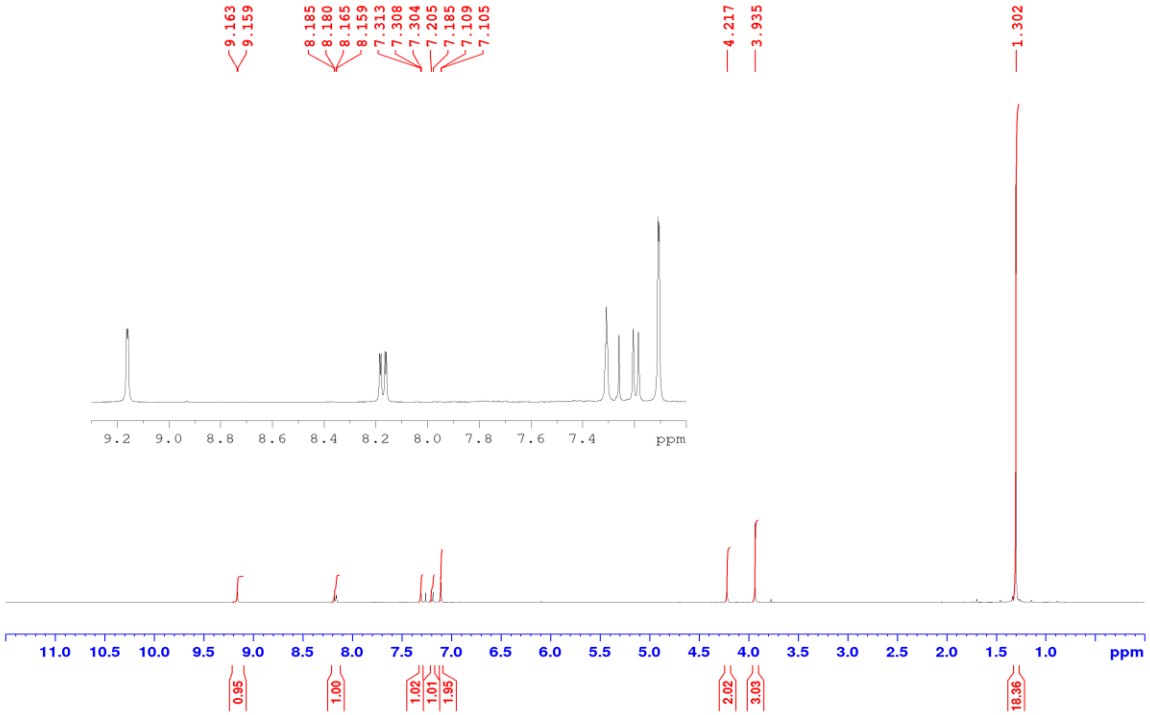

22 (^{13}C NMR, $CDCl_3$, 100 MHz)

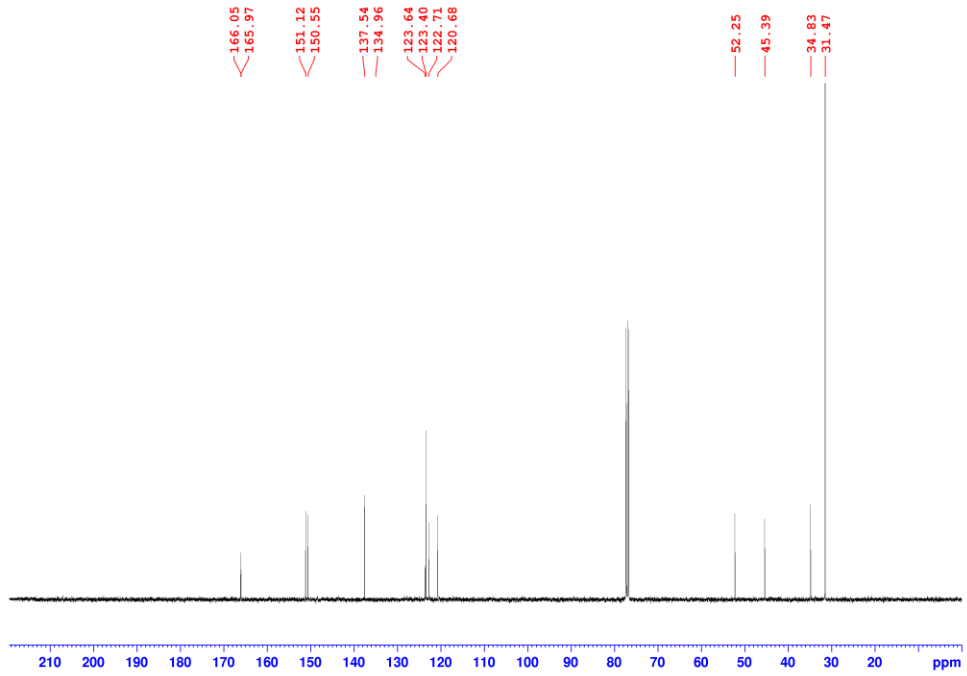

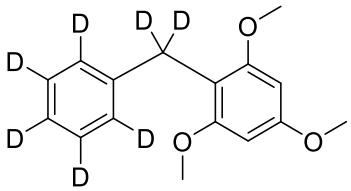

23 (^{1}H NMR, $CDCl_3$, 400 MHz)

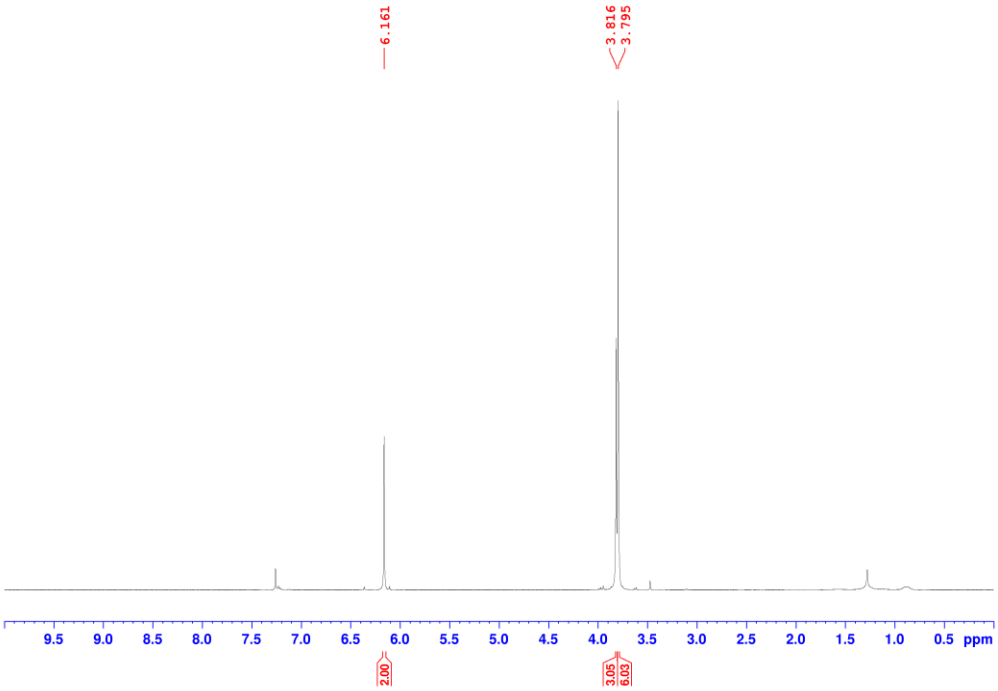

23 (^{13}C NMR, $CDCl_3$, 100 MHz)

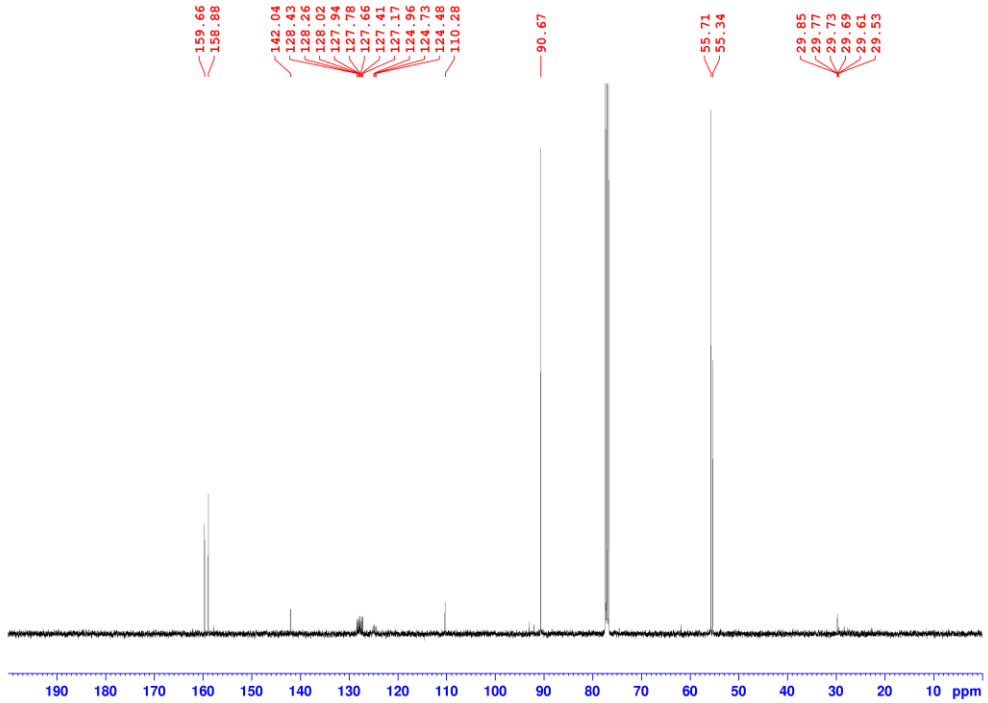

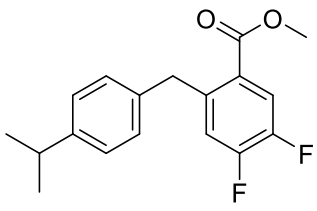

24 (^{1}H NMR, $CDCl_3$, 400 MHz)

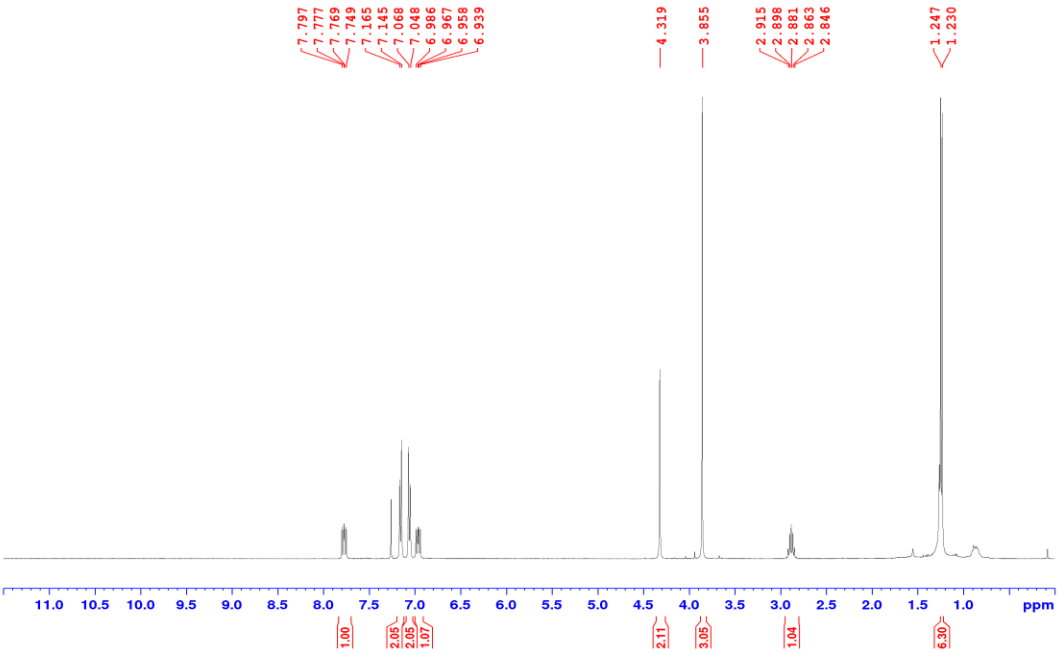

24 (^{13}C NMR, $CDCl_3$, 100 MHz)

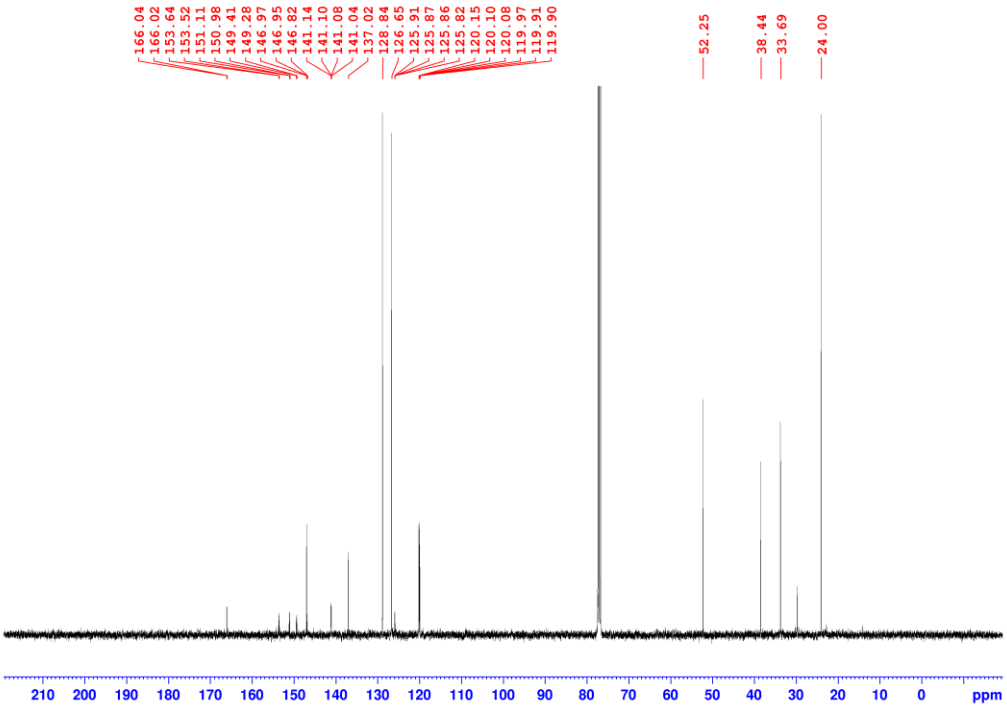

24 (^{19}F NMR, $CDCl_3$, 75 MHz)

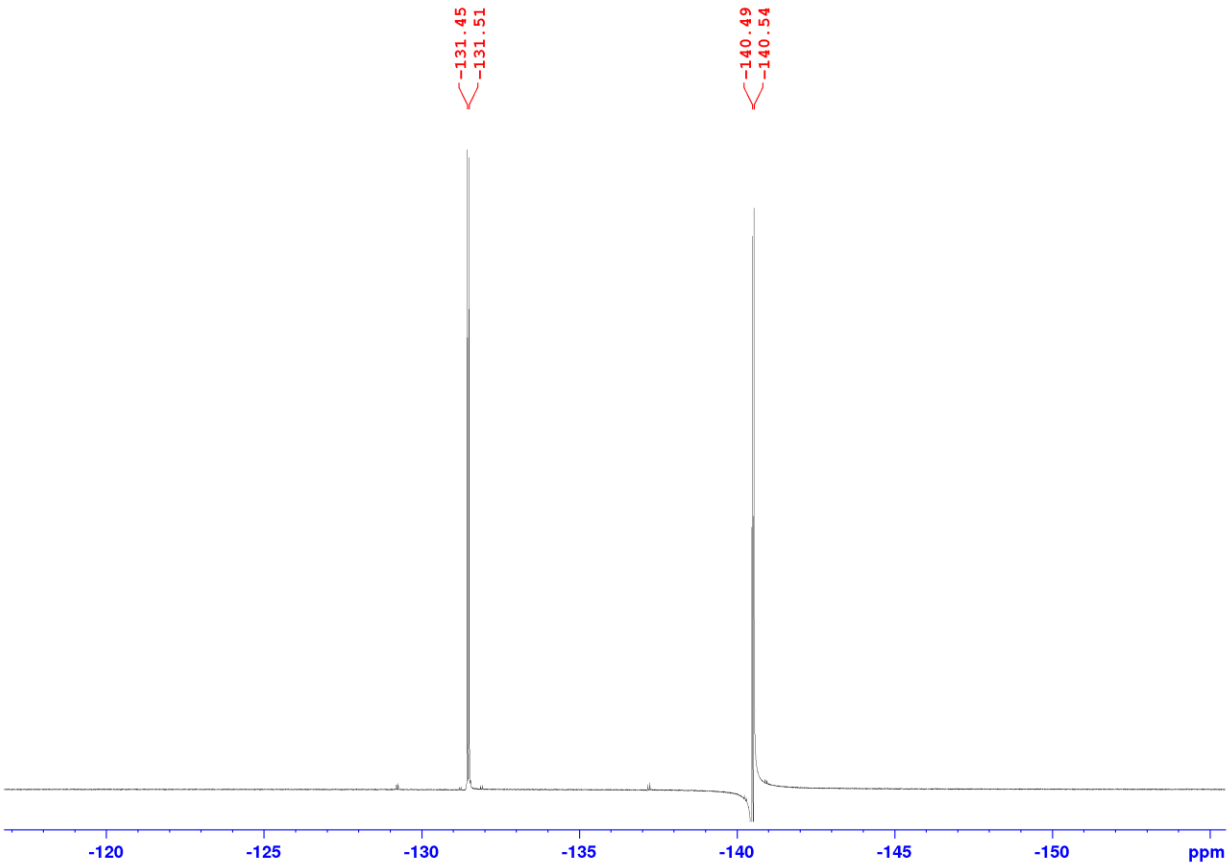

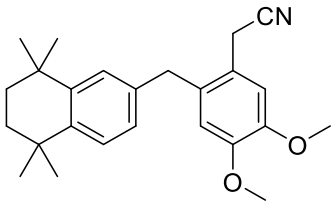

25 (^{1}H NMR, $CDCl_3$, 400 MHz)

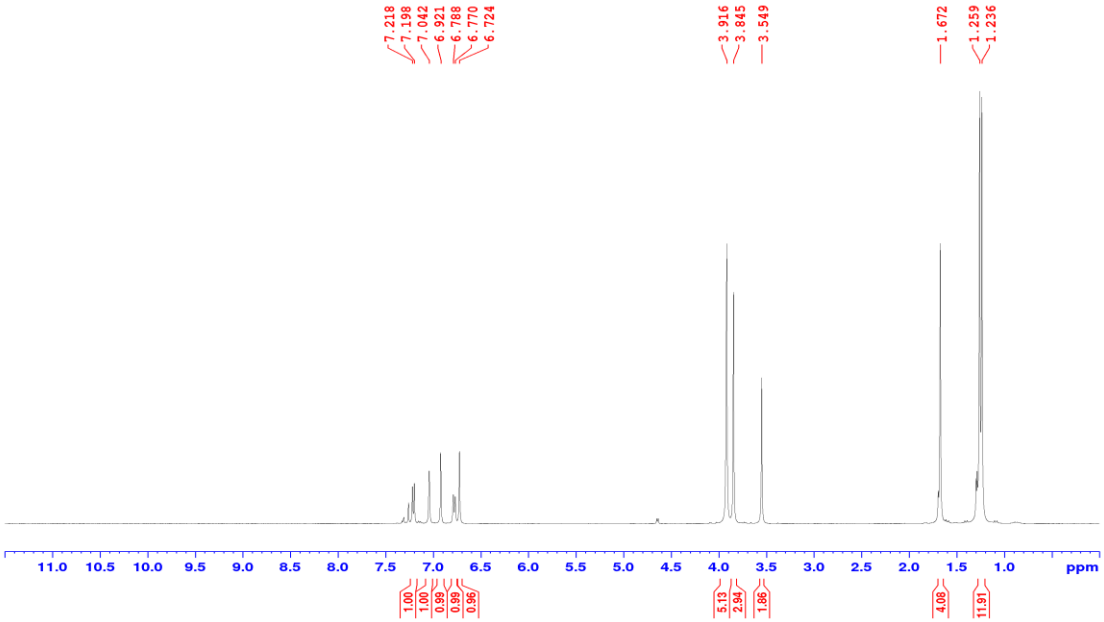

25 (^{13}C NMR, $CDCl_3$, 100 MHz)

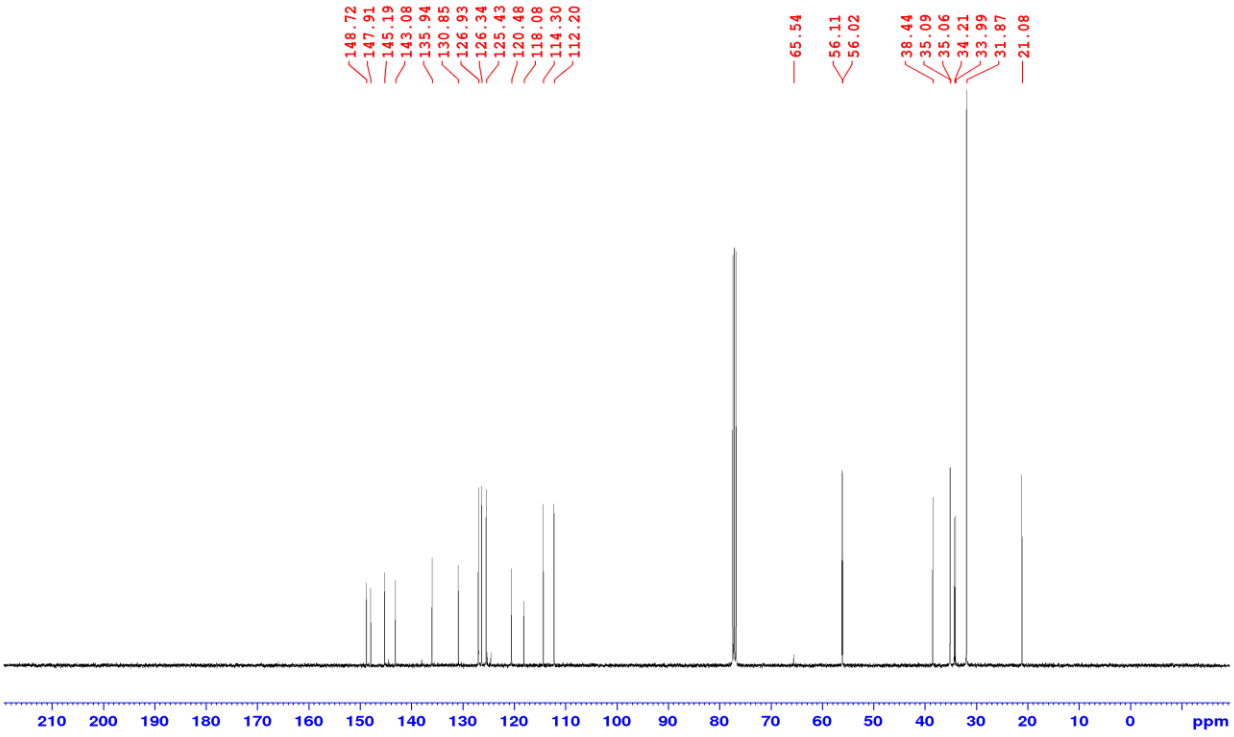

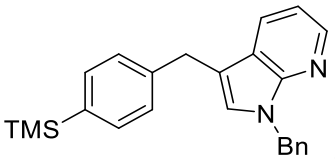

26 (^{1}H NMR, $CDCl_3$, 400 MHz)

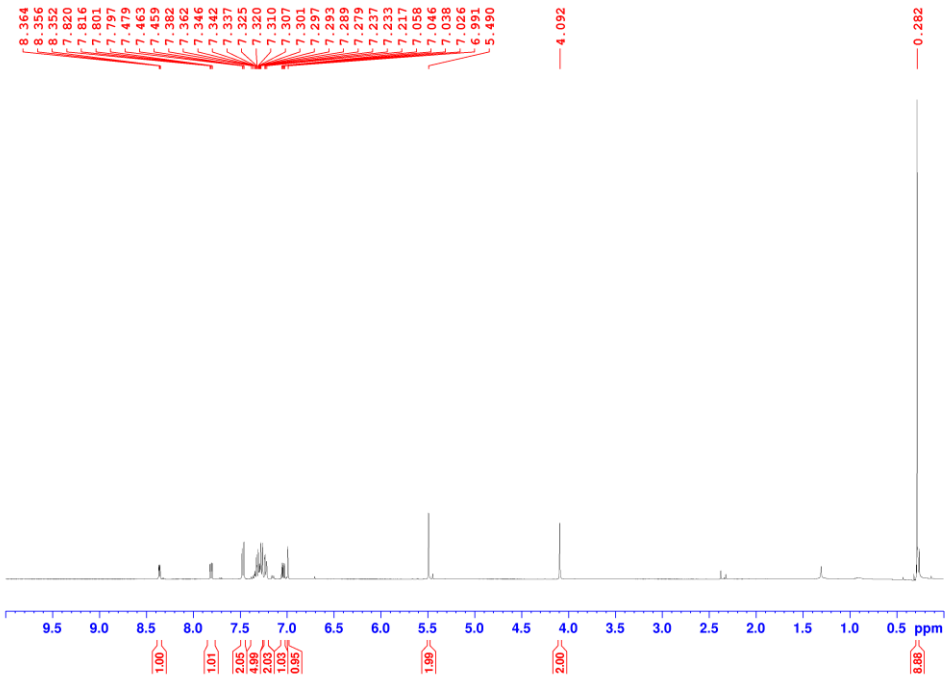

26 (^{13}C NMR, $CDCl_3$, 100 MHz)

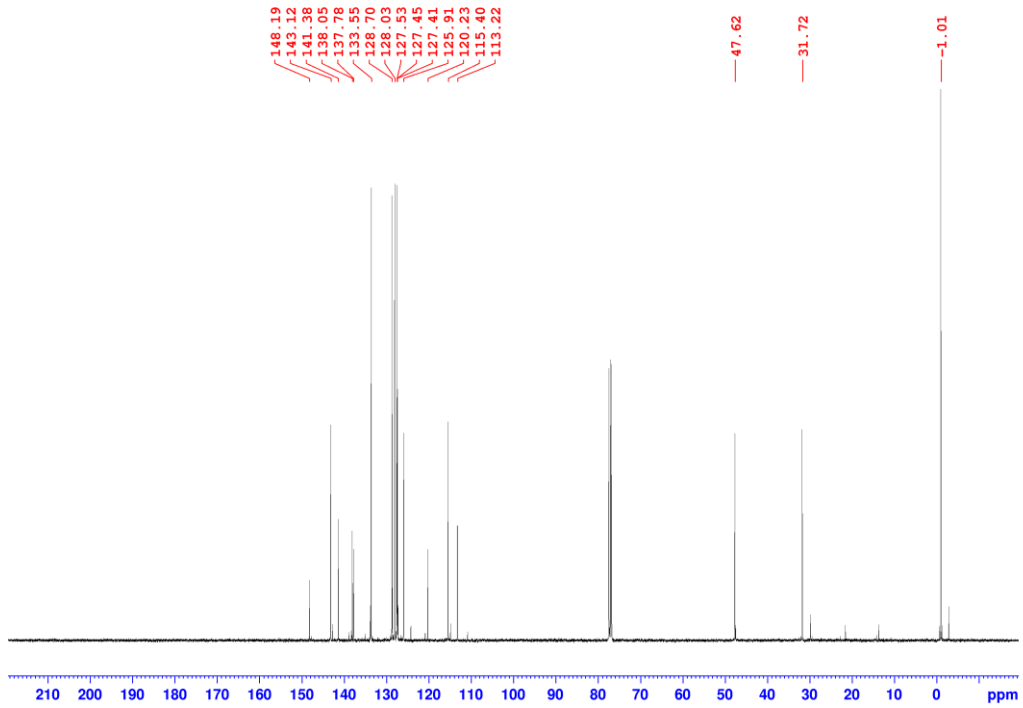

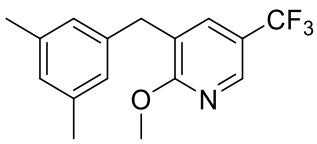

27 (^{1}H NMR, $CDCl_3$, 400 MHz)

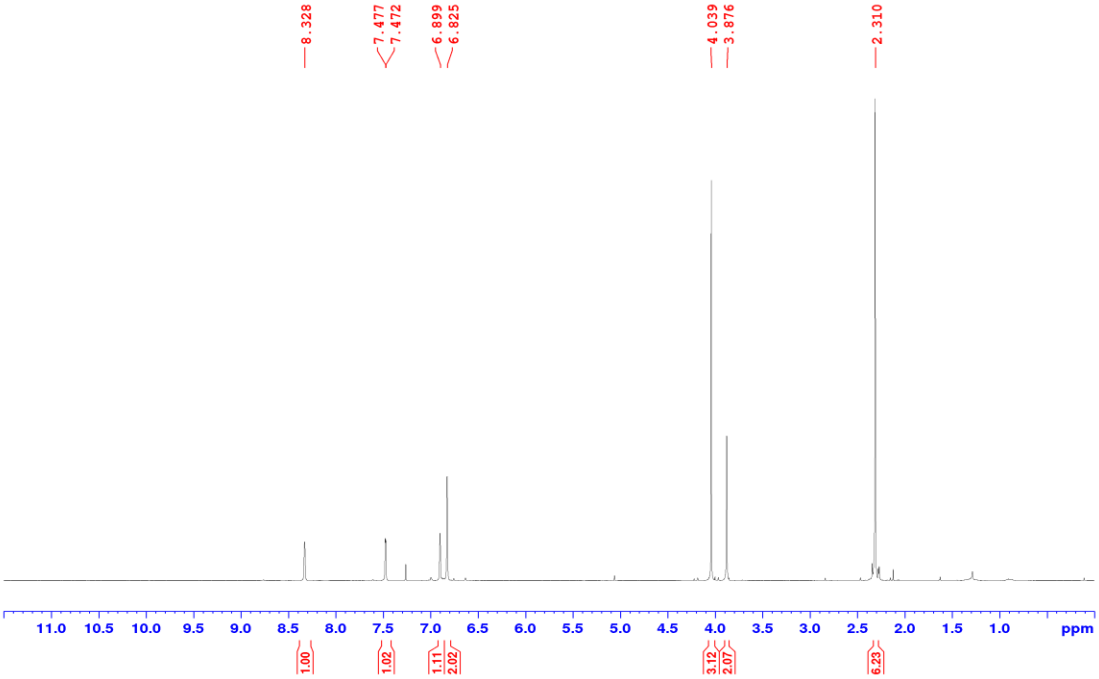

27 (^{13}C NMR, $CDCl_3$, 100 MHz)

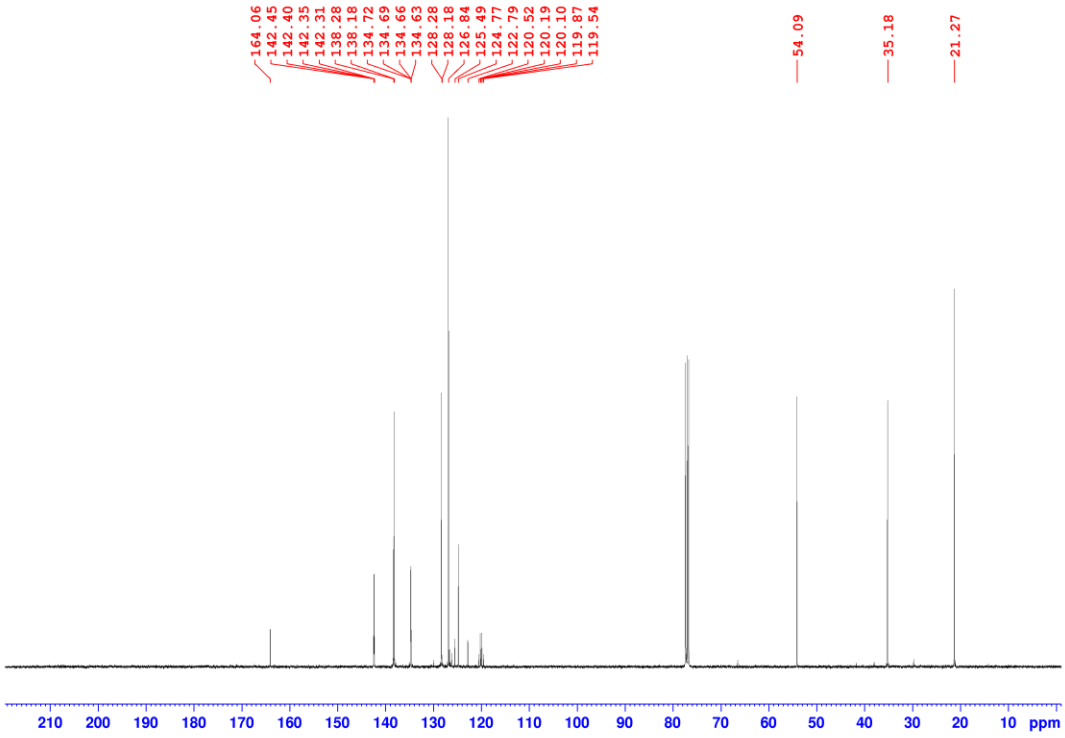

27 (^{19}F NMR, $CDCl_3$, 75 MHz)

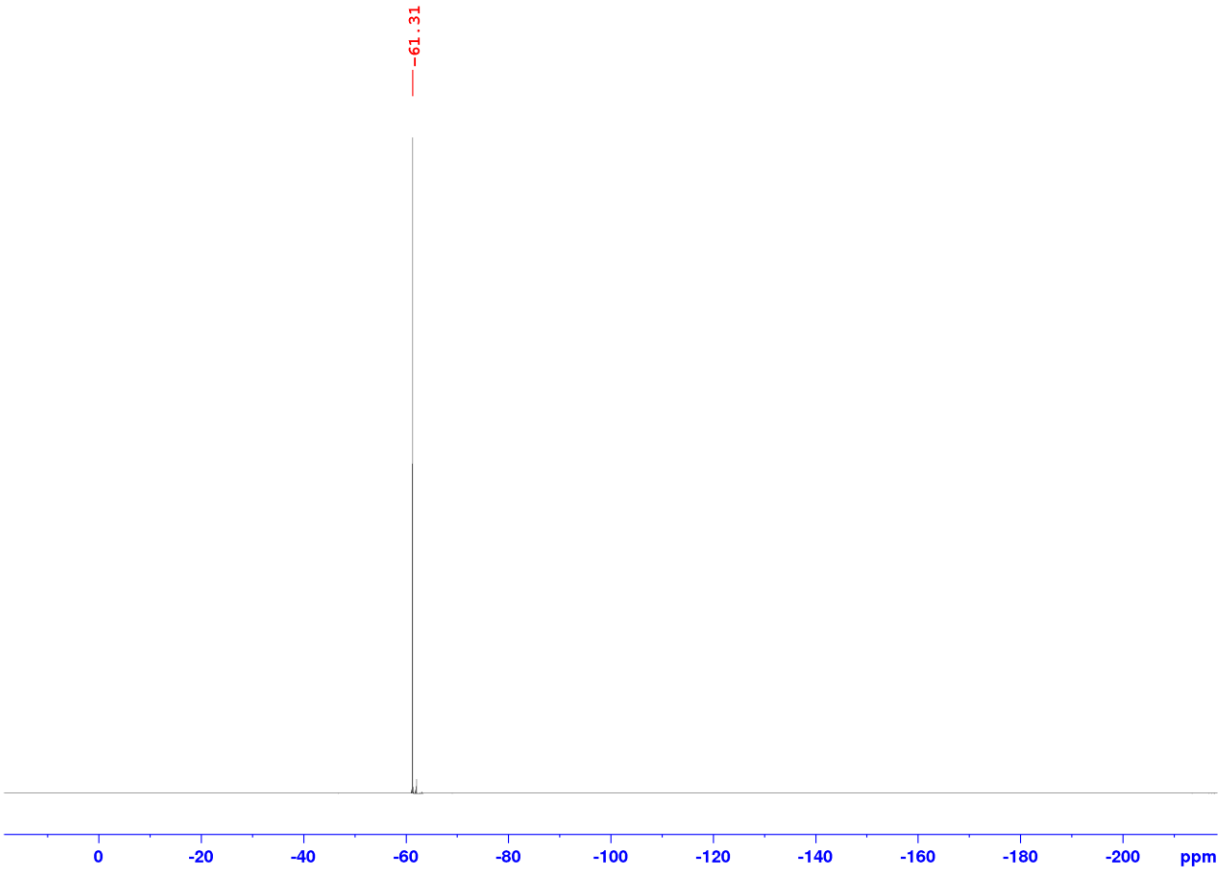

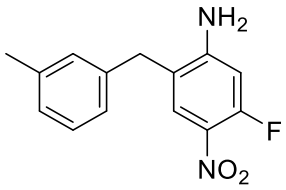

28 (^{1}H NMR, $CDCl_3$, 400 MHz)

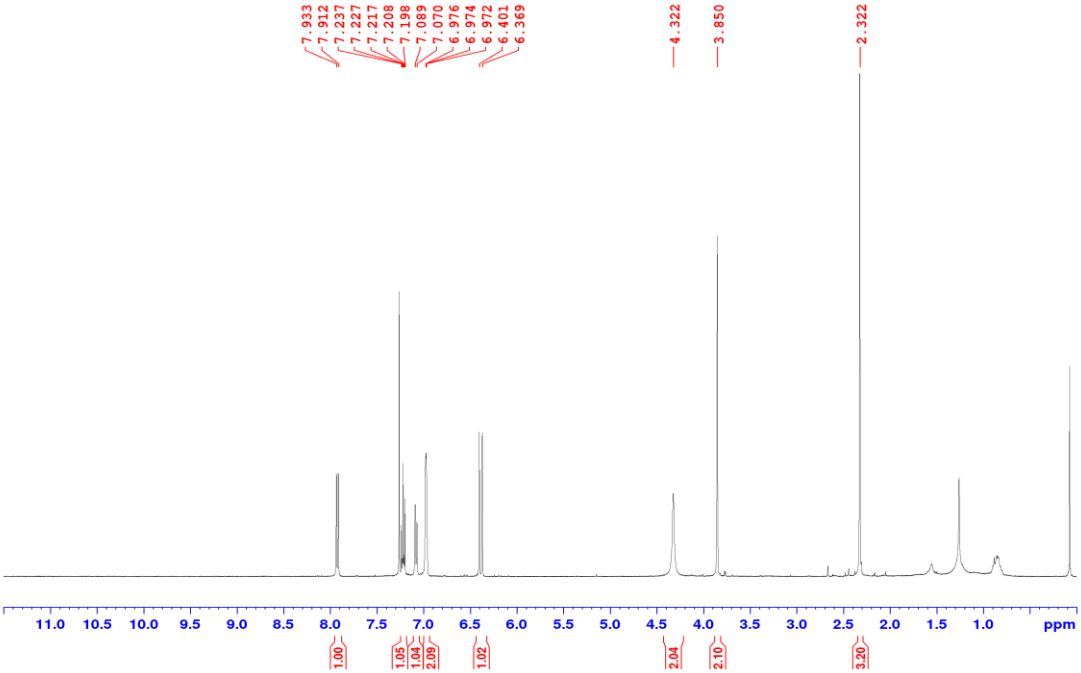

28 (^{13}C NMR, $CDCl_3$, 100 MHz)

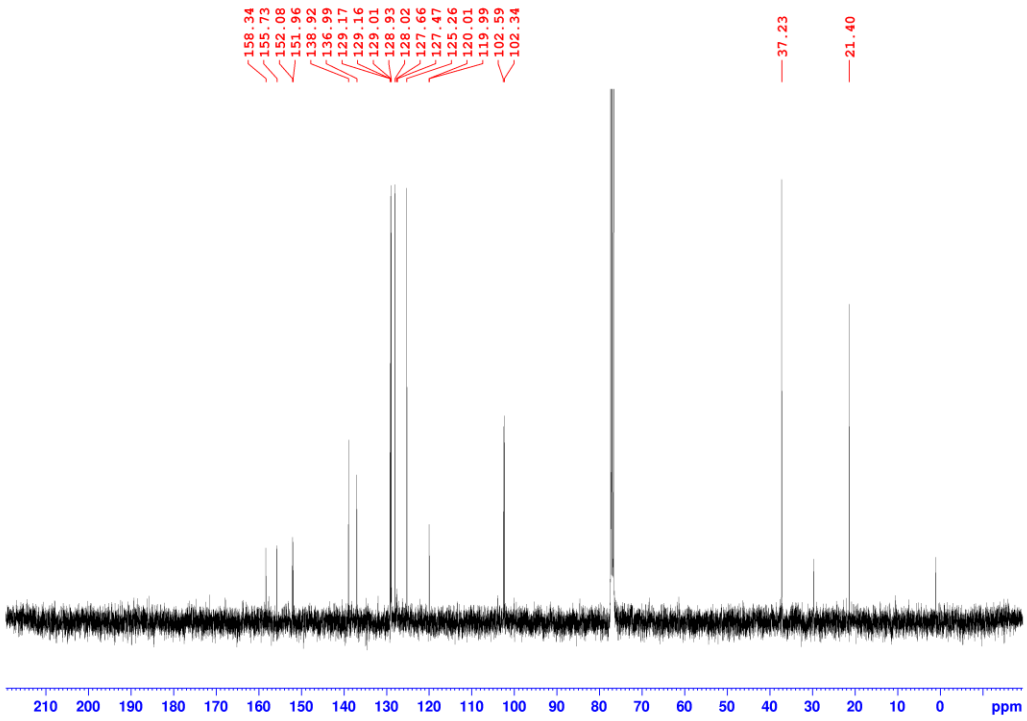

28 (^{19}F NMR, $CDCl_3$, 75 MHz)

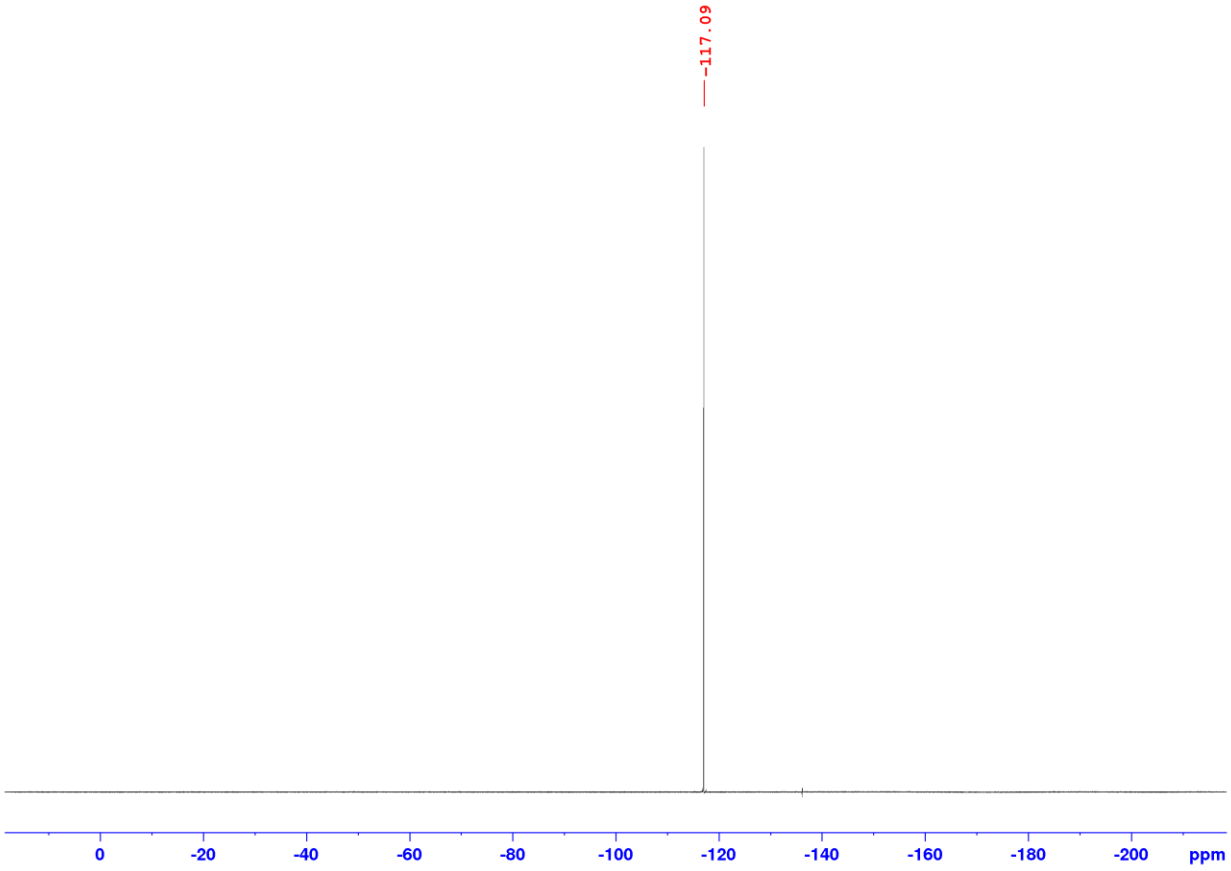

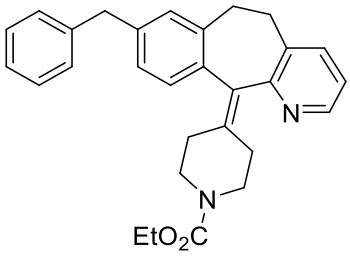

29 (^{1}H NMR, $CDCl_3$, 400 MHz)

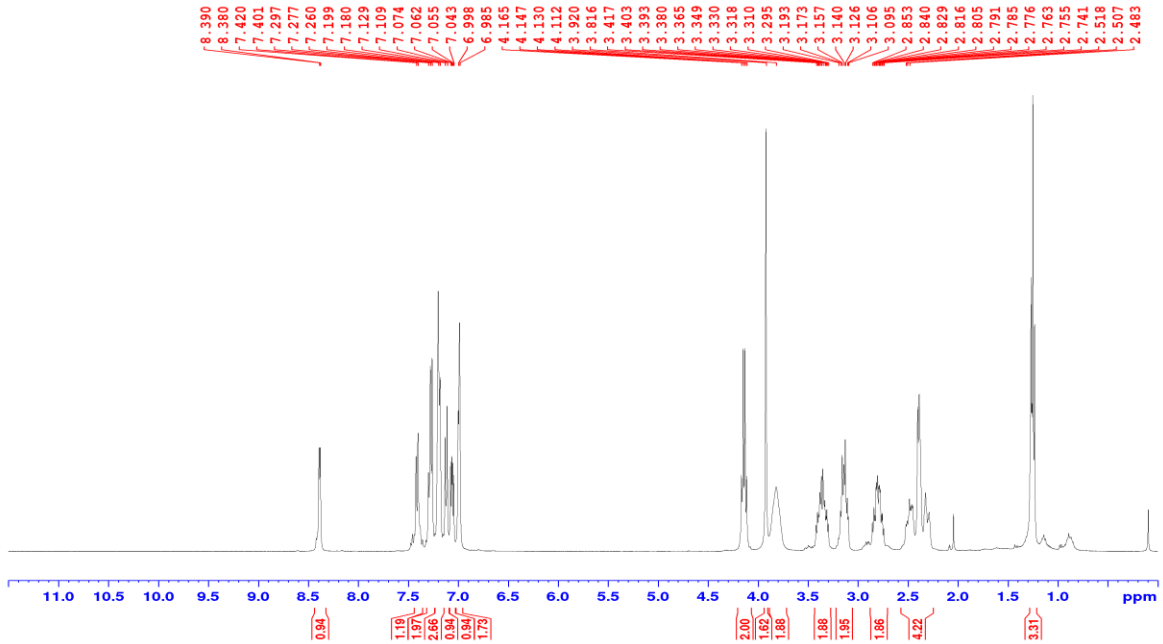

29 (^{13}C NMR, $CDCl_3$, 100 MHz)

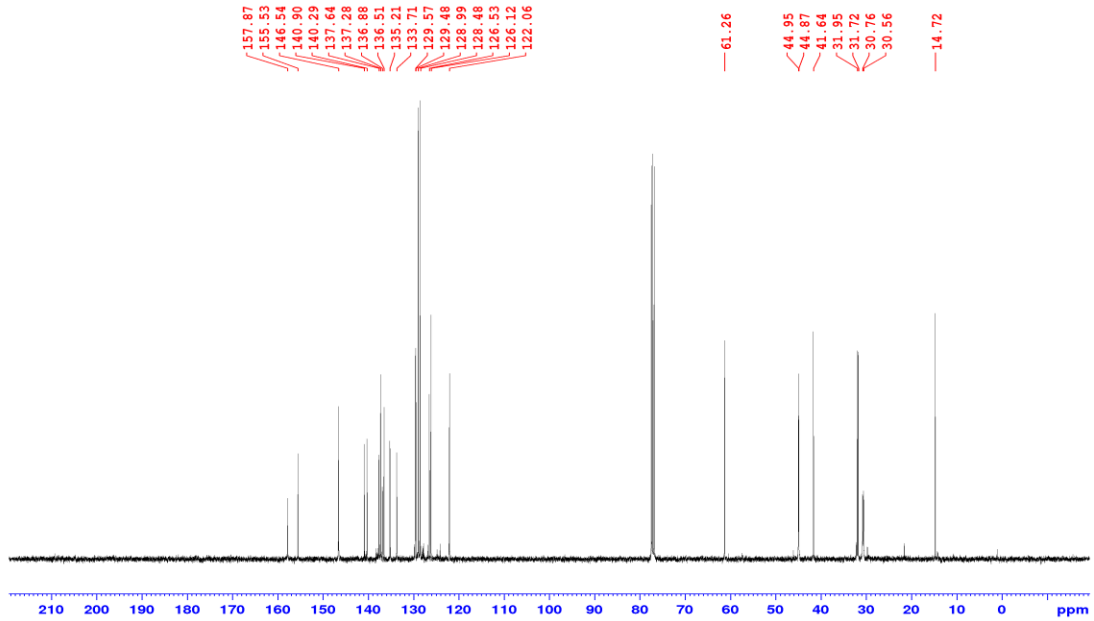

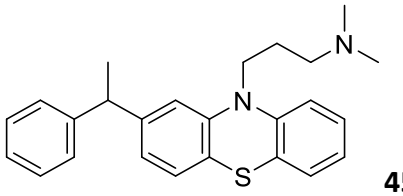

45 (^{1}H NMR, $CDCl_3$, 400 MHz)

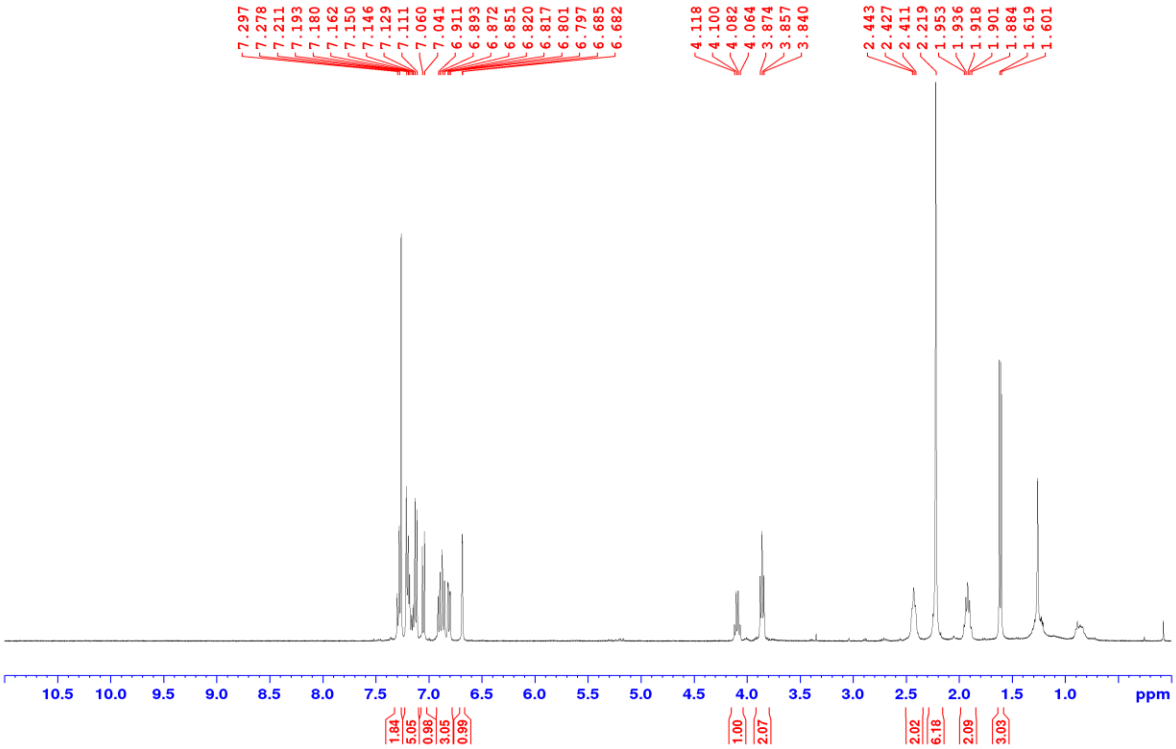

45 (^{13}C NMR, $CDCl_3$, 100 MHz)

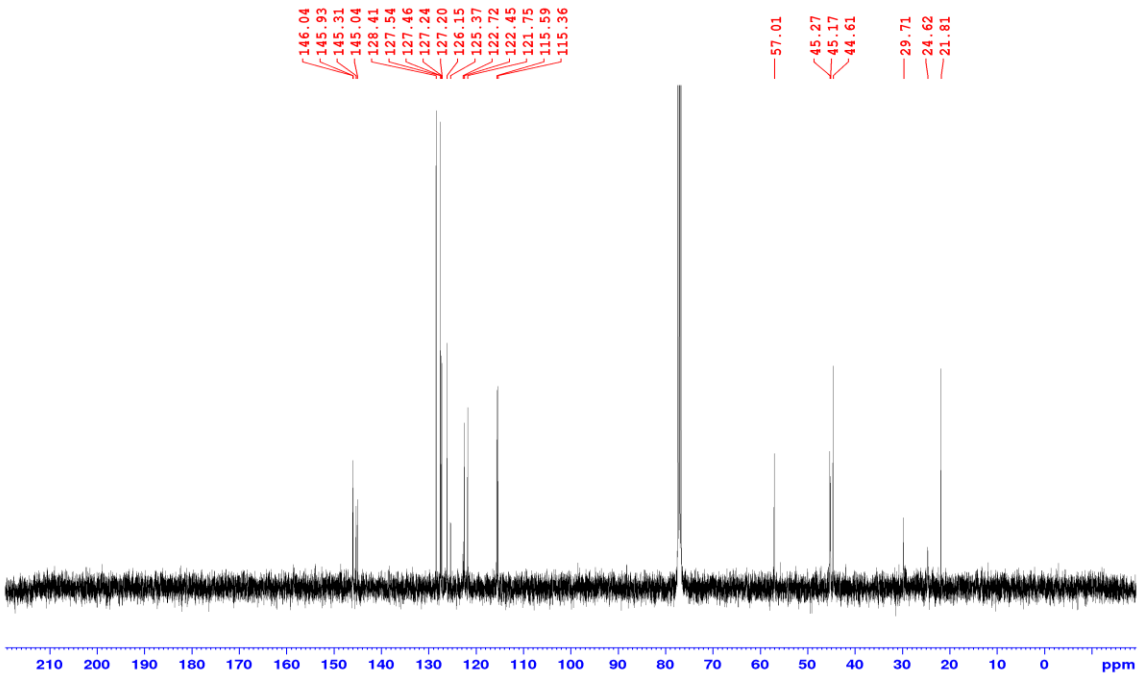

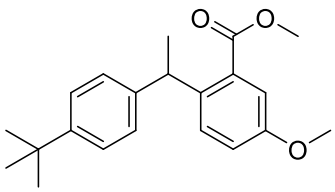

46 (^{1}H NMR, $CDCl_3$, 400 MHz)

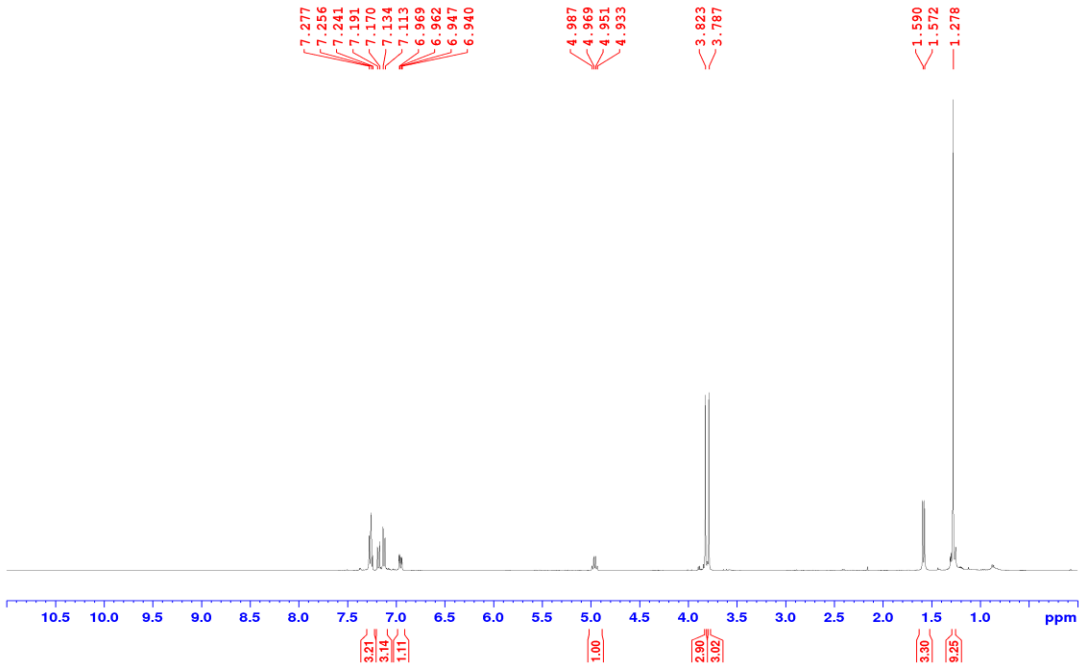

46 (^{13}C NMR, $CDCl_3$, 100 MHz)

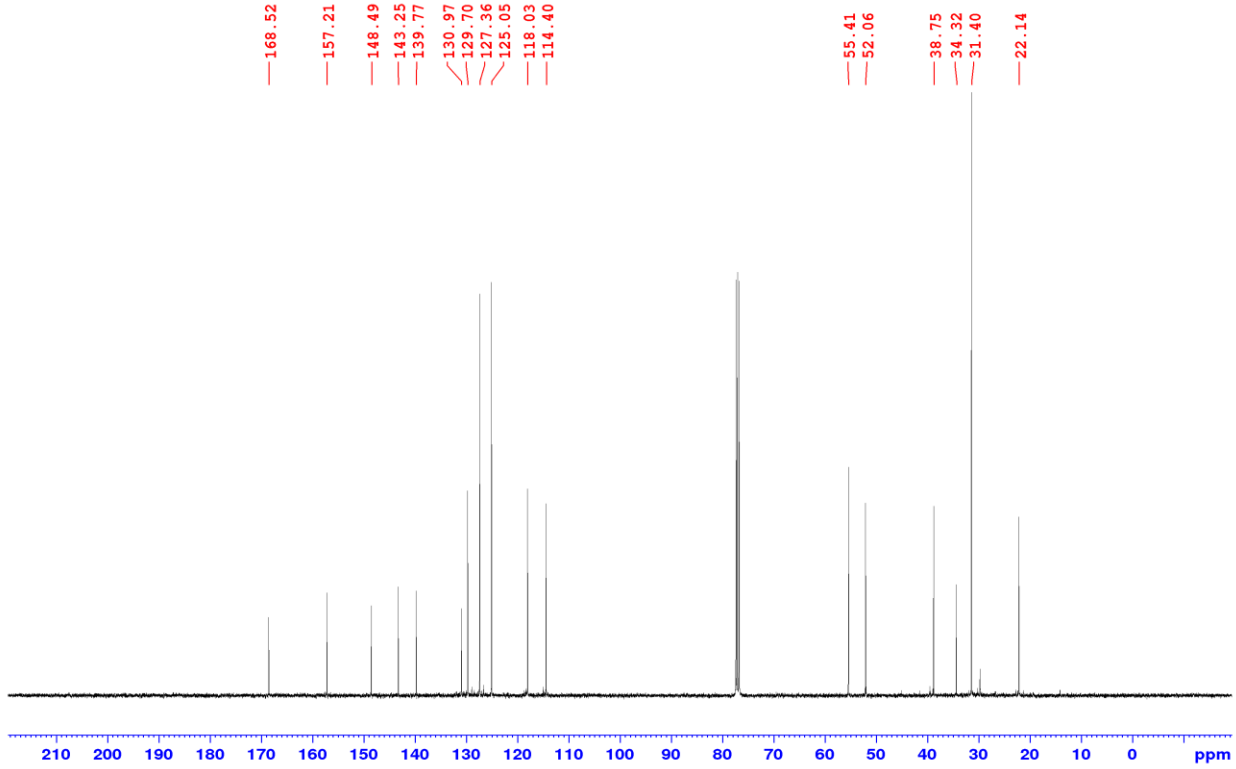

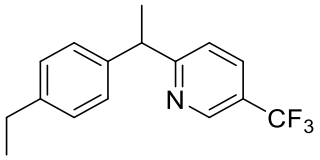

47 (^{1}H NMR, $CDCl_3$, 400 MHz)

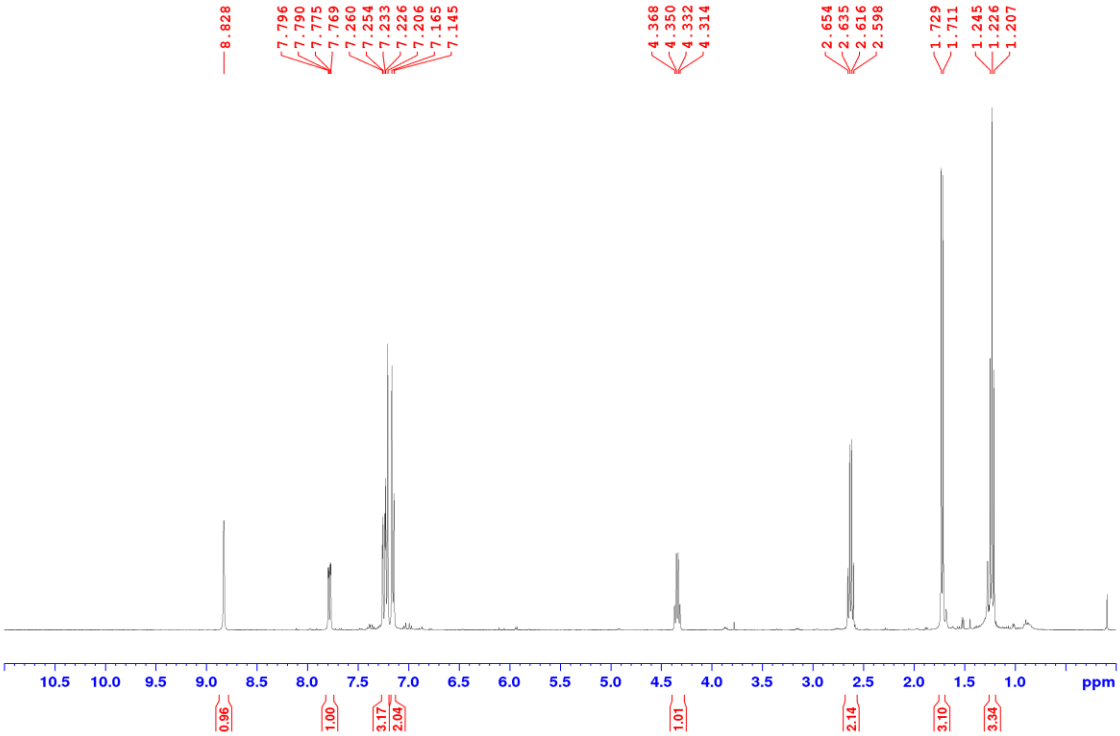

47 (^{13}C NMR, $CDCl_3$, 100 MHz)

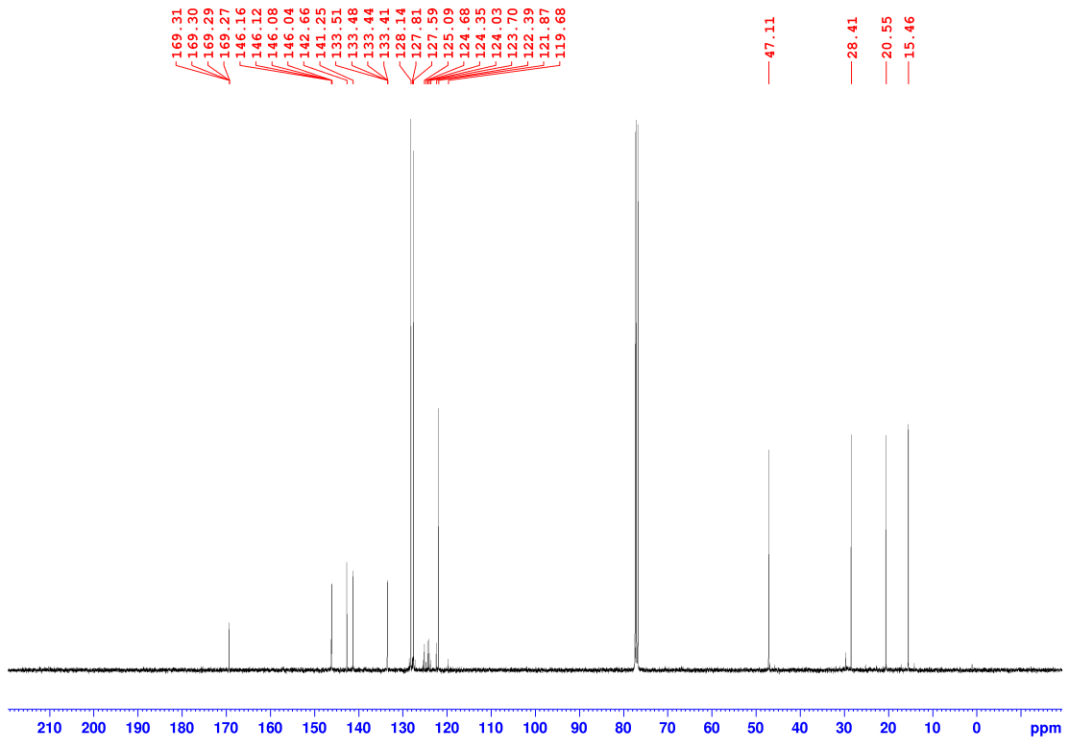

47 (^{19}F NMR, $CDCl_3$, 75 MHz)

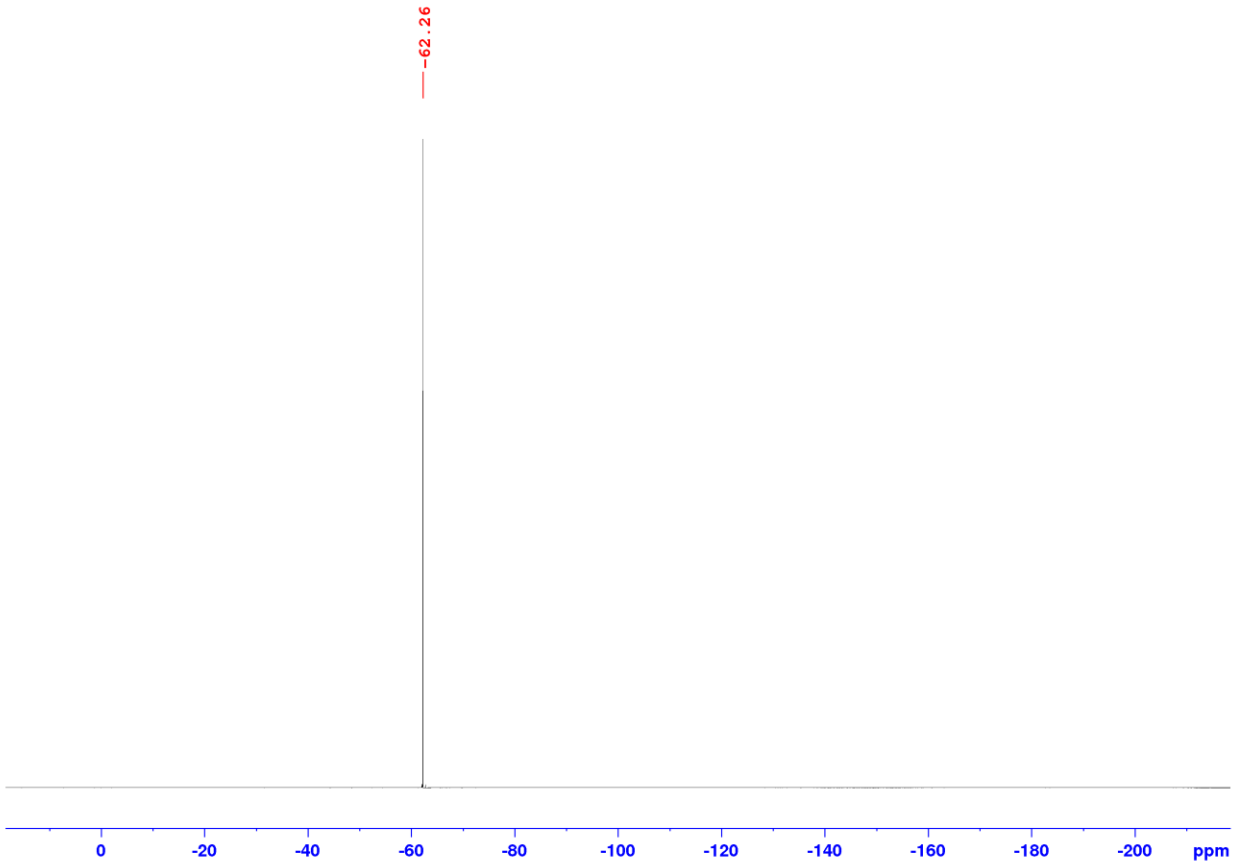

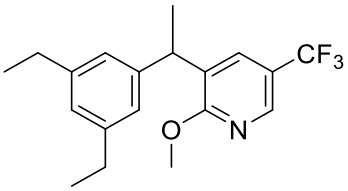

48 (^{1}H NMR, $CDCl_3$, 400 MHz)

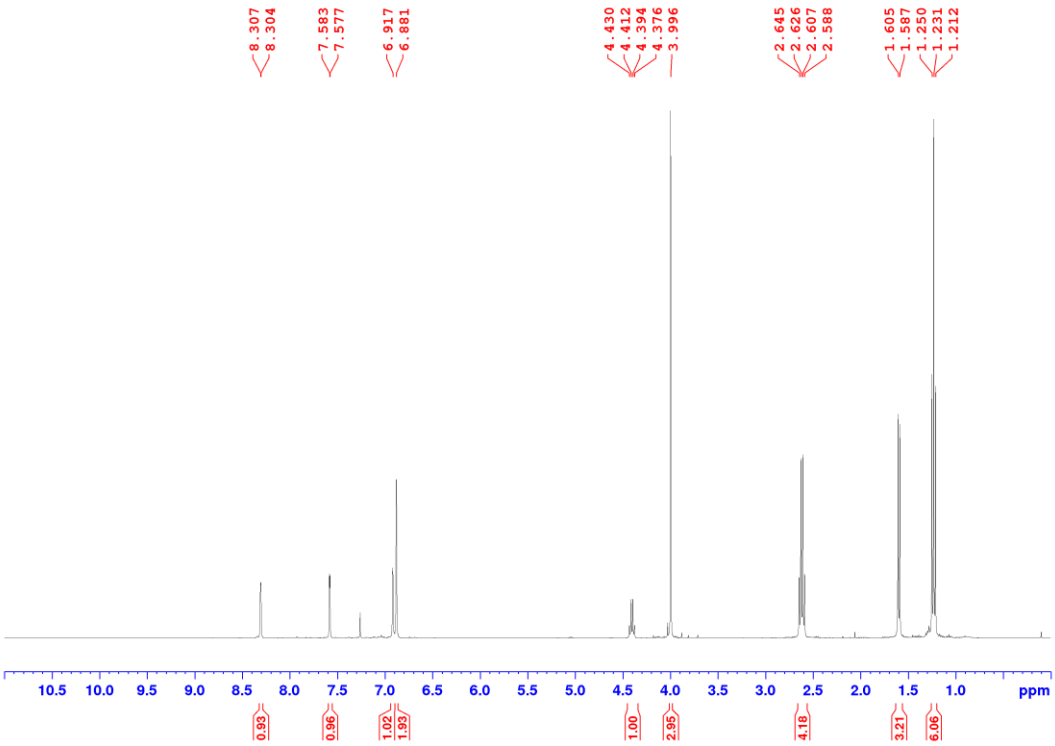

48 (^{13}C NMR, $CDCl_3$, 100 MHz)

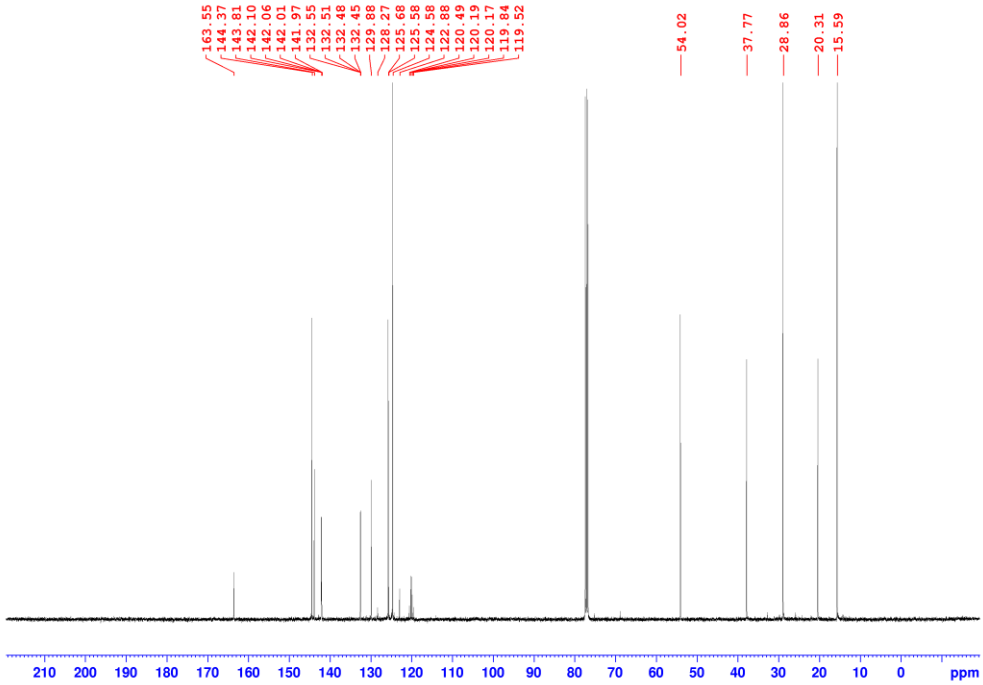

48 (^{19}F NMR, $CDCl_3$, 75 MHz)

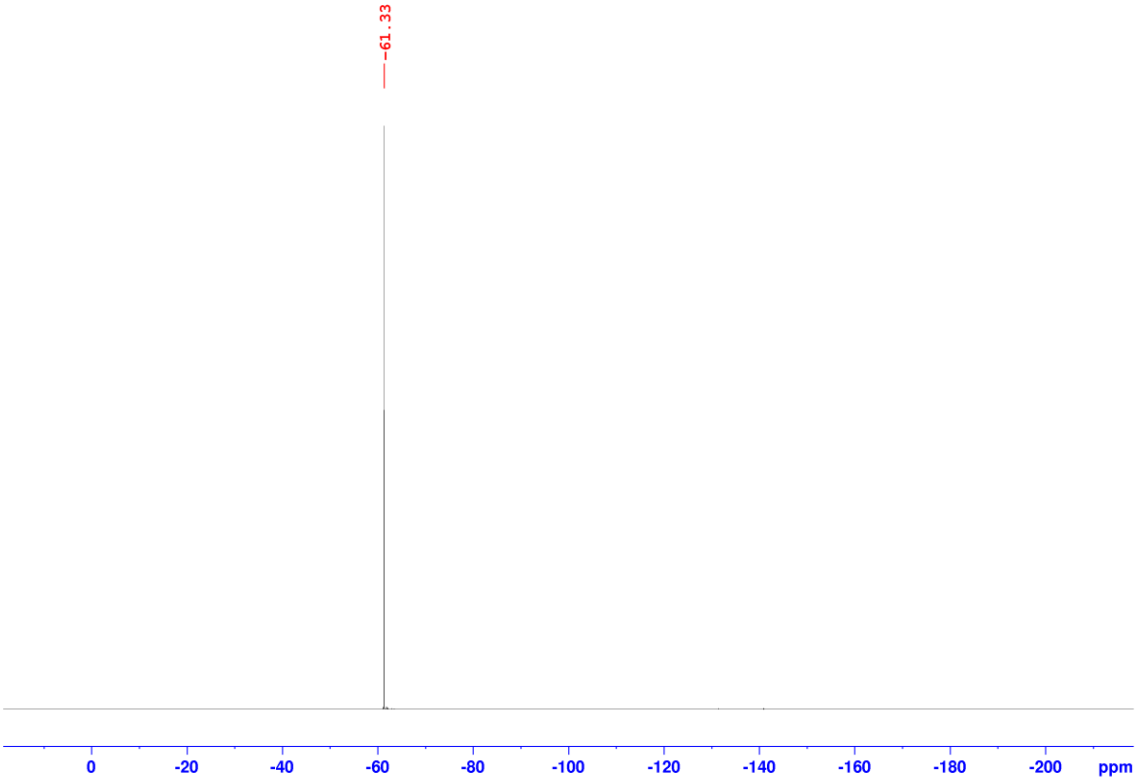

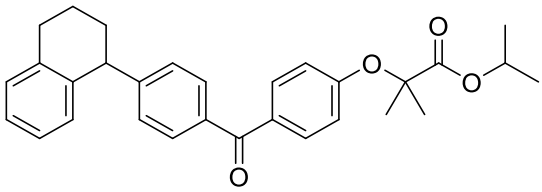

49 (^{1}H NMR, $CDCl_3$, 400 MHz)

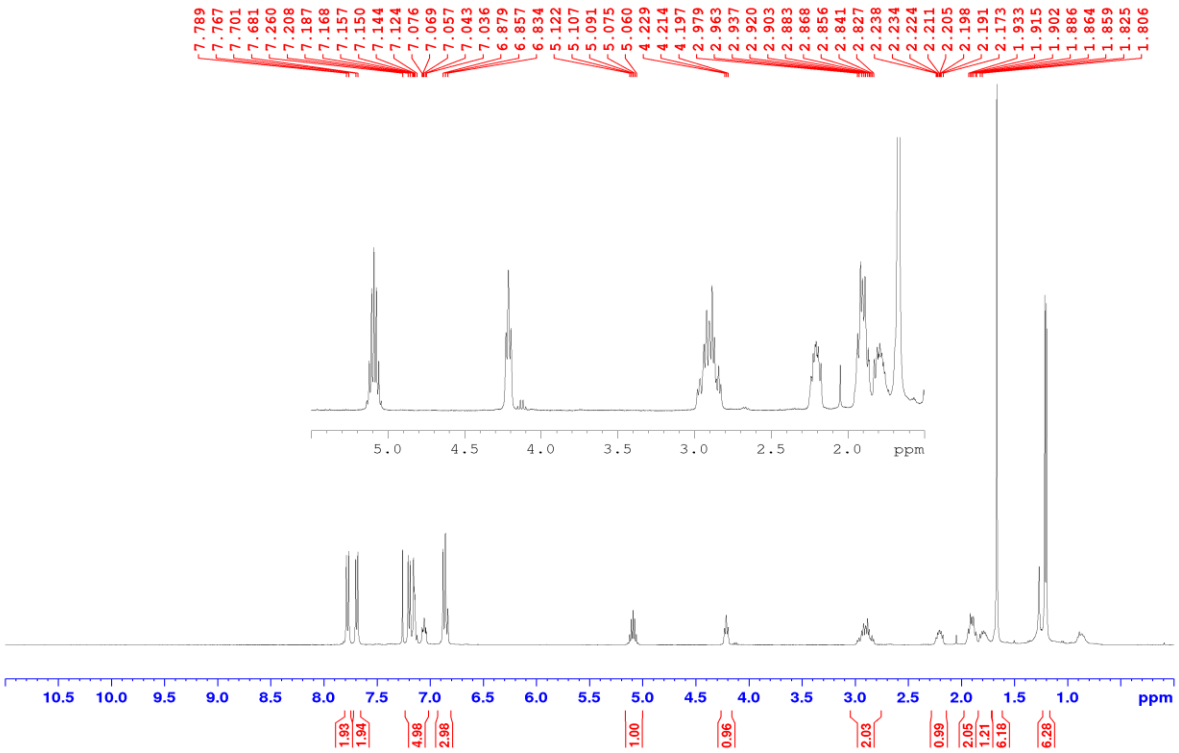

49 (^{13}C NMR, $CDCl_3$, 100 MHz)

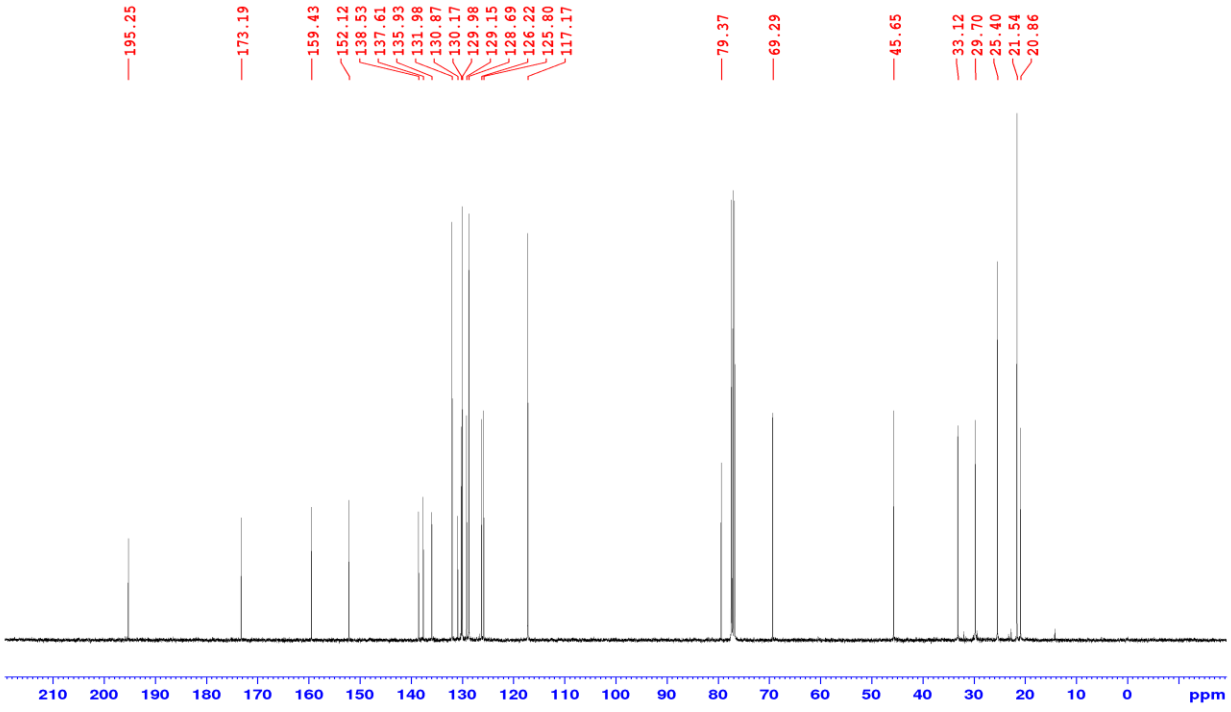

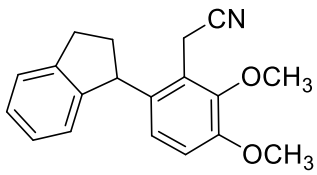

50 (^{1}H NMR, $CDCl_3$, 400 MHz)

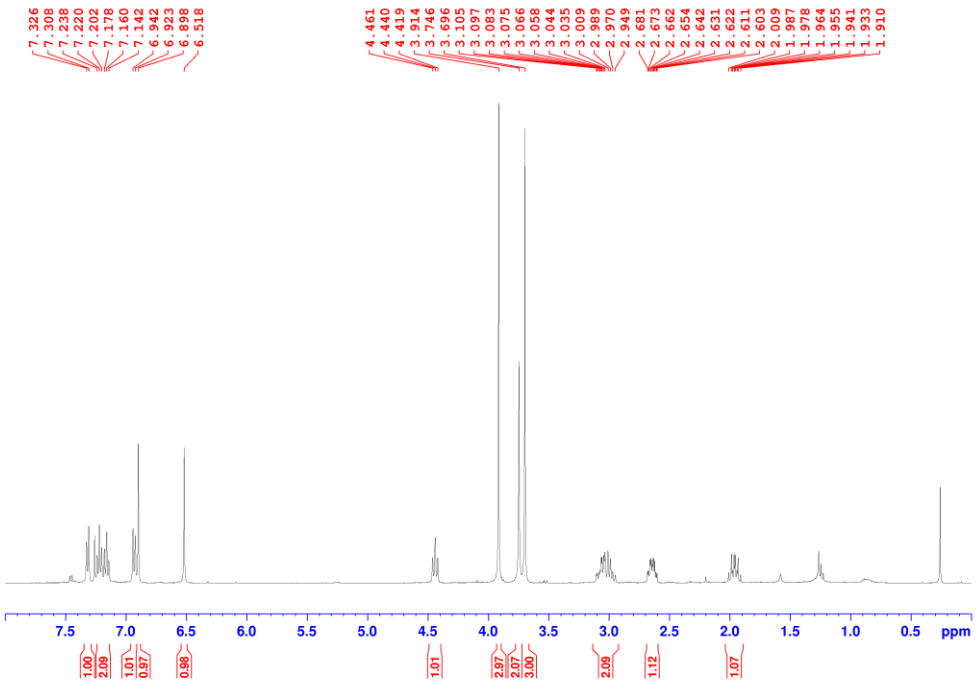

50 (^{13}C NMR, $CDCl_3$, 100 MHz)

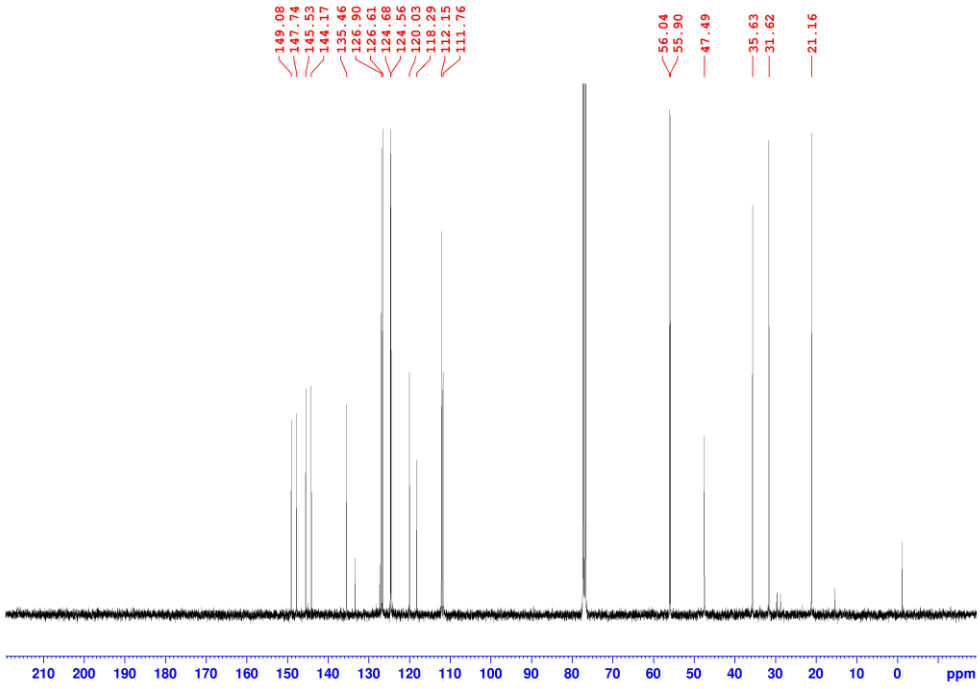

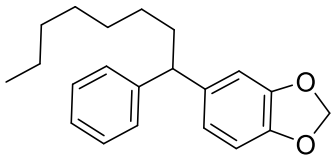

51 (^{1}H NMR, $CDCl_3$, 400 MHz)

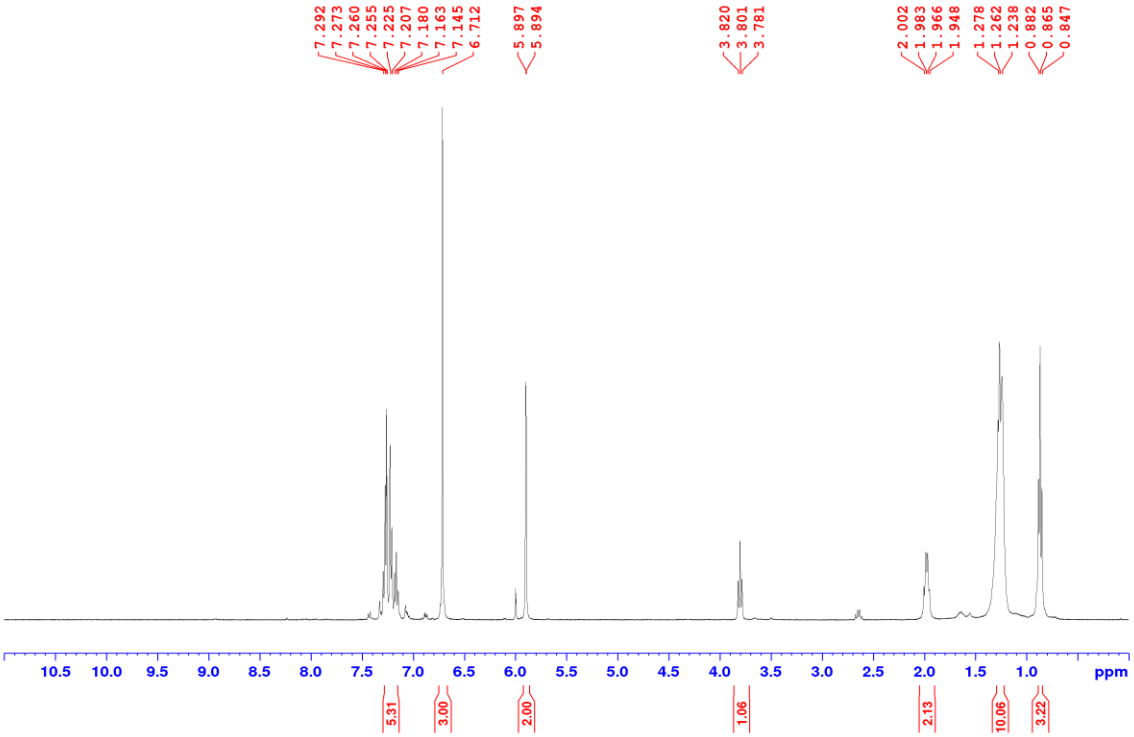

51 (^{13}C NMR, $CDCl_3$, 100 MHz)

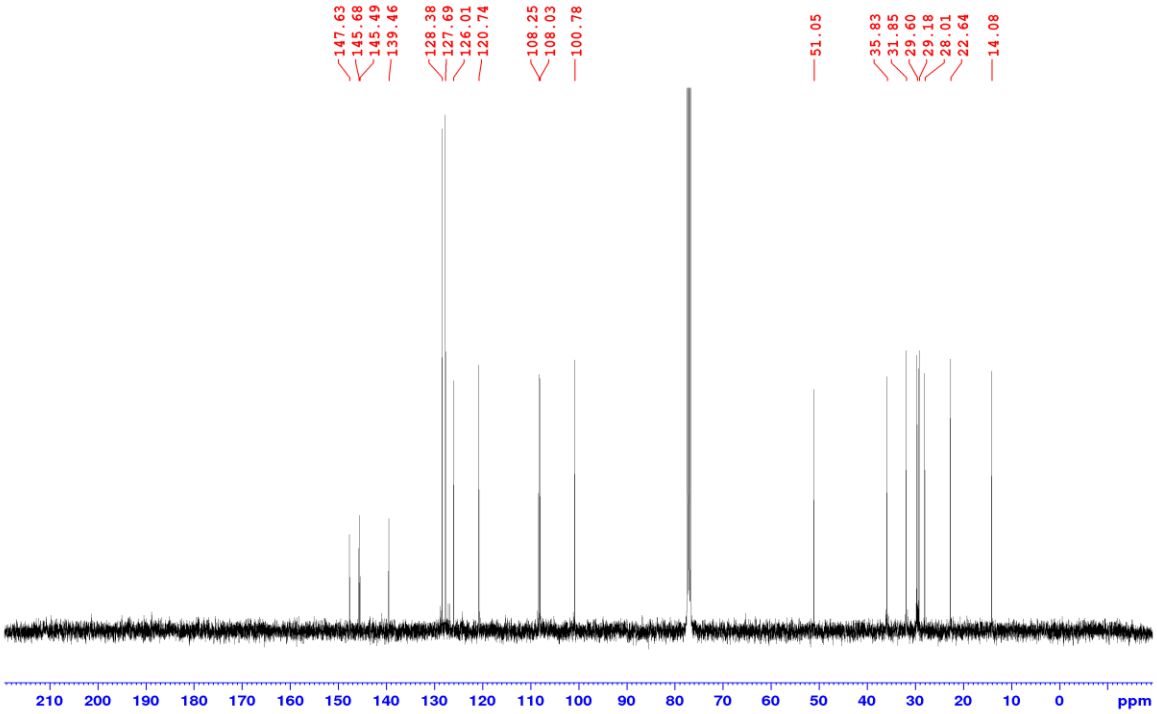

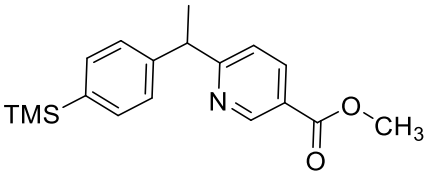

52 (^{1}H NMR, $CDCl_3$, 400 MHz)

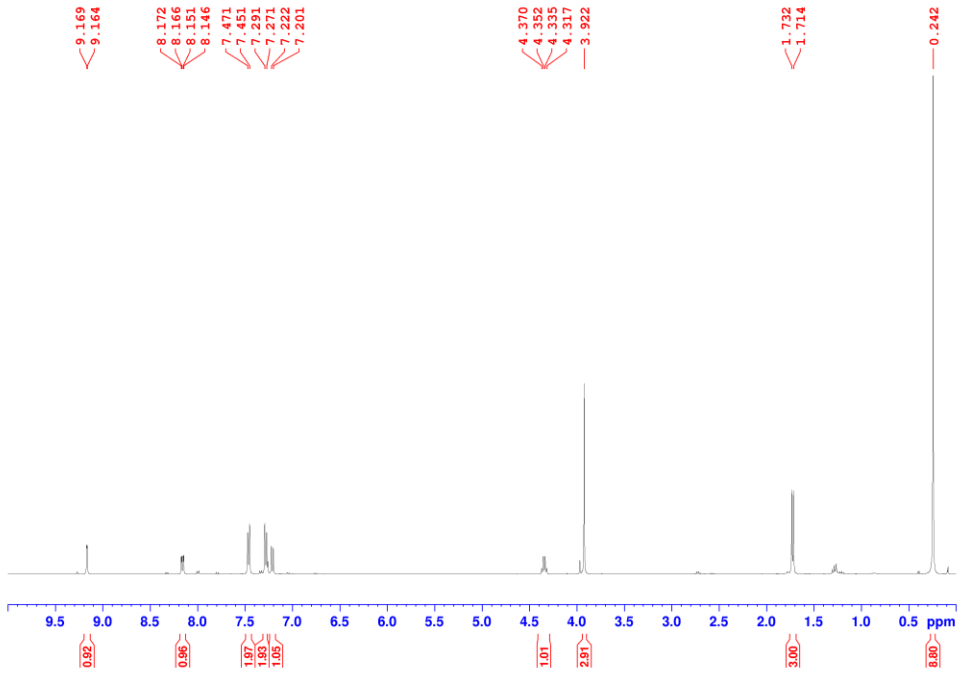

52 (^{13}C NMR, $CDCl_3$, 100 MHz)

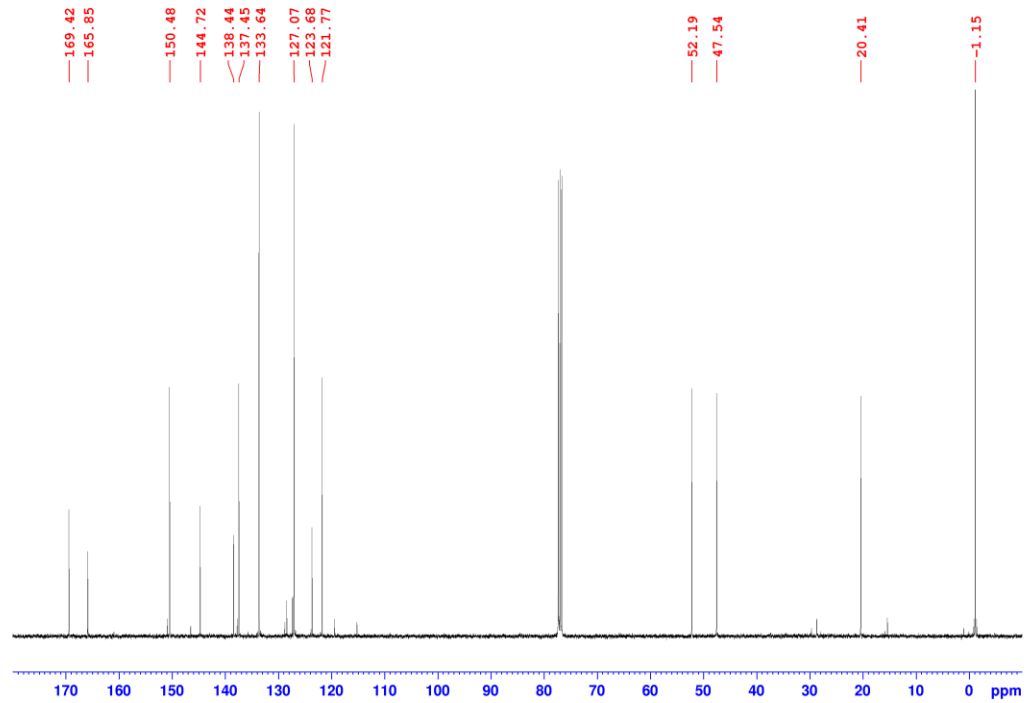

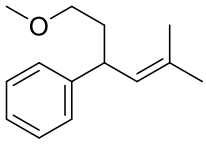

53 (^{1}H NMR, $CDCl_3$, 400 MHz)

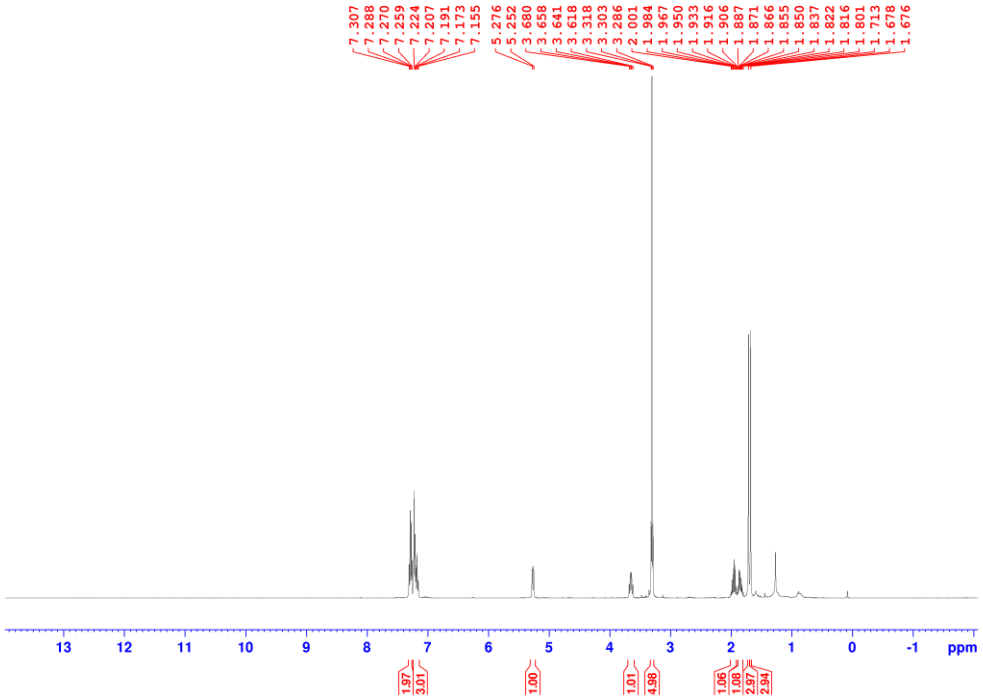

53 (^{13}C NMR, $CDCl_3$, 100 MHz)

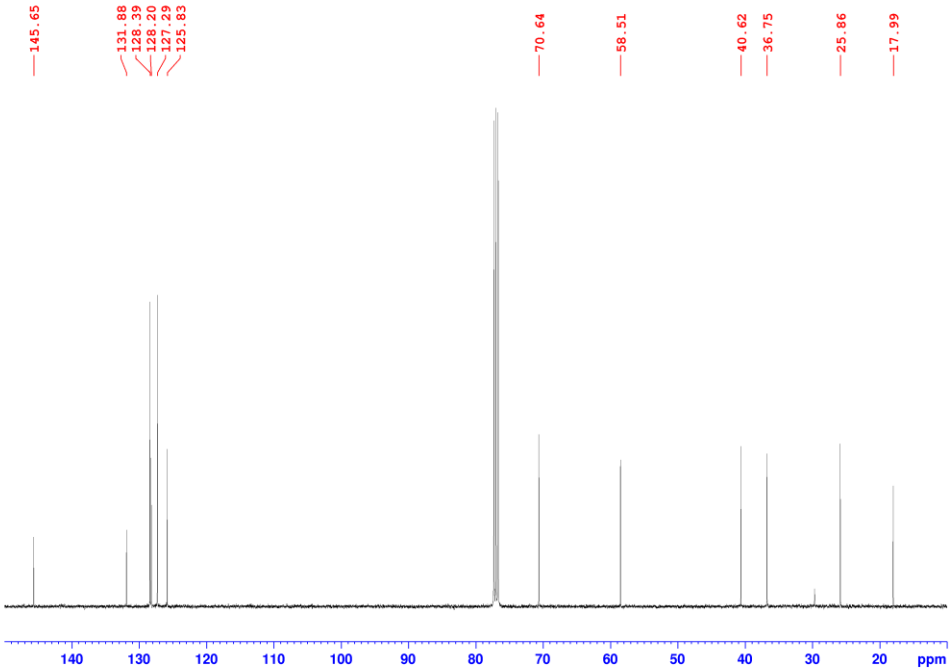

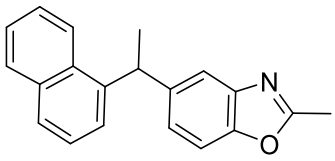

54 (^{1}H NMR, $CDCl_3$, 400 MHz)

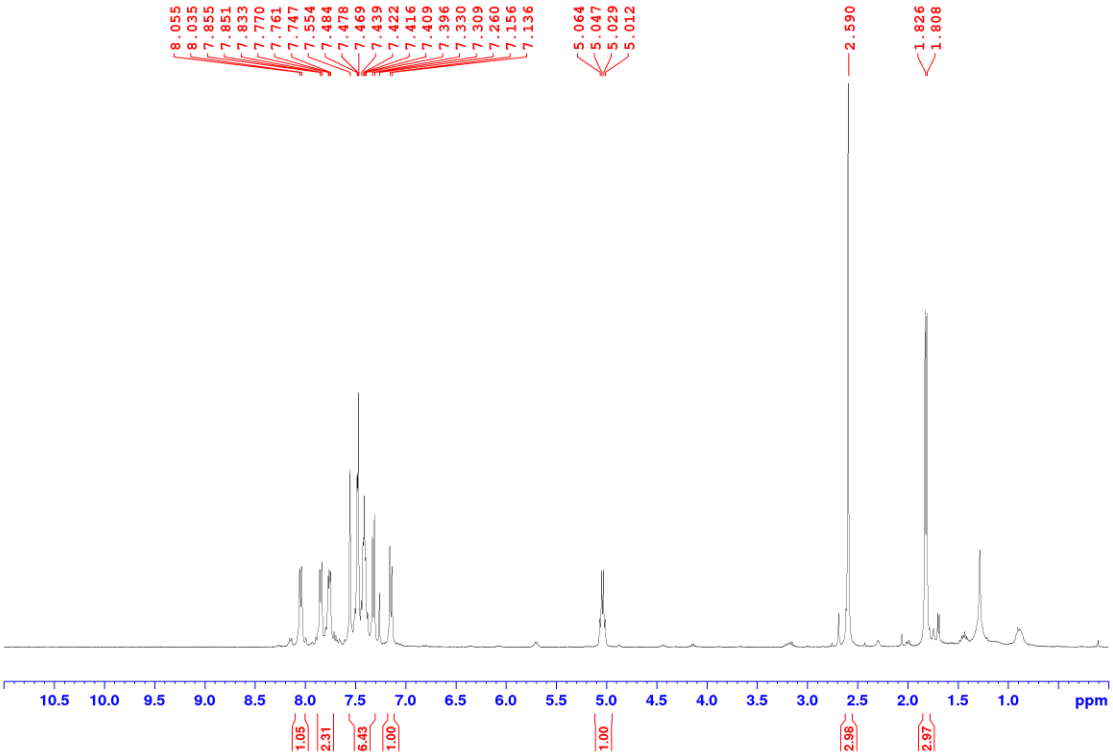

54 (^{13}C NMR, $CDCl_3$, 100 MHz)

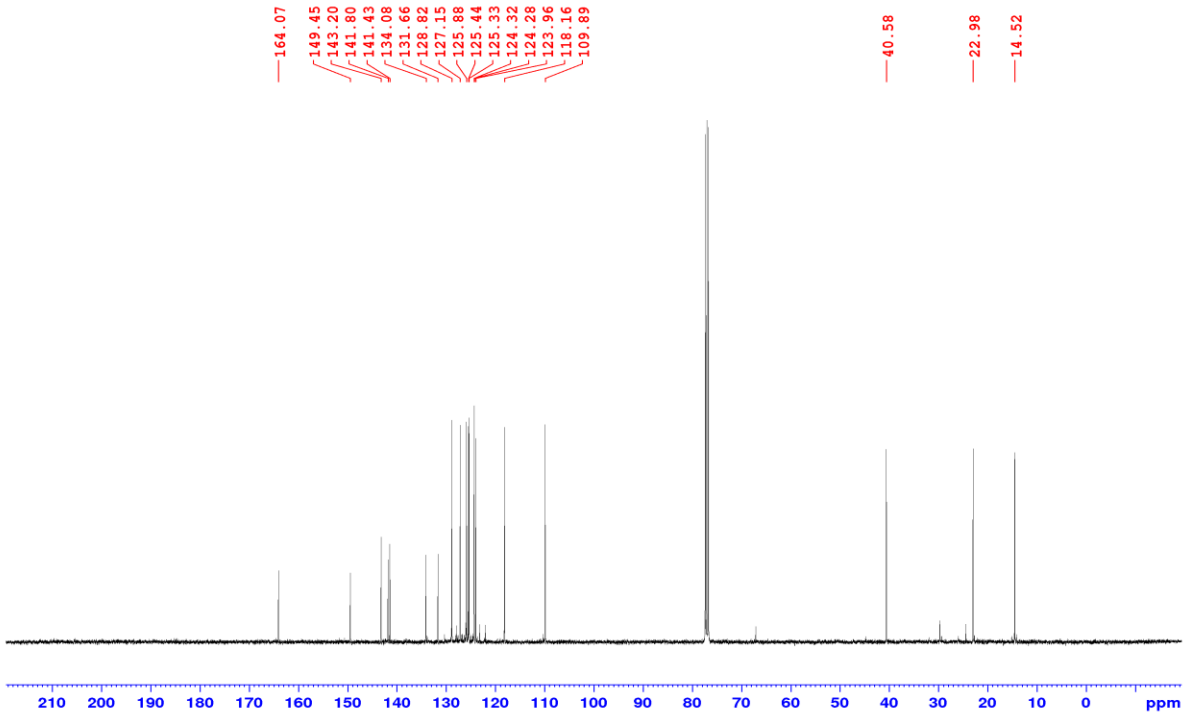

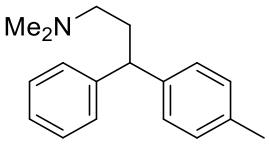

55 (^{1}H NMR, $CDCl_3$, 400 MHz)

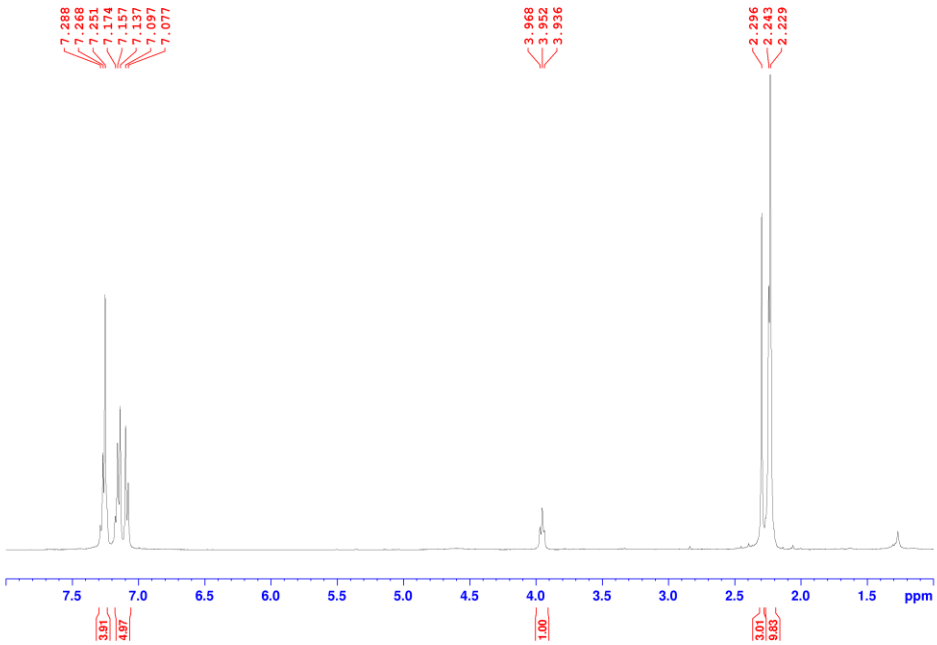

55 (^{13}C NMR, $CDCl_3$, 100 MHz)

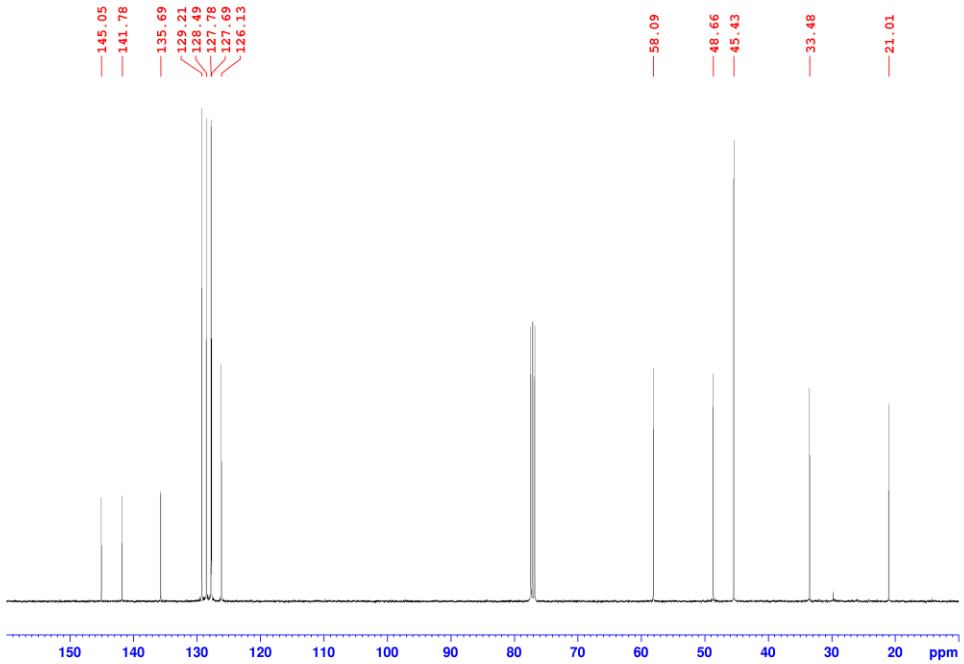

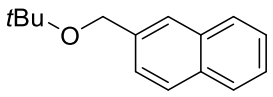

59 (^{1}H NMR, $CDCl_3$, 400 MHz)

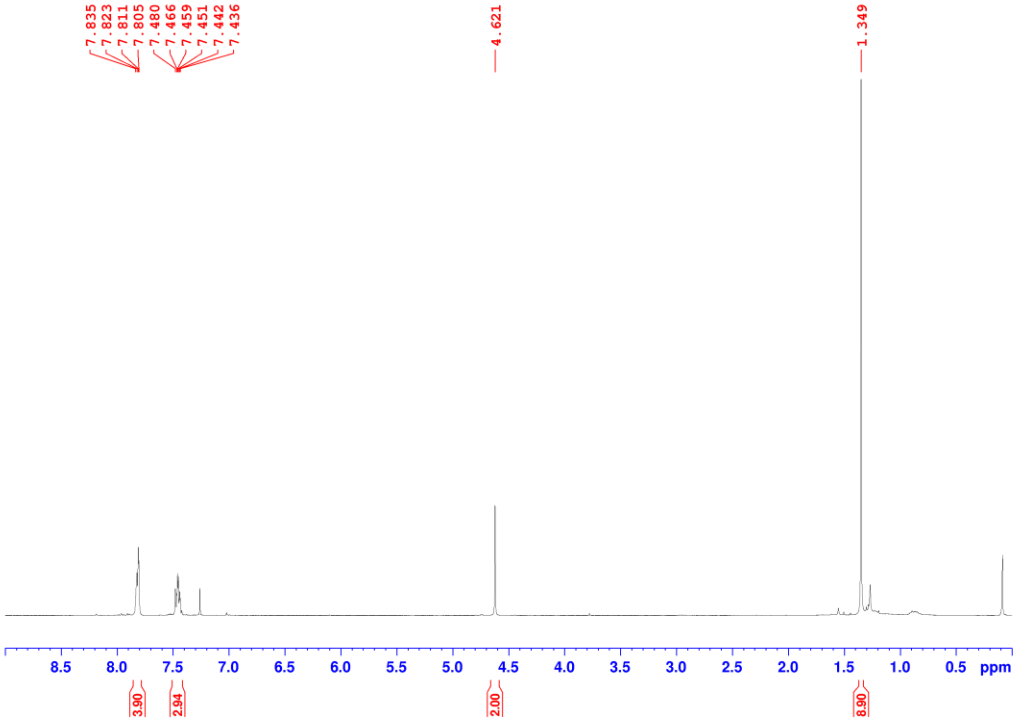

59 (^{13}C NMR, $CDCl_3$, 100 MHz)

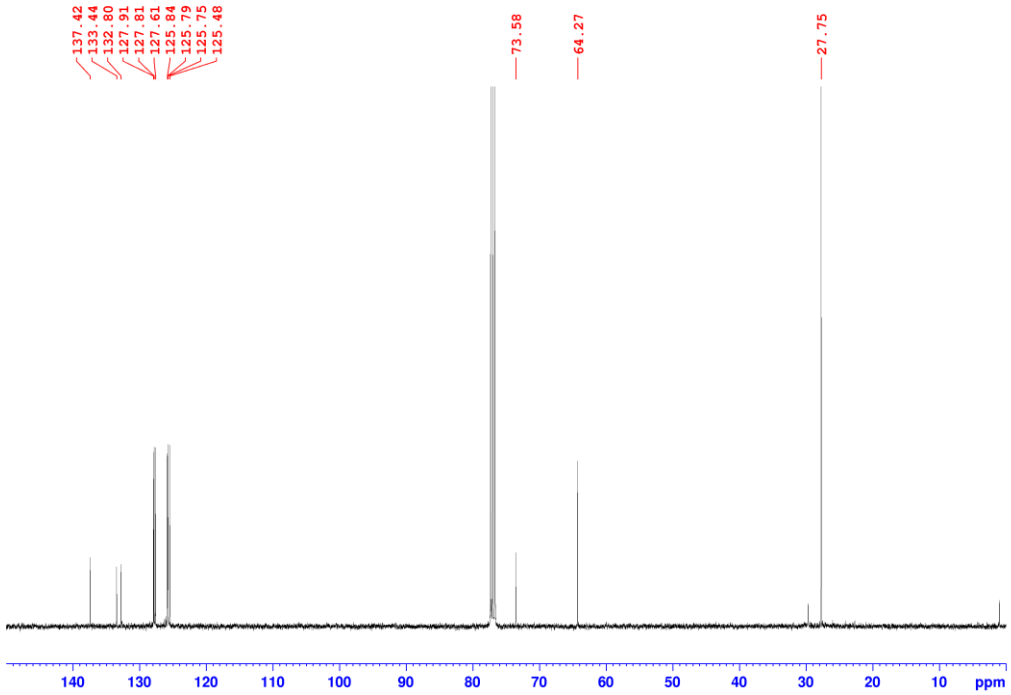

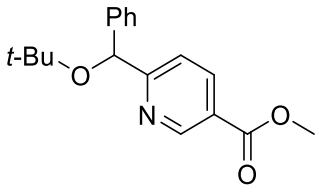

60 (^{1}H NMR, $CDCl_3$, 400 MHz)

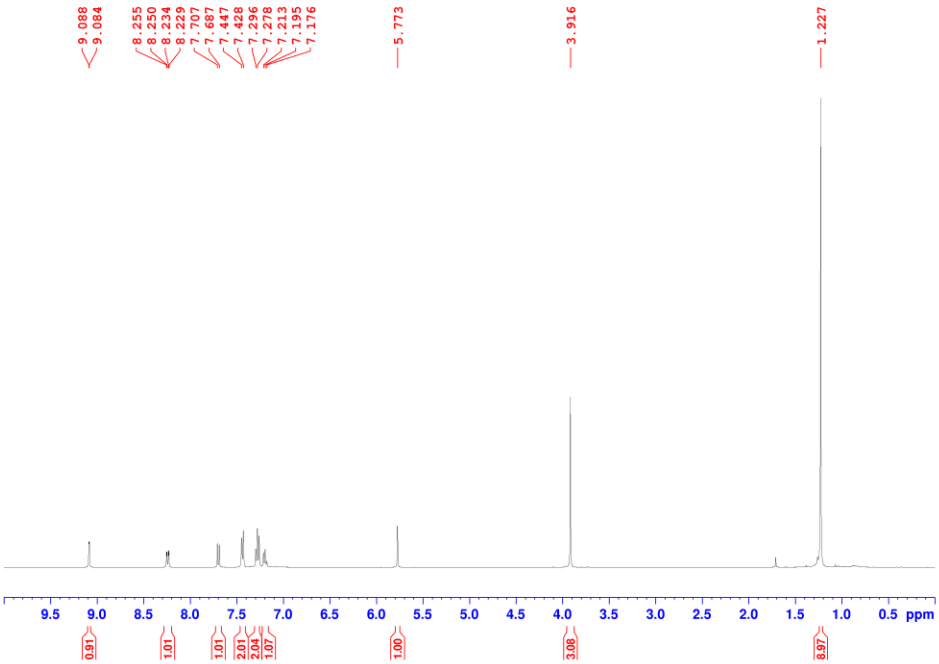

60 (^{13}C NMR, $CDCl_3$, 100 MHz)

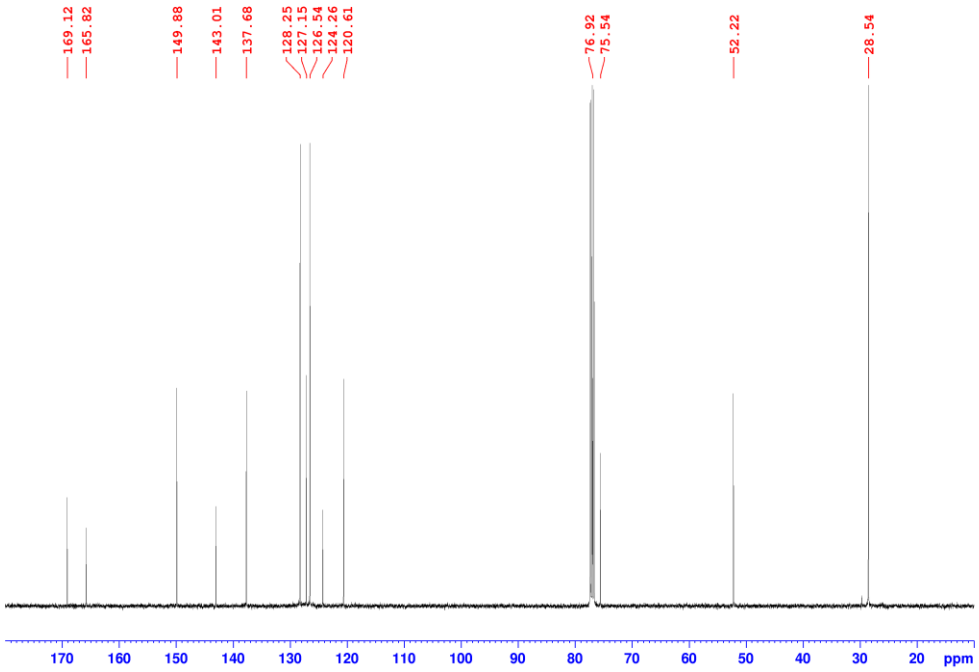

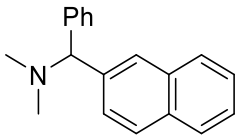

61 (^{1}H NMR, $CDCl_3$, 400 MHz)

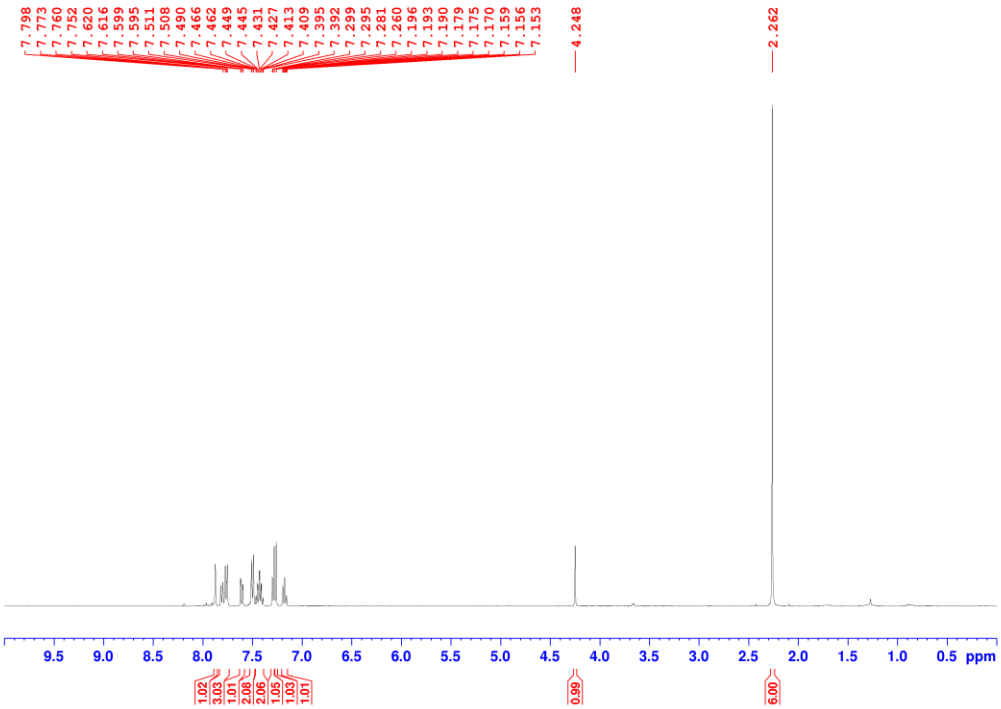

61 (^{13}C NMR, $CDCl_3$, 100 MHz)

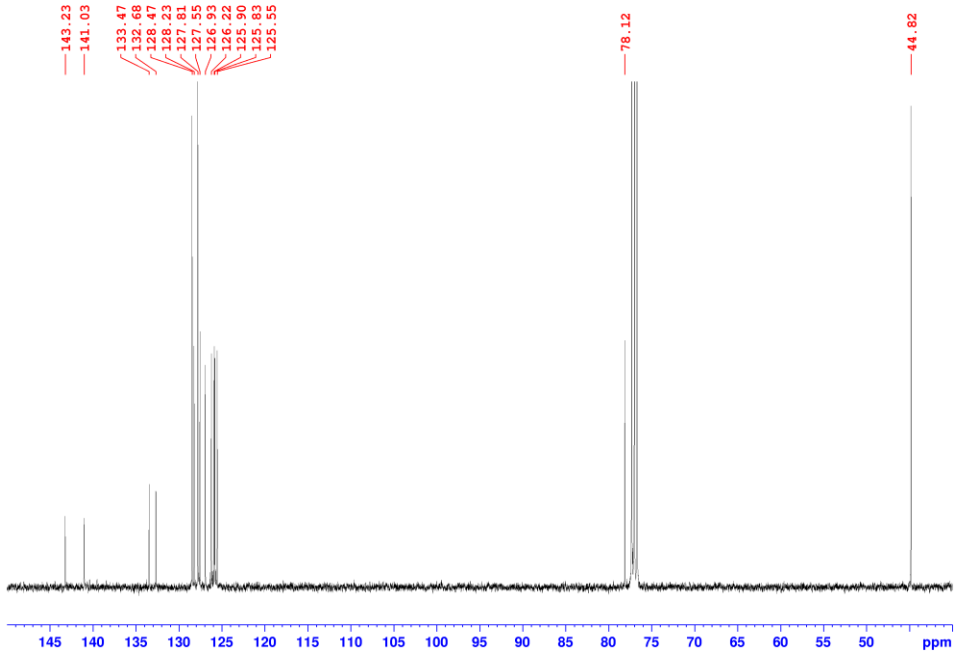

3.2: Nickel-Catalyzed Suzuki-Miyaura Coupling of Silyl Enol Ethers

3.2.1: Experimental Details

Unless otherwise indicated, reagents were obtained from Sigma Aldrich, Acros, Alfa Aesar, Matrix Scientific, Oakwood, or Combi-Blocks, and used as received. Toluene was degassed with N_2 and passed through a PureSolv solvent purification system before use. Unless otherwise indicated, all reactions were carried out in oven-dried glassware inside of a glovebox under an N_2 atmosphere. NMR spectra were collected on a Bruker Avance 400 MHz spectrometer.

((1H-inden-3-yl)oxy)tri*iso*propylsilane,[187] ethyl 3-trimethylsiloxy-2-butenoate,[188] *tert*-butyl(4-*tert*-butylcyclohex-1-enyloxy)dimethylsilane,[189] ((1H-inden-3-yl)oxy)(*tert*-butyl)dimethylsilane,[190] *tert*-butyl((1-(4-trifluoromethylphenyl)prop-1-en-1-yl)oxy)dimethylsilane,[191] and *tert*-butyl((3,4-dihydronaphthalen-1-yl)oxy)dimethylsilane,[192] were all prepared by literature procedures and their characterization data were all in agreement with that reported by the authors.

3.2.1.1:General Procedure D: Nickel-Catalyzed Suzuki-Miyaura coupling of Silyl Enol Ethers

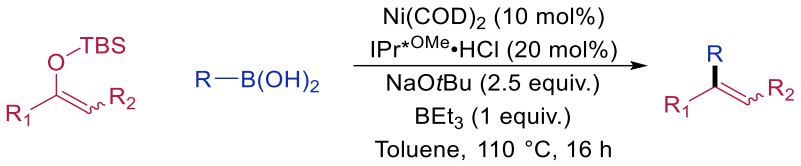

$Ni(COD)_2$ (2.8 mg, 10 mol%, 0.01 mmol), IPr*^{OMe}·HCl (19.6mg, 20 mol%, 0.02 mmol), NaO*t*Bu (24.0 mg, 2.5 equiv, 0.25 mmol), and organoboronic acid (1 equiv, 0.1 mmol) were added to an 8 mL screw-top tube inside of a glovebox. Toluene was added (0.67 mL, 0.15 mol/L) and the mixture was stirred at room temperature for 15 minutes to obtain a transparent orange solution. Next, BEt_3 1.0 M in hexanes (0.1 mL, 1 equiv, 0.1 mmol) was added to the mixture followed by the silyl enol ether (1 equiv, 0.1 mmol). The reaction mixture was then sealed, shipped out of the glovebox, and stirred at 110 °C overnight for approximately 16 hours. The reaction was then quenched with methanol (~2 mL), followed by the addition of 1,3,5-trimethoxybenzene 0.05 M in toluene (1 mL, 0.5 equiv, 0.05 mmol), filtered over silica, and analyzed by GC-MS and ^{1}H NMR.

---

[187] Luttikhedde, H. J. G.; Leino, R.; Lehtonen, A.; Näsman, J. H. *J. Organomet. Chem.* **1998**, *555*, 127–134.
[188] Fleming, I.; Iqbal, J.; Krebs, E.-P. *Tetrahedron* **1983**, *39*, 841–846.
[189] Iwasaki, K.; Wan, K. K.; Oppedisano, A.; Crossley, S. W. M.; Shenvi, R. *J. Am. Chem. Soc.* **2014**, *136*, 1300–1303.
[190] Kang, T.; Cao, W.; Hou, L.; Tang, Q.; Zou, S.; Liu, X.; Feng, X. *Angew. Chem. Int. Ed.* **2019**, *58*, 2464–2468.
[191] Yang, B.; Lu, Z. *J. Org. Chem.* **2016**, *81*, 7288–7300.
[192] Chepiga, K. M.; Feng, Y.; Brunelli, N. A.; Jones, C. W.; Davies, H. M. L. *Org. Lett.* **2013**, *15*, 6136–6139.

3.2.2: Characterization Data and NMR Spectra

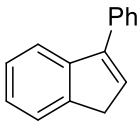

3-phenyl-1-H-indene (94) was prepared from ((1H-inden-3-yl)oxy)(*tert*-butyl)dimethylsilane and phenylboronic acid using General Procedure D. Quantified by ^{1}H NMR relative to 1,3,5-trimethoxybenzene as an internal standard. NMR data were in agreement with the literature, in which the vinylic C–H of the product (6.59 ppm, t, J = 2.0 Hz, 1H)[193] was compared to the methoxy groups of the internal standard (6.10 ppm, s, 9H).[194]

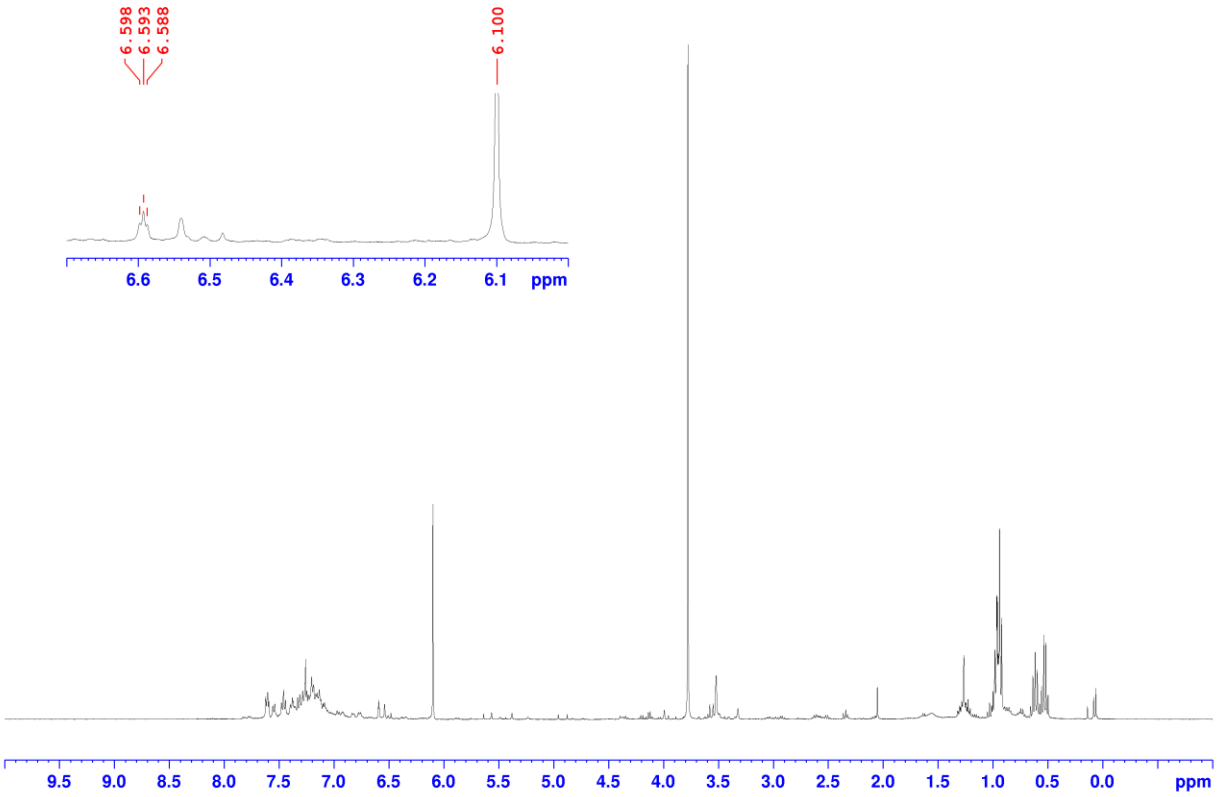

[193] Zheng, H.-X.; Xiao, Z.-F.; Yao, C.-Z.; Li, Q.-Q.; Ning, X.-S.; Kang, Y.-B.; Tang, Y. *Org. Lett.* **2015**, *17*, 6102–6105.
[194] Dabral, S.; Mottweiler, J.; Rinesch, T.; Bolm, C. *Green Chem.* **2015**, *17*, 4908–4912.